UNIVERSIDAD AUTÓNOMA DE MADRID

Programa de Doctorado en Biociencias Moleculares

Doctoral Thesis

Role of SHIP-1 phosphatase in trained immunity modulation

Paula Saz Leal

Madrid, 2018

Departamento de Bioquímica

Facultad de Medicina

Universidad Autónoma de Madrid

Doctoral Thesis

Role of SHIP-1 phosphatase in trained immunity modulation

Memoria presentada por la Licenciada en Bioquímica:

Paula Saz Leal

Para optar al grado de Doctor en Biociencias Moleculares por la Universidad Autónoma de Madrid

Directores de tesis:

Dr. David Sancho Madrid

Dr. Carlos del Fresno Sánchez

Este trabajo se ha realizado en el laboratorio de Inmunobiología de la Fundación-Centro Nacional de Investigaciones Cardiovasculares Carlos III (CNIC).

Madrid, 2018

El Doctor David Sancho Madrid, líder del grupo de investigación de Inmunobiología, y el Doctor Carlos del Fresno Sánchez, investigador posdoctoral senior del mismo laboratorio, ambos de la Fundación-Centro Nacional de Investigaciones Cardiovasculares Carlos III (CNIC),

CERTIFICAN

que **Paula Saz Leal**, Licenciada en Bioquímica y Máster en Biomedicina Molecular, titulaciones obtenidas por la Universidad de Zaragoza y la Universidad Autónoma de Madrid, respectivamente, ha realizado bajo su supervisión el trabajo de Tesis Doctoral: **Role of SHIP-1 phosphatase in trained immunity modulation**.

Para la realización de esta Tesis Doctoral se contó con la financiación de: Beca BES-2015-072699 ("Ayudas para Contratos Predoctorales para la Formación de Doctores 2015") y proyecto SAF2016-79040-R, ambos del Ministerio de Industria, Economía y Competitividad de España (MINECO), Agencia Estatal de Investigación y FEDER (Fondo Europeo para el desarrollo regional); proyecto financiado por la Comisión Europea (635122-PROCROP H2020); proyecto financiado por el Consejo de Investigación europeo (ERC-2016-Consolidator Grant 725091). El CNIC se financia por el MINECO y la fundación Pro-CNIC, y es un Centro de Excelencia Severo Ochoa (SEV-2015-0505).

Revisado el presente trabajo, expresan su conformidad para la presentación del mismo en el Departamento de Bioquímica de la Universidad Autónoma de Madrid, por considerar que reúne los requisitos necesarios para ser sometido a su evaluación ante el tribunal correspondiente para optar al grado de **Doctor en Biociencias Moleculares por la Universidad Autónoma de Madrid.**

Y para que así conste y a los efectos oportunos, firman el presente certificado en Madrid, a 25 de octubre de 2018.

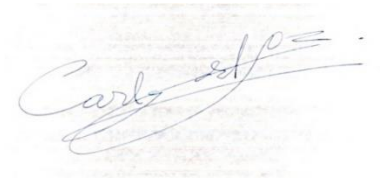

Dr. David Sancho Madrid
Investigador Principal, CNIC
Director de tesis

Dr. Carlos del Fresno Sánchez
Posdoctoral Senior, CNIC
Codirector de tesis

A mi madre

“Lo único imposible

es aquello que no intentas.”

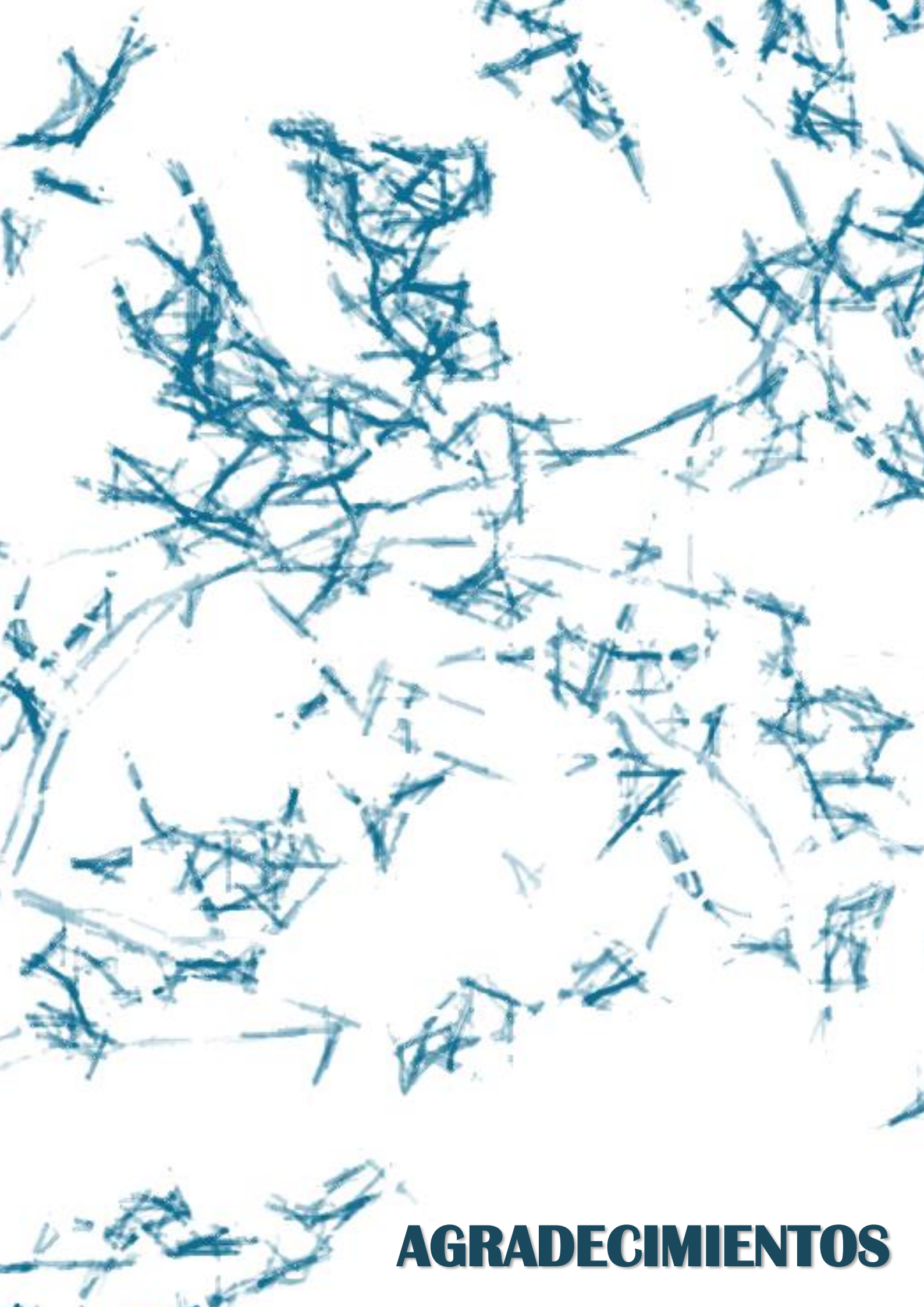

AGRADECIMIENTOS

Y al final…solo queda dar las gracias a todos los que estuvieron en el camino.

Gracias **David**, por darme la oportunidad desde el minuto cero. Gracias por confiar en mí, por enseñarme el duro camino de la ciencia y por apoyarme siempre en mis decisiones. Todo *in parallel*.

Gracias **CArlos**, por recoger al pollito y llevarlo codo a codo hasta el final de viaje. Gracias por enseñarme a hacer ciencia, a ser científica, sin dejar de disfrutar. Y lo más importante, gracias por confiar, por empujarme y creer en mí. (*Fresnada*)

Gracias a todos y cada uno de ***los Sanchos***, porque de todos sin excepción te llevas un pedacito. Gracias a la siempre *British* **Dra. Conejero**, por confiar en mí y por aguantarme en lo mejor... y en lo peor... A **Sarai**, la jefa. A **Pao**, mi italiana caótica. A **Fran**, *I know what you mean*. A **Michel** y su acelerador. A **Joaquín**, por su humor inagotable. Y al "pequeño" **Nacho**, por llegar el último pero hacerse admirar como el primero.

Gracias a cada personita que ha arrimado el hombro en el **CNIC**. Y también gracias a la gente de **Inmunotek**, por ayudarme y hacerlo todo más fácil en este *sprint* final.

Gracias a mi **madre**, que fue y será siempre mi *supermujer*. A mi **padre**, mi ejemplo de lucha y de sacrificio. Y a mi **hermanico**, que siempre será el pequeño, pero siempre está ahí. Gracias a toda mi **familia** y a mis **amigos**, por admirarme y creer en mis ratones, aun sin tener ni idea de lo que estaba hablando. Y gracias a **Ana**, mi ilustradora favorita.

Gracias a mi **pequeñaja**, por enseñarme a ver el *bright side of the life*. Y gracias a **ti**, por tu cariño, por tu apoyo incansable, por tu confianza y por no dejarme caer nunca. Gracias por emprender conmigo este camino, porque sin ti yo no estaría hoy escribiendo estas líneas.

Imagen de portada: Ilustración realizada por Ana Leal Santana.

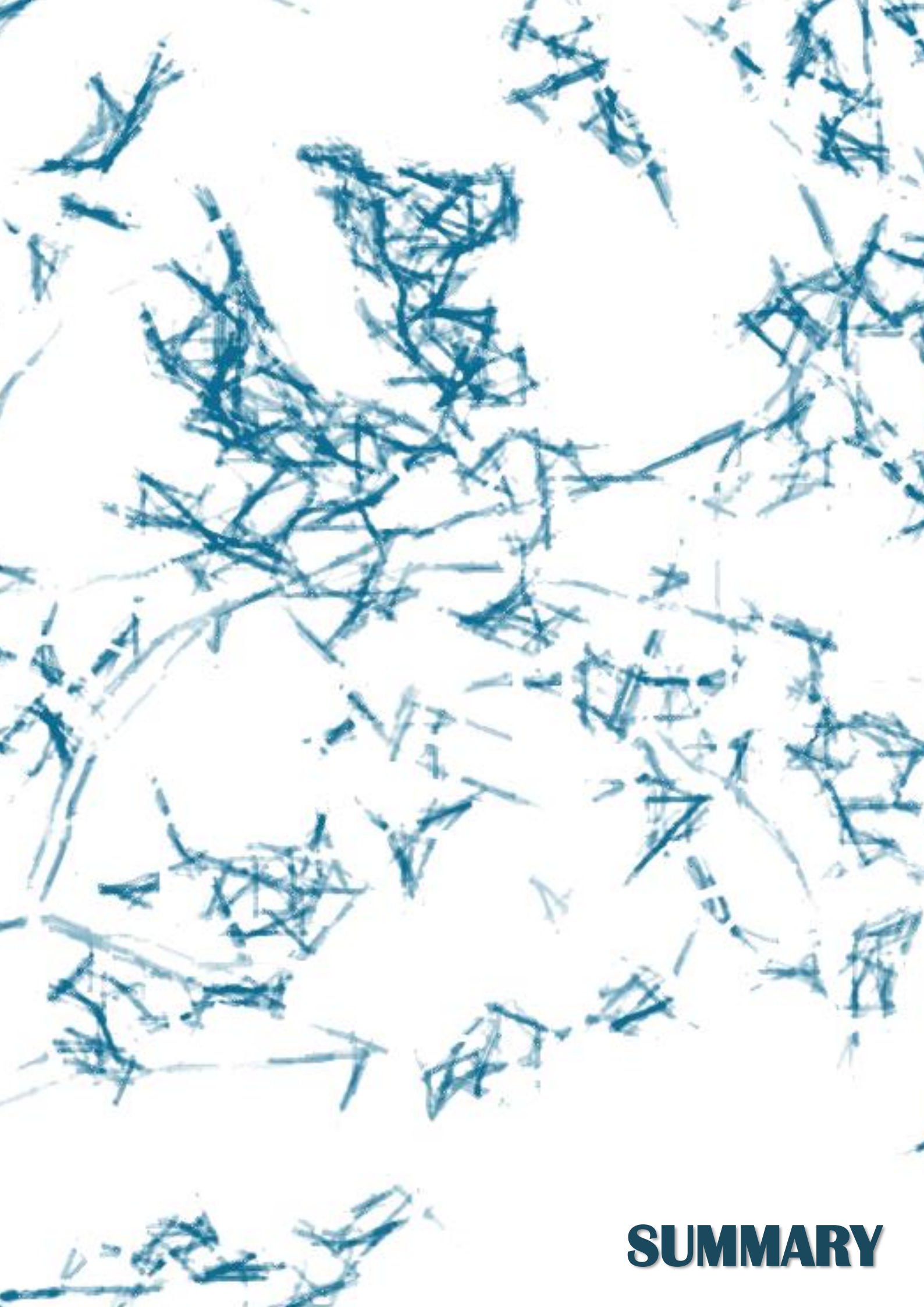

SUMMARY

β-glucan-induced trained immunity in monocytes confers long-term protection against secondary infections through activation of the dendritic cell-associated C-type lectin 1 (Dectin-1)/ Phosphoinositide 3-kinase (PI3K)/ mammalian target of rapamycin (mTOR) pathway. While previous studies have addressed the characterization of this phenomenon, strategies to boost trained immunity deserve further investigation. Src homology 2 (SH2) domain-containing inositol 5'-phosphatase (SHIP)-1 is a hematopoietic-restricted phosphatase that limits PI3K activity and it is able to associate with Dectin-1 receptor. Therefore, we hypothesized that SHIP-1 targeting could modulate trained immunity mediated by Dectin-1 ligands.

Herein, we found that β-glucan-trained macrophages from mice with a myeloid-specific SHIP-1 deletion (LysMΔSHIP-1) enhanced proinflammatory cytokine production in response to lipopolysaccharide (LPS). Following β-glucan training, SHIP-1-deficient macrophages exhibited increased phosphorylation of protein kinase B (also known as Akt, a downstream target of PI3K), and mTOR targets. These overactivation of the signaling pathway correlated with augmented glycolytic metabolism. Furthermore, enhanced training in the absence of SHIP-1 relied on epigenetic reprogramming, including histone methylation and acetylation.

Trained LysMΔSHIP-1 mice produced increased proinflammatory cytokines upon rechallenge *in vivo* and were better protected against systemic *Candida albicans* infection compared with control littermates.

Pharmacological inhibition of SHIP-1 enhanced trained immunity *in vitro* in mouse macrophages and human peripheral blood mononuclear cells (hPBMCs), and also improved protection conferred by immune training with *C. albicans*.

These data establish a proof of concept for improvement of trained immunity, and place SHIP-1 as a target to achieve it.

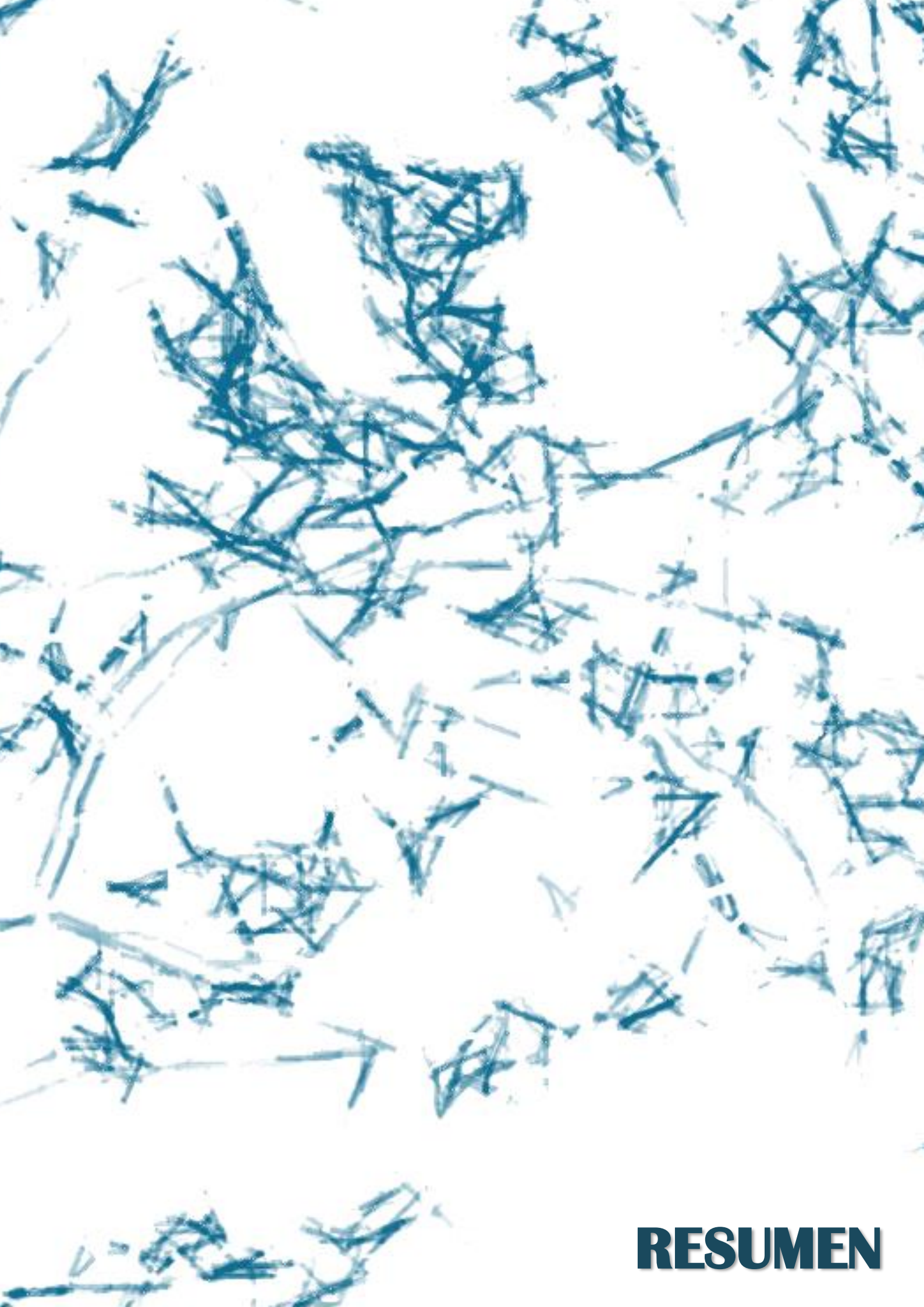

RESUMEN

La inmunidad entrenada inducida por β-glucano en monocitos confiere una protección a largo plazo frente a infecciones secundarias, mediante la activación de la ruta de señalización mediada por la lectina de tipo C asociada a célula dendrítica (en inglés, Dectin-1)/ fosfatidil inositol 3 quinasa (en inglés, PI3K)/ diana de rapamicina en células de mamífero (en inglés, mTOR). Mientras trabajos previos se han centrado en la caracterización de este proceso, no se conocen estrategias para potenciar la inmunidad entrenada. La inositol fosfatasa 5' con dominios de homología 2 a Src 1 (en inglés, SHIP-1) es una fosfatasa que se expresa en el componente hematopoyético, limita la actividad de PI3K y es capaz de asociarse al receptor Dectin-1. Por tanto, hipotetizamos que la regulación de SHIP-1 podría modular la inmunidad entrenada mediada por ligandos de Dectin-1.

En este trabajo encontramos que macrófagos entrenados con β-glucano procedentes de ratones con una depleción específica de SHIP-1 en el compartimento mieloide (LysMΔSHIP-1), producían una mayor cantidad de citoquinas inflamatorias en respuesta a lipopolisacárido. Tras el tratamiento con β-glucano, los macrófagos deficientes en SHIP-1 presentaban mayor fosforilación de la proteína quinasa B (también llamada Akt, diana de PI3K), y de efectores de mTOR. Esta sobreactivación de la ruta de señalización correlacionó con un aumento en el metabolismo glucolítico. Además, este entrenamiento potenciado en ausencia de SHIP-1 se basó en procesos de reprogramación epigenética, concretamente en la metilación y acetilación de histonas.

Los ratones LysMΔSHIP-1 entrenados produjeron más citoquinas proinflamatorias ante un estímulo secundario *in vivo* y, en comparación con ratones silvestres, se protegieron mejor frente a una infección sistémica con *Candida albicans*.

La inhibición química de SHIP-1 potenció la inmunidad entrenada *in vitro* en macrófagos de ratón y células mononucleares de sangre periférica humana y también mejoró la protección conferida por el entrenamiento con *C. albicans*.

Estos datos establecen la prueba de concepto de mejora de inmunidad entrenada y emplazan a SHIP-1 como una diana para conseguirlo.

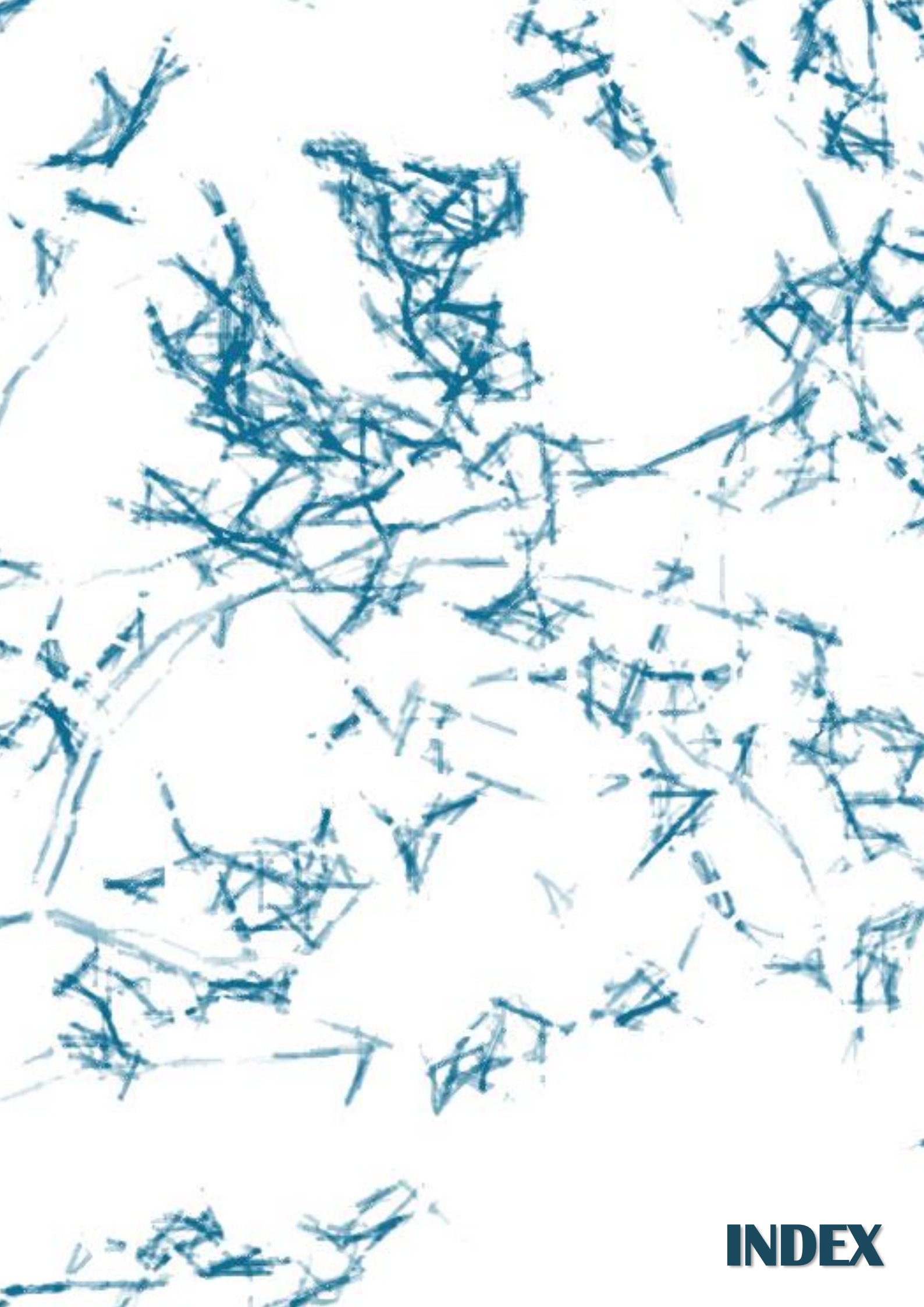

INDEX

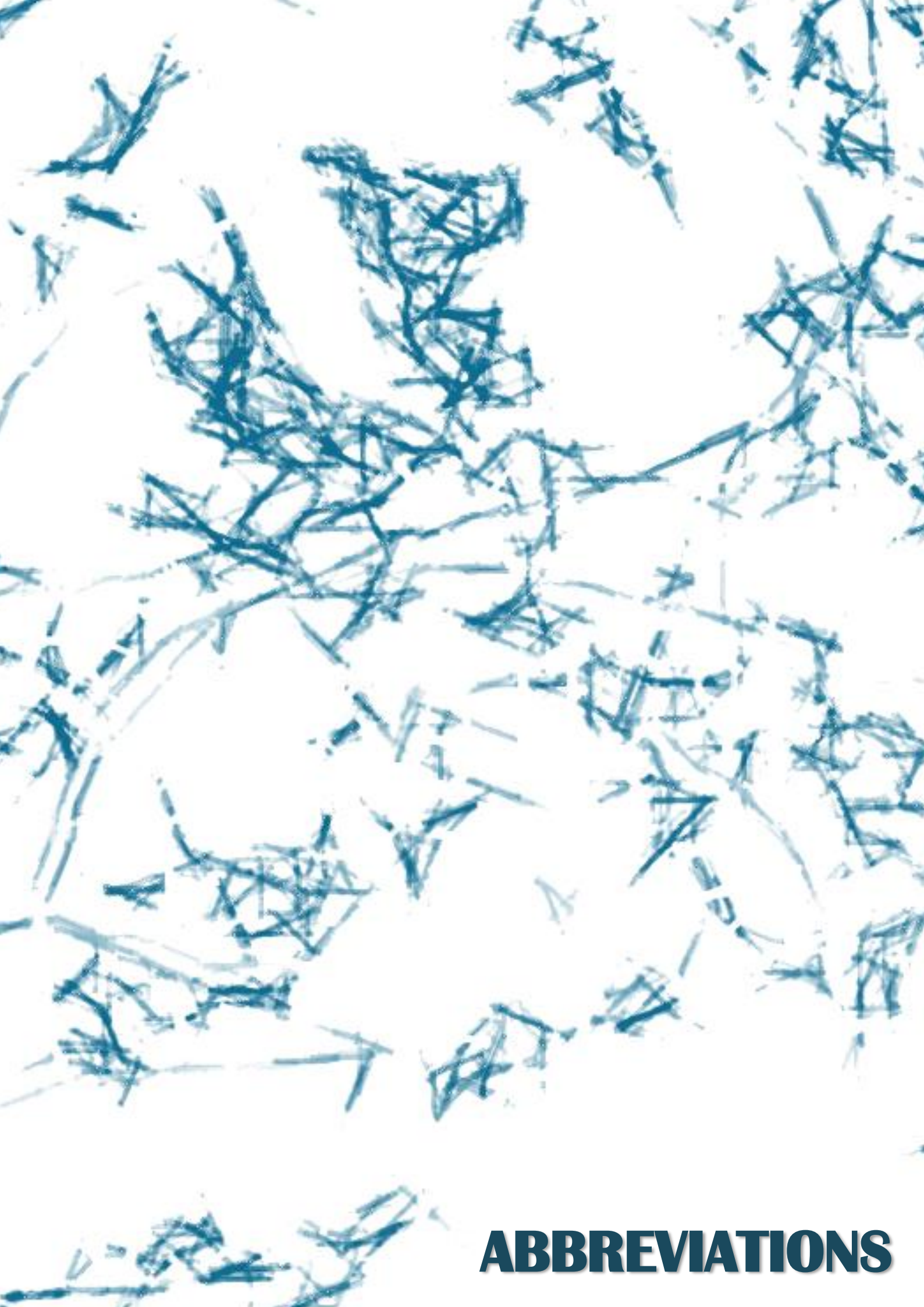

ABBREVIATIONS

Abbreviation	Full name
2DG	2-deoxy-glucose
3AC	3α-aminocholestane
4EBP1	Eukaryotic translation initiation factor 4E (eIF4E)-binding protein 1
AD	Alzheimer's disease
ATP	Adenosine triphosphate
BCG	Bacillus Calmette-Guérin
BMDM	Bone marrow-derived macrophage
cDNA	Complementary DNA
CFU	Colony-forming unit
ChIP	Chromatin immunoprecipitation
CLR	C-type lectin receptor
DAMP	Damage-associated molecular pattern
DC	Dendritic cell
Dectin-1	Dendritic cell-associated C-type lectin 1
DMEM	Dulbecco's Modified Eagle Medium
DNA	Deoxyribonucleic acid
ECAR	Extracellular acidification rate
EDTA	Ethylenediaminetetraacetic acid
EGCG	Epigallocatechin-3-gallate
ELISA	Enzyme-linked immunosorbent assay
FACS	Fluorescence-activated cell sorting
FBS	Fetal bovine serum
FcγR	Fc γ receptor
GM-CSF	Granulocyte-macrophage colony-stimulating factor
H3K27Ac	Acetylation in lysine 27 of histone H3
H3K4me1	Monomethylation in lysine 4 of histone H3
H3K4me3	Trimethylation in lysine 4 of histone H3
hemITAM	Hemi-ITAM
hPBMC	Human peripheral blood mononuclear cell
HSC	Hematopoietic stem cell
IFN-γ	Interferon γ
IL	Interleukin
INPP5	Inositol polyphosphate 5'-phosphatase
ITAM	Immunoreceptor tyrosine-based activatory motif
ITIM	Immunoreceptor tyrosine-based inhibitory motif
LPS	Lipopolysaccharide
LysM	Lysozyme M
LSK	$Lin^{-}Sca\text{-}1^{+}c\text{-}Kit^{+}$ cell
M-CSF	Macrophage colony-stimulating factor
MFI	Mean fluorescence intensity
MPP	Multipotent progenitor
miR / miRNA	Micro-ribonucleic acid
MTA	5'-deoxy-5'-(methylthio)adenosine
Mtb	*Mycobacterium tuberculosis*
mTOR	Mammalian target of rapamycin
mTORC1	Mammalian target of rapamycin complex 1
NK	Natural killer
oxLDL	Oxidized low-density lipoprotein

Abbreviation	Full name
P	Phospho
PAMP	Pathogen-associated molecular pattern
PBS	Phosphate-buffered saline
PI(3,4)P_2	Phosphatidylinositol 3,4-biphosphate
PI(3,4,5)P_3	Phosphatidylinositol 3,4,5-triphosphate
PI3K	Phosphoinositide 3-kinase
PI(4,5)P_2	Phosphatidylinositol 4,5-biphosphate
PRR	Pattern recognition receptor
PTEN	Phosphatase and tensin homolog
qPCR	Quantitative polymerase chain reaction
RBC	Red blood cell
ROS	Reactive oxygen species
RPM	Revolutions per minute
RPMI	Roswell Park Memorial Institute
RT	Room temperature
SH2	Src homology 2
SHIP	SH2 domain-containing inositol 5’-phosphatase
SHIPi	SHIP-1 inhibitor
TCA	Tricarboxylic acid
TLR	Toll-like receptor
TNFα	Tumor necrosis factor α
WB	Western blotting
WGP	Whole glucan particles
WT	Wild-type
YPD	Yeast extract-peptone-dextrose

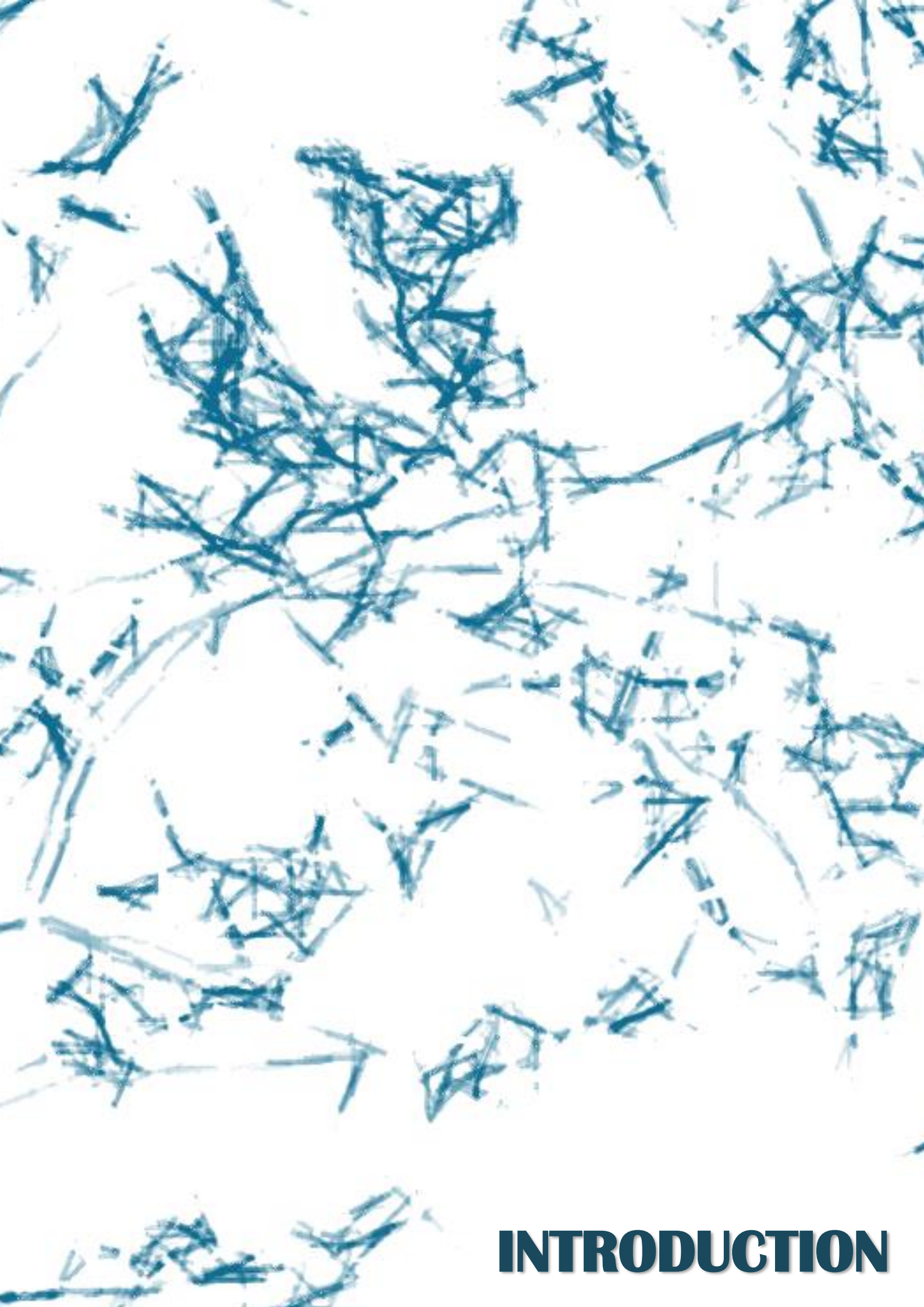

INTRODUCTION

1. Immune system and immunological memory.

1.1. Innate and adaptive immunity.

The vertebrate immune system has been classically divided into two subcomponents: the innate and the adaptive compartment (Janeway et al., 2001, Delves P.J. et al., 2017).

The innate immune system comprises different cellular components, including monocytes, macrophages, neutrophils, dendritic cells (DCs), innate lymphoid cells or natural killer (NK) cells. It emerges as the first line of immune defense, as they trigger immediate effector mechanisms, and it has been classically assumed that innate immune cells are unable to build immunological memory (Janeway et al., 2001, Delves P.J. et al., 2017). Although innate immune cells lack antigen-specific receptors, they possess a variety of surface and intracellular receptors, called pattern-recognition receptors (PRRs). PRRs trigger immune responses after sensing microbial components (pathogen-associated molecular patterns -PAMPs), but also endogenous molecules expressed or released upon tissue damage (damage-associated molecular patterns -DAMPs). Examples of PRRs are Toll-like receptors (TLRs) such as TLR4, that recognizes LPS from Gram-negative bacteria, or C-type lectin receptors (CLRs) such as Dectin-1, that senses the fungal cell wall component β-glucan (Brubaker et al., 2015).

Adaptive immunity, composed by T and B lymphocytes, requires however several days to mount an immune response that, in contrast to innate immunity, is specific for a particular antigen. In this regard, a first encounter with the pathogen enables T and B cells to induce a classical immunological memory based on the generation of specific long-term memory populations, that will allow to respond more efficiently to the same challenge in the future (Janeway et al., 2001, Delves P.J. et al., 2017).

1.2. “Memory” in innate immunity: studies from the past.

The notion that innate immunity is unable to induce immunological memory has been challenged, particularly from studies in organisms that lack adaptive immunity. Studies in plants revealed the development of systemic acquired resistance against a broad variety of pathogens, including virus, bacteria or fungi (Reimer-Michalski and Conrath, 2016, Durrant and Dong, 2004). Likewise, there are also evidences for nonspecific

pathogen-induced immunological memory in distinct species of invertebrates, which only respond to infections by innate immune mechanisms (Milutinovic and Kurtz, 2016).

Moving to vertebrates, early studies revealed that both Bacillus Calmette-Guérin (BCG), the tuberculosis vaccine, and a low-virulent strain of the fungus *Candida albicans* were able to confer protection against lethal systemic candidiasis (Bistoni et al., 1988, van 't Wout et al., 1992) or *Schistosoma mansoni* (Tribouley et al., 1978) in mice lacking adaptive immune system. These data were indicative of the generation of some sort of memory not based on adaptive immunity that interestingly, appeared to be nonspecific for the vaccination challenge. Supporting this notion, different observational and retrospective studies have reported the nonspecific effect of vaccines (Jensen et al., 1993, de Bree et al., 2018), such as the heterologous protection conferred by BCG against infections other than tuberculosis (Butkeviciute et al., 2018, Freyne et al., 2015). Early observations also evidenced the development of endotoxin tolerance, an unresponsive state of innate immune cells to respond against secondary challenges, when they had been pre-exposed to low concentrations of endotoxin (Biswas and Lopez-Collazo, 2009, Lopez-Collazo and del Fresno, 2013). Altogether, the term ‘trained immunity’ has been coined to define this innate immune memory that lead the innate immune system to an enhanced response to secondary challenges (Netea et al., 2011).

2. Trained innate immunity.

2.1. A global overview.

Trained immunity is defined as a memory of innate immune system, where an encounter with a first stimulus (e.g. microbial insult) results in a subsequent enhanced nonspecific response by innate immune cells against a secondary challenge (the same or unrelated), thus providing long-term protection in case of infection (Netea et al., 2016, Netea et al., 2011, Hamon and Quintin, 2016).

In contrast to endotoxin tolerance phenomenon, the memory-induced decreased responsiveness on innate immune cells (Biswas and Lopez-Collazo, 2009), ‘trained immunity’ term has been extensively referred to a memory-induced enhanced

responsiveness (Boraschi and Italiani, 2018), and it will be used in this way throughout this work.

2.1.1. Trained innate immune cells.

Trained immunity properties have been defined for distinct subsets of the innate immune system (Gardiner and Mills, 2016). Several studies demonstrated that NK cell memory can be developed after a previous challenge (Holmes and Bryceson, 2016) with, for instance, cytomegalovirus (Sun et al., 2009) or BCG (Kleinnijenhuis et al., 2014b). Myeloid cells, particularly monocytes and macrophages, have also shown trained immunity properties upon priming with a wide variety of insults (Rusek et al., 2018, Bekkering et al., 2016a). Importantly, trained immunity is independent of adaptive immunity, as demonstrated by the conferred heterologous protection in studies performed on immunodeficient mice lacking B and T cells (Quintin et al., 2012, Kleinnijenhuis et al., 2012, Kleinnijenhuis et al., 2014a, Bistoni et al., 1988).

2.1.2. Training inducers.

A wide variety of stimuli can train innate immune cells, particularly monocytes and macrophages (Leentjens et al., 2018). Among infectious agents, we could enumerate complete microorganisms such as BCG (Kleinnijenhuis et al., 2012) or *C. albicans* (Quintin et al., 2012), or microbial components such as muramyl dipeptide (Ifrim et al., 2014) or the fungal cell wall component β-glucan (Quintin et al., 2012). Not only infectious but also endogenous inducers and metabolites such as oxidized low-density lipoprotein (oxLDL) (Bekkering et al., 2014), uric acid (Crisan et al., 2016a), bovine milk (van Splunter et al., 2018) or mevalonate (Bekkering et al., 2018) can induce trained immunity.

2.1.3. Trained immunity hallmarks.

Trained immunity is characterized by three key hallmarks: increased cytokine production upon rechallenge, changes in the metabolism and epigenetic reprogramming (Netea et al., 2015b, Netea et al., 2015a).

Among those cytokines whose production is augmented after rechallenge in trained cells, we could find proinflammatory tumor necrosis factor α (TNFα), interleukin (IL)-6 and IL-1β (Ifrim et al., 2014, Quintin et al., 2012, Bekkering et al., 2016a, Walachowski et al., 2017). Interferon γ (IFN-γ) has also shown to be modulated, mainly by trained NK cells (Kleinnijenhuis et al., 2014b) (Ifrim et al., 2015). Modulation of IL-

10 varied between studies (Quintin et al., 2012, Ifrim et al., 2013, Bekkering et al., 2016a, Schrum et al., 2018).

A noted shift from oxidative phosphorylation to aerobic glycolysis (Warburg effect) (Liberti and Locasale, 2016), likely due to a faster need of adenosine triphosphate (ATP) production (Liberti and Locasale, 2016), is the main change in cellular metabolism during the induction of β-glucan- (Cheng et al., 2014) or BCG-mediated trained immunity (Arts et al., 2016b). Moreover, glutaminolysis and cholesterol synthesis are non-redundant pathways required for trained immunity to take place (Arts et al., 2016a). Finally, the tricarboxylic acid (TCA) cycle intermediates fumarate (Arts et al., 2016a) or acetyl coenzyme A (Netea et al., 2016) are known to affect histone-modifying enzymes involved in epigenetic reprogramming, the third hallmark of this phenomenon.

Epigenetic reprogramming, mainly mediated by histone modifications, involves chromatin reorganization and is one of the basis for the long-lasting effect of trained immunity (Christ et al., 2016, Netea et al., 2016, van der Heijden et al., 2018, Dominguez-Andres et al., 2018). Genome-wide analyses have revealed the presence of three histone methylation marks, positively associated with gene expression: trimethylation in lysine 4 of histone H3 (H3K4me3) in active promoters, monomethylation in that residue (H3K4me1) that marks enhancers, and acetylation in lysine 27 of histone H3 (H3K27Ac) in both elements (Christ et al., 2016, Netea et al., 2016). Consistent with the presence of these marks, trained immunity induction was prevented in the presence of both histone methylation and acetylation inhibitors (Quintin et al., 2012, Cheng et al., 2014, Ifrim et al., 2014). As a result, epigenetic modifications have been found at the level of important promoters for the training process (Saeed et al., 2014, Kleinnijenhuis et al., 2012), which makes chromatin more accessible and conditions gene expression patterns of trained cells upon stimulation with a secondary challenge.

In addition, recent studies have shown that modulation of bone marrow progenitors is also an integral component of trained immunity (Mitroulis et al., 2018, Kaufmann et al., 2018, Christ et al., 2018, Luo et al., 2015). This supports the long-lasting effect of trained immunity (months and even years) (Kleinnijenhuis et al., 2014a) that is probably hard to attribute only to effects on terminally differentiated mature cells (Netea et al., 2016). Thus, β-glucan (Mitroulis et al., 2018), BCG (Kaufmann et al.,

2018) and even cholesterol-containing western diet (Christ et al., 2018, Luo et al., 2015) were able to reprogram and induce expansion of hematopoietic progenitors such as $Lin^{-}Sca\text{-}1^{+}c\text{-}Kit^{+}$ cells (LSKs) and hematopoietic stem cells (HSCs), with a particular bias to the myeloid lineage. Thus, bone marrow-derived macrophages (BMDMs) generated from previously trained mice were also trained and showed improved clearance of *Mycobacterium tuberculosis* (*Mtb*) infection (Kaufmann et al., 2018).

2.2. *Candida albicans*- and β-glucan-induced training.

2.2.1. Systemic *Candida albicans* infection.

Candida albicans is a dimorphic yeast and an opportunistic fungal pathogen that produces mucosal infections but also invasive candidiasis (Lionakis and Netea, 2013, Poulain, 2015), a systemic infection where kidney is the main target organ (Lionakis et al., 2011). Systemic candidiasis is the fourth leading cause of nosocomial bloodstream infection in the United States and mortality exceeds 40% (Lionakis and Netea, 2013).

Regarding host immune response, innate PRRs recognize various PAMPs of *Candida*. β-glucan is a polysaccharide that constitutes the main cell wall component of certain bacteria and fungi (El Khoury et al., 2012), including *C. albicans* (Poulain and Jouault, 2004). Importantly, Dectin-1 is required for β-glucan recognition (Brown and Gordon, 2001) and control of fungal infections (Taylor et al., 2007). Furthermore, TLR2 and TLR4 sense mannans whereas TLR9 within the cytosol recognizes fungal deoxyribonucleic acid (DNA); mannose receptor recognizes mannose-rich *Candida* structures (Lionakis and Netea, 2013).

Upon a primary systemic infection, monocytes/macrophages are key phagocytic cells for protection against invasive candidiasis (Ngo et al., 2014, Qian et al., 1994, Dominguez-Andres et al., 2017), but it is also proposed that other immune cell types, including DCs (Whitney et al., 2014) or NK cells (Bar et al., 2014) may play a role. Notably, protection against systemic candidiasis is adaptive immunity-independent as shown by mice lacking both B and T cells (Jensen et al., 1993, Bar et al., 2014). Eventually, neutrophils are essential as final effectors for host defense against systemic *C. albicans* infection (Dejima et al., 2011).

2.2.2. *Candida*-induced protection against secondary infections.

Exposure to a low-virulent strain (PCA-2) or to a low dose of virulent (SC5314) *C. albicans*, as well as to β-glucan, protect mice from secondary lethal systemic

candidiasis (Bistoni et al., 1986, Quintin et al., 2012, Bistoni et al., 1988) or heterologous *Staphylococcus aureus* septicaemia (Di Luzio and Williams, 1978, Bistoni et al., 1986, Cheng et al., 2014, Marakalala et al., 2013). This acquired resistance does not rely on T, B or NK cells (Bistoni et al., 1986, Quintin et al., 2012, Bistoni et al., 1988), based on studies with mice lacking the adaptive immune system or treated with NK cell-depleting anti-asialo ganglioside-monosialic acid antibody, respectively. Nevertheless, this protection occurs in a myeloid-dependent manner, as protection was prevented by affecting macrophage function or monocyte recruitment (Bistoni et al., 1986, Quintin et al., 2012, Cheng et al., 2014, Bistoni et al., 1988). Moreover, mice pre-injected with both *Candida* and β-glucan, produce increased levels of TNFα, IL-6, IL-1β or IL-10 in serum when they are treated with LPS a week after, with variations in the cytokines depending on the model used (Quintin et al., 2012, Garcia-Valtanen et al., 2017, Arts et al., 2016a).

2.2.3. Molecular mechanisms involved in trained immunity development.

To define molecular mechanisms at the intracellular level, several trained immunity *in vitro* models have been developed. *In vitro* sensing of β-glucan or heat-killed *C. albicans* induces trained immunity in human monocytes (Cheng et al., 2014), hPBMCs (Ifrim et al., 2013, Quintin et al., 2012), purified murine splenic monocytes (Garcia-Valtanen et al., 2017), peritoneal macrophages or BMDMs (Walachowski et al., 2017). These models are usually characterized by 24 hours of stimulation with the training inducer followed by a resting period without stimulus, and a final secondary challenge with the same or unrelated insult (Quintin et al., 2012, Ifrim et al., 2014). Of note, the resting period is a critical step, as it tries to reflect *in vitro* the long-lasting effect of trained immunity. While some studies in hPBMCs and monocytes followed a 6- or 7-day resting period (Quintin et al., 2012, Ifrim et al., 2014), other studies (Ifrim et al., 2013), especially in BMDMs (Walachowski et al., 2017), shortened or abolished this step. As a prototypical model, monocytes or macrophages can be primed with β-glucan, washed, rested and secondarily rechallenged with LPS (Walachowski et al., 2017, Cheng et al., 2014). As final outcome, although TNFα has become the most prototypical readout, increase in IL-6 and IL-1β production have been also demonstrated upon secondary challenge (Quintin et al., 2012, Ifrim et al., 2014, Bekkering et al., 2016a, Walachowski et al., 2017). Changes in IL-10 are more controversial, as some studies showed no effect upon training (Quintin et al., 2012),

whereas other also appreciated an increase (Bekkering et al., 2016a, Garcia-Valtanen et al., 2017). Finally, although not consistently evaluated, some reports also showed a β-glucan-dependent increase in viability, which could also support a final effect on enhanced immune response (Bekkering et al., 2016a, Garcia-Valtanen et al., 2017).

Training of monocytes requires sensing of β-glucan by Dectin-1 receptor **(Figure I1)**, as inhibition of the receptor with laminarin abolished training induction, as well as Dectin-1-deficient individuals failed to mount the trained response (Quintin et al., 2012). This Dectin-1-mediated training mostly relies on the activation of the PI3K/mTOR pathway **(Figure I1)** (Cheng et al., 2014). Consistently, β-glucan stimulation induced phosphorylation of Akt, a downstream target of PI3K, mTOR and mTOR targets. Moreover, both the PI3K inhibitor wortmannin and the mTOR inhibitor rapamycin prevented induction of training (Cheng et al., 2014, Arts et al., 2016a).

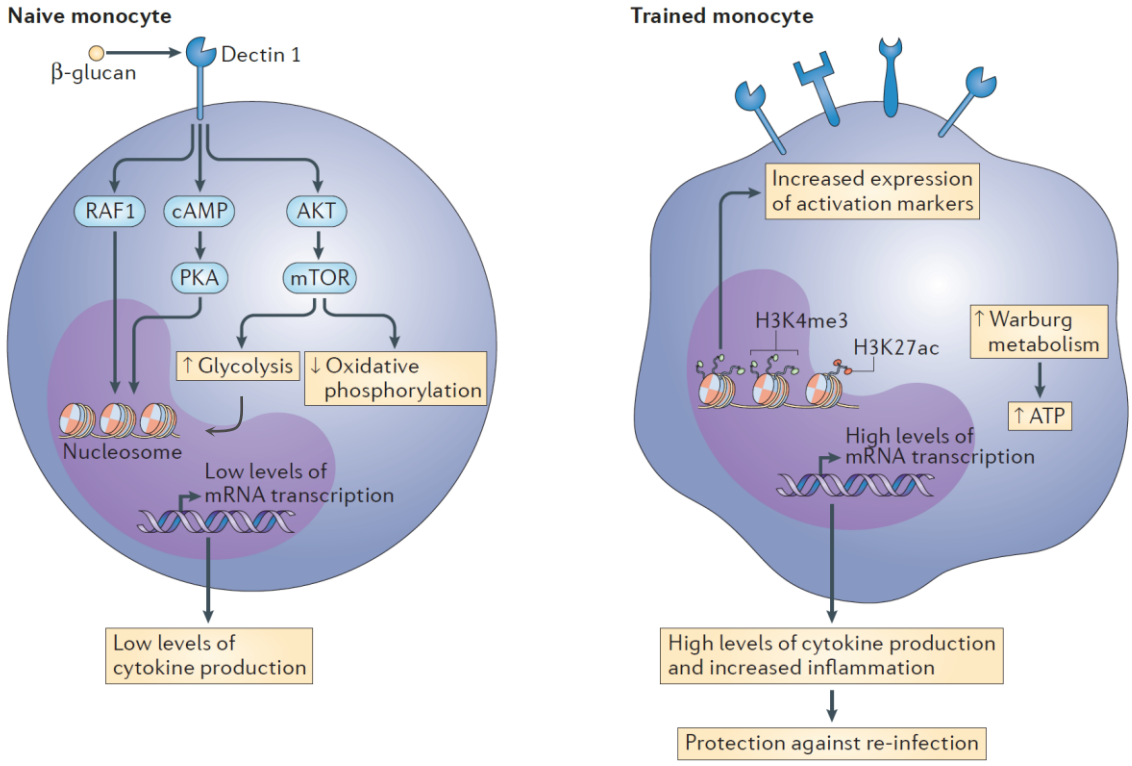

Figure I1. Integration of signaling and metabolic pathways in β-glucan-trained monocytes. (Adapted from (Netea et al., 2015a)). Recognition of β-glucan by Dectin-1 induces activation of Akt/mTOR pathway, among others, and metabolic rewiring, leading to epigenetic reprogramming of naïve monocytes. As a result, the β-glucan-trained cells shift towards glycolytic metabolism (a process known as Warburg effect), and display persistent epigenetic modifications, resulting in a stronger inflammatory phenotype upon rechallenge.

At the metabolic level, switch to glycolysis is the main signature of β-glucan trained monocytes **(Figure I1)**. Indeed, the transcriptome of these cells revealed an induced expression of genes involved in the glycolytic pathway (Cheng et al., 2014). Furthermore, β-glucan trained monocytes showed a reduced oxygen consumption, increased glucose uptake and elevated lactate production on day 7 post-training (Cheng et al., 2014, Arts et al., 2016a). In addition, glutamine and cholesterol metabolism, and the TCA cycle, but not the pentose phosphate pathway, are also important metabolic pathways in β-glucan-induced trained immunity (Arts et al., 2016a, Dominguez-Andres et al., 2018).

β-glucan training of monocytes/macrophages results in a global increase in histone H3 activating marks, mainly methylation and acetylation **(Figure I1)**, revealed by genome-wide chromatin immunoprecipitation (ChIP)-seq assays (Quintin et al., 2012, Saeed et al., 2014). Thus, H3K4me3 and H3K27Ac accumulation was found at promoters of important trained immunity-associated genes, including *TNFα, IL-6, DECTIN-1* or mTOR pathway genes (Quintin et al., 2012, Cheng et al., 2014). Consistently, immune training with *C. albicans* or β-glucan was prevented in the presence of the histone methyltransferase inhibitor 5′-deoxy-5′-(methylthio)adenosine (MTA) but not when pre-treating with the histone demethylase inhibitor pargyline, used as a control (Quintin et al., 2012, Cheng et al., 2014, Ifrim et al., 2014). Likewise, supporting also the importance of acetylation, pre-incubation with the histone acetyltransferase inhibitor epigallocatechin-3-gallate (EGCG) before β-glucan stimulation also abolished trained immunity induction (Ifrim et al., 2014). Resveratrol, by activating the deacetylase sirtuin-1 had an identical effect (Cheng et al., 2014). Consistent with the divergent response observed during endotoxin tolerance phenomenon, the epigenetic program triggered in β-glucan trained macrophages differed from the one found in LPS-tolerant macrophages (Saeed et al., 2014, Foster et al., 2007, Hoeksema and de Winther, 2016). Moreover, the tolerant state could be reverted when stimulating those cells with β-glucan (Novakovic et al., 2016).

3. SHIP-1 phosphatase.

3.1. Regulation of PI3K/Akt pathway by inositol phosphatases.

The class I PI3Ks are a large family of enzymes that are able to phosphorylate the phosphatidylinositol 4,5-biphosphate ($PI(4,5)P_2$) to generate phosphatidylinositol

(3,4,5)-triphosphate (PI(3,4,5)P_3) on the inner layer of the plasma membrane. Upon PI3K activation, the protein kinase Akt is recruited to the membrane, where it gets activated by different mechanisms (Eramo and Mitchell, 2016) **(Figure I2)**. This Akt activation allows further activation of mTOR complex 1 (mTORC1) and subsequent mTOR targets such as eukaryotic translation initiation factor 4E (eIF4E)-binding protein 1 (4EBP1) or ribosomal protein S6 (Dibble and Cantley, 2015). In this way, PI3K/Akt signaling has shown to regulate a plethora of processes including cell growth, proliferation, survival, autophagy, cell cycle progression, glucose uptake and metabolism (Eramo and Mitchell, 2016, Martini et al., 2014).

PI3K activity is tightly counterbalanced by inositol 5'-phosphatases. PI(3,4,5)P_3, product of PI3K, is dephosphorylated to yield phosphatidylinositol 3,4-biphosphate (PI(3,4)P_2) by SHIP-1, its homolog SHIP-2, the inositol polyphosphate 5'-phosphatase (INPP5) E, the skeletal muscle- and kidney-enriched inositol phosphatase or the proline-rich inositol polyphosphate 5'-phosphatase. On the other hand, the phosphatase and tensin homolog (PTEN) also antagonizes PI3K activity by dephosphorylating PI(3,4,5)P_3 in position 3, giving rise to PI(4,5)P_2 **(Figure I2)** (Eramo and Mitchell, 2016, Billcliff and Lowe, 2014, Erneux et al., 2016).

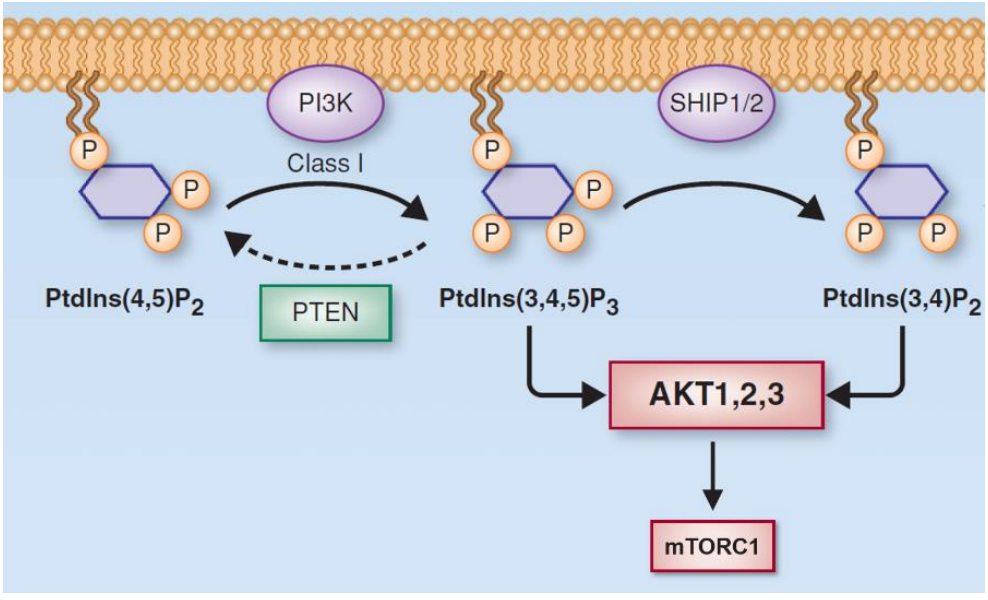

Figure I2. Regulation of PI3K pathway by inositol phosphatases. (Adapted from (Vo and Fruman, 2015)). PI(4,5)P_2 is phosphorylated by class I PI3Ks to transiently generate PI(3,4,5)P_3. PI(3,4,5)P_3 is dephosphorylated by PTEN and SHIP to yield PI(4,5)P_2 or PI(3,4)P_2, respectively. Akt is recruited to the membrane to be activated via binding PI(3,4,5)P_3, and PI(3,4)P_2 in some contexts. Akt, once activated, regulates a plethora of downstream pathways via mTORC1 phosphorylation.

3.2. SHIP-1 expression and regulation.

Among inositol 5'-phosphatases, SHIP-1 phosphatase is encoded by the *INPP5D* gene and is predominantly expressed in the hematopoietic compartment, including HSCs, T, B and NK cells and the myeloid compartment, but also in osteoblasts (Kerr, 2011, Hazen et al., 2009). Although sharing 38% sequence homology, the expression pattern and function clearly differ from its homolog SHIP-2, as the latter is ubiquitously expressed (Rohrschneider et al., 2000). Finally, SHIP-1 expression can be regulated by proteasomal degradation (Ruschmann et al., 2010) or by micro-ribonucleic acid (miRNA or miR)-mediated degradation of transcripts, in particular by miR-155 (O'Connell et al., 2010).

Apart from the expression pattern, a second determinant of SHIP-1 signaling is its cell location, as recruitment to the plasma membrane is crucial for SHIP-1 to have access to its substrate PI(3,4,5)P_3 (Pauls and Marshall, 2017). SHIP-1 recruitment to the plasma membrane can occur in association with adaptor proteins, scaffold proteins or by direct association with intracellular receptor chains via its SH2 domain. Direct binding can involve interaction with immunoreceptor tyrosine-based inhibitory motif (ITIM)-containing receptors such as Fc γ receptor (FcγR) IIB (Ono et al., 1996) or Ly49 receptor in NK cells (Wang et al., 2002). SHIP-1 binds not only to inhibitory, but also to immunoreceptor tyrosine-based activation motifs (ITAM) such as the present in the B cell receptor (Pauls and Marshall, 2017, Manno et al., 2016) or hemi-ITAMs (hemITAM)-containing activatory receptors such as Dectin-1 (Blanco-Menendez et al., 2015). In summary, SHIP-1 phosphatase has shown to interact with cytokine, growth factor but also with immune receptors, thus emerging as an intrinsic brake of immune cell signaling (Pauls and Marshall, 2017).

3.3. SHIP-1 biology and cellular function.

Considering its role in dampening receptor signaling, SHIP-1 affects different functions of a wide variety of cell subsets (Pauls and Marshall, 2017, Kerr, 2011). The phosphatase plays a role in maintaining the niche that supports HSC quiescence in the hematopoietic compartment (Hazen et al., 2009). Regarding adaptive immune system, SHIP-1 controls B cell development and function (Brauweiler et al., 2000).T cell priming and effector functions are also affected, as SHIP-1-deficient mice showed both increased regulatory T cells (Collazo et al., 2009, Collazo et al., 2012) and enhanced type 1 versus type 2 helper T cell ratio (Tarasenko et al., 2007). Moreover,

SHIP-1 regulates survival, homeostasis, repertoire diversity and IFN-γ production in NK cells (Gumbleton et al., 2017, Gumbleton et al., 2015, Trotta et al., 2005). In addition, SHIP-1 is also needed for DCs to efficiently prime T cells (Neill et al., 2007, Antignano et al., 2010a, Gold et al., 2015, Gold et al., 2016).

Importantly, SHIP-1 plays a prominent role in myeloid biology and has shown to impact diverse macrophage effector functions (Kerr, 2011, Conde et al., 2011). On one hand, it is widely accepted that SHIP-1 negatively regulates multiple types of phagocytosis, including those mediated by FcγRs or complement receptor 3 (Cox et al., 2001, Tamura et al., 2009, Yao et al., 2017). However, while some studies have claimed that SHIP-1-deficient macrophages or granulocyte-macrophage colony-stimulating factor (GM-CSF) bone-marrow-derived cells produced elevated levels of reactive oxygen species (ROS) (Ganesan et al., 2006, Blanco-Menendez et al., 2015, Wang et al., 2014), other showed that SHIP-1 enhanced this production (Kamen et al., 2008). Regarding inflammatory cytokines, the role of SHIP-1 is also controversial. While some studies claimed that SHIP-1 contributed to cytokine production in macrophages (Hadidi et al., 2012), including LPS- and FcγR-induced proinflammatory cytokines (An et al., 2005, Ganesan et al., 2006), other authors conversely showed lower production in SHIP-1-deficient BMDMs (Fang et al., 2004). Although not formally addressed, these divergences could rely on differential regulation of TLR signaling by PI3K/Akt pathway depending on the context (Pourrajab et al., 2015, Troutman et al., 2012). Finally, a critical role is attributed to SHIP-1 in endotoxin tolerance, as SHIP-1-deficient BMDMs were hyperresponsive to LPS and they did not develop endotoxin tolerance (Sly et al., 2004).

As result of the negative regulatory role of SHIP-1 in such a variety of cells and functions, SHIP-1-deficient mice display many inflammatory disorders including splenomegaly, hematopoietic abnormalities, autoantibody-mediated autoimmunity, allergic airway inflammation, consolidating pneumonia and Crohn's disease-like ileitis (Helgason et al., 1998, Kerr et al., 2011, Maxwell et al., 2011, Oh et al., 2007). Lung and gut pathologies of these germline SHIP-1 knockout mice are characterized by abundant myeloid infiltration (Helgason et al., 1998, Kerr et al., 2011). Interestingly, specific deletion in either B cells, T cells, or DCs alone did not result in spontaneous allergic airway inflammation (Gold et al., 2015), although SHIP-1 absence in B cells led to an autoantibody-mediated disease (O'Neill et al., 2011). Remarkably, the

combined deletion of SHIP-1 in T and myeloid cells led also to mucosal inflammatory disease (Park et al., 2014), although the specific deletion of SHIP-1 only in the myeloid compartment did not recapitulate any of these inflammatory symptoms (Maxwell et al., 2014).

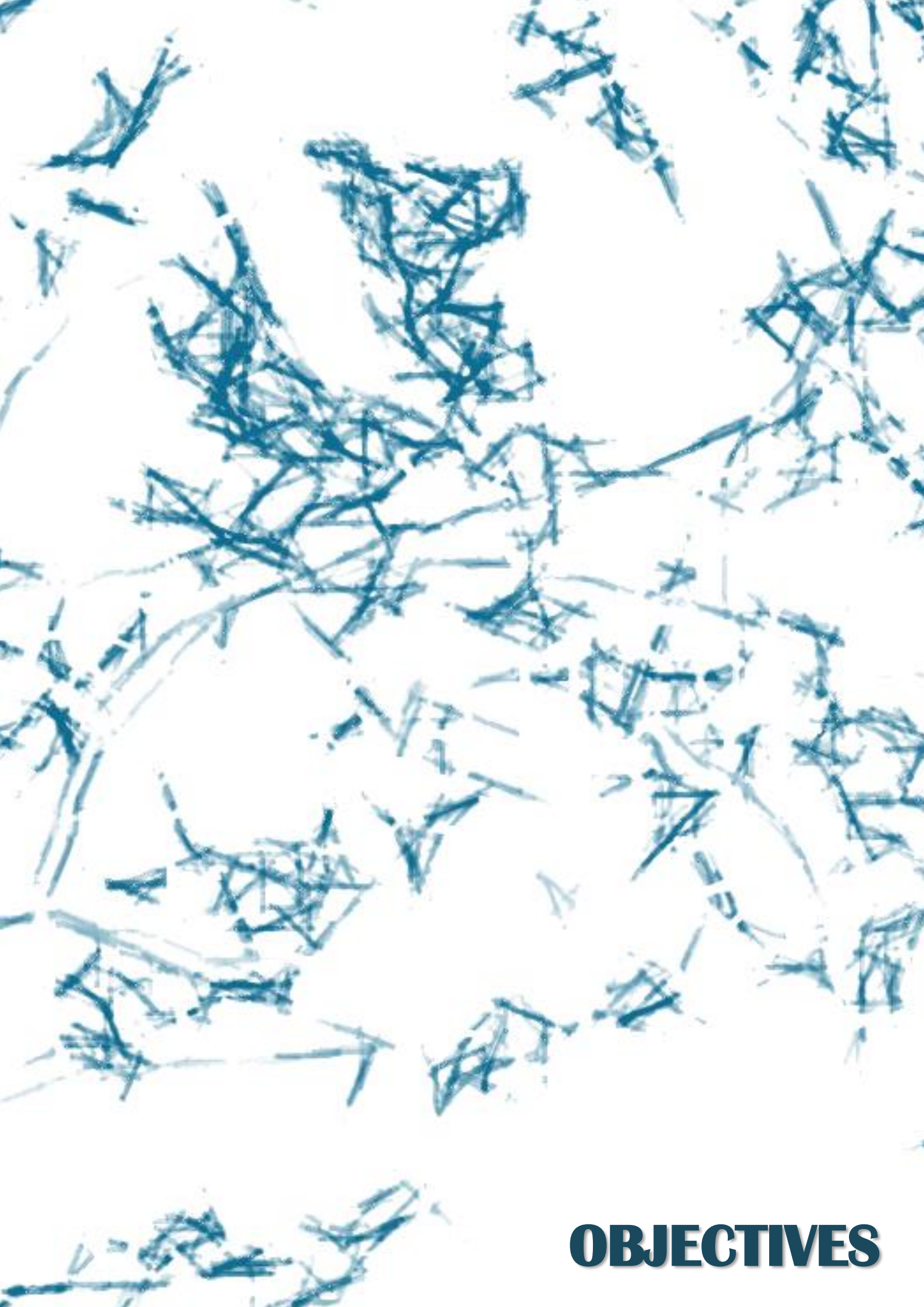

OBJECTIVES

Taking into consideration first that trained immunity induced by *C. albicans* and β-glucan in myeloid cells relies on Dectin-1 receptor and PI3K-dependent mechanisms, and second, that SHIP-1 phosphatase counterbalances PI3K function and is able to associate to Dectin-1, the general aim of this work was to evaluate whether SHIP-1 targeting in myeloid cells could modulate β-glucan- and/or *C. albicans*-mediated immune training. For this purpose, the specific objectives of this thesis were:

1. Evaluate the phenotype of trained SHIP-1-deficient macrophages *in vitro*, analyzing hallmarks of trained immunity.

2. Address the effect of the specific deletion of SHIP-1 in the myeloid compartment in trained immunity properties *in vivo* and resistance to secondary infection in mice.

3. Explore the chemical inhibition of SHIP-1 as a potential tool to modulate trained immunity.

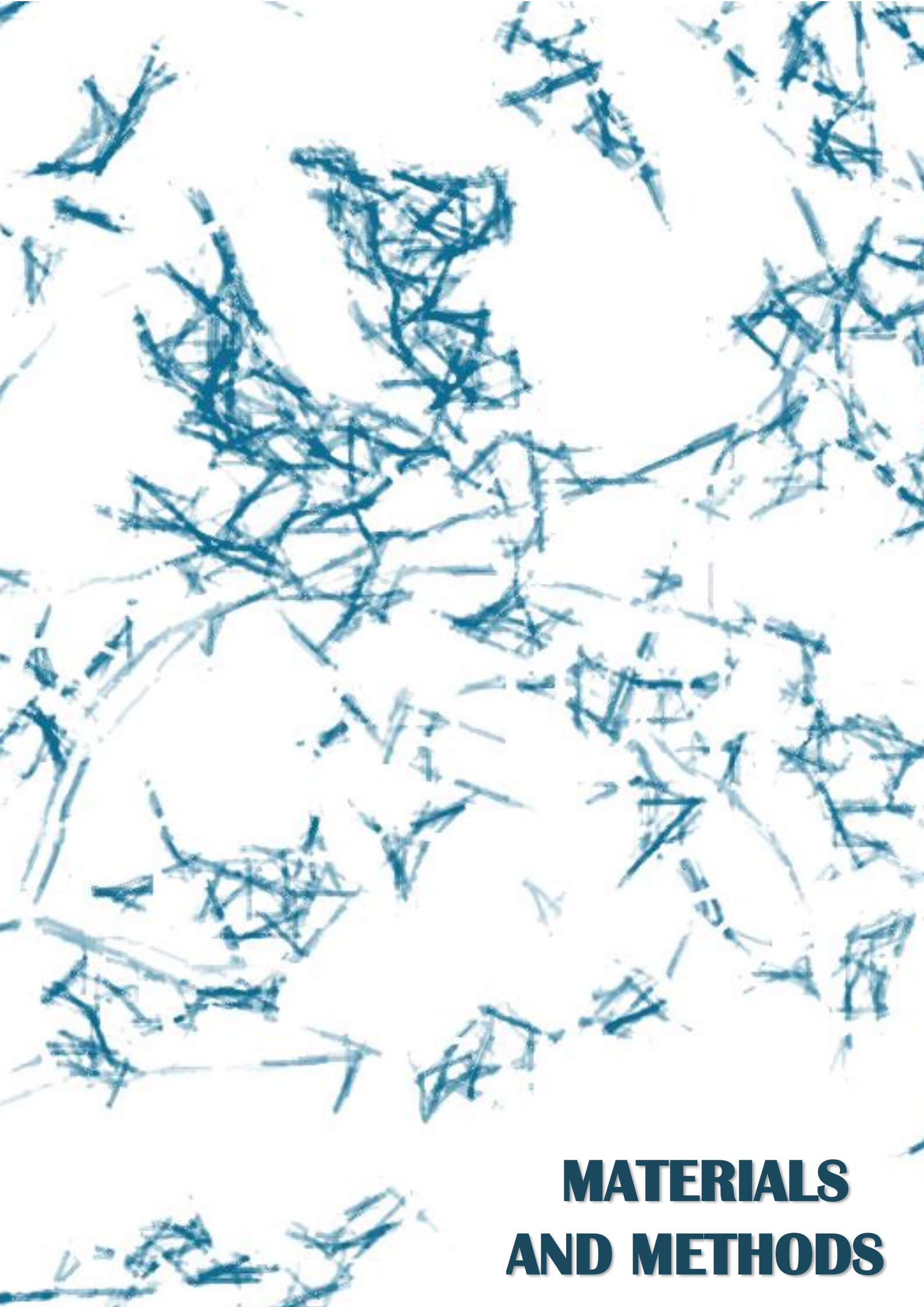

MATERIALS AND METHODS

1. *Candida albicans*.

The clinical isolate *Candida albicans* SC5314 (Pitarch et al., 2016) was kindly provided by Professor Concha Gil (Complutense University, Madrid, Spain). The fungus was regularly refreshed and was grown on yeast extract-peptone-dextrose (YPD)-agar plates (Sigma) at 30ºC for 48h, in order to maintain the degree of virulence.

2. Mouse strains and cells.

Mice, all in C57BL/6 background, were bred at CNIC under specific pathogen-free conditions. Mouse colonies included Wild-type C57BL/6J (WT used for SHIP-1 inhibition experiments), and conditional knockout mice under the control of the myeloid-specific promoter Lysozyme M (LysM): $LysM^{+/+}SHIP\text{-}1^{flox/flox}$ (WT) and $LysM^{Cre/+}SHIP\text{-}1^{flox/flox}$ (LysMΔSHIP-1) (Collazo et al., 2012), which were kept as littermates. Experiments were conducted with 8- to 12-weeks-old age-matched mice (regardless gender). All animal procedures were reviewed and approved by Animal Ethics Committee at the CNIC, Madrid Autonomous University Ethics Committee, and the Community of Madrid authority. All animal procedures were compliant with the EU Directive 2010/63/EU and Recommendation 2007/526/EC regarding the protection of animals used for experimental and other scientific purposes, enforced by the Spanish law under Real Decreto 1201/2005. Mice were allocated randomly in the different experimental procedures.

Mouse bone marrow-derived macrophage differentiation. To obtain BMDMs, both tibiae and femurs were collected, flushed with phosphate-buffered saline (PBS, Gibco) and spun down at 1650 revolutions per minute (rpm) for 5 minutes at 4º C. Cells were lysed using red blood cell (RBC) Lysis Buffer (Sigma) for 3 minutes at room temperature (RT) and filtered through 70 µm cell strainers (BD Biosciences). Cell suspensions were resuspended in Roswell Park Memorial Institute (RPMI) 1640 medium (Sigma) supplemented with 10% heat-inactivated fetal bovine serum (FBS, Sigma), 1 mM pyruvate (Lonza), 100 µM non-essential aminoacids (Thermo Fisher Scientific), 2 mM L-glutamine, 100 U/ml penicillin, 100 µg/ml streptomycin (all three from Lonza) and 50 µM 2-mercaptoethanol (Merck), herein called R10; and plated in non-treated cell culture plates (100 x 15 mm, Corning) at 37ºC for 5 days, in a ratio of 20 plates per mouse. This medium was supplemented with macrophage colony

stimulating factor (M-CSF) from 30% mycoplasma-free L929 cell supernatant. To that end, L929 cell line (ATCC® CCL-1™) was grown in R10 on 175 cm^2 cell culture flasks (Stemcell) and supernatants were obtained by filtering 15-days long cultures over 0.22 µm Stericup Filter unit (Merck Millipore). At day 5, BMDMs were washed with PBS, detached in PBS supplemented with 5 mM ethylenediaminetetraacetic acid (EDTA, Life Technologies, and resulting buffer was called PBS/EDTA), counted by CASY® cell counter (Innovatis AG), plated in R10 on treated or non-treated cell culture plates depending on the assay at the required concentration and rested overnight before any stimulation.

3. Human peripheral blood mononuclear cells.

Buffy coats from healthy volunteers were obtained from Andalusian Biobank after approval by the local Instituto de Salud Carlos III (ISCIII) Research Ethics Committee (PI 36_2017).

hPBMCs were isolated from those buffy coats by differential centrifugation on Biocoll Separating Solution (Cultek) at 700g for 30 minutes following the manufacturers' instructions. hPBMCs-containing ring was washed twice in PBS and spun down at 1650 rpm for 5 minutes. Pellet was resuspended in Dulbecco's Modified Eagle Medium (DMEM, Sigma) supplemented with 10% heat-inactivated FBS, 100 µM non-essential aminoacids, 2 mM L-glutamine, 100 U/ml penicillin, 100 µg/ml streptomycin and 50 µM 2-mercaptoethanol, herein called D10, counted by CASY® cell counter, plated and rested 2 hours before stimulation.

4. Trained immunity *in vitro* models.

BMDMs. BMDMs (10^5) were plated in 96-well cell-culture treated plates (200-µl final volume, Corning) and stimulated with R10 or 100 µg/ml β-glucan (whole glucan particles, WGP) for 24h. Then, cells were washed and rested 3 days in culture medium (R10). At day 4, unless indicated, BMDMs were washed again and primed with 25 ng/ml IFN-γ (BD Biosciences) for 24h. On day 5, a final wash was performed, and cells were stimulated with R10 or 1 µg/ml *Escherichia coli* LPS (EK, Invivogen). To analyze IL-1β production, following 4 hours of LPS challenge, cells were further stimulated for 2 hours with 5 mM ATP (Sigma), needed for inflammasome activation and pro-IL-1β processing (Schroder and Tschopp, 2010), and supernatants were harvested for

enzyme-linked immunosorbent assay (ELISA). For TNFα and IL-6, supernatants were collected after 24h of LPS stimulation.

When required, BMDMs were pre-incubated for 30 minutes prior to β-glucan stimulation with 500 µM 5′-deoxy-5′-(methylthio)adenosine (MTA, Sigma), 6 µM Pargyline (Sigma), 50 µM Resveratrol (Sigma), 50 µM epigallocatechin-3-gallate (EGCG, Sigma) or SHIP-1 inhibitor (SHIPi, 3α-aminocholestane, 3AC, Calbiochem) at the indicated doses. Inhibitors were also added after the first wash-out, before the resting period.

To assess receptor expression and cell viability, $6 \cdot 10^5$ BMDMs were plated in non-treated 24-well plates in order to facilitate their detaching for further fluorescence-activated cell sorting (FACS) (1200-µl final volume, Corning) and followed the training scheme described above. Dectin-1 expression was evaluated at day 0 prior to β-glucan addition. Cell viability and TLR4 expression were assessed on day 5 before LPS stimulation. At indicated times, cells were collected in PBS/EDTA and stained on ice-cold FACS Buffer (PBS/EDTA plus 3% FBS) for flow cytometry analysis.

For western blotting (WB) assays, $3 \cdot 10^6$ BMDMs were plated in non-treated 6-well plates (3-ml final volume, Corning) and stimulated with R10 or 200 µg/ml β-glucan for given times. This increased concentration of β-glucan was used to maintain the mass:cell ratio used for 96-well plates.

To address metabolic status, $3 \cdot 10^6$ BMDMs were plated in non-treated 6-well plates (3-ml final volume, Corning) and followed the training scheme described above but training with 200 µg/ml β-glucan (to keep mass:cell ratio). At day 4, without IFN-γ priming, cells were detached in PBS/EDTA, plated at 10^5 cells/well in 96-well Seahorse cell culture plates (200-µl final volume, Agilent Technologies) in sixtuplicates and rested overnight in R10 prior to the Seahorse XF glycolysis stress test (Agilent Technologies). When glycolytic metabolism was evaluated just after overnight stimulation with β-glucan, BMDMs (10^5) were directly plated in 96-well Seahorse cell culture plates (200-µl final volume, Agilent Technologies) and stimulated with R10 or 100 µg/ml β-glucan the day after.

hPBMCs. Total hPBMCs ($5 \cdot 10^5$) were plated in cell culture treated 96-well plates (200-µl final volume) and stimulated with 100 µg/ml β-glucan for 24h. Then, cells were washed and rested 6 days in culture medium (R10). At day 7, PBMCs were stimulated

with 1 µg/ml LPS (EK). When required, hPBMCs were pre-incubated for 30 minutes prior to β-glucan stimulation with 10 µM 3AC. Inhibitor was also added after the first wash-out, before the resting period. To assess cell viability, $3 \cdot 10^6$ total hPBMCs were plated in non-treated 24-well plates (1200-µl final volume, Corning) and followed the training scheme described here. At day 7, prior to LPS stimulation, cells were collected in PBS/EDTA and stained on ice-cold FACS Buffer for flow cytometry analysis.

For normalization of cytokine production to the number of cells recovered, the fold cell number in each condition was calculated as follows: (live cell number/live non-trained WT cell number in average). In case of SHIP-1 inhibition experiments, 3AC non-treated cells were used as reference. Thus, cytokine production was normalized per cell number as (absolute cytokine value/fold cell number described above) in each condition.

5. *In vivo* models.

Mice were trained with either two intraperitoneal injections of 1 mg β-glucan particles on days −7 and −4 or $2 \cdot 10^4$ *Candida albicans* intravenously on day -7. Sterile PBS was used as control. When required, mice were intraperitoneally treated with 0.11 mg 3AC on days -8 and -7. 3AC was diluted in PBS 0.3% hydroxypropylcellulose (Sigma), with buffer alone used as control. As a reference, the secondary challenge (described next) was considered as day 0.

One week later, mice were challenged intraperitoneally with PBS or 5 µg *E. coli* LPS (serotype O55:B5, Sigma) and blood was collected 60 minutes later to assess serum TNFα or 90 minutes later to evaluate serum IL-1β and IL-6. Serum was obtained by high-speed centrifugation of blood for 15 minutes. Alternatively, mice were lethally infected with $2 \cdot 10^6$ *C. albicans* and monitored daily for weight, general health and survival, following the institutional guidance.

For quantitative polymerase chain reaction (qPCR) analysis of renal cytokines, RNA was purified from whole kidneys harvested in QIazol Lysis Reagent (Qiagen) at day 2 post-infection (p.i.). Kidney fungal burden at indicated time points p.i. was determined by plating organ homogenates obtained mechanically over 70 µm cell strainers (BD Biosciences) after slicing the tissue, in serial ten-fold dilutions on YPD

agar plates. Colony-forming units (CFUs) were counted after growth at 30ºC for 48 hours and data are shown as CFUs per total kidney.

6. ELISA.

Mouse cytokines were analyzed in supernatants of BMDMs or sera using the following reagents: for IL-1β, Mouse IL-1β/IL-1F2 DuoSet, R&D Systems; for IL-6, Purified rat anti-mouse IL-6, Biotin rat anti-mouse IL-6 -both from BD Biosciences- and Streptavidin Horseradish Peroxidase Conjugate from Invitrogen; for TNFα: OptEIA ELISA kit (BD Biosciences) or TNFα DuoSet (R&D Systems). TNFα in serum was quantified by using Mouse TNFα DuoSet (R&D Systems).

Human cytokines were analyzed in supernatants of hPBMCs by using the Human IL-1β/IL-1F2 Duoset, Human IL-6 Duoset and Human TNFα DuoSet kits, all from R&D Systems.

7. Western Blotting.

Culture medium was removed form plated cells and cell lysates were prepared in radioimmunoprecipitation assay buffer containing protease and phosphatase inhibitors (Roche). Samples were run on Mini-PROTEAN TGX PRECAST Gels and transferred onto a nitrocellulose membrane (both from Bio-Rad Laboratories) for blotting with the following antibodies: β-Actin (C4) and SHIP-1 (P1C1) from Santa Cruz; phospho (p)Akt (Ser473, #4058S), Akt (#2920S), pS6 (Ser235/236, #4858T) and p4EBP1 (Thr37/46, #9459S), all from Cell Signaling. Alexa Fluor-680 (Life Technologies) or Qdot-800 (Rockland) conjugated secondary antibodies were used. Gels were visualized in an Odyssey instrument (LI-COR) and band intensity was quantified by using ImageJ software (Bitplane).

8. Antibodies and flow cytometry.

Samples were stained with the appropriate antibody cocktails in ice-cold FACS Buffer at 4ºC for 15 minutes. Antibodies included mouse Phycoerythrin-anti-TLR4 (BioLegend) and Alexa 647-anti-Dectin-1 (Bio-Rad). Dead cells were excluded by Hoechst 33258 (Invitrogen) incorporation. Purified anti-FcγRIII/II (2.4G2, TONBO Bioscience) was used to block murine Fc-receptors at 4ºC for 10 minutes in all the

stainings. Events were acquired using FACSCanto 3L (BD Biosciences). Data were analyzed with FlowJo software (Tree Star).

9. Glycolytic flux evaluation.

The assay was performed in DMEM supplemented with 1 mM glutamine, 100 µg/ml penicillin and 100 µg/ml streptomycin. The pH was adjusted to 7.4 with KOH (herein called Seahorse medium). Cells were washed with PBS and 175 µl of Seahorse medium was added. Plates were incubated at 37°C without CO_2 for 1h prior to the assay. Extracellular acidification rate (ECAR) was determined by using the glycolysis stress test in an XF-96 Extracellular Flux Analyzer (Agilent Technologies). Three consecutive measurements were performed under basal conditions and after sequential addition of 80 mM glucose (Merck), 9 µM oligomycin A (Sigma) and 500 mM 2-deoxy-glucose (2DG, Sigma). As shown in **Figure M1**, basal and maximal glycolysis were defined as ECAR (mpH) after addition of glucose and oligomycin, respectively. Glycolytic reserve was defined as the difference between maximal and basal glycolysis.

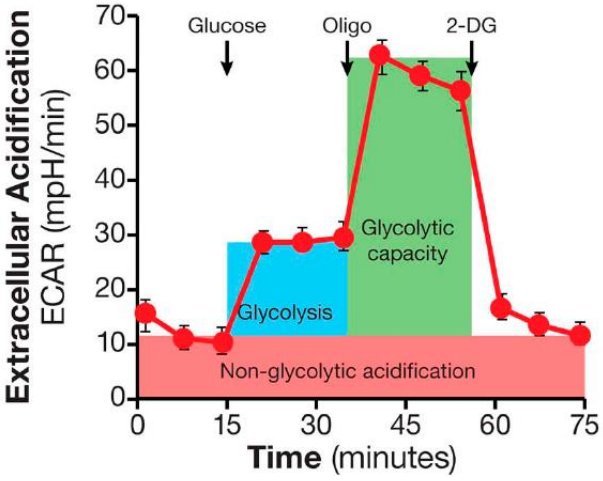

Figure M1. Profile of key parameters of glycolytic function resulting from glycolysis stress test. (Taken from (Pike Winer and Wu, 2014)). Basal glycolysis (or glycolysis) is defined as ECAR (mpH) upon saturating addition of glucose (blue area under the curve). Maximal glycolysis (or glycolytic capacity) is defined as maximum ECAR (mpH) reached following the addition of oligomycin (oligo), which effectively shuts down oxidative phosphorylation and results into glycolysis at maximum capacity (light green area). 2-deoxyglucose (2DG) fully abolishes glycolysis. Glycolytic reserve indicates the capability of a cell to respond to an energetic demand and is calculated by subtracting basal from maximal glycolysis.

10. Chromatin Immunoprecipitation analysis.

Chromatin ImmunoPrecipitation (ChIP) was performed using the Magna ChIP A – Chromatin Immunoprecipitation kit together with the ChIPAb+ Trimethyl-Histone H3 (Lys4) (H3K4me3) – ChIP validated antibody, both from Millipore-Merck, following the provider's instructions. Cells were fixed with 1% formaldehyde for 10 minutes at RT, exposed to glycine to quench unreacted formaldehyde and washed twice with ice-cold PBS supplemented with the provided protease inhibitor cocktail. After scraping the cells in ice-cold PBS, they were pelleted, lysed and sonicated for 15 minutes (30 seconds on/30 seconds off) at high intensity by using a Bioruptor UCD-200TM-TX water bath sonicator (Diagenode). Sonicates were diluted and incubated with antibodies plus protein A magnetic beads for 1 hour with rotation at 4 ºC. Beads were magnetically collected and washed extensively. Protein-DNA complexes were disrupted from the beads upon proteinase-K treatment and recovered DNA was purified.

Immunoprecipitated DNA and input DNA were amplified by means of qPCR with specific primers for the promoter region of TNFα (Fw: 5'-CAACTTTCCAAACCCTCTGC-3'; Rv: 5'-CTGGCTAGTCCCTTGCTGTC-3') with input DNA to generate a standard curve. ChIP data are represented as a percentage of input.

11. RNA extraction and quantitative PCR.

RNeasy Plus Mini Kit, from Qiagen, was used for RNA extraction. Complementary DNA (cDNA) was prepared using the High Capacity cDNA reverse transcription kit (Applied Biosystems). qPCR was performed in a 7900-FAST-384 instrument (Applied Biosystems) by using the GoTaq qPCR master mix from Promega. Primers used in this work (synthetized by Sigma) were as follows: β-actin Fw: 5′-GGCTGTATTCCCCTCCATCG-3′; β-actin Rv: 5′-CCAGTTGGTAACAATGCCATGT-3′; IL-1β Fw: 5'-CTGAACTCAACTGTGAAATGCCA-3'; IL-1β Rv: 5'-AAAGGTTTGGAAGCAGCCCT-3'; IL-6 Fw: CCGTGTGGTTACATCTACCCT-3'; IL-6 Rv: 5'-CGTGGTTCTGTTGATGACAGT-3' TNFα Fw: 5'-CCCTCACACTCAGATCATCTTCT-3'; TNFα Rv: 5'-GCTACGACGTGGGCTACAG-3'; messenger RNA levels were normalized to β-Actin expression. Data are shown as relative expression to β-Actin (ΔΔCt).

12. Quantification and statistical analysis.

The statistical analyses were performed using Prism software (GraphPad Software). Unless specified, statistical significance for comparison between two sample groups with a normal distribution (Shapiro-Wilk test for normality) was determined by two-tailed paired or unpaired Student's t-test. When groups were too small to estimate normality, Gaussian distribution was assumed. Comparison of survival curves was carried out by Log-rank (Mantel-Cox) test. Outliers were identified by means of Tukey's range test. Differences were considered significant at $p < 0.05$ as indicated. Except when specified, only significant differences are shown. As indicated in figure legends, either a representative experiment or pool are shown, and the number of repetitions of each experiment and number of experimental units (either cultures or mice) is indicated. *In vitro* experiments are shown as a pool of experiments, where linked WT-LysMΔSHIP-1 dots represent independent cultures that were processed within the same experiment. In this way, an internal comparison between genotypes can be visually done. Different conditions within the same genotype in a particular experiment, although not connected by a matter of clarity, were also paired analyzed and statistically significant differences are indicated by hashes (#).

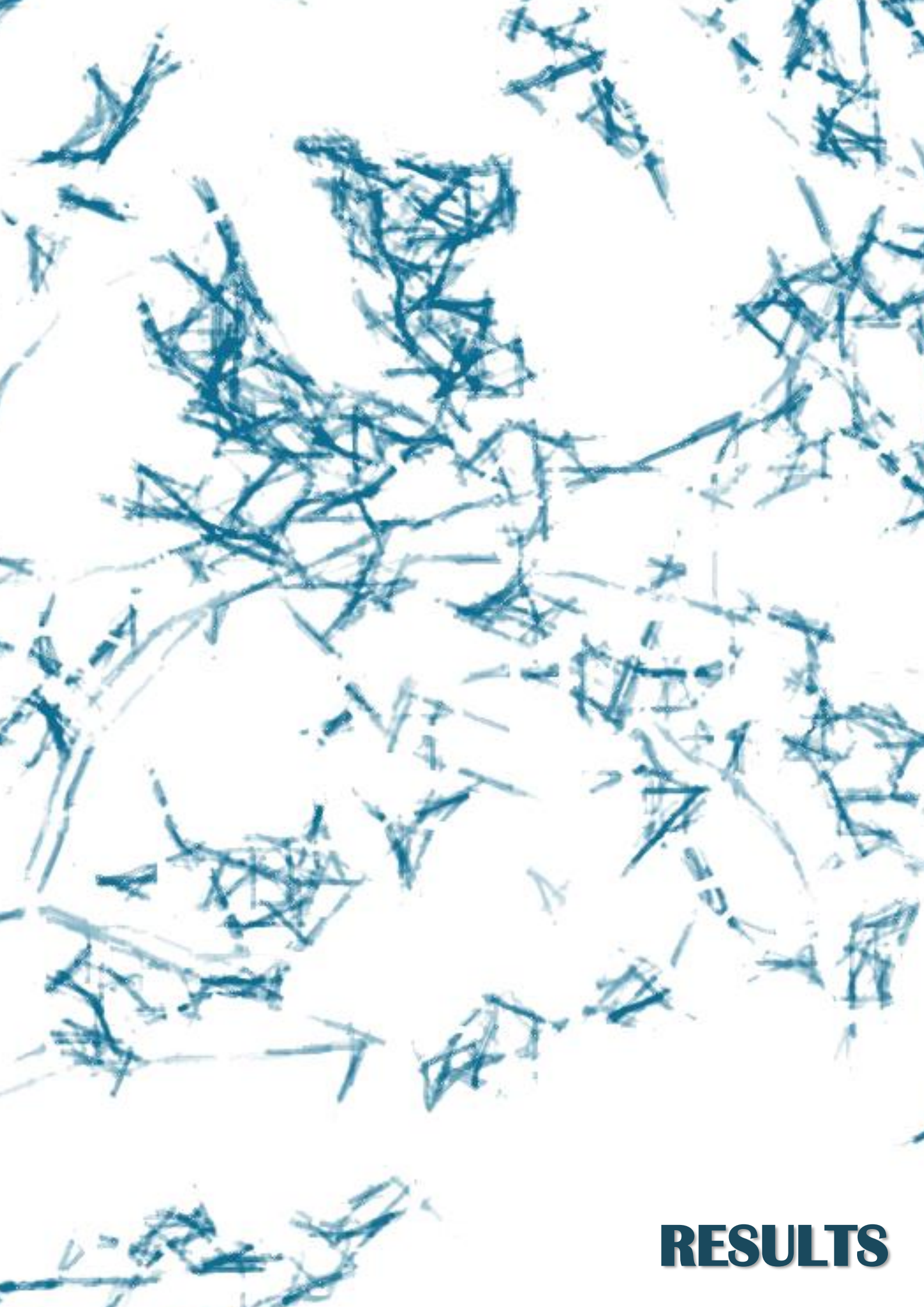

RESULTS

1. Setting up a working *in vitro* model of trained immunity in mouse bone marrow-derived macrophages.

1.1. Experimental design of a trained immunity model.

To explore trained immunity modulation by myeloid cells, we designed a long-term trained immunity *in vitro* model for mouse macrophages, by adapting a published scheme for hPBMCs (Quintin et al., 2012). It consisted of 24 hours of stimulation with WGP from *Saccharomyces cerevisiae*, a purified particulate β-glucan which is a well-established ligand for Dectin-1 receptor (Rosas et al., 2008), followed by a wash with fresh medium and a 3-day long resting period. Afterwards, BMDMs were primed with IFN-γ and stimulated the day after with LPS as heterologous secondary challenge. Medium was replaced before each step. TNFα, as prototypical trained immunity cytokine, was measured in supernatants 1 day later **(Figure R1A)**.

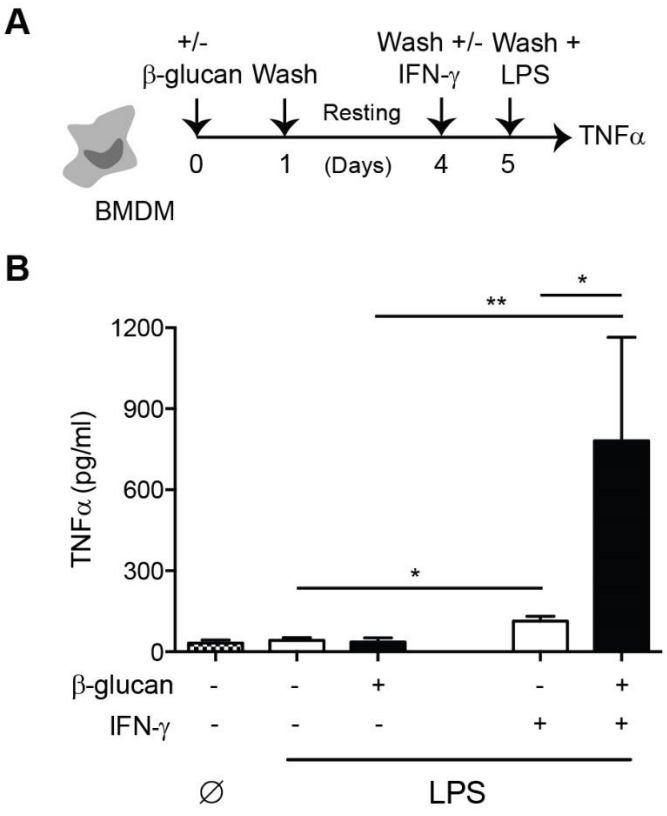

Figure R1. Experimental set-up of a trained immunity *in vitro* model in mouse BMDMs. (A) Graphical scheme of trained immunity *in vitro* model applied to WT BMDMs. Briefly, BMDMs were trained with 100 µg/ml of β-glucan. Cells were washed with fresh medium and rested for 3 days. At day 4, BMDMs were primed with 25 ng/ml of IFN-γ for 24 hours and finally rechallenged with 1 µg/ml of LPS. TNFα was analyzed one day after. **(B)** BMDMs were stimulated (+) or not (-) with β-glucan, washed, rested and primed at day 4 (+) or not (-) with IFN-γ prior to LPS stimulation, according to A. (Ø) represent BMDMs with no stimulation. TNFα in supernatants after 24 hours of LPS exposure was analyzed. Mean + SEM from 5 independent experiments is shown. *p < 0.05, **p < 0.01, paired Student's t-test.

Compared to non-trained BMDMs, previous β-glucan priming increased TNFα production in response to LPS challenge 5 days later **(Figure R1B)**, reproducing trained immunity (Quintin et al., 2012). Of note, IFN-γ priming was needed to detect LPS-induced cytokine production, regardless of the induction of training **(Figure R1B)**, and therefore was included when applying this *in vitro* model.

1.2. SHIP-1 protein is induced upon β-glucan stimulation.

To address the relevance of SHIP-1 phosphatase in Dectin-1-triggered trained immunity, BMDMs were stimulated with β-glucan and the expression of SHIP-1 was analyzed. In accordance with previous studies (O'Connell et al., 2009, Zhou et al., 2006), SHIP-1 was expressed in steady state conditions in BMDMs. Compared to this basal expression level, β-glucan stimulation resulted in further induction of the phosphatase 24 hours later, with no plating-dependent effect on that induction **(Figure R2)**. This would suggest that the phosphatase could play a role in β-glucan-induced trained immunity.

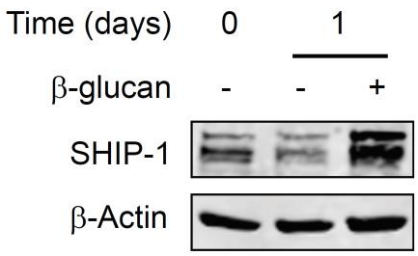

Figure R2. SHIP-1 expression in BMDMs. BMDMs were exposed (+) or not (-) to β-glucan for 1 day. SHIP-1 expression was analyzed by WB and normalized to β-Actin. Representative experiment of 3 performed.

2. Characterization of trained SHIP-1-deficient macrophages.

2.1. Efficient SHIP-1 deletion in LysMΔSHIP-1 macrophages.

To further address the role of SHIP-1 in trained immunity phenomenon, we took advantage of the LysMΔSHIP-1 mouse model (Collazo et al., 2012). Consistently, BMDMs derived from these mice lacked expression of SHIP-1 phosphatase **(Figure R3)**.

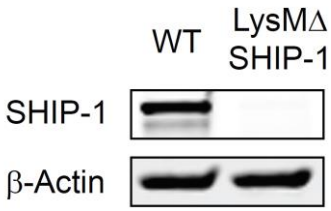

Figure R3. SHIP-1 protein is depleted in LysMΔSHIP-1 BMDMs. SHIP-1 expression in WT versus LysMΔSHIP-1 BMDMs was analyzed by WB and normalized to β-Actin. Representative experiment of 6 performed.

2.2. Expression of trained immunity-associated receptors is not affected by SHIP-1.

We first evaluated the surface expression of the receptors involved in the sensing of both the training stimulus and the secondary challenge. Expression of Dectin-1, receptor for β-glucan, was comparable between WT and SHIP-1-deficient macrophages before training induction **(Figure R4)**.

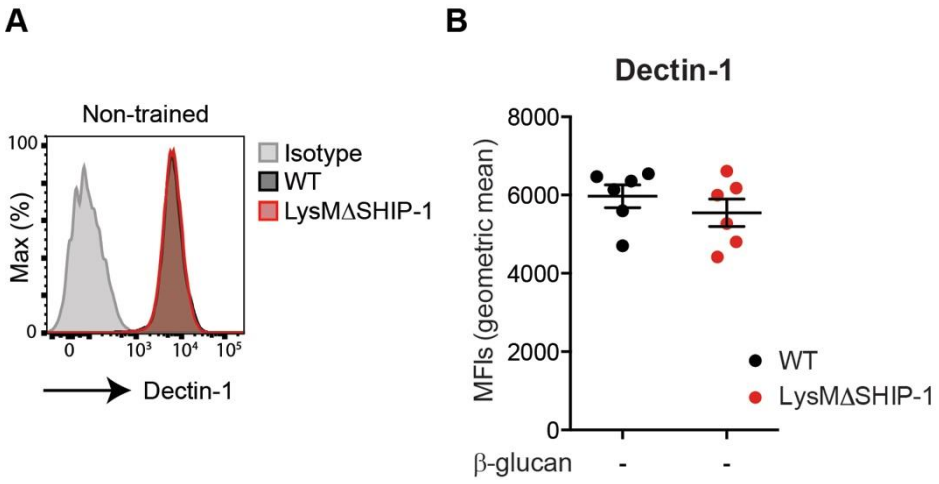

Figure R4. Equivalent Dectin-1 surface expression on BMDMs in the absence of SHIP-1. Dectin-1 expression in WT and LysMΔSHIP-1 BMDMs before β-glucan stimulation was analyzed by FACS. **(A)** FACS histograms representative of 4 independent experiments; **(B)** individual data and mean ± SEM of mean fluorescence intensity (MFI) from a pool of 2 experiments are shown. (B) Each dot represents an independent cell culture and 3 BMDM cultures per experiment were performed.

We also checked the expression of the LPS receptor TLR4 at day 5 prior to LPS challenge, in BMDMs previously trained or not with β-glucan. There were no differences in the expression levels of TLR4 between non-trained and trained BMDMs, as well as among WT and SHIP-1-deficient macrophages in each experimental

condition **(Figure R5)**. These data would rule out a differential capacity of sensing relevant PAMPs for our study due to the lack of SHIP-1 in BMDMs.

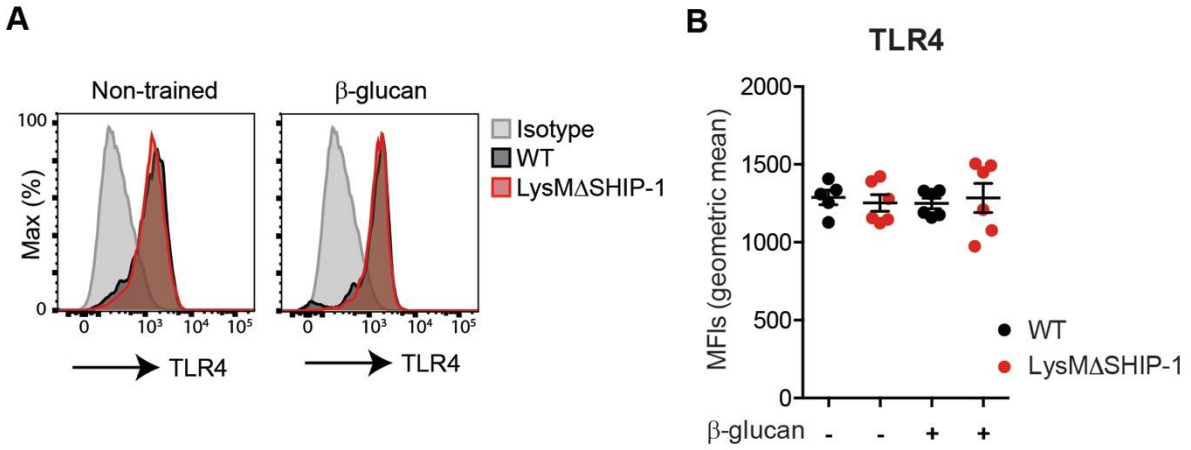

Figure R5. TLR4 expression on BMDMs is not affected by training or SHIP-1 deficiency. TLR4 expression in WT and LysMΔSHIP-1 BMDMs before LPS stimulation according to model in Figure R1A was analyzed by flow cytometry. **(A)** FACS histograms from non-trained (left panel) or β-glucan-trained (right panel) BMDMs representative of 4 independent experiments; **(B)** individual data and mean ± SEM of MFI from a pool of 2 experiments are shown. Each dot represents an independent cell culture and 3 BMDM cultures per experiment were performed.

2.3. SHIP-1 deletion does not affect trained macrophage numbers.

β-glucan-induced training has been shown to increase cell viability of mouse splenic (Garcia-Valtanen et al., 2017) and human monocytes (Bekkering et al., 2016a). Thereby, we evaluated cell number after applying our *in* vitro model and prior to LPS rechallenge. Concurring with previous results, β-glucan training also increased the number of viable WT BMDMs compared to non-trained cells **(Figure R6)**. Noteworthy, non-trained SHIP-1-deficient BMDMs revealed higher numbers compared to their WT counterparts. However, cells from both genotypes displayed comparable relative numbers upon training conditions **(Figure R6)**. Taking these facts into consideration and to ensure the analysis of cell-intrinsic responses, as previously described (Bekkering et al., 2016a), whenever evaluating trained immunity parameters, such as cytokine production, data were normalized to the relative cell number present in each condition.

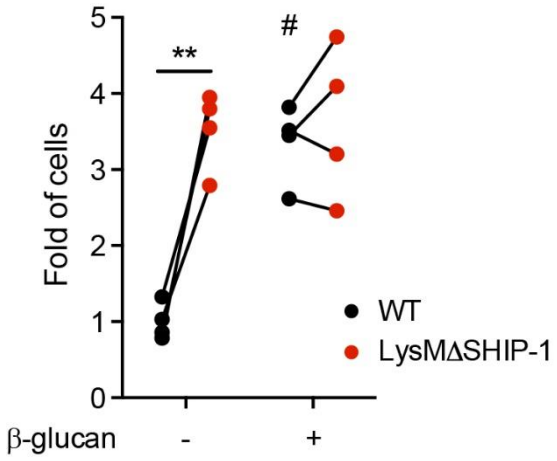

Figure R6. Relative number of BMDMs recovered after training and before LPS stimulation. WT and LysMΔSHIP-1 BMDMs were exposed (+) or not (-) to β-glucan and IFN-γ-primed according to model in Figure R1A. At day 5 and before LPS stimulation, the number of viable BMDMs was determined by FACS based on Hoechst 33258 exclusion. Fold of cells was calculated by dividing live cell number in each experimental condition by the average number of WT non-trained cells in all the experiments. Individual data from 4 independent experiments are shown. $^{**}p < 0.01$, paired Student's t-test comparing WT and LysMΔSHIP-1. $\#p < 0.05$, paired Student's t-test comparing stimulated or not with β-glucan within the same genotype.

3. SHIP-1 deletion boosts β-glucan-induced training in macrophages.

3.1. SHIP-1 modulates cytokine production upon β-glucan training.

To formally evaluate the role of SHIP-1 phosphatase in trained immunity, WT and LysMΔSHIP-1 BMDMs were trained with β-glucan, washed, rested and further rechallenged with LPS. While IL-6 and TNFα were evaluated after 24 hours of LPS exposure, IL-1β was measured upon 4 hours of LPS stimulation plus 2 additional hours of ATP (needed for inflammasome activation and pro-IL-1β processing, (Schroder and Tschopp, 2010) **(Figure R7A)**. Importantly, these analyses were performed on cells washed up to three times, with no remaining cytokines in the medium of β-glucan-trained BMDMs before LPS stimulation.

First, SHIP-1 deletion did not impact on the LPS-induced inflammatory response under non-trained conditions **(Figure R7B).** Pre-incubation of BMDMs with β-glucan led to greater production of LPS-induced IL-1β and TNFα **(Figure R7B, left and right panel)**. Remarkably, upon training conditions, the absence of SHIP-1 in macrophages resulted in an overproduction of these trained immunity-associated proinflammatory cytokines **(Figure R7B, left and right panel)**. Nevertheless, this trained immunity phenomenon was not observed in terms of IL-6 production in this setting, as trained

WT BMDMs even produced significantly less cytokine than non-trained counterparts, with no effect of SHIP-1 phosphatase deletion **(Figure R7B, middle panel)**. These data reflect that SHIP-1 adjusts LPS-induced proinflammatory cytokine production during β-glucan training, with some specificity depending on the cytokine analyzed.

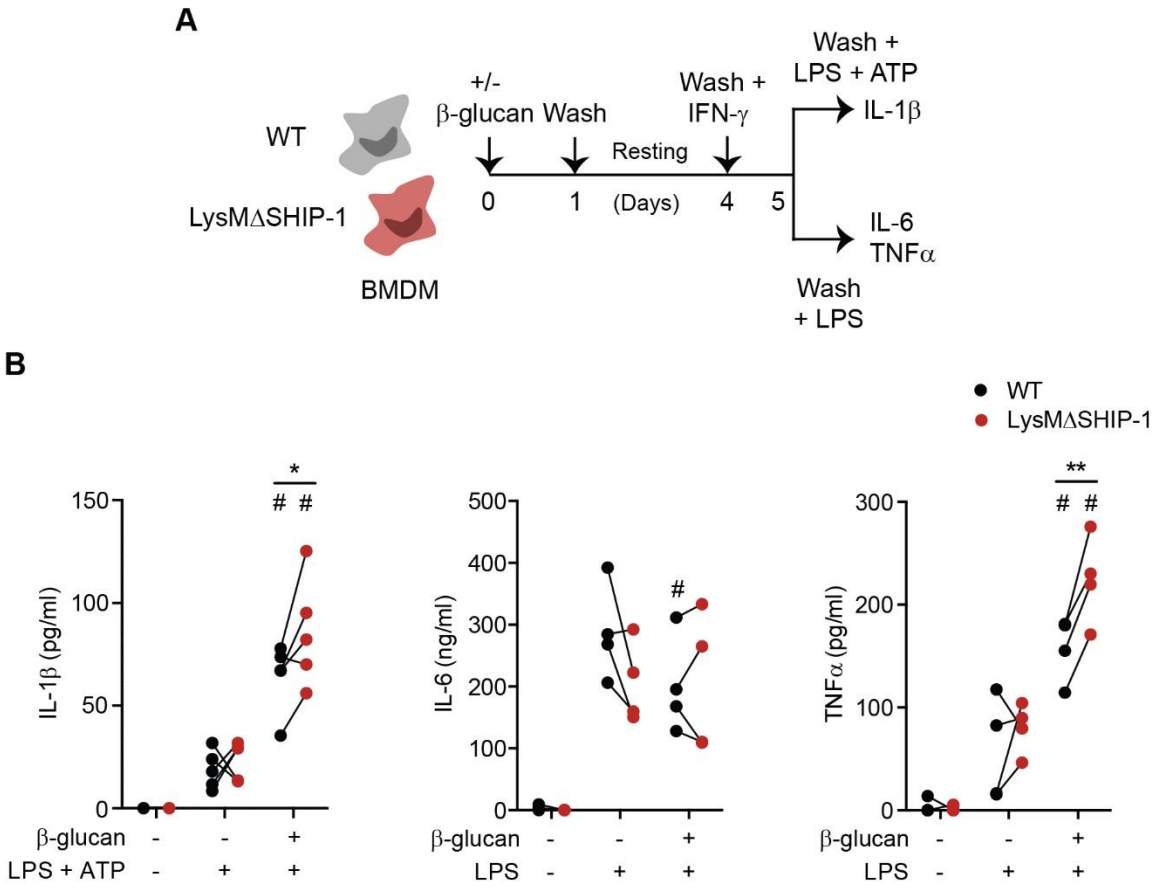

Figure R7. Trained SHIP-1-deficient macrophages show enhanced production of IL-1β and TNFα. **(A)** Scheme of trained immunity *in vitro* model applied to WT and LysMΔSHIP-1 BMDMs. As indicated in Figure R1A, BMDMs were trained with β-glucan and cells were washed and rested for 3 days. At day 4, BMDMs were primed with IFN-γ for 24 hours and finally rechallenged with LPS. IL-6 and TNFα were analyzed after 24 hours. For IL-1β, LPS stimulation (4 hours) was followed by ATP addition for another 2 hours. **(B)** BMDMs were stimulated (+) or not (-) with β-glucan or LPS (+ ATP for IL-1β), and IL-1β (left panel), IL-6 (middle panel) and TNFα production (right panel) were analyzed in supernatants according to A. Independent experiments (N=4-5) are shown. *p < 0.05, **p < 0.01, paired Student's t-test comparing WT and LysMΔSHIP-1. #p < 0.05, paired Student's t-test comparing stimulated or not with β-glucan within the same genotype.

3.2. SHIP-1 regulates molecular and metabolic hallmarks of trained immunity.

Considering that SHIP-1 deficiency boosts the production of proinflammatory cytokines, the final hallmark of trained immunity at the molecular level, we addressed

whether other key features of this phenomenon were also modulated by the phosphatase.

3.2.1. SHIP-1 absence leads to overactivation of trained immunity-related molecular pathway.

PI3K/Akt signaling is a canonical molecular pathway implicated in the development of trained responses (Cheng et al., 2014, Arts et al., 2016b). Thereby, we first evaluated phosphorylation of Akt kinase upon β-glucan exposure in BMDMs. As shown in **Figure R8**, in WT BMDMs, Akt was phosphorylated in response to β-glucan in a time-dependent manner, peaking at 30 minutes of stimulation, similar to human monocytes (Cheng et al., 2014).

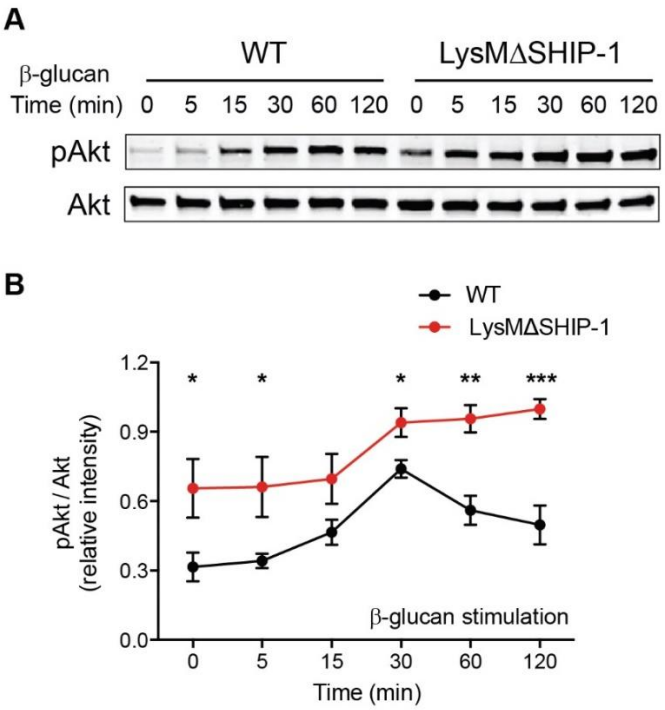

Figure R8. β-glucan-induced Akt phosphorylation is increased in SHIP-1-deficient macrophages. WT and LysMΔSHIP-1 BMDMs were exposed to β-glucan for the indicated time and pAkt and Akt were analyzed by WB. **(A)** Representative gel of 5 experiments performed. **(B)** Quantification of WB kinetics by ImageJ software. Relative band intensity is shown. Mean ± SEM from a pool of 5 experiments performed. *$p < 0.05$, **$p < 0.01$, ***p<0.001, paired Student's t-test comparing WT and LysMΔSHIP-1 at any time point.

Furthermore, SHIP-1-deficient macrophages showed increased and sustained phosphorylation of this kinase over time **(Figure R8)**. Remarkably, a basal increase in Akt phosphorylation was found in LysMΔSHIP-1 macrophages, which concurs with previous results (Antignano et al., 2010b, Rajaram et al., 2009). However, this did not

result in an eventual cytokine overproduction unless β-glucan-induced training was established **(Figure R7B)**.

We also assessed the phosphorylation of downstream effectors of the pathway in response to β-glucan, particularly two mTOR targets: the ribosomal protein S6 and 4EBP1 (Dibble and Cantley, 2015). In WT BMDMs, while S6 displayed two ways of phosphorylation, activation of 4EBP1 peaked at 5-15 minutes post-challenge **(Figure R9)**. Again, SHIP-1-deficient macrophages revealed an increased phosphorylation of these targets that was more patent at later time points **(Figure R9)**.

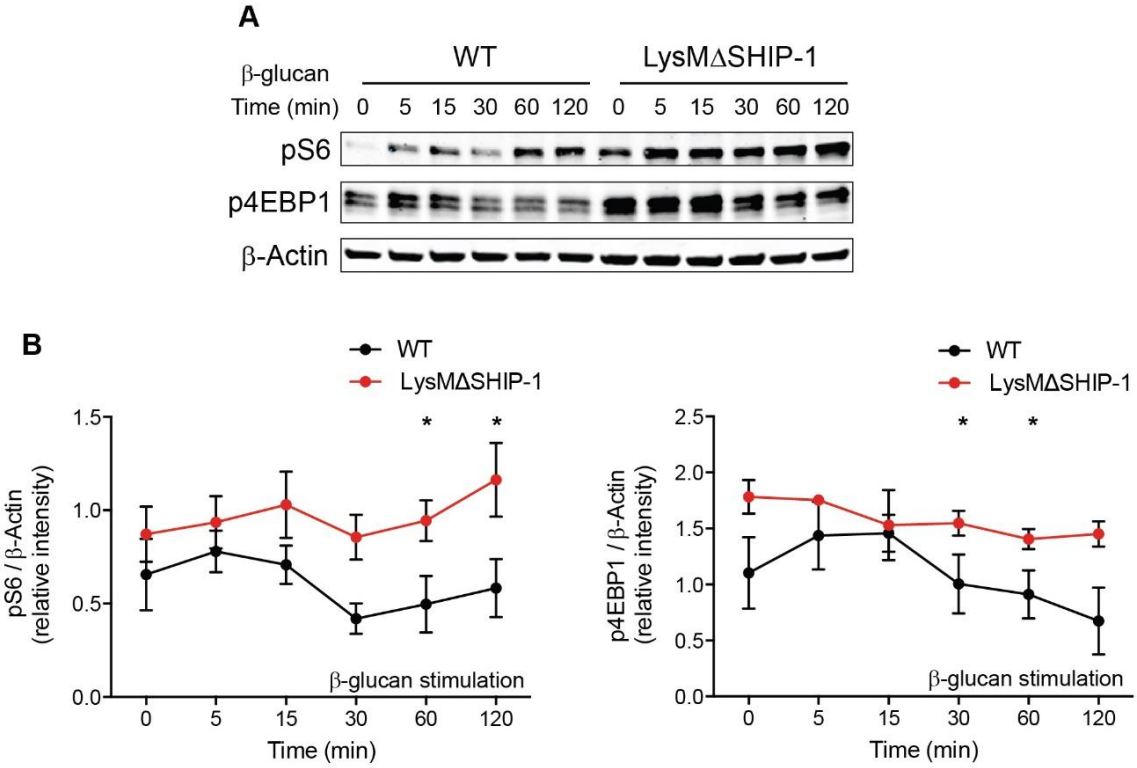

Figure R9. Augmented phosphorylation of mTOR targets upon β-glucan in the absence of SHIP-1. WT and LysMΔSHIP-1 BMDMs were exposed to β-glucan for the indicated time and pS6, p4EBP1 and β-Actin were analyzed by WB. **(A)** Representative gel of 5 experiments performed. **(B)** Quantification of WB kinetics for pS6 (left panel) and p4EBP1 (right panel) by ImageJ software. Relative band intensity is shown. Mean ± SEM from a pool of 5 experiments performed. *$p < 0.05$, paired Student's t-test comparing WT and LysMΔSHIP-1 at any time point.

3.2.2. SHIP-1 deficiency results in enhanced glycolysis.

Regarding metabolic changes, we assessed the extent of the glycolytic switch induced by β-glucan by measuring the ECAR in a glycolysis stress test, prior to the LPS rechallenge according to **Figure R7A**. Training with β-glucan increased the ECAR of WT BMDMs 5 days later **(Figure R10)**. This was reflected at different levels, including

basal glycolysis **(Figure R10B)**, maximal glycolysis **(Figure R10C)** and the glycolytic reserve **(Figure R10D)**, which reveals the extent of the glycolytic capacity of these cells. Importantly, this switch to glycolysis was significantly more pronounced for all parameters of the glycolytic function in the case of trained SHIP-1-deficient macrophages **(Figure R10)**. Of note, concurring with data on signaling pathway activation **(Figure R8)**, a steady state enhanced glycolysis was detected in LysMΔSHIP-1 BMDMs **(Figure R10)**, but it did not result in higher cytokine production unless β-glucan-induced training was established **(Figure R7B)**.

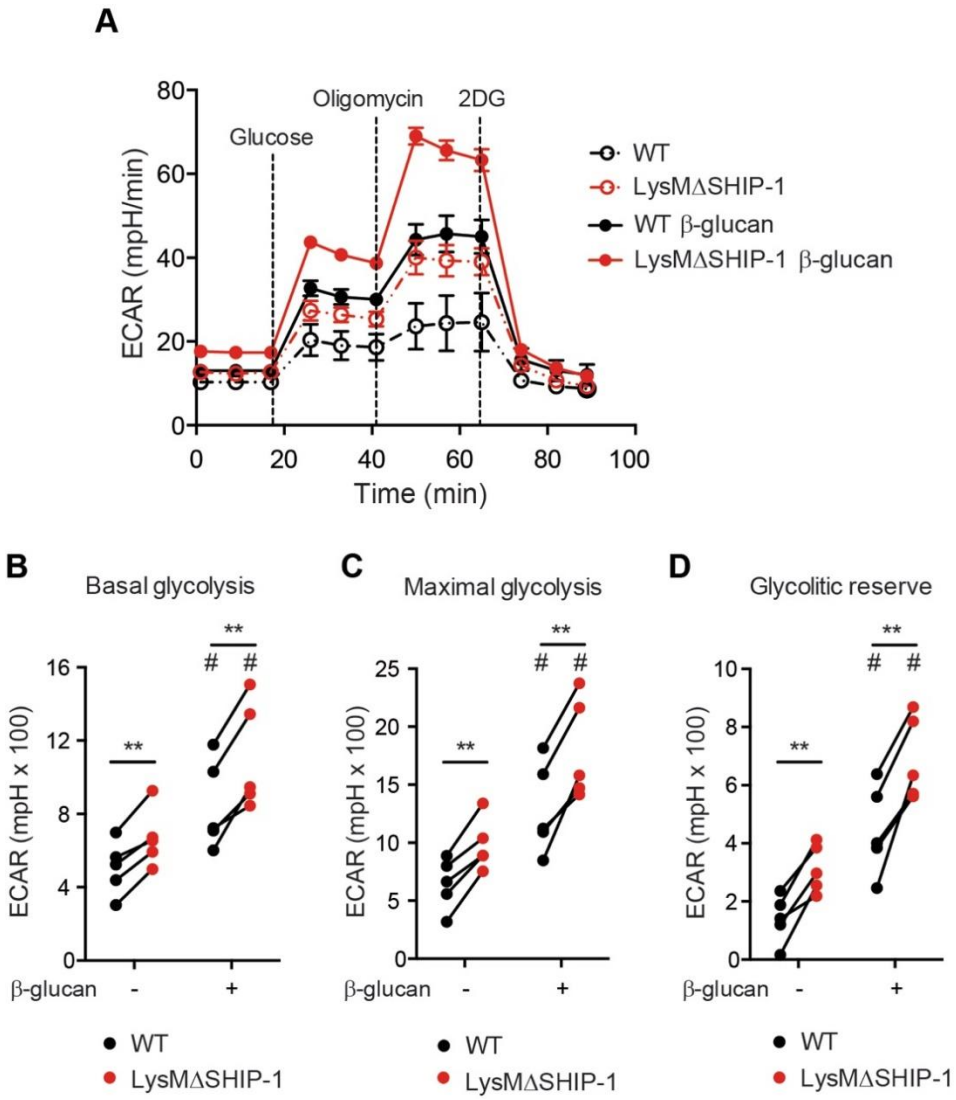

Figure R10. Boosted glycolytic shift in SHIP-1-deficient BMDMs prior to LPS challenge. According to Figure R7A, WT and LysMΔSHIP-1 BMDMs were left untreated (dashed lines) or treated for 1 day with β-glucan (solid lines), washed, rested for 3 days and re-plated in equal numbers for determination of ECAR. ECAR in a glycolysis stress test was analyzed upon sequential addition of glucose, oligomycin and 2DG as indicated **(A)**. **(B)** Analysis of basal glycolysis, **(C)** maximal glycolysis and **(D)** glycolytic reserve. Mean ± SEM (A) or individual data (B-D) of 5 independent cultures are shown. (B-D) **p < 0.01, paired Student's t-test comparing WT and LysMΔSHIP-1. #p< 0.05, paired Student's t-test comparing within the same genotype stimulated or not with β-glucan.

We wondered whether this differential switch in the metabolism reflected a change developed along to the training process or whether it took place upon β-glucan priming. To address that, we evaluated glycolysis after an overnight β-glucan stimulation **(Figure R11)**.

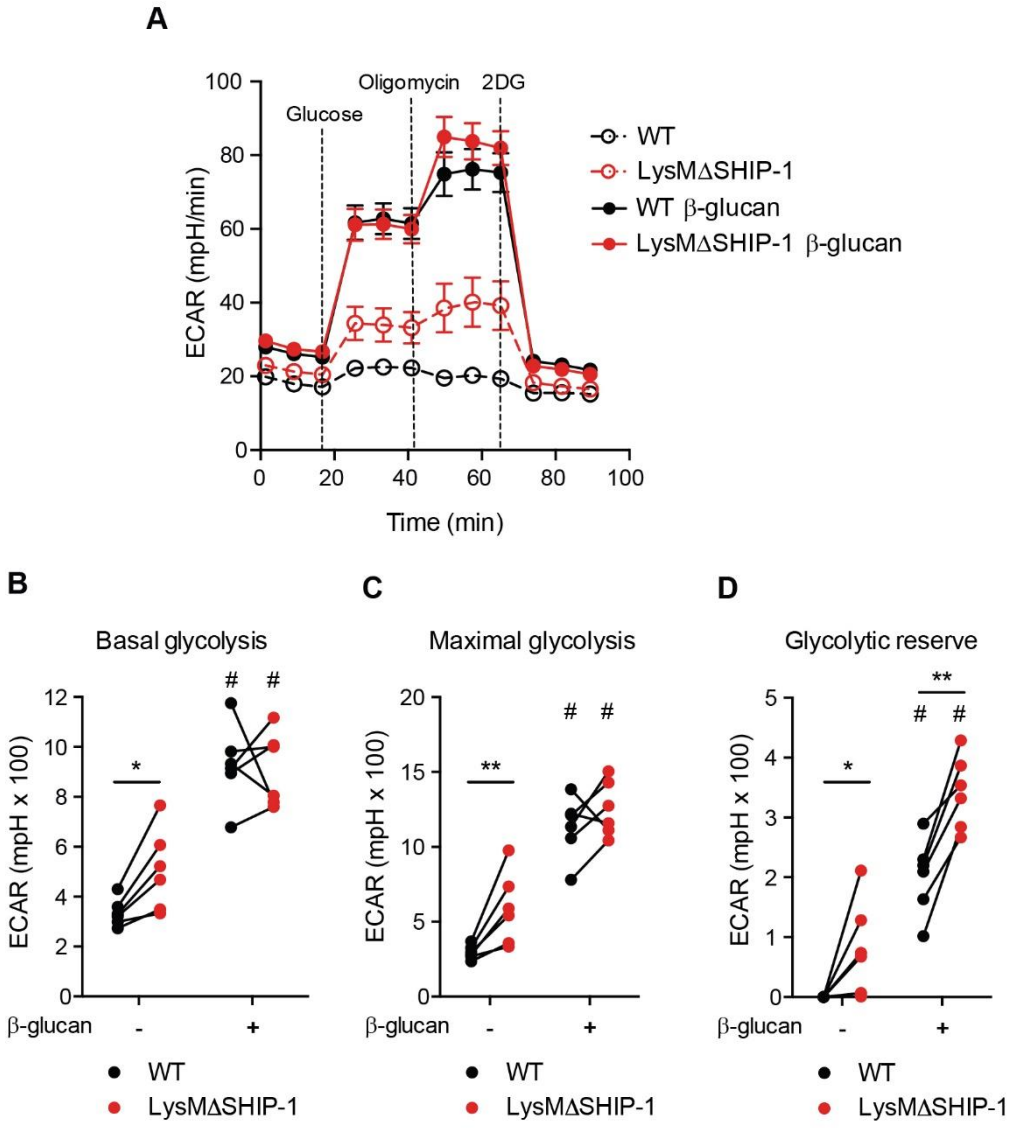

Figure R11. SHIP-1 controls the extent of the early glycolytic metabolism. WT and LysMΔSHIP-1 BMDMs were left untreated (dashed lines) or treated overnight with β-glucan (solid lines) and ECAR was determined. ECAR in a glycolysis stress test was analyzed upon sequential addition of glucose, oligomycin and 2DG as indicated **(A)**. **(B)** Analysis of basal glycolysis, **(C)** maximal glycolysis and **(D)** glycolytic reserve. Mean ± SEM (A) or individual data (B-D) of 6 independent cultures are shown**.** (B-D) **p* < 0.05, ***p* < 0.01, paired Student's t-test comparing WT and LysMΔSHIP-1. #*p*< 0.05, paired Student's t-test comparing stimulated or not with β-glucan within the same genotype.

This revealed that basal **(Figure R11B)** and maximal glycolysis **(Figure R11C),** and the glycolytic reserve **(Figure R11D)** were already increased in β-glucan primed

WT BMDMs. However, only the glycolytic reserve was further increased in the absence of SHIP-1, suggesting that this is the first metabolic difference associated to SHIP-1-deficient BMDMs upon β-glucan training. Again, and consistently with previous results, an enhanced glycolysis was detected in unstimulated LysMΔSHIP-1 BMDMs **(Figure R11)**. Taking altogether, these results indicate that SHIP-1 controls the extent of the glycolytic metabolism.

3.3. SHIP-1-induced effect relies on epigenetic histone modification.

Epigenetic reprogramming is one of the key steps in the induction of trained immunity (Christ et al., 2016, Netea et al., 2016, van der Heijden et al., 2018, Dominguez-Andres et al., 2018). To address whether the regulatory role of SHIP-1 on trained immunity relied on epigenetics, we trained BMDMs as before and, at day 5 prior to LPS stimulation, we checked the presence of histone modifications by a ChIP assay. Particularly, we evaluated H3K4me3, at the level of TNFα promoter (Quintin et al., 2012, Saeed et al., 2014) **(Figure 12A)**.

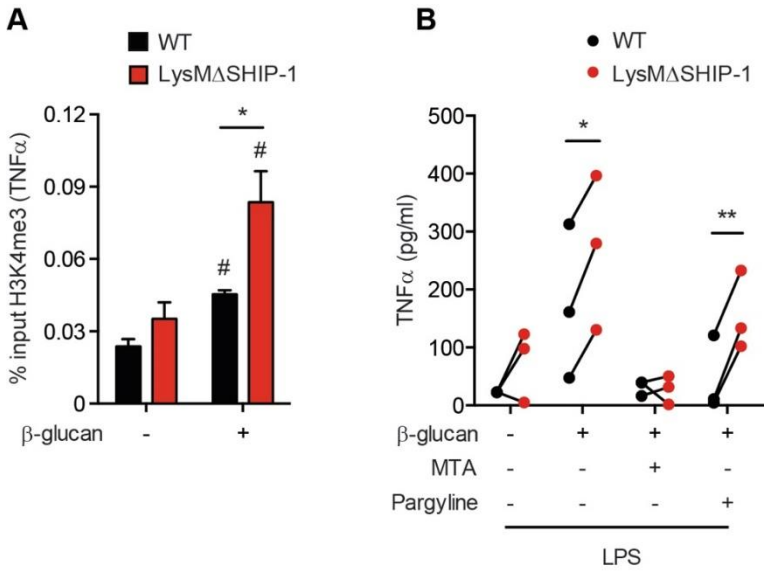

Figure R12. Histone methylation is critical for SHIP-1-mediated regulation of β-glucan training. **(A)** According to Figure R7A, WT and LysMΔSHIP-1 BMDMs were trained (+) or not (-) with β-glucan for 1 day, washed, rested for 4 days and ChIP against H3K4me3 was performed. Enrichment of that epigenetic mark on the TNFα promoter was analyzed by qPCR. Mean + SEM of 5 experiments performed is shown. *p < 0.05, paired Student's t-test comparing WT and LysMΔSHIP-1. #p< 0.05, paired Student's t-test comparing within the same genotype stimulated or not with β-glucan. **(B)** WT and LysMΔSHIP-1 BMDMs were incubated (+) or not (-) with the methyltransferase inhibitor MTA or the histone demethylase inhibitor pargyline for 30 minutes previous to β-glucan training and after washing it out. TNFα production was analyzed in supernatants after LPS stimulation according to model in Figure R7A. Individual data corresponding to 3 independent experiments are shown. *p < 0.05, **p < 0.01, paired Student's t-test comparing WT and LysMΔSHIP-1.

The training with β-glucan specifically enriched the presence of this activating epigenetic mark, which reflects a more open chromatin **(Figure R12A)**. Moreover, this histone mark was much more abundant when training was induced in the absence of SHIP-1 **(Figure R12A)**, concurring with final enhanced TNFα production **(Figure R7B)**.

To formally assess whether the SHIP-1-mediated effect on trained immunity depended on this epigenetic reprogramming coined after β-glucan stimulation, we trained BMDMs as in **Figure R7A**, but in the presence of epigenetic inhibitors. BMDMs were pre-treated for 30 minutes before β-glucan stimulation with different inhibitors, which were also included after the first wash-out. While MTA is a methyltransferase inhibitor that has been shown to prevent training induction, pargyline is a demethylase inhibitor which has been described not to have any effect in the training process (Quintin et al., 2012). Thus, pre-incubation with MTA inhibitor abolished all the SHIP-1-mediated effect on β-glucan training, revealed in terms of TNFα production **(Figure R12B)**. However, SHIP-1-dependent overproduction of TNFα was preserved when pargyline was present during training development **(Figure R12B)**.

Finally, trained immunity development also relies on acetylation of histones, particularly on H3K27Ac (Saeed et al., 2014). EGCG is a histone acetyltransferase inhibitor that has been shown to abolish the training (Ifrim et al., 2014). Moreover, resveratrol activates the histone deacetylase sirtuin 1, which results in an equivalent effect (Cheng et al., 2014). Taking this into account, we trained BMDMs as before, but now in the presence of these epigenetic inhibitors, separately. Again, enhanced training in SHIP-1-deficient macrophages, revealed by TNFα overproduction, was abolished when cells were pre-treated with any of the histone acetylation inhibitors, either EGCG or resveratrol **(Figure R13)**.

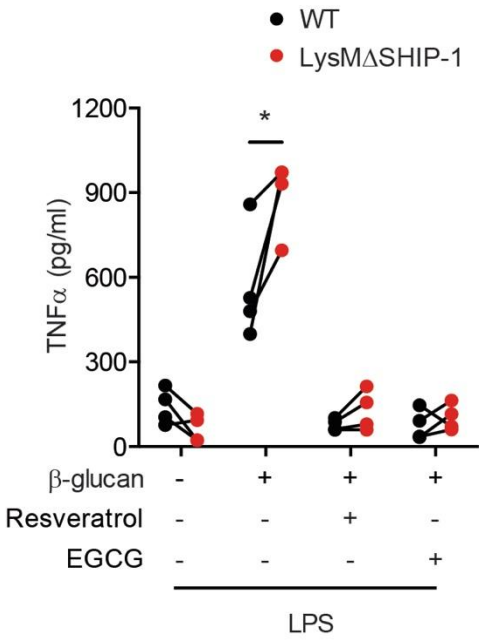

Figure R13. SHIP-1-dependent enhanced training relies on histone acetylation. WT and LysMΔSHIP-1 BMDMs were incubated (+) or not (-) with the histone acetyltransferase inhibitor EGCG or the histone deacetylase activator resveratrol for 30 minutes previous to β-glucan training when indicated (+) and after washing it out. TNFα production was analyzed in supernatants after LPS stimulation according to model in Figure R7A. Individual data corresponding to 4 independent experiments are shown. *p < 0.05, paired Student's t-test comparing WT and LysMΔSHIP-1.

These results highlight SHIP-1 as a regulator of trained immunity by dampening the Akt/mTOR molecular pathway and the glycolytic switch, and relying on the epigenetic reprogramming induced by β-glucans, paradigms of the training process.

4. Myeloid-specific deletion of SHIP-1 improves trained immunity *in vivo.*

4.1. Enhanced β-glucan-induced training in LysMΔSHIP-1 mice.

The generation of trained immunity *in vivo* leads to cross-protection against diverse secondary infections (Hamon and Quintin, 2016, Netea et al., 2016, Netea et al., 2011), being PI3K signaling the canonical molecular pathway in myeloid cells implicated in the development of that trained response (Cheng et al., 2014, Arts et al., 2016b). On the other hand, SHIP-1-deficient macrophages showed heightened trained immunity properties compared to their WT counterparts *in vitro*.

To explore whether training is also regulated *in vivo* by SHIP-1 in the myeloid compartment, as shown *in vitro*, mice were consecutively injected twice with β-glucan, as described (Cheng et al., 2014, Arts et al., 2016a). Initially, to investigate the

regulatory role of myeloid SHIP-1 on cytokine production under that trained conditions, mice were subjected to an LPS-induced endotoxemia model (Arts et al., 2016a) and serum proinflammatory cytokines, such as IL-1β, IL-6 and TNFα were measured **(Figure R14A)**. Of note, under non-trained conditions, myeloid SHIP-1 deficiency only affected LPS-induced IL-6 production **(Figure R14B, middle panel).**

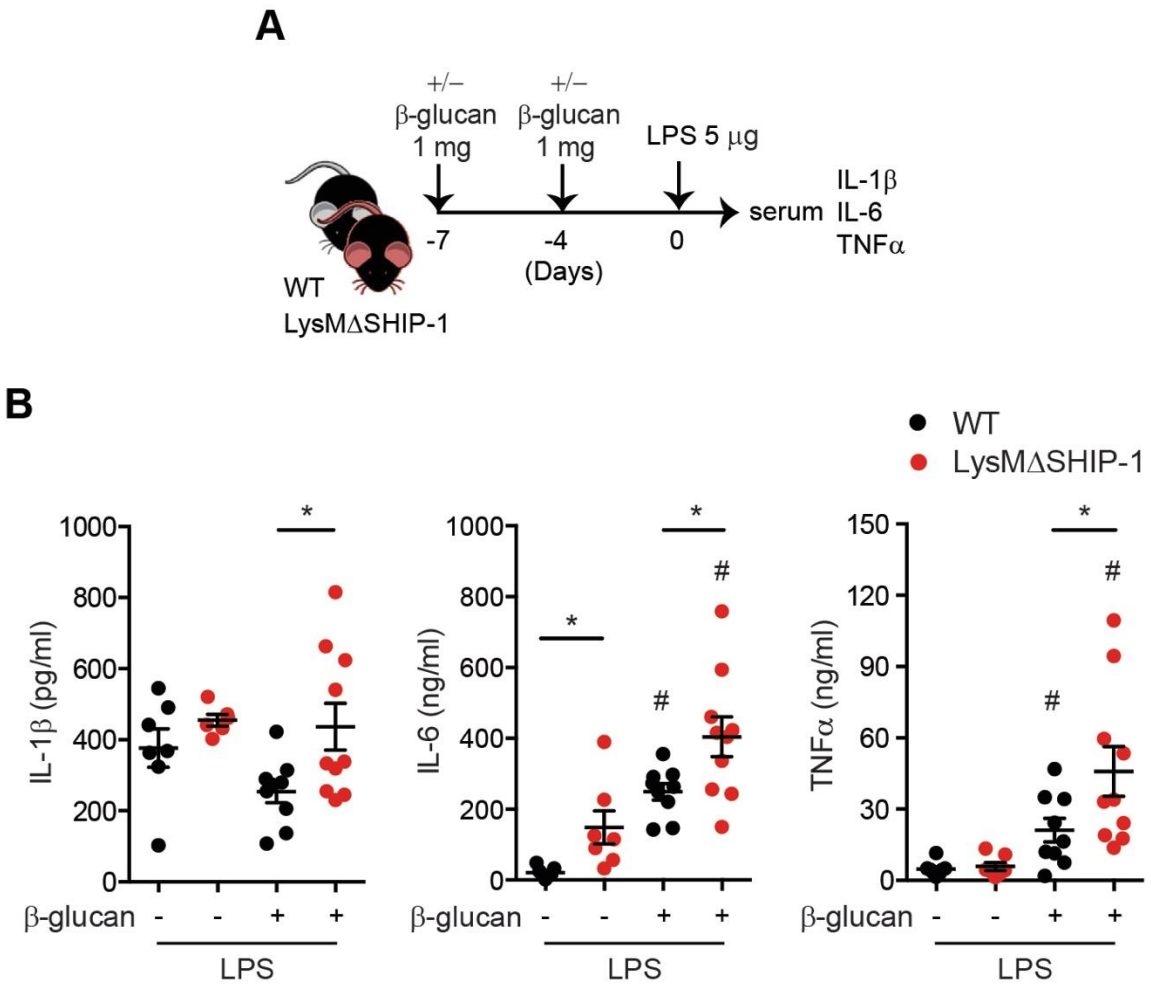

Figure R14. β-glucan-trained LysMΔSHIP-1 mice show a boosted production of inflammatory cytokines in response to LPS. **(A)** *In vivo* training model by two consecutive intraperitoneal administrations of 1 mg of β-glucan and subsequent stimulation with 5 μg of LPS. Serum proinflammatory cytokines, including IL-1β, IL-6 and TNFα were measured. **(B)** WT and LysMΔSHIP-1 mice were trained (+) or not (-) and rechallenged with LPS according to A. Serum was collected 60 (TNFα) or 90 min (IL-1β and IL-6) afterwards. Mean ± SEM of 2 pooled experiments is shown, including at least 5 mice per condition. *p < 0.05, unpaired Student's t-test comparing WT and LysMΔSHIP-1. #p < 0.05, unpaired Student's t-test comparing the same genotype stimulated or not with β-glucan.

LPS-induced levels of IL-6 and TNFα were increased in sera of WT mice receiving the β-glucan pre-treatment **(Figure R14B, middle and right panels)**, indicative of training induction (Quintin et al., 2012), while no training effect was observed for IL-1β in WT mice **(Figure R14B, left panel)**. Importantly, and consistent

with former results *in vitro*, serum levels of all IL-1β, IL-6 and TNFα were further augmented in trained SHIP-1-deficient mice compared to trained WT counterparts **(Figure R14B)**. These data reflect an exacerbated inflammatory response in trained LysMΔSHIP-1 mice and support the regulatory role of SHIP-1 on training also *in vivo*.

Additionally, trained immunity has been revealed as a protective response against lethal systemic *C. albicans* infection, through a mechanism relying on monocytes and macrophages (Quintin et al., 2012). Thus, in order to demonstrate whether the enhanced trained immunity observed in SHIP-1-deficient mice would influence the protection to a secondary infection, after the training with β-glucan, mice were infected with a lethal dose of the clinical isolate *C. albicans* SC5314 (Pitarch et al., 2016) **(Figure R15A)** and survival was monitored.

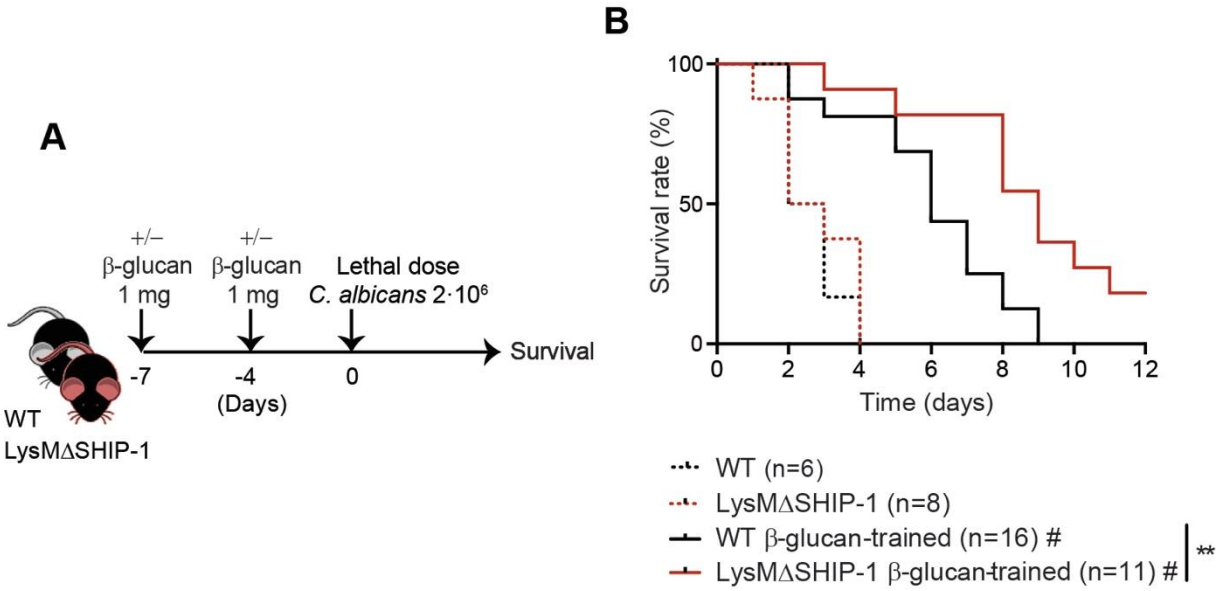

Figure R15. β-glucan-trained LysMΔSHIP-1 mice are better protected against lethal candidiasis. **(A)** *In vivo* training model by two consecutive intraperitoneal administrations of 1 mg of β-glucan and secondary lethal intravenous infection with $2 \cdot 10^6$ *C. albicans*. **(B)** WT and LysMΔSHIP-1 mice were trained (solid lines) or not (dashed lines) and infected according to A. Survival was monitored. A pool of 2 experiments is shown including between 6 and 16 mice per group. $^{**}p < 0.01$, Log-rank test between WT and LysMΔSHIP-1 mice. $\#p < 0.05$, Log-rank test comparing β-glucan-trained or not within the same genotype.

As shown in **Figure R15B (dashed lines)**, all non-trained mice rapidly succumbed upon systemic candidiasis, indicating that SHIP-1 expression in the myeloid compartment is redundant for the primary response to lethal candidiasis. Nevertheless, trained immunity was induced by β-glucan as it expanded the lifespan of WT mice **(Figure R15B, solid lines)**. This confirms that even in such harsh infectious conditions, trained immunity-mediated protection takes place. Importantly,

this conferred protection was further improved in LysMΔSHIP-1 mice, even with survivor animals at the end of the procedure **(Figure R15B, solid lines)**. This observation indicated that SHIP-1 deletion in the myeloid compartment boosts the development of β-glucan-induced trained immunity protection against lethal infections *in vivo*.

4.2. Improved *C. albicans*-conferred trained immunity in LysMΔSHIP-1 mice.

It has been described that the encounter with a nonlethal dose of *C. albicans* protects mice against a secondary lethal reinfection with the same pathogen (Quintin et al., 2012). Thereby, we trained mice with a low dose of *C. albicans*. One week later, we subjected mice to a lethal systemic candidiasis as above **(Figure R16A)**.

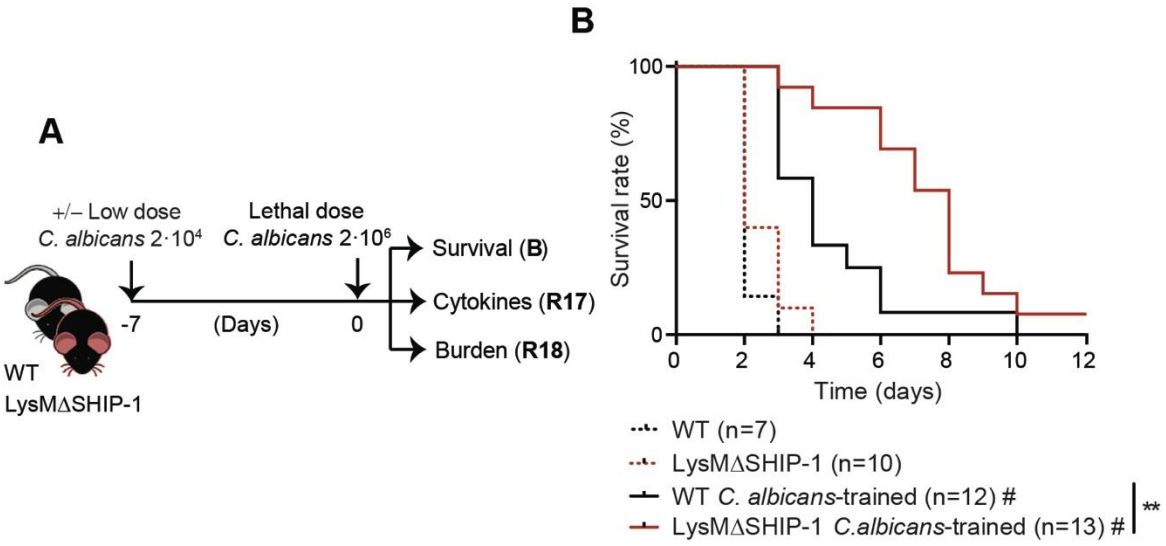

Figure R16. *C. albicans*-trained LysMΔSHIP-1 mice are better protected against lethal reinfection. **(A)** *In vivo* training model by intravenous infection with a low dose of *C. albicans* ($2{\cdot}10^4$) and secondary lethal reinfection with $2{\cdot}10^6$ *Candida albicans* one week later. **(B)** WT and LysMΔSHIP-1 mice were trained (solid lines) or not (dashed lines) and infected according to A. Survival was monitored. A pool of 2 experiments is shown including between 7 and 13 mice per group as indicated. $^{**}p < 0.01$, Log-rank test between WT and LysMΔSHIP-1 mice. #$p < 0.05$, Log-rank test comparing *C. albicans*-trained or not within the same genotype.

Similar to **Figure R15**, non-trained mice died equally, starting as soon as day 2 post-infection **(Figure R16B, dashed lines)**. Concurring with results on β-glucan, trained immunity induced by *Candida* prolonged the survival of WT mice **(Figure R16B,**

solid lines). Again, mice with a specific deletion of SHIP-1 in the myeloid compartment were more resistant against such a harsh infection **(Figure R16B, solid lines)**.

To more deeply characterize mechanisms that could support the enhanced survival observed in trained LysMΔSHIP-1 mice, we harvested kidneys from trained animals at day 2 post-secondary infection, as most of non-trained ones had already deceased. We first evaluated the abundance of trained immunity-involved cytokines in the whole kidney. Correlating to what had been observed *in vitro*, renal IL-1β and TNFα production was increased in *Candida*-lethally infected kidneys from trained LysMΔSHIP-1 mice **(Figure R17, left and right panel)**. Again, no effect was appreciable when assessing IL-6 cytokine **(Figure R17, middle panel)**.

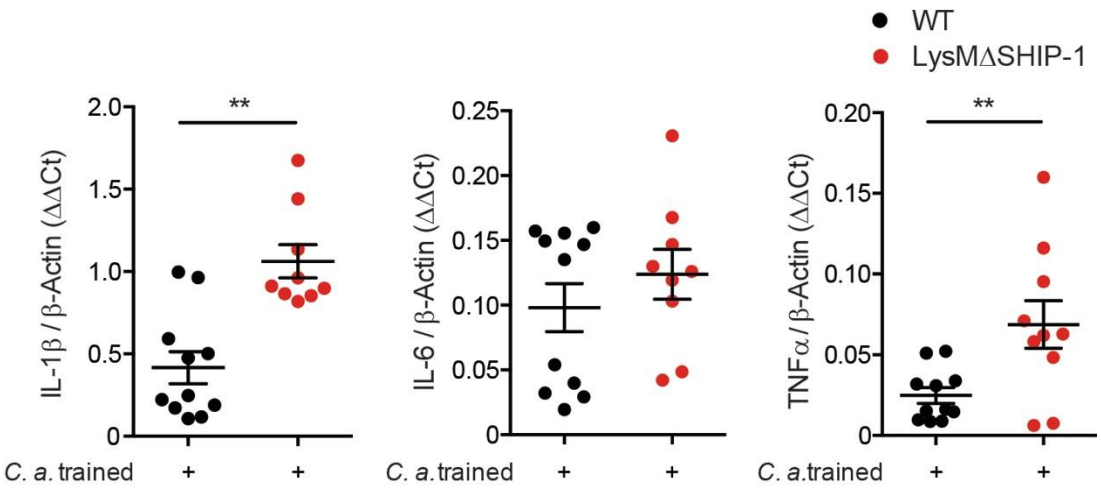

Figure R17. Increased levels of renal inflammatory cytokines in *C. albicans*-trained LysMΔSHIP-1 mice. WT and LysMΔSHIP-1 mice were trained according to Figure R16A. Total renal cytokines at day 2 post-secondary infection were evaluated in trained mice by qPCR and referred to β-Actin levels. Single dots correspond to individual mice. Mean ± SEM of 3 pooled experiments is shown, including at least 9 mice per condition. **p< 0.01, unpaired Student's t-test comparing WT and LysMΔSHIP-1.

Next, we evaluated renal fungal burden from those kidneys at different time points. Compared to WT mice, training in the absence of SHIP-1 led to a decreased amount of fungus in the infected kidneys, reaching statistical significance at day 3 post-infection **(Figure R18)**. These results could explain the increased survival that was appreciated afterwards in LysMΔSHIP-1 mice **(Figure R16B)**.

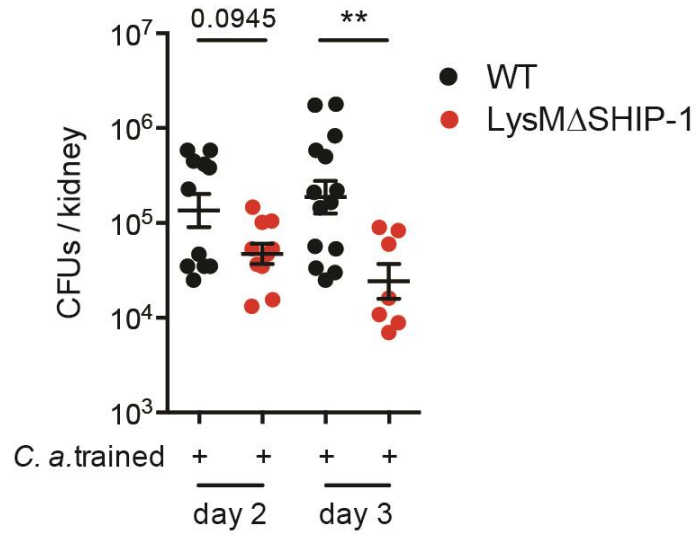

Figure R18. *C. albicans*-trained LysMΔSHIP-1 mice show decreased renal fungal burden. WT and LysMΔSHIP-1 mice were trained according to Figure R16A. Renal fungal burden, determined as CFUs in total kidney, was evaluated at day 2 and 3 post-secondary infection in trained mice. Single dots correspond to individual mice. Mean ± SEM of 3 pooled experiments is shown, including at least 7 mice per condition. **p< 0.01, unpaired Student's t-test comparing WT and LysMΔSHIP-1.

Altogether, these data indicate that SHIP-1 deficiency in the myeloid compartment modulates β-glucan- and *Candida*-induced trained immunity *in vivo*, improving response to pathogen-specific or heterologous challenges.

5. Trained immunity is enhanced upon pharmacological SHIP-1 inhibition.

The great relevance of the PI3K pathway in pathologies such as cancer, has promoted the study of the phosphatase SHIP-1 as a potential therapeutic target (Fernandes et al., 2013). To that end, distinct SHIP-1 inhibitors, such as 3AC (SHIPi) (Brooks et al., 2010), have been developed. In order to extrapolate our results to a more clinically relevant context, we decided to use that inhibitor as a potential therapeutical tool to harness trained immunity.

5.1 SHIP-1 inhibition boosts mouse immune training.

5.1.1. *In vitro*.

First, we tested the use of SHIPi *in vitro*. We applied our characterized trained immunity *in vitro* model to WT BMDMs **(Figure R7A)**, but now including the pharmacological inhibition of SHIP-1 during training induction. Thus, macrophages were pre-exposed

to different doses of 3AC (SHIPi, IC50=13.5 μM; (Brooks et al., 2015)) 30 minutes before β-glucan stimulation and the inhibitor was also added after the first wash-out. TNFα was used as a prototypical readout after resting and secondary LPS stimulation **(Figure R19A)**.

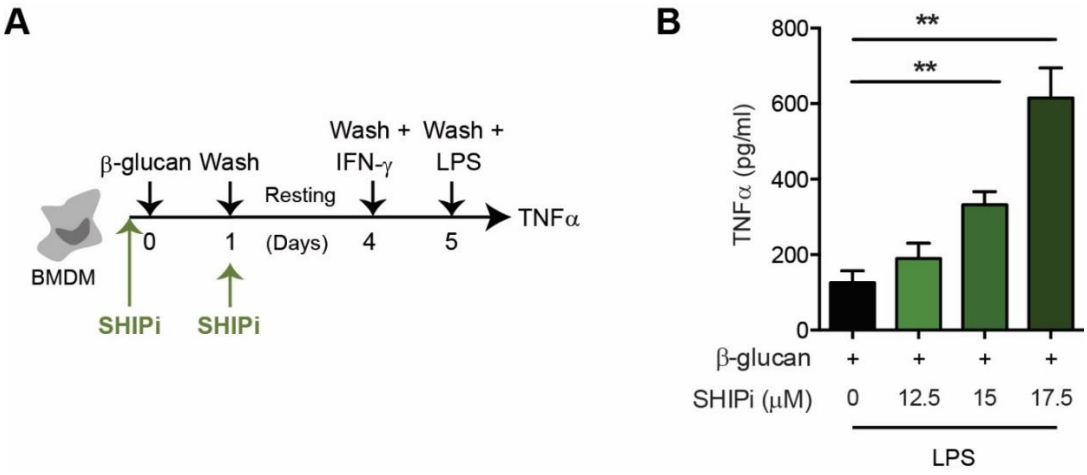

Figure R19. SHIP-1-inhibited trained BMDMs show enhanced trained immunity *in vitro*. **(A)** *In vitro* experimental model applied to BMDMs, indicating when the SHIPi 3AC was added. BMDMs were incubated with SHIPi 30 minutes before β-glucan stimulation and the inhibitor was also included after the first wash-out at the indicated concentrations in B. **(B)** TNFα production was analyzed in supernatants of β-glucan-trained cells after LPS stimulation according to model in A. 4 independent experiments are shown. Data are represented as mean + SEM. Significance was assessed by paired Student's t-test between SHIPi-treated and non-treated cells. **p < 0.01.

As illustrated in **Figure R19B**, and compared to SHIPi non-treated β-glucan trained WT BMDMs, SHIP-1 inhibition increased LPS-induced TNFα production in a dose-dependent manner. Concurring with the narrow activity curve described for 3AC (Brooks et al., 2015), small differences in the concentration of the SHIPi resulted in relevant variations on final TNFα production. Of note, this measurement was only performed in β-glucan-trained cells, as non-trained BMDMs did not survive the 5 day-long *in vitro* culture in the presence of 3AC, while the inhibitor did not affect survival of trained BMDMs. This result indicates the conceivable use of this inhibitor as a therapeutic tool to improve trained immunity.

5.1.2. *In vivo.*

In order to assess whether SHIP-1 inhibitor could be used under *in vivo* infectious conditions, we took advantage of the *Candida albicans*-induced trained immunity model described before **(Figure R16A)**. Mice were subjected twice in consecutive days to SHIPi intraperitoneal administration **(Figure R20A)**, according to a published

'pulsatile' regimen (Gumbleton et al., 2017). The second day of 3AC administration coincided with training with the low dose of *C. albicans* infection. One week afterwards, mice were lethally infected with the same fungus and survival was monitored. Concurring with previous results, non-trained mice rapidly succumbed, and inhibition of SHIP-1 did not affect survival of non-trained mice **(Figure R20B, dashed lines)**, suggesting that the phosphatase is redundant during *C. albicans* lethal infection. Importantly, SHIP-1 inhibition further improved the protection to systemic candidiasis conferred by *C. albicans* training, **(Figure R20B, solid lines)**, indicating that chemical inhibition of SHIP-1 boosts trained immunity *in vivo*.

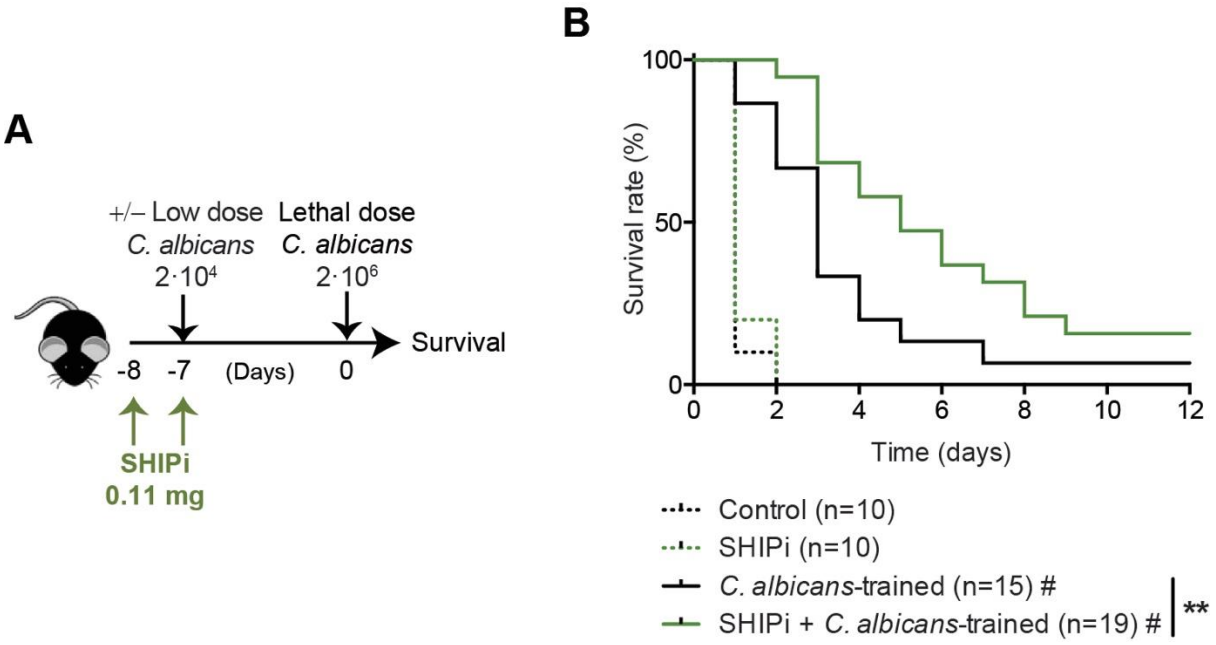

Figure R20. SHIP-1 inhibition improves training-based protection against lethal candidiasis. **(A)** *In vivo* model of training by a systemic infection with a low dose of *Candida albicans* ($2{\cdot}10^4$) in the presence of SHIP-1i followed by a second lethal challenge ($2{\cdot}10^6$) with the same pathogen. When indicated, 0.11 mg of the inhibitor was administered intraperitoneally. **(B)** Survival curve of diluent-(Control) or SHIPi-treated mice according to model in A. A pool of 2 experiments is shown including between 10 and 19 mice per group. $^{**}p < 0.01$, Log-rank test between SHIPi-treated or not under the same experimental conditions (either trained or not). $\#p < 0.05$, Log-rank test comparing *C. albicans*-trained or not under the same treatment (either control or SHIPi-treated).

5.2. Enhanced trained immunity in human peripheral blood mononuclear cells by inhibiting SHIP-1.

Finally, we wondered whether SHIP-1-mediated enhancement of trained immunity could also work on human cells. For that, we tested the SHIPi inhibitor in hPBMCs from buffy coats obtained from healthy donors. Cells were subjected to a well-established trained immunity model *in vitro* for those cells (Quintin et al., 2012), but exposing them

to SHIP-1 inhibitor 30 minutes before β-glucan training. Next, hPBMCs were washed out, keeping them in SHIPi-containing medium and rested for 6 days. Finally, they were rechallenged with LPS and cytokines involved in the trained immunity phenomenon were evaluated **(Figure R21A)**. As happening with mouse BMDMs, detection of cytokines was only performed in β-glucan-trained hPBMCs, as SHIPi was toxic for non-trained cells. Notably, the administration to hPBMCs of 10 μM of SHIPi during β-glucan training increased the production of IL-1β, IL-6 and TNFα after LPS stimulation **(Figure R21B)**.

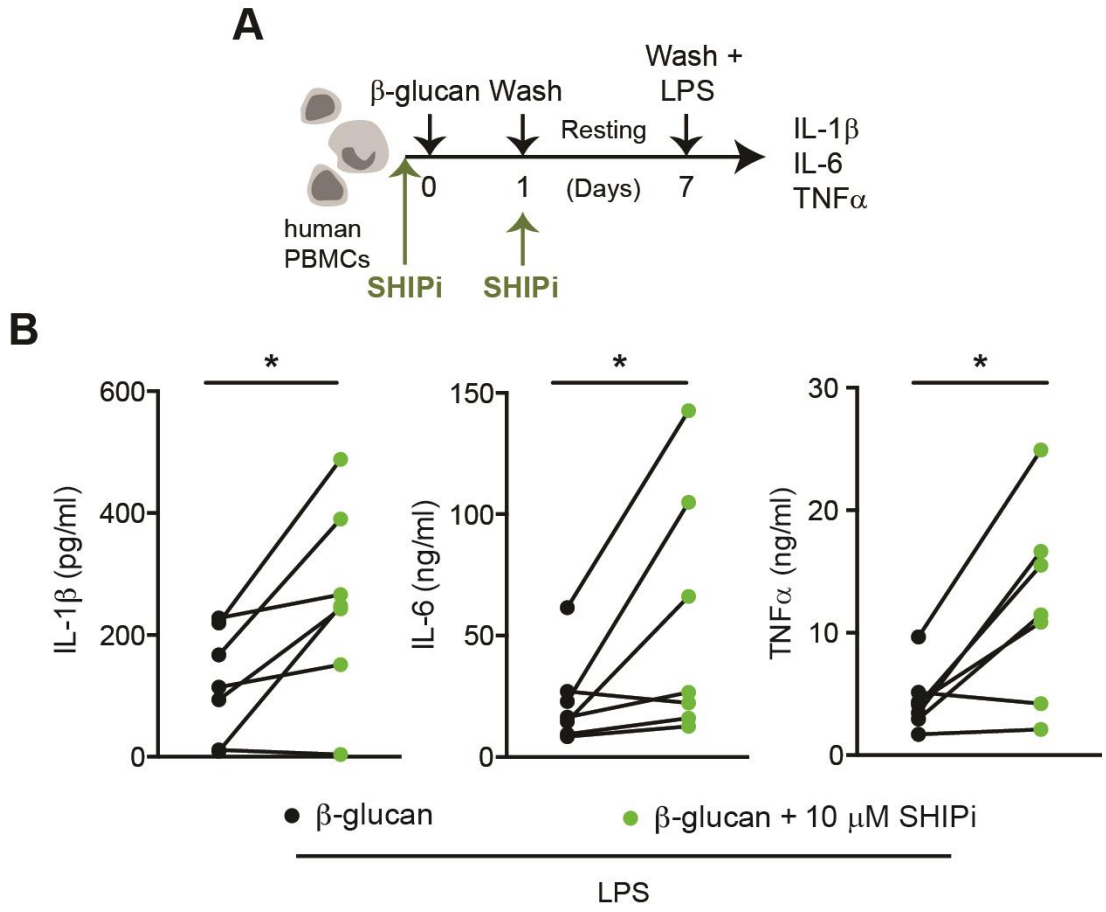

Figure R21. SHIP-1 inhibition boosts trained immunity in hPBMCs. **(A)** *In vitro* experimental model applied to hPBMCs, indicating when SHIPi was added. Briefly, hPBMCs were pre-exposed to 10 μM SHIPi and trained with 100 μg/ml β-glucan. Cells were washed and rested in SHIPi-containing medium for 6 days. Finally, hPBMCs were rechallenged with 1 μg/ml of LPS and proinflammatory cytokines were measured after 24 hours. **(B)** IL-1β, IL-6 and TNFα production was analyzed in supernatants of β-glucan-trained hPBMCs after LPS stimulation according to model in A. Samples from 7 independent buffy coats are shown. *$p < 0.05$, paired Student's t-test between SHIP-1i-treated and non-treated cells.

Thus, our data indicate that SHIP-1 can be targeted with pharmacological inhibitors both in mice and human cells to boost trained immunity.

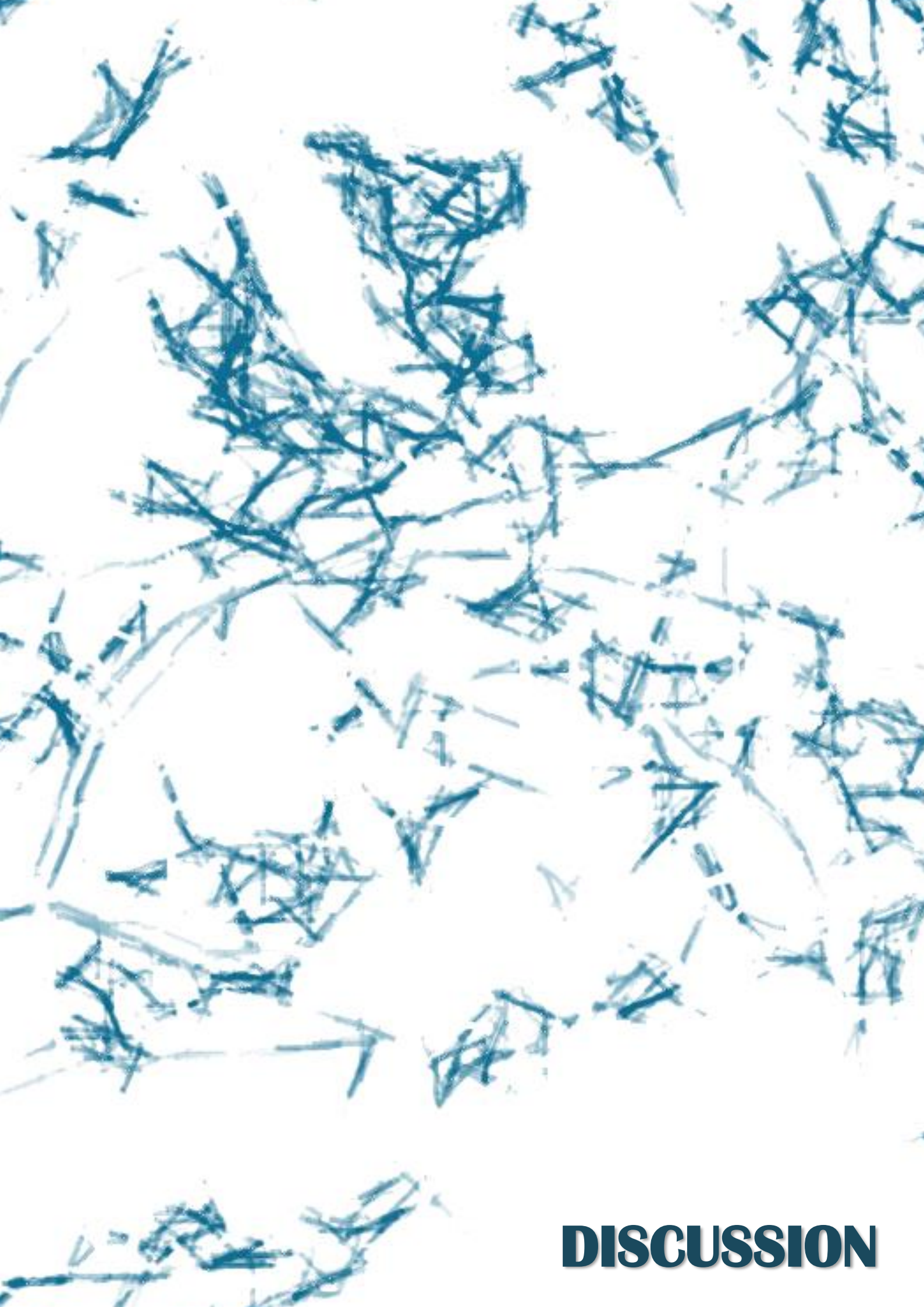

DISCUSSION

Development of trained immunity upon diverse triggering stimulus such as β-glucan (Cheng et al., 2014) or BCG vaccine (Arts et al., 2016b) relies on activation of the PI3K/Akt pathway. In fact, both β-glucan- and BCG-induced trainings were abolished in the presence of the PI3K inhibitor wortmannin (Cheng et al., 2014, Buffen et al., 2014). On the other hand, former results in our laboratory indicated that Dectin-1, the main β-glucan receptor (Rosas et al., 2008), associates to SHIP-1 (Blanco-Menendez et al., 2015), a phosphatase critically involved in PI3K regulation (Eramo and Mitchell, 2016). Taking this into account, we initially hypothesized that modulation of PI3K activity via SHIP-1 targeting, could result in the improvement of trained immunity induced by Dectin-1 ligands such as β-glucan or *Candida albicans*.

1. Role of SHIP-1 upon β-glucan-/*Candida*-induced training.

In accordance with previous studies (O'Connell et al., 2009, Zhou et al., 2006), SHIP-1 protein was expressed in BMDMs in steady state conditions. Moreover, β-glucan stimulation augmented the basal expression of the phosphatase, which suggested a likely involvement of SHIP-1 in β-glucan-induced immune training of these myeloid cells. As summarized in **Figure D1**, SHIP-1 depletion led to an intrinsic enhancement of cytokine production in trained macrophages, particularly of TNFα and IL-1β, proinflammatory cytokines previously associated with trained immunity (Quintin et al., 2012, Ifrim et al., 2014, Bekkering et al., 2016a, Walachowski et al., 2017). This outcome was accompanied by increased PI3K/Akt/mTOR pathway activation and enhancement of other trained immunity hallmarks such as the switch to glycolytic metabolism. That boosted immune training relied on epigenetic reprogramming, as both histone methylation and acetylation were key processes for SHIP-1-mediated effect on this trained immunity. *In vivo*, this turned into increased cytokine production upon rechallenge and better protection against reinfection in trained mice with a specific deletion of SHIP-1 in the myeloid compartment. Increase in proinflammatory cytokines and improved protection upon training were also achieved by means of SHIP-1 chemical inhibition and, finally, translated to trained hPBMCs.

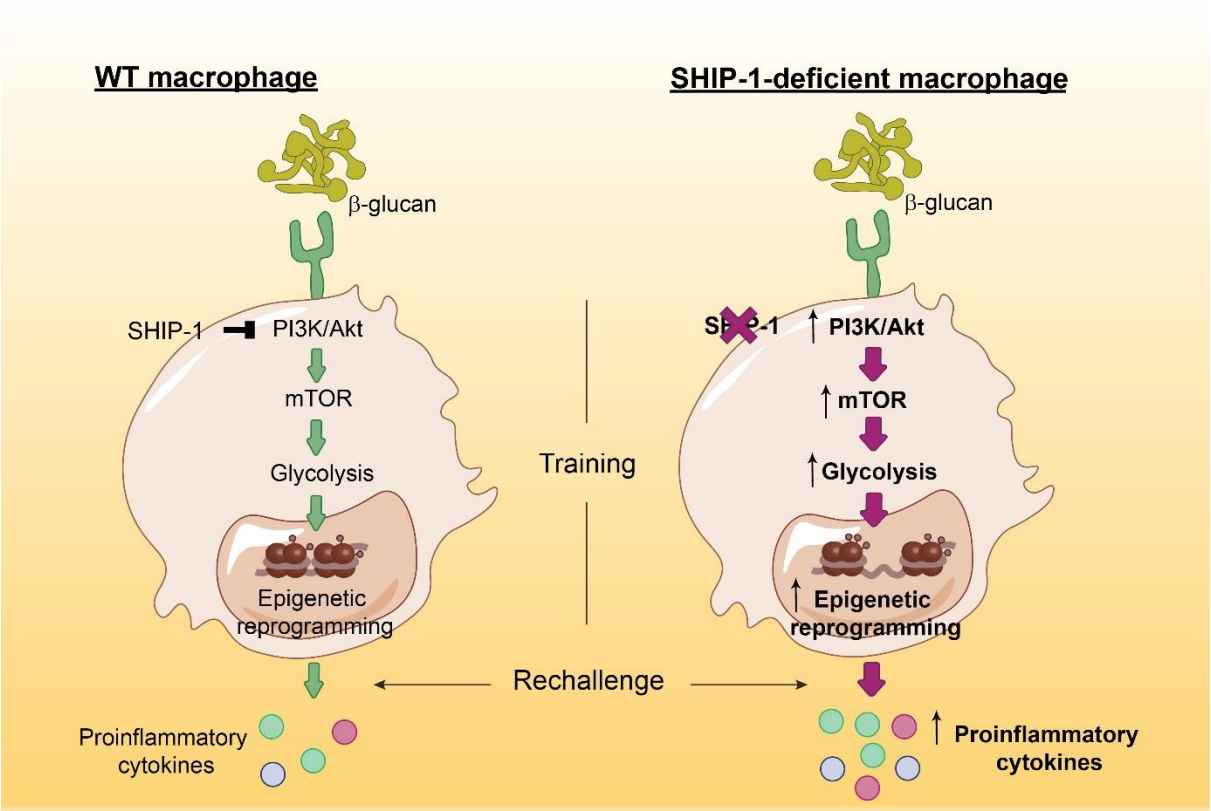

Figure D1. Working model for SHIP-1-mediated effect on trained immunity at the molecular level. In WT macrophages, β-glucan training leads to activation of PI3K/Akt/mTOR pathway, which results in a switch to glycolysis and epigenetic reprogramming. Upon stimulation with a secondary challenge, trained cells produce high levels of proinflammatory cytokines such as IL-1β or TNFα (left). Under SHIP-1-deficient settings, β-glucan priming results in an increased pathway activation, an enhanced shift to glycolytic metabolism and a more pronounced epigenetic reprogramming. Consistently, upon rechallenge, SHIP-1-deficient or SHIP-1-inhibited trained macrophages overproduce these proinflammatory cytokines (right).

In vitro β-glucan-mediated induction of trained immunity has been previously described for human mononuclear phagocytes (Cheng et al., 2014), hPBMCs (Ifrim et al., 2013), purified murine splenic monocytes (Garcia-Valtanen et al., 2017), peritoneal macrophages and BMDMs (Walachowski et al., 2017). Compared to the latter study in BMDMs, where establishing a short-term trained immunity *in vitro* model (Walachowski et al., 2017)**,** here we set up a long-term *in vitro* scheme, which better resembles the long-lasting effect that it is reached in this phenomenon. In our 6-day long *in vitro* protocol for BMDM training and challenge, a previous IFN-ɣ priming to detect any TNFα production upon LPS stimulation was needed, regardless of the β-glucan training induction. This concurs with classical activation of mouse macrophages, which establishes that these cells need a combination of two signals to be activated, a priming step and a triggering stimulus. For *in vitro* activation of mouse peritoneal macrophages

and BMDMs, a generally established protocol consists of priming macrophages with IFN-ɣ and subsequent stimulation, for instance, with a TLR ligand such as LPS (Mosser and Zhang, 2008). This two-step protocol allows the detection of cytokine production such as TNFα in response to LPS (Holden et al., 2014). This indeed would concur with the fact that BMDM differentiation in presence of M-CSF results in macrophages with a M2-like polarized state that could need to be primed to overcome M2 polarization and produce proinflammatory mediators upon TLR ligand stimulation (Ushach and Zlotnik, 2016, Hamilton, 2008). Supporting the notion that the use of IFN-ɣ for priming cytokine production is a particular feature of the mouse BMDM *in vitro* model, this priming was not necessary for any of the other *in vivo* or *in vitro* models tested. This fact also includes hPBMCs, where we reproduced an established and previously published trained immunity *in vitro* model (Quintin et al., 2012).

β-glucan training and, additionally, SHIP-1 absence in β-glucan-trained macrophages, enhanced the production of IL-1β and TNFα. Conversely, neither training nor the SHIP-1-mediated effect was observed for IL-6 in BMDMs. The lack of effect in this particular cytokine could be explained by specific features of the *in vitro* model, such as the high IL-6 production detected already in non-trained conditions (in the order of ng/ml). Moreover, SHIP-1-dependent modulation of training was not observed either in terms of renal IL-6 *in vivo*. It has been described that, upon a particular stimulus, the involvement of differential molecular pathways accounts for diverse expression patterns of IL-6 compared to IL-1β and TNFα (Palmer et al., 2008, Lim et al., 2014, Khalaf et al., 2010, Keller et al., 2006). These pathways could be selectively modulated following β-glucan training and, in turn, differentially regulated by SHIP-1 upon training conditions. On the other hand, no training effect was appreciable for serum IL-1β *in vivo* upon challenge with LPS, whereas IL-6 was increased in non-trained LysMΔSHIP-1 mice, which could be explained because of the kinetics, dosage or experimental settings used (Quintin et al., 2012, Arts et al., 2016a). Still, the production of all these trained immunity-associated cytokines was boosted in SHIP-1-deficient mice upon β-glucan training.

We barely appreciated effect of SHIP-1 on direct LPS-triggered production of proinflammatory cytokines, as no differences between WT and SHIP-1-deficient macrophages were found under non-trained conditions. This could be controversial according to previous studies claiming that SHIP-1 expression in macrophages

modulates cytokine production (An et al., 2005, Sly et al., 2004). The difference could reside on the fact that BMDMs in our model were stimulated with LPS after 5 days of *in vitro* procedure and not immediately after differentiation. Interestingly, the lack of effect of SHIP-1 without training would be reinforced by the similar epigenetic status found in non-trained WT versus SHIP-1-deficient BMDMs, as the amount of activating H3K4me3 mark at the TNFα promoter was equivalent. As epigenetics controls macrophage phenotype (de Groot and Pienta, 2018), a plausible explanation would be that this period in culture affected LPS-associated epigenetic modifications independently of SHIP-1 in non-trained cells, what would lead to a comparable response, but the analysis of BMDMs at day 0 would be needed to address this hypothesis. In any case, our data indicate that SHIP-1 regulates cytokine production upon trained conditions.

PI3K-induced Akt signaling pathway controls a plethora of key processes including cell growth, proliferation and survival (Eramo and Mitchell, 2016). Some studies have associated trained immunity induction with enhanced survival, specifically described for murine spleen-derived and human monocytes (Garcia-Valtanen et al., 2017, Bekkering et al., 2016a). Consistent with them, we recovered increased number of live WT cells upon β-glucan priming. Other studies however, have not considered a potential increase in viability upon training, and did not evaluate trained immunity readouts in a cell-based manner (Quintin et al., 2012, Cheng et al., 2014, Saeed et al., 2014). Thereby, the final outcome could be overestimated due to an augmented number of cells. To ensure a cell-intrinsic analysis of trained immunity parameters, we plated cells equally before the assay (e.g. for glycolytic flux evaluation) or normalized cytokine production to the relative number of cells per condition. When doing that, we still observed an intrinsic effect on cytokine production and other hallmarks associated with trained immunity, further enhanced by SHIP-1 deletion or inhibition. This would accord with a previous study on human monocytes, where training was maintained after normalization to cell counts (Bekkering et al., 2016a). Nevertheless, it would disagree with the study from Garcia-Valtanen and colleagues, where an increased survival and not the β-glucan training effect explained the elevated cytokine production in spleen-derived and human monocytes. These divergences could be explicated because of the dosage, β-glucan source, glucan form or experimental settings, but

experimental procedures should be unified to make studies comparable and more reproducible.

Consistent with regulation of PI3K signaling pathway, Akt overactivation upon SHIP-1 deletion entails a survival advantage that has been previously described (Liu et al., 1999, Rothchild et al., 2016, Antignano et al., 2010a). This fact was reproduced in non-trained SHIP-1-deficient BMDMs, whose numbers at the end of the *in vitro* protocol was approximately three-fold compared to their WT counterparts. However, although β-glucan training increased survival of WT cells, the number of β-glucan-trained cells was comparable between WT and LysMΔSHIP-1 BMDMs. This could suggest either a maximal survival or proliferative capacity of SHIP-1-deficient macrophages in basal conditions that cannot be further increased upon training.

The increased basal Akt phosphorylation found in SHIP-1-deficient BMDMs concurred with a similar trend on the activation of mTOR targets. Consistently, a steady state increase in glycolytic metabolism also occurred in SHIP-1-deficient BMDMs although it was further increased upon β-glucan training. However, this basally increased pathway activation and glycolytic switch was not translated into differential epigenetic modifications under non-trained conditions. Subsequently, it did not result in higher cytokine production upon rechallenge unless β-glucan-induced trained immunity was established, indicating a specific role of SHIP-1 upon training. Altogether, these data suggest that SHIP-1 deficiency generates a pro-glycolytic state that allows a divergent epigenetic reprogramming and a boosted inflammatory response only upon β-glucan-trained conditions.

From our results *in vivo*, we are placing SHIP-1 as a target to improve β-glucan- and *C. albicans*-induced myeloid-dependent trained immunity, grounded in the conditional myeloid deletion of SHIP-1 driven by the LysM promoter. Cre recombinase, under the control of this myeloid promoter, has been extensively used to evaluate functions in monocytes and macrophages (Zhu et al., 2014, Han et al., 2013, Schappe et al., 2018), but also targets other populations such as neutrophils (Cross et al., 1988, Clausen et al., 1999). Although neutrophils are key mediators in *C. albicans* immune response (Dejima et al., 2011), there were no differences in the primary response to the fungus between WT and LysMΔSHIP-1 mice unless trained immunity was induced. Moreover, immune training has not been described for neutrophils, while a

fundamental role for C-C chemokine receptor type 2-expressing cells such as inflammatory monocytes and macrophages has been established (Quintin et al., 2012). These data, together with results *in vivo*, allow us to consider that the observed phenotype relies essentially in monocytes/macrophages. Nevertheless, evaluation of the intrinsic activity of neutrophils in WT and LysMΔSHIP-1 mice, under both non-trained and trained conditions, would merit further investigation to formally discard an effect on this population.

Enhancement of trained immunity by SHIP-1 targeting would concur with impaired induction of endotoxin tolerance under SHIP-1-deficient settings (Sly et al., 2004), as both innate memory processes could be considered as antagonistic. Thus, it would be interesting to further study whether SHIP-1-dependent metabolism could tip the scale toward the development of one memory program or the other in innate immune cells.

Beyond SHIP-1 involvement, a key novelty of this work is the proof of concept of trained immunity improvement. To our knowledge, no strategies to potentiate the beneficial inflammatory behavior of trained innate immune cells have been proposed. In this line, in a short-term model of trained immunity *in vitro*, the exogenous addition of recombinant GM-CSF showed an accessory contribution to prime macrophages (Walachowski et al., 2017). However, GM-CSF was not directly involved in the β-glucan-mediated long-lasting mechanism and could prime additional signals through the mitogen-activated protein kinase pathway (Borriello et al., 2016). Conversely, we are showing an intrinsic improvement by acting on the canonical trained immunity pathway, together with a long-lasting effect also appreciable *in vivo.*

2. SHIP-1 inhibition.

In addition to SHIP-1 genetic targeting, we are providing a pharmacological approach to reach it, namely, the use of the SHIP-1 inhibitor 3AC. This inhibitor provided a dose-dependent modulation on cytokine production in trained BMDMs. This fact would allow a gradual modulation of trained immunity which could be adjusted depending on the desired effect. For instance, immune training could be boosted at maximum in case of

a harsh infection but could be also controlled to avoid excessive inflammation if needed.

Due to the regulatory effect of SHIP-1 in receptor-triggered inflammatory responses (Pauls and Marshall, 2017), germline-deficient SHIP-1 mice display reduced lifespan due to gross inflammatory abnormalities, including splenomegaly, hematopoietic abnormalities, autoantibody-mediated autoimmunity, consolidating pneumonia and Crohn's disease-like ileitis (Helgason et al., 1998, Kerr et al., 2011, Maxwell et al., 2011). Considering this excessive inflammation upon SHIP-1 deficiency, 3AC *in vivo* administration has to be tightly regulated to avoid pleiotropic detrimental effects. Daily administration of 3AC has been used (Brooks et al., 2015, Fernandes et al., 2015), with no apparent effect on morbidity neither recapitulating the phenotype of full SHIP-1-deficient mice. Nevertheless, a pulsatile but not extended dosing strategy of 3AC *in vivo* has been described as successful anti-tumor immunotherapy (Gumbleton et al., 2017). Notably, this administration schedule was of particular interest for us to achieve SHIP-1 inhibition only during the training phase, not influencing directly the response to secondary lethal *Candida albicans*. Moreover, this regime allows to reduce toxic or side effects although still, they cannot be completely excluded.

Indeed, in our hands, 3AC administration led to undesired toxicity in non-trained cells, both in BMDMs and hPBMCs. Thus, in the design of therapeutic uses of 3AC in the context of trained immunity, it is reasonable that both 3AC and the training stimulus should be administered at the same time to prevent deleterious effects of SHIPi. On the other hand, other pan-SHIP inhibitors (Fuhler et al., 2012, Russo et al., 2015) and, more importantly, specific SHIP-1 inhibitors (K118) (Brooks et al., 2015, Srivastava et al., 2016) have been also developed and tested. The existence of these battery of inhibitors opens the possibility to be also used for trained immunity modulation.

It has been described that the SHIP-1 inhibitor 3AC could influence other mature cells than macrophages such as T cells (Collazo et al., 2012, Fernandes et al., 2015, Brooks et al., 2015) and NK cells (Fernandes et al., 2015). Concurring with this, 3AC administration enhanced anti-tumor effector functions of $CD8^+$ T cells and NK cells (Gumbleton et al., 2017). Although 3AC could be influencing this cells, it is important to consider that the primary response to systemic candidiasis is independent of T cells (Jensen et al., 1993), and mainly relies on innate immune cells such as neutrophils

(Dejima et al., 2011), NK cells for neutrophil licensing (Bar et al., 2014) and monocytes (Ngo et al., 2014, Lionakis, 2014). Moreover, the *C. albicans*-induced training model that we have used is independent of T/B lymphocytes and NK cells, relying on myeloid cells (Quintin et al., 2012). This statement is also based on studies using the LysM-Cre recombinase mouse model (Cheng et al., 2014). All these facts would reinforce the involvement of the innate rather than the adaptive immunity in the increased protection we observed, however we cannot rule out effects of 3AC in T or B cells that could occur in parallel and/or influence the final outcome *in vivo*. Finally, systemic inhibition of SHIP-1 could also influence other non-myeloid cells such as NK cells, where indeed trained immunity features have been also described (Hammer and Romagnani, 2017). In any case, considering the potential therapeutic use of SHIPi *in vivo* to enhance innate immune training, it would be interesting to fully dissect the actual cellular mechanism involved in its beneficial effect.

Modulation of myeloid progenitors in the bone marrow has been shown as an integral component of trained immunity (Mitroulis et al., 2018, Kaufmann et al., 2018). Trained immunity inducers such as β-glucan (Mitroulis et al., 2018) or BCG (Kaufmann et al., 2018) expanded bone marrow progenitors including LSK and HSCs, with a particular bias to the myeloid lineage (multipotent progenitors -MPPs- and granulocyte-macrophage progenitors). This expansion was associated with metabolic, epigenetic and transcriptional reprogramming of those progenitors (Kaufmann et al., 2018, Mitroulis et al., 2018) and finally resulted in reprogramming of trained-BMDMs and improved clearance of *Mtb* (Kaufmann et al., 2018). On the other hand, it has been also proved that 3AC administration expanded the HSC compartment (Brooks et al., 2015), including LSKs, HSCs and MPPs. This expansion was accompanied by an increase in serum granulocyte colony-stimulating factor (Brooks et al., 2015), also augmented in bone marrow extracellular fluid upon training (Mitroulis et al., 2018). Taking altogether, further studies would be needed to decipher whether SHIP-1 could be also involved in trained immunity modulation by influencing bone marrow progenitors. In this regard, transfer of what Gumbleton and colleagues called hematolymphoid cells (bone marrow and splenocytes) from tumor-challenged, 3AC-treated, long-term surviving mice, protected naïve recipients against tumor challenge (Gumbleton et al., 2017). This transferred protective immunological memory could emerge from an expansion of the T cell memory compartment due to SHIP-1 inhibition;

however, it could also be possible a training effect mediated by SHIP-1 inhibitor on transferred bone marrow progenitors.

3. Expanding the implication of SHIP-1 in trained immunity.

Our data directly link β-glucan-mediated training with SHIP-1. Nevertheless, it would not be surprising the involvement of this phosphatase in some other trained-related contexts, especially those mediated by PI3K/Akt signaling pathway.

For instance, BCG vaccination promotes trained responses against a variety of pathogens (Kleinnijenhuis et al., 2014a, Kleinnijenhuis et al., 2012, de Bree et al., 2018) and confers cross-protection to *Candida albicans* (Kleinnijenhuis et al., 2012) or human viral infections (Arts et al., 2018b). Interestingly, BCG vaccination induced the expression of the miR-155 (Huang et al., 2015) through PI3K signaling pathway in macrophages (Ghorpade et al., 2012). Notably, miR-155 is known to repress SHIP-1 through direct interaction with the phosphatase RNA (O'Connell et al., 2009). In fact, this repression occurred upon BCG-triggered responses (Wang et al., 2014), resulting in modulation of ROS production by macrophages (Wang et al., 2014) and apoptotic cell death (Huang et al., 2015, Ghorpade et al., 2012). Thus, SHIP-1 could be a direct mediator of BCG-induced trained responses. In addition, SHIP-1 displayed an inhibitory function in the nucleotide-binding oligomerization domain-containing protein 2 signaling (Conde et al., 2012), the BCG-mediated trained immunity pathway (Kleinnijenhuis et al., 2012, Arts et al., 2015), what could make interesting the combined use of SHIP-1 inhibitor with BCG to improve its training protective effect. In this way, SHIP-1 inhibition could represent a broad strategy to boost trained immunity.

Trained immunity has been also proposed as adjunctive immunotherapy in cancer (Netea et al., 2017, Buffen et al., 2014, Stevens et al., 2016). On one hand, the enhanced effector functions of trained innate immune cells would help to eliminate microbes that could promote antigen-dependent lymphoproliferation (Stevens et al., 2016). Moreover, immune training could enhance anti-tumor immunity by reversing the immunosuppressive tumor microenvironment (Netea et al., 2017, Buffen et al., 2014, Stevens et al., 2016). In this regard, a correlation has been established between BCG-mediated training and bladder cancer (Buffen et al., 2014). Single nucleotide polymorphisms in autophagy genes that correlated with increased training, were also

associated with better prognosis in BCG-treated patients suffering bladder cancer (Buffen et al., 2014). On the other hand and considering the great relevance of PI3K pathway in cancer (Martini et al., 2014), there are also increasing applications of SHIP-1 antagonists, including 3AC, with successful results in cancer treatment (Brooks et al., 2010, Fuhler et al., 2012, Gumbleton et al., 2017). Taking this into account, together with the improvement of trained immunity by SHIP-1 inhibition, it would be interesting to study the combo effect of SHIP-1 inhibition plus training induction in cancer immunotherapy.

Although enhanced innate immune responses in trained immunity raise as an important host defense mechanism against infections, several maladaptive states that are based on excessive inflammation could result from trained immunity induction (Netea et al., 2016, Leentjens et al., 2018). In this regard, diverse endogenous danger signals from injured tissues can trigger long-term reprogramming of cytokine production through epigenetic regulation of transcriptional program (Crisan et al., 2016b). Atherosclerosis has been extensively postulated as an example of such diseases (Christ et al., 2016, Leentjens et al., 2018, Bekkering et al., 2013). This is supported by oxLDL-mediated induction of trained immunity in human monocytes (Bekkering et al., 2016a, Bekkering et al., 2014) together with the trained immunity-like phenotype present in circulating monocytes from symptomatic atherosclerosis patients (Bekkering et al., 2016b). In this sense, metabolic and epigenetic reprogramming of innate immune cells could also sustain the proinflammatory phenotype observed during cardiovascular diseases (Hoogeveen et al., 2018).

hPBMCs from patients with gout also display enhanced proinflammatory cytokine production, likely due to a harmful uric acid-induced training (Crisan et al., 2016a, Crisan et al., 2017). Moreover, monocytes and macrophages of a wide variety of autoimmune diseases and autoinflammatory disorders, such as rheumatoid arthritis, systemic lupus erythematosus (Arts et al., 2018a) or Hyper-IgD syndrome (Bekkering et al., 2018) share a constitutive and damaging trained immunity-like phenotype in terms of cytokine production, metabolic changes and/or epigenetic rewiring. Under these settings, caution is needed about the potential deleterious effects of trained immunity in all these inflammatory processes, where SHIP-1 activators (Ong et al., 2007, Viernes et al., 2014) such as AQX-1125 (Stenton et al., 2013b, Stenton et al.,

2013a) rather than inhibitors, could be potentially used to ameliorate an excessive and detrimental activation of trained immunity.

On the other hand, it has been shown that a single peripheral acute LPS administration induced microglia immune training, which led to microglial metabolic and epigenetic reprogramming, correlating with increased brain proinflammatory cytokines and exacerbated pathology in Alzheimer's disease (AD) and stroke (Wendeln et al., 2018). Moreover, in the context of microglial priming, trained immunity has been postulated to contribute to brain aging (Haley et al., 2017) and neuropsychiatric disorders (Salam et al., 2017). Although the role of SHIP-1 phosphatase in microglia and AD pathology is not fully understood (Malik et al., 2015), these evidences would suggest that SHIP-1 inhibition, by boosting microglia-dependent training, could be detrimental for neurological disorders and stroke.

In summary, our data indicate that the trained immunity process can be boosted. Moreover, SHIP-1 targeting by means of inhibitors could be proposed as potential pharmacological tools to improve trained immunity **(Figure D2)**.

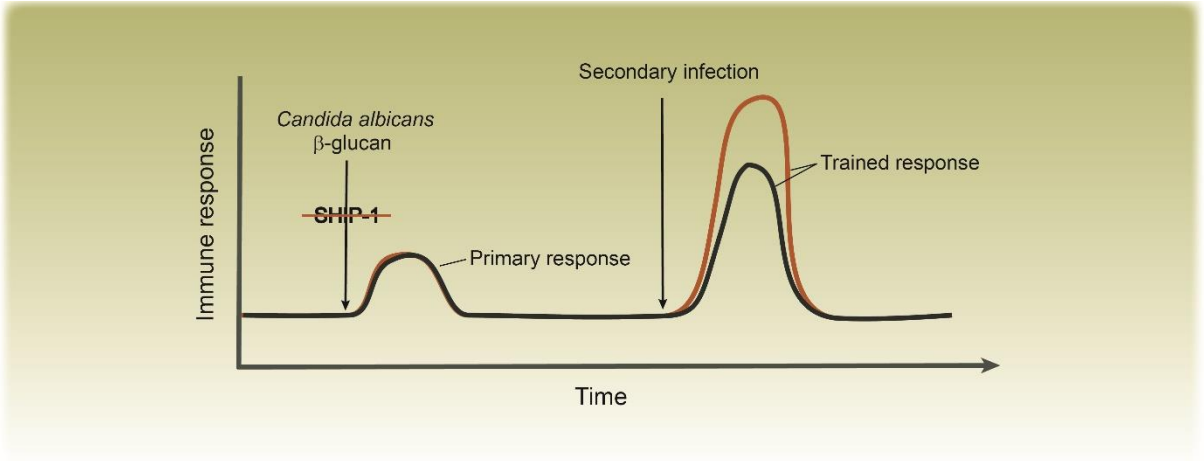

Figure D2. Enhanced trained immunity phenomenon by targeting SHIP-1. Compared to previous described induction of trained immunity (black line), SHIP-1 targeting during *Candida albicans* or β-glucan priming results in an enhanced trained immune response upon a secondary challenge (brown line), which is protective under infectious settings.

This phenomenon has emerged as a potent branch for innate host defense, being postulated that trained immunity could be applied to reversion of sepsis-induced endotoxin tolerance (Novakovic et al., 2016) and especially treatment of infections (Quintin et al., 2012, Cheng et al., 2014). Nevertheless**,** deciphering mechanisms whereby it may be boosted will be crucial to face new challenges such as increasing

virulent and drug-resistant infections, and to design new-generation vaccines that combine both adaptive and innate immune memory (Netea et al., 2016, van der Meer et al., 2015).

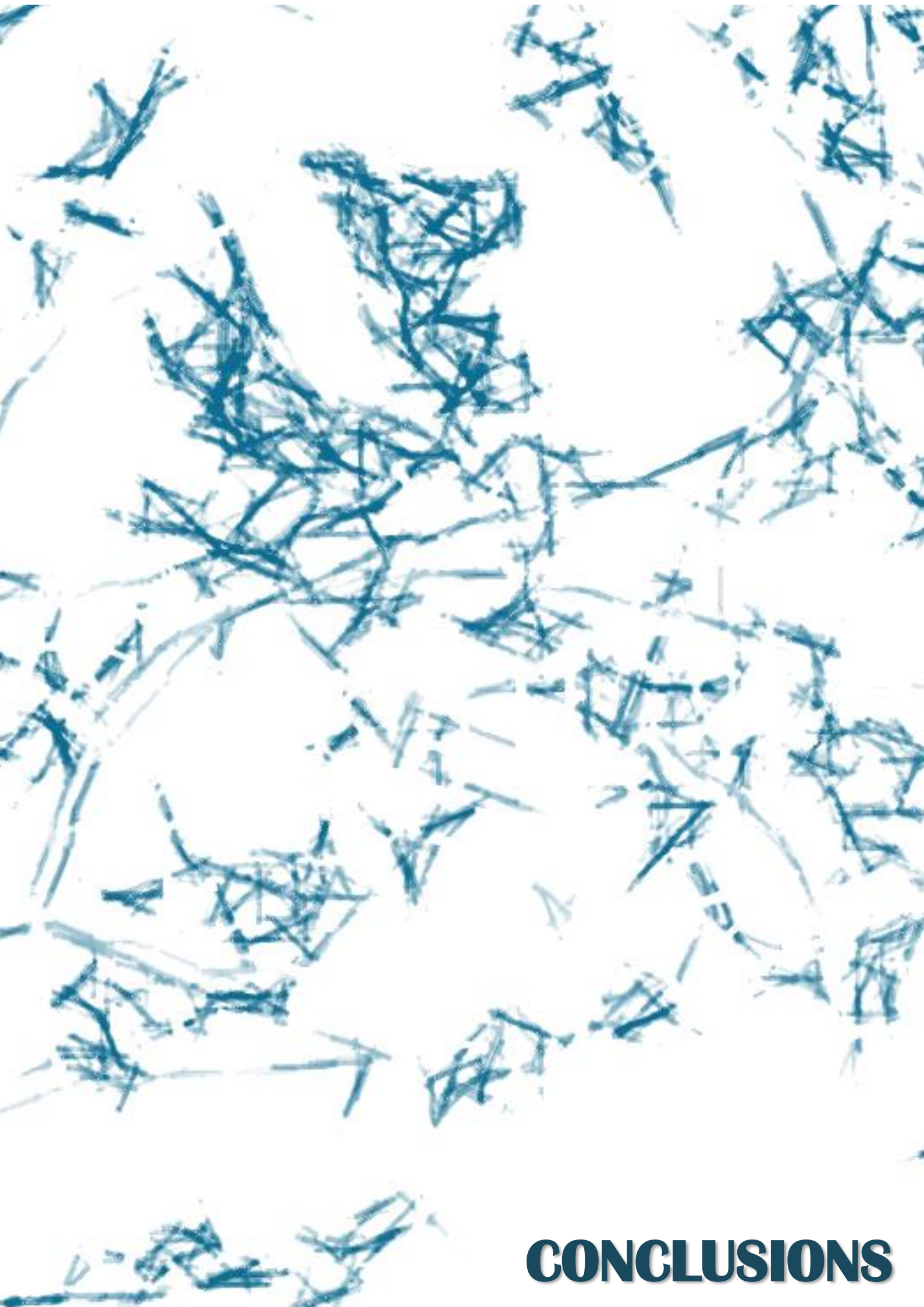

CONCLUSIONS

1. The lack of SHIP-1 in macrophages boosts β-glucan-induced trained immunity, leading to increased LPS-induced production of IL-1β and TNFα.

2. β-glucan-trained SHIP-1-deficient macrophages exhibit increased trained immunity molecular pathway activation and a more pronounced switch to glycolysis.

3. The enhanced β-glucan training in macrophages through SHIP-1 deletion relies on epigenetic reprogramming, particularly on histone methylation and acetylation.

4. β-glucan-trained mice with a specific SHIP-1 deletion in the myeloid compartment show an enhanced production of trained immunity-associated cytokines upon heterologous rechallenge and a better protection against secondary *Candida albicans* infection.

5. Myeloid specific SHIP-1-deficient mice trained with a low dose of *Candida albicans* show increased renal proinflammatory cytokines and improved response against a lethal reinfection.

6. Pharmacological inhibition of SHIP-1 boosts trained immunity in macrophages *in vitro* and improves protection to secondary lethal candidiasis conferred by *Candida albicans* training in *vivo*.

7. Trained immunity in human peripheral blood mononuclear cells is enhanced by SHIP-1 inhibition.

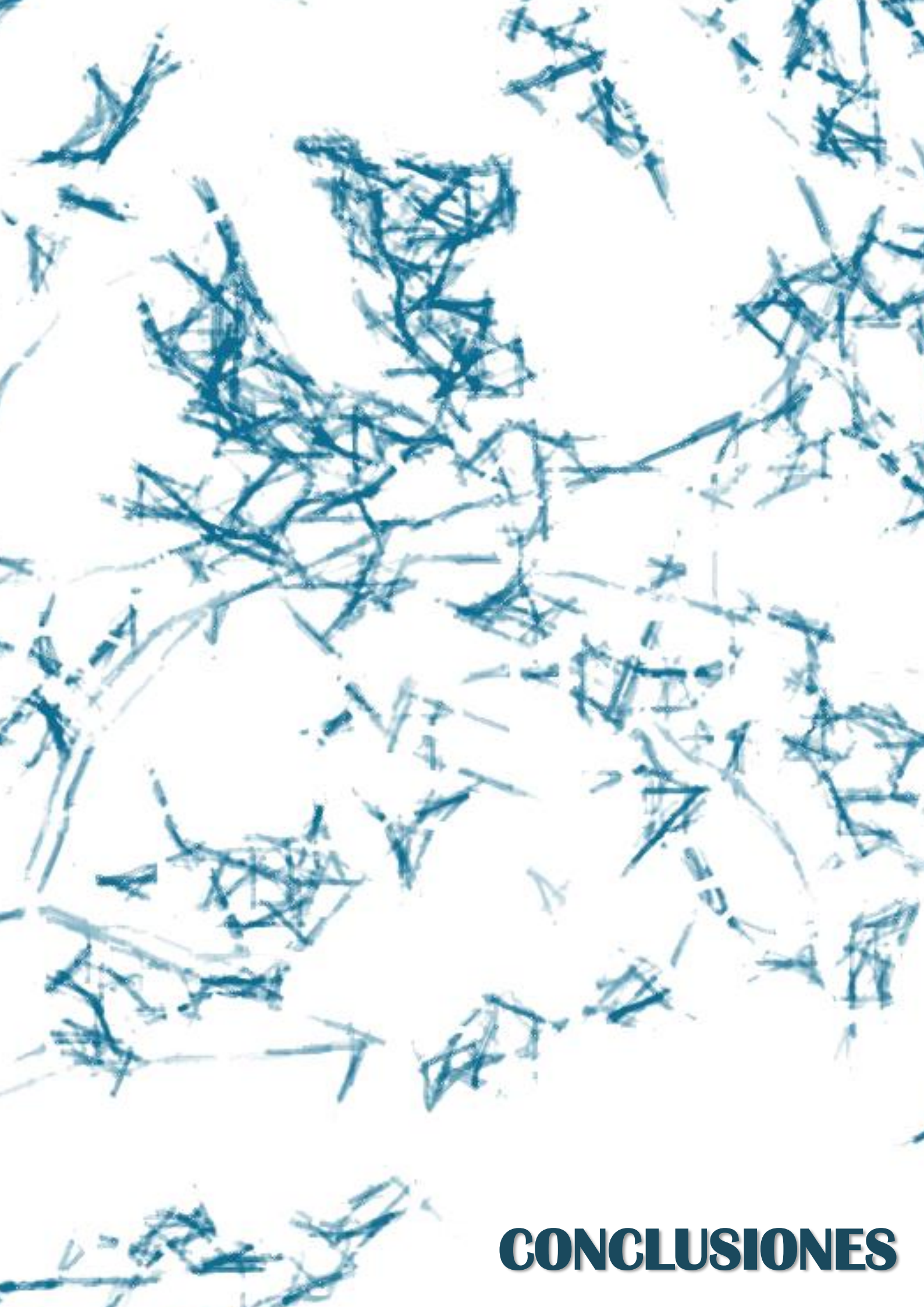

CONCLUSIONES

1. La ausencia de SHIP-1 en macrófagos potencia la inmunidad entrenada inducida por β-glucano, lo que resulta en una mayor producción de IL-1β y TNFα en respuesta a LPS.

2. Los macrófagos deficientes en SHIP-1 entrenados con β-glucano muestran una activación mayor de la ruta de señalización que media la inmunidad entrenada y un cambio a glucólisis más pronunciado.

3. La mejora del entrenamiento con β-glucano mediante la ausencia de SHIP-1 depende de procesos de reprogramación epigenética, en particular de metilación y acetilación de histonas.

4. Los ratones que portan una depleción específica de SHIP-1 en el compartimento mieloide y son entrenados con β-glucano, producen una mayor cantidad de citoquinas asociadas al proceso de inmunidad entrenada cuando son expuestos a un estímulo heterólogo, y se protegen mejor frente a una infección secundaria con *Candida albicans*.

5. Ratones deficientes en SHIP-1 en células mieloides y entrenados con una dosis baja de *Candida albicans*, producen más citoquinas proinflamatorias en el riñón y se protegen mejor frente a una reinfección letal.

6. La inhibición farmacológica de SHIP-1 potencia la inmunidad entrenada en macrófagos *in vitro* y mejora la protección conferida por el entrenamiento con *Candida albicans* frente a una candidiasis secundaria letal.

7. La inmunidad entrenada en células mononucleares de sangre periférica humana se potencia mediante la inhibición de SHIP-1.

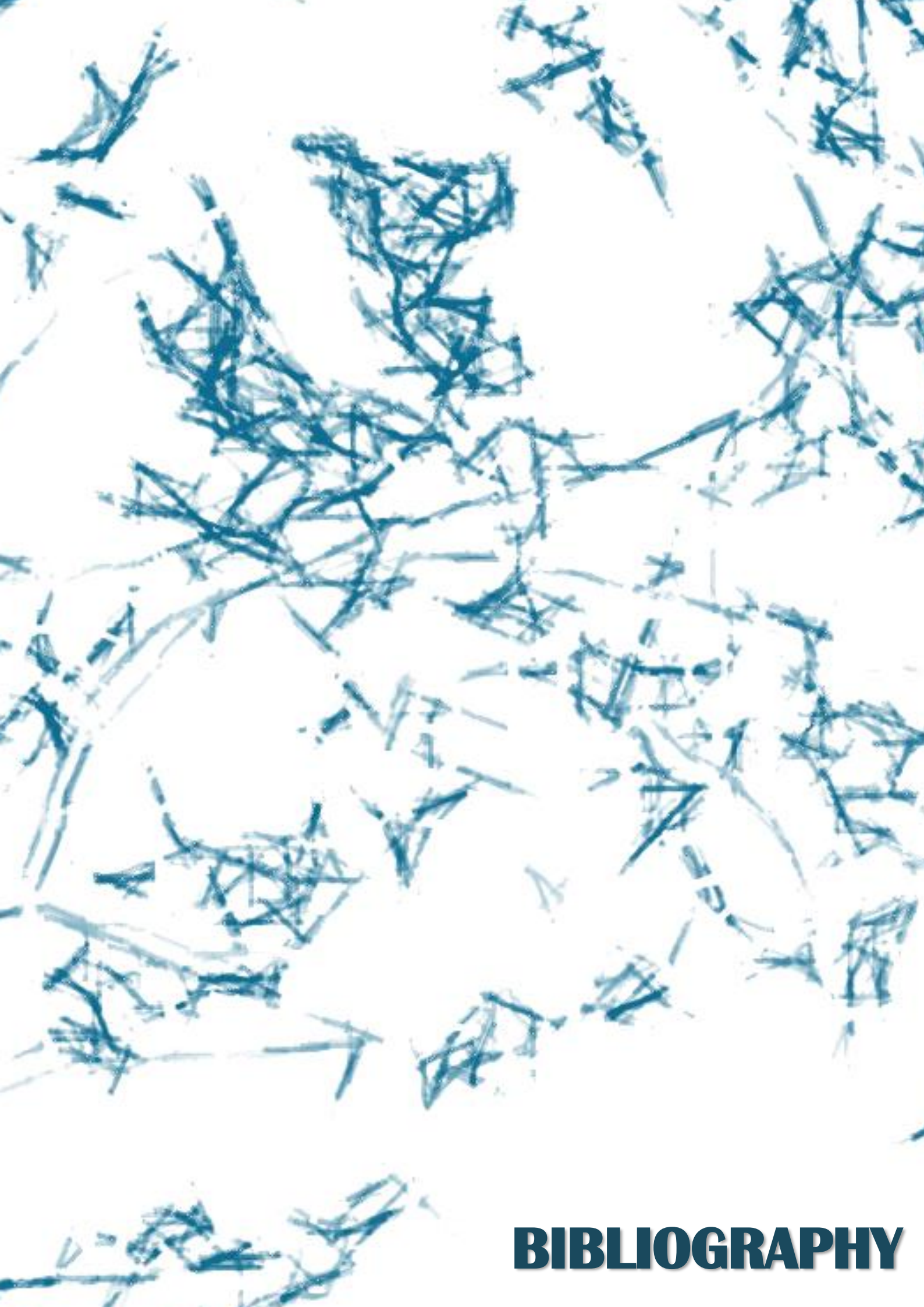

BIBLIOGRAPHY

AN, H., XU, H., ZHANG, M., ZHOU, J., FENG, T., QIAN, C., QI, R. & CAO, X. 2005. Src homology 2 domain-containing inositol-5-phosphatase 1 (SHIP1) negatively regulates TLR4-mediated LPS response primarily through a phosphatase activity- and PI-3K-independent mechanism. *Blood,* 105**,** 4685-4692.

ANTIGNANO, F., IBARAKI, M., KIM, C., RUSCHMANN, J., ZHANG, A., HELGASON, C. D. & KRYSTAL, G. 2010a. SHIP is required for dendritic cell maturation. *J Immunol,* 184**,** 2805-2813.

ANTIGNANO, F., IBARAKI, M., RUSCHMANN, J., JAGDEO, J. & KRYSTAL, G. 2010b. SHIP negatively regulates Flt3L-derived dendritic cell generation and positively regulates MyD88-independent TLR-induced maturation. *J Leukoc Biol,* 88**,** 925-935.

ARTS, R. J., BLOK, B. A., VAN CREVEL, R., JOOSTEN, L. A., AABY, P., BENN, C. S. & NETEA, M. G. 2015. Vitamin A induces inhibitory histone methylation modifications and down-regulates trained immunity in human monocytes. *J Leukoc Biol,* 98**,** 129-136.

ARTS, R. J., NOVAKOVIC, B., TER HORST, R., CARVALHO, A., BEKKERING, S., LACHMANDAS, E., RODRIGUES, F., SILVESTRE, R., CHENG, S. C., WANG, S. Y., HABIBI, E., GONCALVES, L. G., MESQUITA, I., CUNHA, C., VAN LAARHOVEN, A., VAN DE VEERDONK, F. L., WILLIAMS, D. L., VAN DER MEER, J. W., LOGIE, C., O'NEILL, L. A., DINARELLO, C. A., RIKSEN, N. P., VAN CREVEL, R., CLISH, C., NOTEBAART, R. A., JOOSTEN, L. A., STUNNENBERG, H. G., XAVIER, R. J. & NETEA, M. G. 2016a. Glutaminolysis and Fumarate Accumulation Integrate Immunometabolic and Epigenetic Programs in Trained Immunity. *Cell Metab,* 24**,** 807-819.

ARTS, R. J. W., CARVALHO, A., LA ROCCA, C., PALMA, C., RODRIGUES, F., SILVESTRE, R., KLEINNIJENHUIS, J., LACHMANDAS, E., GONCALVES, L. G., BELINHA, A., CUNHA, C., OOSTING, M., JOOSTEN, L. A. B., MATARESE, G., VAN CREVEL, R. & NETEA, M. G. 2016b. Immunometabolic Pathways in BCG-Induced Trained Immunity. *Cell Rep,* 17**,** 2562-2571.

ARTS, R. J. W., JOOSTEN, L. A. B. & NETEA, M. G. 2018a. The Potential Role of Trained Immunity in Autoimmune and Autoinflammatory Disorders. *Front Immunol,* 9**,** 298.

ARTS, R. J. W., MOORLAG, S., NOVAKOVIC, B., LI, Y., WANG, S. Y., OOSTING, M., KUMAR, V., XAVIER, R. J., WIJMENGA, C., JOOSTEN, L. A. B., REUSKEN, C., BENN, C. S., AABY, P., KOOPMANS, M. P., STUNNENBERG, H. G., VAN CREVEL, R. & NETEA, M. G. 2018b. BCG Vaccination Protects against Experimental Viral Infection in Humans through the Induction of Cytokines Associated with Trained Immunity. *Cell Host Microbe,* 23**,** 89-100 e5.

BAR, E., WHITNEY, P. G., MOOR, K., REIS E SOUSA, C. & LEIBUNDGUT-LANDMANN, S. 2014. IL-17 regulates systemic fungal immunity by controlling the functional competence of NK cells. *Immunity,* 40**,** 117-127.

BEKKERING, S., ARTS, R. J. W., NOVAKOVIC, B., KOURTZELIS, I., VAN DER HEIJDEN, C., LI, Y., POPA, C. D., TER HORST, R., VAN TUIJL, J., NETEA-MAIER, R. T., VAN DE VEERDONK, F. L., CHAVAKIS, T., JOOSTEN, L. A. B., VAN DER MEER, J. W. M., STUNNENBERG, H., RIKSEN, N. P. & NETEA, M.

G. 2018. Metabolic Induction of Trained Immunity through the Mevalonate Pathway. *Cell,* 172**,** 135-146 e9.

BEKKERING, S., BLOK, B. A., JOOSTEN, L. A., RIKSEN, N. P., VAN CREVEL, R. & NETEA, M. G. 2016a. In Vitro Experimental Model of Trained Innate Immunity in Human Primary Monocytes. *Clin Vaccine Immunol,* 23**,** 926-933.

BEKKERING, S., JOOSTEN, L. A., VAN DER MEER, J. W., NETEA, M. G. & RIKSEN, N. P. 2013. Trained innate immunity and atherosclerosis. *Curr Opin Lipidol,* 24**,** 487-492.

BEKKERING, S., QUINTIN, J., JOOSTEN, L. A., VAN DER MEER, J. W., NETEA, M. G. & RIKSEN, N. P. 2014. Oxidized low-density lipoprotein induces long-term proinflammatory cytokine production and foam cell formation via epigenetic reprogramming of monocytes. *Arterioscler Thromb Vasc Biol,* 34**,** 1731-1738.

BEKKERING, S., VAN DEN MUNCKHOF, I., NIELEN, T., LAMFERS, E., DINARELLO, C., RUTTEN, J., DE GRAAF, J., JOOSTEN, L. A., NETEA, M. G., GOMES, M. E. & RIKSEN, N. P. 2016b. Innate immune cell activation and epigenetic remodeling in symptomatic and asymptomatic atherosclerosis in humans in vivo. *Atherosclerosis,* 254**,** 228-236.

BILLCLIFF, P. G. & LOWE, M. 2014. Inositol lipid phosphatases in membrane trafficking and human disease. *Biochem J,* 461**,** 159-175.

BISTONI, F., VECCHIARELLI, A., CENCI, E., PUCCETTI, P., MARCONI, P. & CASSONE, A. 1986. Evidence for macrophage-mediated protection against lethal Candida albicans infection. *Infect Immun,* 51**,** 668-674.

BISTONI, F., VERDUCCI, G., PERITO, S., VECCHIARELLI, A., PUCCETTI, P., MARCONI, P. & CASSONE, A. 1988. Immunomodulation by a low-virulence, agerminative variant of Candida albicans. Further evidence for macrophage activation as one of the effector mechanisms of nonspecific anti-infectious protection. *J Med Vet Mycol,* 26**,** 285-299.

BISWAS, S. K. & LOPEZ-COLLAZO, E. 2009. Endotoxin tolerance: new mechanisms, molecules and clinical significance. *Trends Immunol,* 30**,** 475-487.

BLANCO-MENENDEZ, N., DEL FRESNO, C., FERNANDES, S., CALVO, E., CONDE-GARROSA, R., KERR, W. G. & SANCHO, D. 2015. SHIP-1 Couples to the Dectin-1 hemITAM and Selectively Modulates Reactive Oxygen Species Production in Dendritic Cells in Response to Candida albicans. *J Immunol,* 195**,** 4466-4478.

BORASCHI, D. & ITALIANI, P. 2018. Innate Immune Memory: Time for Adopting a Correct Terminology. *Front Immunol,* 9**,** 799.

BORRIELLO, F., IANNONE, R., DI SOMMA, S., LOFFREDO, S., SCAMARDELLA, E., GALDIERO, M. R., VARRICCHI, G., GRANATA, F., PORTELLA, G. & MARONE, G. 2016. GM-CSF and IL-3 Modulate Human Monocyte TNF-alpha Production and Renewal in In Vitro Models of Trained Immunity. *Front Immunol,* 7**,** 680.

BRAUWEILER, A. M., TAMIR, I. & CAMBIER, J. C. 2000. Bilevel control of B-cell activation by the inositol 5-phosphatase SHIP. *Immunol Rev,* 176**,** 69-74.

BROOKS, R., FUHLER, G. M., IYER, S., SMITH, M. J., PARK, M. Y., PARAISO, K. H., ENGELMAN, R. W. & KERR, W. G. 2010. SHIP1 inhibition increases

immunoregulatory capacity and triggers apoptosis of hematopoietic cancer cells. *J Immunol,* 184**,** 3582-3589.

BROOKS, R., IYER, S., AKADA, H., NEELAM, S., RUSSO, C. M., CHISHOLM, J. D. & KERR, W. G. 2015. Coordinate expansion of murine hematopoietic and mesenchymal stem cell compartments by SHIPi. *Stem Cells,* 33**,** 848-858.

BROWN, G. D. & GORDON, S. 2001. Immune recognition. A new receptor for beta-glucans. *Nature,* 413**,** 36-37.

BRUBAKER, S. W., BONHAM, K. S., ZANONI, I. & KAGAN, J. C. 2015. Innate immune pattern recognition: a cell biological perspective. *Annu Rev Immunol,* 33**,** 257-290.

BUFFEN, K., OOSTING, M., QUINTIN, J., NG, A., KLEINNIJENHUIS, J., KUMAR, V., VAN DE VOSSE, E., WIJMENGA, C., VAN CREVEL, R., OOSTERWIJK, E., GROTENHUIS, A. J., VERMEULEN, S. H., KIEMENEY, L. A., VAN DE VEERDONK, F. L., CHAMILOS, G., XAVIER, R. J., VAN DER MEER, J. W., NETEA, M. G. & JOOSTEN, L. A. 2014. Autophagy controls BCG-induced trained immunity and the response to intravesical BCG therapy for bladder cancer. *PLoS Pathog,* 10**,** e1004485.

BUTKEVICIUTE, E., JONES, C. E. & SMITH, S. G. 2018. Heterologous effects of infant BCG vaccination: potential mechanisms of immunity. *Future Microbiol,* 13**,** 1193-1208.

CHENG, S. C., QUINTIN, J., CRAMER, R. A., SHEPARDSON, K. M., SAEED, S., KUMAR, V., GIAMARELLOS-BOURBOULIS, E. J., MARTENS, J. H., RAO, N. A., AGHAJANIREFAH, A., MANJERI, G. R., LI, Y., IFRIM, D. C., ARTS, R. J., VAN DER VEER, B. M., DEEN, P. M., LOGIE, C., O'NEILL, L. A., WILLEMS, P., VAN DE VEERDONK, F. L., VAN DER MEER, J. W., NG, A., JOOSTEN, L. A., WIJMENGA, C., STUNNENBERG, H. G., XAVIER, R. J. & NETEA, M. G. 2014. mTOR- and HIF-1alpha-mediated aerobic glycolysis as metabolic basis for trained immunity. *Science,* 345**,** 1250684.

CHRIST, A., BEKKERING, S., LATZ, E. & RIKSEN, N. P. 2016. Long-term activation of the innate immune system in atherosclerosis. *Semin Immunol,* 28**,** 384-393.

CHRIST, A., GUNTHER, P., LAUTERBACH, M. A. R., DUEWELL, P., BISWAS, D., PELKA, K., SCHOLZ, C. J., OOSTING, M., HAENDLER, K., BASSLER, K., KLEE, K., SCHULTE-SCHREPPING, J., ULAS, T., MOORLAG, S., KUMAR, V., PARK, M. H., JOOSTEN, L. A. B., GROH, L. A., RIKSEN, N. P., ESPEVIK, T., SCHLITZER, A., LI, Y., FITZGERALD, M. L., NETEA, M. G., SCHULTZE, J. L. & LATZ, E. 2018. Western Diet Triggers NLRP3-Dependent Innate Immune Reprogramming. *Cell,* 172**,** 162-175 e14.

CLAUSEN, B. E., BURKHARDT, C., REITH, W., RENKAWITZ, R. & FORSTER, I. 1999. Conditional gene targeting in macrophages and granulocytes using LysMcre mice. *Transgenic Res,* 8**,** 265-277.

COLLAZO, M. M., PARAISO, K. H., PARK, M. Y., HAZEN, A. L. & KERR, W. G. 2012. Lineage extrinsic and intrinsic control of immunoregulatory cell numbers by SHIP. *Eur J Immunol,* 42**,** 1785-1795.

COLLAZO, M. M., WOOD, D., PARAISO, K. H., LUND, E., ENGELMAN, R. W., LE, C. T., STAUCH, D., KOTSCH, K. & KERR, W. G. 2009. SHIP limits immunoregulatory capacity in the T-cell compartment. *Blood,* 113**,** 2934-2944.

CONDE, C., GLOIRE, G. & PIETTE, J. 2011. Enzymatic and non-enzymatic activities of SHIP-1 in signal transduction and cancer. *Biochem Pharmacol,* 82**,** 1320-1334.

CONDE, C., RAMBOUT, X., LEBRUN, M., LECAT, A., DI VALENTIN, E., DEQUIEDT, F., PIETTE, J., GLOIRE, G. & LEGRAND, S. 2012. The inositol phosphatase SHIP-1 inhibits NOD2-induced NF-kappaB activation by disturbing the interaction of XIAP with RIP2. *PLoS One,* 7**,** e41005.

COX, D., DALE, B. M., KASHIWADA, M., HELGASON, C. D. & GREENBERG, S. 2001. A regulatory role for Src homology 2 domain-containing inositol 5'-phosphatase (SHIP) in phagocytosis mediated by Fc gamma receptors and complement receptor 3 (alpha(M)beta(2); CD11b/CD18). *J Exp Med,* 193**,** 61-71.

CRISAN, T. O., CLEOPHAS, M. C., OOSTING, M., LEMMERS, H., TOENHAKE-DIJKSTRA, H., NETEA, M. G., JANSEN, T. L. & JOOSTEN, L. A. 2016a. Soluble uric acid primes TLR-induced proinflammatory cytokine production by human primary cells via inhibition of IL-1Ra. *Ann Rheum Dis,* 75**,** 755-762.

CRISAN, T. O., CLEOPHAS, M. C. P., NOVAKOVIC, B., ERLER, K., VAN DE VEERDONK, F. L., STUNNENBERG, H. G., NETEA, M. G., DINARELLO, C. A. & JOOSTEN, L. A. B. 2017. Uric acid priming in human monocytes is driven by the AKT-PRAS40 autophagy pathway. *Proc Natl Acad Sci U S A,* 114**,** 5485-5490.

CRISAN, T. O., NETEA, M. G. & JOOSTEN, L. A. 2016b. Innate immune memory: Implications for host responses to damage-associated molecular patterns. *Eur J Immunol,* 46**,** 817-828.

CROSS, M., MANGELSDORF, I., WEDEL, A. & RENKAWITZ, R. 1988. Mouse lysozyme M gene: isolation, characterization, and expression studies. *Proc Natl Acad Sci U S A,* 85**,** 6232-6236.

DE BREE, L. C. J., KOEKEN, V., JOOSTEN, L. A. B., AABY, P., BENN, C. S., VAN CREVEL, R. & NETEA, M. G. 2018. Non-specific effects of vaccines: Current evidence and potential implications. *Semin Immunol*. pii:S-1044-5323(18)30011-3

DE GROOT, A. E. & PIENTA, K. J. 2018. Epigenetic control of macrophage polarization: implications for targeting tumor-associated macrophages. *Oncotarget,* 9**,** 20908-20927.

DEJIMA, T., SHIBATA, K., YAMADA, H., HARA, H., IWAKURA, Y., NAITO, S. & YOSHIKAI, Y. 2011. Protective role of naturally occurring interleukin-17A-producing gammadelta T cells in the lung at the early stage of systemic candidiasis in mice. *Infect Immun,* 79**,** 4503-4510.

DELVES P.J., MARTIN S.J., BURTON D.R. & I.M., R. 2017. *Roitt's Essential Immunology*, Wiley-Blackwell.

DI LUZIO, N. R. & WILLIAMS, D. L. 1978. Protective effect of glucan against systemic Staphylococcus aureus septicemia in normal and leukemic mice. *Infect Immun,* 20**,** 804-810.

DIBBLE, C. C. & CANTLEY, L. C. 2015. Regulation of mTORC1 by PI3K signaling. *Trends Cell Biol,* 25**,** 545-555.

DOMINGUEZ-ANDRES, J., FEO-LUCAS, L., MINGUITO DE LA ESCALERA, M., GONZALEZ, L., LOPEZ-BRAVO, M. & ARDAVIN, C. 2017. Inflammatory Ly6C(high) Monocytes Protect against Candidiasis through IL-15-Driven NK Cell/Neutrophil Activation. *Immunity,* 46**,** 1059-1072 e4.

DOMINGUEZ-ANDRES, J., NOVAKOVIC, B., LI, Y., SCICLUNA, B. P., GRESNIGT, M. S., ARTS, R. J. W., OOSTING, M., MOORLAG, S., GROH, L. A., ZWAAG, J., KOCH, R. M., TER HORST, R., JOOSTEN, L. A. B., WIJMENGA, C., MICHELUCCI, A., VAN DER POLL, T., KOX, M., PICKKERS, P., KUMAR, V., STUNNENBERG, H. & NETEA, M. G. 2018. The Itaconate Pathway Is a Central Regulatory Node Linking Innate Immune Tolerance and Trained Immunity. *Cell Metab*. pii:S1550-4131(18)30568-0.

DURRANT, W. E. & DONG, X. 2004. Systemic acquired resistance. *Annu Rev Phytopathol,* 42**,** 185-209.

EL KHOURY, D., CUDA, C., LUHOVYY, B. L. & ANDERSON, G. H. 2012. Beta glucan: health benefits in obesity and metabolic syndrome. *J Nutr Metab,* 2012**,** 851362.

ERAMO, M. J. & MITCHELL, C. A. 2016. Regulation of PtdIns(3,4,5)P3/Akt signalling by inositol polyphosphate 5-phosphatases. *Biochem Soc Trans,* 44**,** 240-252.

ERNEUX, C., GHOSH, S., RAMOS, A. R. & EDIMO, W. E. 2016. New Functions of the Inositol Polyphosphate 5-Phosphatases in Cancer. *Curr Pharm Des,* 22**,** 2309-2314.

FANG, H., PENGAL, R. A., CAO, X., GANESAN, L. P., WEWERS, M. D., MARSH, C. B. & TRIDANDAPANI, S. 2004. Lipopolysaccharide-Induced Macrophage Inflammatory Response Is Regulated by SHIP. *The Journal of Immunology,* 173**,** 360-366.

FERNANDES, S., BROOKS, R., GUMBLETON, M., PARK, M. Y., RUSSO, C. M., HOWARD, K. T., CHISHOLM, J. D. & KERR, W. G. 2015. SHIPi Enhances Autologous and Allogeneic Hematolymphoid Stem Cell Transplantation. *EBioMedicine,* 2**,** 205-213.

FERNANDES, S., IYER, S. & KERR, W. G. 2013. Role of SHIP1 in cancer and mucosal inflammation. *Ann N Y Acad Sci,* 1280**,** 6-10.

FOSTER, S. L., HARGREAVES, D. C. & MEDZHITOV, R. 2007. Gene-specific control of inflammation by TLR-induced chromatin modifications. *Nature,* 447**,** 972-978.

FREYNE, B., MARCHANT, A. & CURTIS, N. 2015. BCG-associated heterologous immunity, a historical perspective: experimental models and immunological mechanisms. *Trans R Soc Trop Med Hyg,* 109**,** 46-51.

FUHLER, G. M., BROOKS, R., TOMS, B., IYER, S., GENGO, E. A., PARK, M. Y., GUMBLETON, M., VIERNES, D. R., CHISHOLM, J. D. & KERR, W. G. 2012. Therapeutic potential of SH2 domain-containing inositol-5'-phosphatase 1 (SHIP1) and SHIP2 inhibition in cancer. *Mol Med,* 18**,** 65-75.

GANESAN, L. P., JOSHI, T., FANG, H., KUTALA, V. K., RODA, J., TROTTA, R., LEHMAN, A., KUPPUSAMY, P., BYRD, J. C., CARSON, W. E., CALIGIURI, M. A. & TRIDANDAPANI, S. 2006. FcgammaR-induced production of superoxide and inflammatory cytokines is differentially regulated by SHIP through its influence on PI3K and/or Ras/Erk pathways. *Blood,* 108**,** 718-725.

GARCIA-VALTANEN, P., GUZMAN-GENUINO, R. M., WILLIAMS, D. L., HAYBALL, J. D. & DIENER, K. R. 2017. Evaluation of trained immunity by beta-1, 3 (d)-glucan on murine monocytes in vitro and duration of response in vivo. *Immunol Cell Biol,* 95**,** 601-610.

GARDINER, C. M. & MILLS, K. H. 2016. The cells that mediate innate immune memory and their functional significance in inflammatory and infectious diseases. *Semin Immunol,* 28**,** 343-350.

GHORPADE, D. S., LEYLAND, R., KUROWSKA-STOLARSKA, M., PATIL, S. A. & BALAJI, K. N. 2012. MicroRNA-155 is required for Mycobacterium bovis BCG-mediated apoptosis of macrophages. *Mol Cell Biol,* 32**,** 2239-2253.

GOLD, M. J., ANTIGNANO, F., HUGHES, M. R., ZAPH, C. & MCNAGNY, K. M. 2016. Dendritic-cell expression of Ship1 regulates Th2 immunity to helminth infection in mice. *Eur J Immunol,* 46**,** 122-130.

GOLD, M. J., HUGHES, M. R., ANTIGNANO, F., HIROTA, J. A., ZAPH, C. & MCNAGNY, K. M. 2015. Lineage-specific regulation of allergic airway inflammation by the lipid phosphatase Src homology 2 domain-containing inositol 5-phosphatase (SHIP-1). *J Allergy Clin Immunol,* 136**,** 725-736 e2.

GUMBLETON, M., SUDAN, R., FERNANDES, S., ENGELMAN, R. W., RUSSO, C. M., CHISHOLM, J. D. & KERR, W. G. 2017. Dual enhancement of T and NK cell function by pulsatile inhibition of SHIP1 improves antitumor immunity and survival. *Sci Signal,* 10, 5353.

GUMBLETON, M., VIVIER, E. & KERR, W. G. 2015. SHIP1 intrinsically regulates NK cell signaling and education, resulting in tolerance of an MHC class I-mismatched bone marrow graft in mice. *J Immunol,* 194**,** 2847-2854.

HADIDI, S., ANTIGNANO, F., HUGHES, M. R., WANG, S. K., SNYDER, K., SAMMIS, G. M., KERR, W. G., MCNAGNY, K. M. & ZAPH, C. 2012. Myeloid cell-specific expression of Ship1 regulates IL-12 production and immunity to helminth infection. *Mucosal Immunol,* 5**,** 535-543.

HALEY, M. J., BROUGH, D., QUINTIN, J. & ALLAN, S. M. 2017. Microglial Priming as Trained Immunity in the Brain. *Neuroscience*. pii: S030-4522(17)30929-6.

HAMILTON, J. A. 2008. Colony-stimulating factors in inflammation and autoimmunity. *Nat Rev Immunol,* 8**,** 533-544.

HAMMER, Q. & ROMAGNANI, C. 2017. About Training and Memory: NK-Cell Adaptation to Viral Infections. *Adv Immunol,* 133**,** 171-207.

HAMON, M. A. & QUINTIN, J. 2016. Innate immune memory in mammals. *Semin Immunol,* 28**,** 351-358.

HAN, M. S., JUNG, D. Y., MOREL, C., LAKHANI, S. A., KIM, J. K., FLAVELL, R. A. & DAVIS, R. J. 2013. JNK expression by macrophages promotes obesity-induced insulin resistance and inflammation. *Science,* 339**,** 218-222.

HAZEN, A. L., SMITH, M. J., DESPONTS, C., WINTER, O., MOSER, K. & KERR, W. G. 2009. SHIP is required for a functional hematopoietic stem cell niche. *Blood,* 113**,** 2924-2933.

HELGASON, C. D., DAMEN, J. E., ROSTEN, P., GREWAL, R., SORENSEN, P., CHAPPEL, S. M., BOROWSKI, A., JIRIK, F., KRYSTAL, G. & HUMPHRIES, R. K. 1998. Targeted disruption of SHIP leads to hemopoietic perturbations, lung pathology, and a shortened life span. *Genes Dev,* 12**,** 1610-1620.

HOEKSEMA, M. A. & DE WINTHER, M. P. 2016. Epigenetic Regulation of Monocyte and Macrophage Function. *Antioxid Redox Signal,* 25**,** 758-774.

HOLDEN, J. A., ATTARD, T. J., LAUGHTON, K. M., MANSELL, A., O'BRIEN-SIMPSON, N. M. & REYNOLDS, E. C. 2014. Porphyromonas gingivalis lipopolysaccharide weakly activates M1 and M2 polarized mouse macrophages but induces inflammatory cytokines. *Infect Immun,* 82**,** 4190-4203.

HOLMES, T. D. & BRYCESON, Y. T. 2016. Natural killer cell memory in context. *Semin Immunol,* 28**,** 368-376.

HOOGEVEEN, R. M., NAHRENDORF, M., RIKSEN, N. P., NETEA, M. G., DE WINTHER, M. P. J., LUTGENS, E., NORDESTGAARD, B. G., NEIDHART, M., STROES, E. S. G., CATAPANO, A. L. & BEKKERING, S. 2018. Monocyte and haematopoietic progenitor reprogramming as common mechanism underlying chronic inflammatory and cardiovascular diseases. *Eur Heart J,* 39**,** 3521-3527.

HUANG, J., JIAO, J., XU, W., ZHAO, H., ZHANG, C., SHI, Y. & XIAO, Z. 2015. MiR-155 is upregulated in patients with active tuberculosis and inhibits apoptosis of monocytes by targeting FOXO3. *Mol Med Rep,* 12**,** 7102-7108.

IFRIM, D. C., JOOSTEN, L. A., KULLBERG, B. J., JACOBS, L., JANSEN, T., WILLIAMS, D. L., GOW, N. A., VAN DER MEER, J. W., NETEA, M. G. & QUINTIN, J. 2013. Candida albicans primes TLR cytokine responses through a Dectin-1/Raf-1-mediated pathway. *J Immunol,* 190**,** 4129-4135.

IFRIM, D. C., QUINTIN, J., JOOSTEN, L. A., JACOBS, C., JANSEN, T., JACOBS, L., GOW, N. A., WILLIAMS, D. L., VAN DER MEER, J. W. & NETEA, M. G. 2014. Trained immunity or tolerance: opposing functional programs induced in human monocytes after engagement of various pattern recognition receptors. *Clin Vaccine Immunol,* 21**,** 534-545.

IFRIM, D. C., QUINTIN, J., MEERSTEIN-KESSEL, L., PLANTINGA, T. S., JOOSTEN, L. A., VAN DER MEER, J. W., VAN DE VEERDONK, F. L. & NETEA, M. G. 2015. Defective trained immunity in patients with STAT-1-dependent chronic mucocutaneaous candidiasis. *Clin Exp Immunol,* 181**,** 434-440.

JANEWAY, C. A., JR., TRAVERS, P., WALPORT, M. & J.D., C. 2001. *Immunobiology: The immune system in health and disease,* Garland Science.

JENSEN, J., WARNER, T. & BALISH, E. 1993. Resistance of SCID mice to Candida albicans administered intravenously or colonizing the gut: role of polymorphonuclear leukocytes and macrophages. *J Infect Dis,* 167**,** 912-919.

KAMEN, L. A., LEVINSOHN, J., CADWALLADER, A., TRIDANDAPANI, S. & SWANSON, J. A. 2008. SHIP-1 increases early oxidative burst and regulates phagosome maturation in macrophages. *J Immunol,* 180**,** 7497-7505.

KAUFMANN, E., SANZ, J., DUNN, J. L., KHAN, N., MENDONCA, L. E., PACIS, A., TZELEPIS, F., PERNET, E., DUMAINE, A., GRENIER, J. C., MAILHOT-LEONARD, F., AHMED, E., BELLE, J., BESLA, R., MAZER, B., KING, I. L., NIJNIK, A., ROBBINS, C. S., BARREIRO, L. B. & DIVANGAHI, M. 2018. BCG Educates Hematopoietic Stem Cells to Generate Protective Innate Immunity against Tuberculosis. *Cell,* 172**,** 176-190 e19.

KELLER, C., HELLSTEN, Y., STEENSBERG, A. & PEDERSEN, B. K. 2006. Differential regulation of IL-6 and TNF-alpha via calcineurin in human skeletal muscle cells. *Cytokine,* 36**,** 141-147.

KERR, W. G. 2011. Inhibitor and activator: dual functions for SHIP in immunity and cancer. *Ann N Y Acad Sci,* 1217**,** 1-17.

KERR, W. G., PARK, M. Y., MAUBERT, M. & ENGELMAN, R. W. 2011. SHIP deficiency causes Crohn's disease-like ileitis. *Gut,* 60**,** 177-188.

KHALAF, H., JASS, J. & OLSSON, P. E. 2010. Differential cytokine regulation by NF-kappaB and AP-1 in Jurkat T-cells. *BMC Immunol,* 11**,** 26.

KLEINNIJENHUIS, J., QUINTIN, J., PREIJERS, F., BENN, C. S., JOOSTEN, L. A., JACOBS, C., VAN LOENHOUT, J., XAVIER, R. J., AABY, P., VAN DER MEER, J. W., VAN CREVEL, R. & NETEA, M. G. 2014a. Long-lasting effects of BCG vaccination on both heterologous Th1/Th17 responses and innate trained immunity. *J Innate Immun,* 6**,** 152-158.

KLEINNIJENHUIS, J., QUINTIN, J., PREIJERS, F., JOOSTEN, L. A., IFRIM, D. C., SAEED, S., JACOBS, C., VAN LOENHOUT, J., DE JONG, D., STUNNENBERG, H. G., XAVIER, R. J., VAN DER MEER, J. W., VAN CREVEL, R. & NETEA, M. G. 2012. Bacille Calmette-Guerin induces NOD2-dependent nonspecific protection from reinfection via epigenetic reprogramming of monocytes. *Proc Natl Acad Sci U S A,* 109**,** 17537-17542.

KLEINNIJENHUIS, J., QUINTIN, J., PREIJERS, F., JOOSTEN, L. A., JACOBS, C., XAVIER, R. J., VAN DER MEER, J. W., VAN CREVEL, R. & NETEA, M. G. 2014b. BCG-induced trained immunity in NK cells: Role for non-specific protection to infection. *Clin Immunol,* 155**,** 213-219.

LEENTJENS, J., BEKKERING, S., JOOSTEN, L. A. B., NETEA, M. G., BURGNER, D. P. & RIKSEN, N. P. 2018. Trained Innate Immunity as a Novel Mechanism Linking Infection and the Development of Atherosclerosis. *Circ Res,* 122**,** 664-669.

LIBERTI, M. V. & LOCASALE, J. W. 2016. The Warburg Effect: How Does it Benefit Cancer Cells? *Trends Biochem Sci,* 41**,** 211-218.

LIM, M. X., PNG, C. W., TAY, C. Y., TEO, J. D., JIAO, H., LEHMING, N., TAN, K. S. & ZHANG, Y. 2014. Differential regulation of proinflammatory cytokine expression by mitogen-activated protein kinases in macrophages in response to intestinal parasite infection. *Infect Immun,* 82**,** 4789-4801.

LIONAKIS, M. S. 2014. New insights into innate immune control of systemic candidiasis. *Med Mycol,* 52**,** 555-564.

LIONAKIS, M. S., LIM, J. K., LEE, C. C. & MURPHY, P. M. 2011. Organ-specific innate immune responses in a mouse model of invasive candidiasis. *J Innate Immun,* 3**,** 180-199.

LIONAKIS, M. S. & NETEA, M. G. 2013. Candida and host determinants of susceptibility to invasive candidiasis. *PLoS Pathog,* 9**,** e1003079.

LIU, Q., SASAKI, T., KOZIERADZKI, I., WAKEHAM, A., ITIE, A., DUMONT, D. J. & PENNINGER, J. M. 1999. SHIP is a negative regulator of growth factor receptor-mediated PKB/Akt activation and myeloid cell survival. *Genes Dev,* 13**,** 786-791.

LOPEZ-COLLAZO, E. & DEL FRESNO, C. 2013. Pathophysiology of endotoxin tolerance: mechanisms and clinical consequences. *Crit Care,* 17**,** 242.

LUO, Y., CHEN, G. L., HANNEMANN, N., IPSEIZ, N., KRONKE, G., BAUERLE, T., MUNOS, L., WIRTZ, S., SCHETT, G. & BOZEC, A. 2015. Microbiota from Obese Mice Regulate Hematopoietic Stem Cell Differentiation by Altering the Bone Niche. *Cell Metab,* 22**,** 886-894.

MALIK, M., PARIKH, I., VASQUEZ, J. B., SMITH, C., TAI, L., BU, G., LADU, M. J., FARDO, D. W., REBECK, G. W. & ESTUS, S. 2015. Genetics ignite focus on microglial inflammation in Alzheimer's disease. *Mol Neurodegener,* 10**,** 52.

MANNO, B., OELLERICH, T., SCHNYDER, T., CORSO, J., LOSING, M., NEUMANN, K., URLAUB, H., BATISTA, F. D., ENGELKE, M. & WIENANDS, J. 2016. The Dok-3/Grb2 adaptor module promotes inducible association of the lipid phosphatase SHIP with the BCR in a coreceptor-independent manner. *Eur J Immunol,* 46**,** 2520-2530.

MARAKALALA, M. J., WILLIAMS, D. L., HOVING, J. C., ENGSTAD, R., NETEA, M. G. & BROWN, G. D. 2013. Dectin-1 plays a redundant role in the immunomodulatory activities of beta-glucan-rich ligands in vivo. *Microbes Infect,* 15**,** 511-515.

MARTINI, M., DE SANTIS, M. C., BRACCINI, L., GULLUNI, F. & HIRSCH, E. 2014. PI3K/AKT signaling pathway and cancer: an updated review. *Ann Med,* 46**,** 372-383.

MAXWELL, M. J., DUAN, M., ARMES, J. E., ANDERSON, G. P., TARLINTON, D. M. & HIBBS, M. L. 2011. Genetic segregation of inflammatory lung disease and autoimmune disease severity in SHIP-1-/- mice. *J Immunol,* 186**,** 7164-7175.

MAXWELL, M. J., SRIVASTAVA, N., PARK, M. Y., TSANTIKOS, E., ENGELMAN, R. W., KERR, W. G. & HIBBS, M. L. 2014. SHIP-1 deficiency in the myeloid compartment is insufficient to induce myeloid expansion or chronic inflammation. *Genes Immun,* 15**,** 233-240.

MILUTINOVIC, B. & KURTZ, J. 2016. Immune memory in invertebrates. *Semin Immunol,* 28**,** 328-342.

MITROULIS, I., RUPPOVA, K., WANG, B., CHEN, L. S., GRZYBEK, M., GRINENKO, T., EUGSTER, A., TROULLINAKI, M., PALLADINI, A., KOURTZELIS, I., CHATZIGEORGIOU, A., SCHLITZER, A., BEYER, M., JOOSTEN, L. A. B., ISERMANN, B., LESCHE, M., PETZOLD, A., SIMONS, K., HENRY, I., DAHL, A., SCHULTZE, J. L., WIELOCKX, B., ZAMBONI, N., MIRTSCHINK, P., COSKUN, U., HAJISHENGALLIS, G., NETEA, M. G. & CHAVAKIS, T. 2018. Modulation of Myelopoiesis Progenitors Is an Integral Component of Trained Immunity. *Cell,* 172**,** 147-161 e12.

MOSSER, D. M. & ZHANG, X. 2008. Activation of murine macrophages. *Curr Protoc Immunol,* Chapter 14**,** Unit 14 2.

NEILL, L., TIEN, A. H., REY-LADINO, J. & HELGASON, C. D. 2007. SHIP-deficient mice provide insights into the regulation of dendritic cell development and function. *Exp Hematol,* 35**,** 627-639.

NETEA, M. G., JOOSTEN, L. A., LATZ, E., MILLS, K. H., NATOLI, G., STUNNENBERG, H. G., O'NEILL, L. A. & XAVIER, R. J. 2016. Trained immunity: A program of innate immune memory in health and disease. *Science,* 352**,** aaf1098.

NETEA, M. G., JOOSTEN, L. A., VAN DER MEER, J. W., KULLBERG, B. J. & VAN DE VEERDONK, F. L. 2015a. Immune defence against Candida fungal infections. *Nat Rev Immunol,* 15**,** 630-42.

NETEA, M. G., JOOSTEN, L. A. B. & VAN DER MEER, J. W. M. 2017. Hypothesis: stimulation of trained immunity as adjunctive immunotherapy in cancer. *J Leukoc Biol,* 102**,** 1323-1332.

NETEA, M. G., LATZ, E., MILLS, K. H. G. & O&APOS;NEILL, L. A. J. 2015b. Innate immune memory: a paradigm shift in understanding host defense. *Nature immunology.*16, 675-679.

NETEA, M. G., QUINTIN, J. & VAN DER MEER, J. W. 2011. Trained immunity: a memory for innate host defense. *Cell Host Microbe,* 9**,** 355-361.

NGO, L. Y., KASAHARA, S., KUMASAKA, D. K., KNOBLAUGH, S. E., JHINGRAN, A. & HOHL, T. M. 2014. Inflammatory monocytes mediate early and organ-specific innate defense during systemic candidiasis. *J Infect Dis,* 209**,** 109-119.

NOVAKOVIC, B., HABIBI, E., WANG, S. Y., ARTS, R. J. W., DAVAR, R., MEGCHELENBRINK, W., KIM, B., KUZNETSOVA, T., KOX, M., ZWAAG, J., MATARESE, F., VAN HEERINGEN, S. J., JANSSEN-MEGENS, E. M., SHARIFI, N., WANG, C., KERAMATI, F., SCHOONENBERG, V., FLICEK, P., CLARKE, L., PICKKERS, P., HEATH, S., GUT, I., NETEA, M. G., MARTENS, J. H. A., LOGIE, C. & STUNNENBERG, H. G. 2016. beta-Glucan Reverses the Epigenetic State of LPS-Induced Immunological Tolerance. *Cell,* 167**,** 1354-1368 e14.

O'CONNELL, R. M., CHAUDHURI, A. A., RAO, D. S. & BALTIMORE, D. 2009. Inositol phosphatase SHIP1 is a primary target of miR-155. *Proc Natl Acad Sci U S A,* 106**,** 7113-7118.

O'CONNELL, R. M., KAHN, D., GIBSON, W. S., ROUND, J. L., SCHOLZ, R. L., CHAUDHURI, A. A., KAHN, M. E., RAO, D. S. & BALTIMORE, D. 2010. MicroRNA-155 promotes autoimmune inflammation by enhancing inflammatory T cell development. *Immunity,* 33**,** 607-619.

O'NEILL, S. K., GETAHUN, A., GAULD, S. B., MERRELL, K. T., TAMIR, I., SMITH, M. J., DAL PORTO, J. M., LI, Q. Z. & CAMBIER, J. C. 2011. Monophosphorylation of CD79a and CD79b ITAM motifs initiates a SHIP-1 phosphatase-mediated inhibitory signaling cascade required for B cell anergy. *Immunity,* 35**,** 746-756.

OH, S. Y., ZHENG, T., BAILEY, M. L., BARBER, D. L., SCHROEDER, J. T., KIM, Y. K. & ZHU, Z. 2007. Src homology 2 domain-containing inositol 5-phosphatase

1 deficiency leads to a spontaneous allergic inflammation in the murine lung. *J Allergy Clin Immunol,* 119**,** 123-131.

ONG, C. J., MING-LUM, A., NODWELL, M., GHANIPOUR, A., YANG, L., WILLIAMS, D. E., KIM, J., DEMIRJIAN, L., QASIMI, P., RUSCHMANN, J., CAO, L. P., MA, K., CHUNG, S. W., DURONIO, V., ANDERSEN, R. J., KRYSTAL, G. & MUI, A. L. 2007. Small-molecule agonists of SHIP1 inhibit the phosphoinositide 3-kinase pathway in hematopoietic cells. *Blood,* 110**,** 1942-1949.

ONO, M., BOLLAND, S., TEMPST, P. & RAVETCH, J. V. 1996. Role of the inositol phosphatase SHIP in negative regulation of the immune system by the receptor Fc(gamma)RIIB. *Nature,* 383**,** 263-266.

PALMER, C. D., MUTCH, B. E., WORKMAN, S., MCDAID, J. P., HORWOOD, N. J. & FOXWELL, B. M. 2008. Bmx tyrosine kinase regulates TLR4-induced IL-6 production in human macrophages independently of p38 MAPK and NFkappaB activity. *Blood,* 111**,** 1781-1788.

PARK, M. Y., SRIVASTAVA, N., SUDAN, R., VIERNES, D. R., CHISHOLM, J. D., ENGELMAN, R. W. & KERR, W. G. 2014. Impaired T-cell survival promotes mucosal inflammatory disease in SHIP1-deficient mice. *Mucosal Immunol,* 7**,** 1429-1439.

PAULS, S. D. & MARSHALL, A. J. 2017. Regulation of immune cell signaling by SHIP1: A phosphatase, scaffold protein and potential therapeutic target. *Eur J Immunol.*47, 932-945.

PIKE WINER, L. S. & WU, M. 2014. Rapid analysis of glycolytic and oxidative substrate flux of cancer cells in a microplate. *PLoS One,* 9**,** e109916.

PITARCH, A., NOMBELA, C. & GIL, C. 2016. Seroprofiling at the Candida albicans protein species level unveils an accurate molecular discriminator for candidemia. *J Proteomics,* 134**,** 144-162.

POULAIN, D. 2015. Candida albicans, plasticity and pathogenesis. *Crit Rev Microbiol,* 41**,** 208-217.

POULAIN, D. & JOUAULT, T. 2004. Candida albicans cell wall glycans, host receptors and responses: elements for a decisive crosstalk. *Curr Opin Microbiol,* 7**,** 342-349.

POURRAJAB, F., YAZDI, M. B., ZARCH, M. B., ZARCH, M. B. & HEKMATIMOGHADDAM, S. 2015. Cross talk of the first-line defense TLRs with PI3K/Akt pathway, in preconditioning therapeutic approach. *Mol Cell Ther,* 3**,** 4.

QIAN, Q., JUTILA, M. A., VAN ROOIJEN, N. & CUTLER, J. E. 1994. Elimination of mouse splenic macrophages correlates with increased susceptibility to experimental disseminated candidiasis. *J Immunol,* 152**,** 5000-5008.

QUINTIN, J., SAEED, S., MARTENS, J. H. A., GIAMARELLOS-BOURBOULIS, E. J., IFRIM, D. C., LOGIE, C., JACOBS, L., JANSEN, T., KULLBERG, B. J., WIJMENGA, C., JOOSTEN, L. A. B., XAVIER, R. J., VAN DER MEER, J. W. M., STUNNENBERG, H. G. & NETEA, M. G. 2012. Candida albicans infection affords protection against reinfection via functional reprogramming of monocytes. *Cell Host Microbe,* 12**,** 223-232.

RAJARAM, M. V., BUTCHAR, J. P., PARSA, K. V., CREMER, T. J., AMER, A., SCHLESINGER, L. S. & TRIDANDAPANI, S. 2009. Akt and SHIP modulate

Francisella escape from the phagosome and induction of the Fas-mediated death pathway. *PLoS One,* 4**,** e7919.

REIMER-MICHALSKI, E. M. & CONRATH, U. 2016. Innate immune memory in plants. *Semin Immunol,* 28**,** 319-327.

ROHRSCHNEIDER, L. R., FULLER, J. F., WOLF, I., LIU, Y. & LUCAS, D. M. 2000. Structure, function, and biology of SHIP proteins. *Genes Dev,* 14**,** 505-520.

ROSAS, M., LIDDIARD, K., KIMBERG, M., FARO-TRINDADE, I., MCDONALD, J. U., WILLIAMS, D. L., BROWN, G. D. & TAYLOR, P. R. 2008. The induction of inflammation by dectin-1 in vivo is dependent on myeloid cell programming and the progression of phagocytosis. *J Immunol,* 181**,** 3549-3557.

ROTHCHILD, A. C., SISSONS, J. R., SHAFIANI, S., PLAISIER, C., MIN, D., MAI, D., GILCHRIST, M., PESCHON, J., LARSON, R. P., BERGTHALER, A., BALIGA, N. S., URDAHL, K. B. & ADEREM, A. 2016. MiR-155-regulated molecular network orchestrates cell fate in the innate and adaptive immune response to Mycobacterium tuberculosis. *Proc Natl Acad Sci U S A,* 113**,** 6172-6181.

RUSCHMANN, J., HO, V., ANTIGNANO, F., KURODA, E., LAM, V., IBARAKI, M., SNYDER, K., KIM, C., FLAVELL, R. A., KAWAKAMI, T., SLY, L., TURHAN, A. G. & KRYSTAL, G. 2010. Tyrosine phosphorylation of SHIP promotes its proteasomal degradation. *Exp Hematol,* 38**,** 392-402, 402 e1.

RUSEK, P., WALA, M., DRUSZCZYNSKA, M. & FOL, M. 2018. Infectious Agents as Stimuli of Trained Innate Immunity. *Int J Mol Sci,* 19.

RUSSO, C. M., ADHIKARI, A. A., WALLACH, D. R., FERNANDES, S., BALCH, A. N., KERR, W. G. & CHISHOLM, J. D. 2015. Synthesis and initial evaluation of quinoline-based inhibitors of the SH2-containing inositol 5'-phosphatase (SHIP). *Bioorg Med Chem Lett,* 25**,** 5344-5348.

SAEED, S., QUINTIN, J., KERSTENS, H. H., RAO, N. A., AGHAJANIREFAH, A., MATARESE, F., CHENG, S. C., RATTER, J., BERENTSEN, K., VAN DER ENT, M. A., SHARIFI, N., JANSSEN-MEGENS, E. M., TER HUURNE, M., MANDOLI, A., VAN SCHAIK, T., NG, A., BURDEN, F., DOWNES, K., FRONTINI, M., KUMAR, V., GIAMARELLOS-BOURBOULIS, E. J., OUWEHAND, W. H., VAN DER MEER, J. W., JOOSTEN, L. A., WIJMENGA, C., MARTENS, J. H., XAVIER, R. J., LOGIE, C., NETEA, M. G. & STUNNENBERG, H. G. 2014. Epigenetic programming of monocyte-to-macrophage differentiation and trained innate immunity. *Science,* 345**,** 1251086.

SALAM, A. P., PARIANTE, C. M. & ZUNSZAIN, P. 2017. Innate Immune Memory: Implications for Microglial Function and Neuroprogression. *Mod Trends Pharmacopsychiatry,* 31**,** 67-78.

SCHAPPE, M. S., SZTEYN, K., STREMSKA, M. E., MENDU, S. K., DOWNS, T. K., SEEGREN, P. V., MAHONEY, M. A., DIXIT, S., KRUPA, J. K., STIPES, E. J., ROGERS, J. S., ADAMSON, S. E., LEITINGER, N. & DESAI, B. N. 2018. Chanzyme TRPM7 Mediates the Ca(2+) Influx Essential for Lipopolysaccharide-Induced Toll-Like Receptor 4 Endocytosis and Macrophage Activation. *Immunity,* 48**,** 59-74 e5.

SCHRODER, K. & TSCHOPP, J. 2010. The inflammasomes. *Cell,* 140**,** 821-32.

SCHRUM, J. E., CRABTREE, J. N., DOBBS, K. R., KIRITSY, M. C., REED, G. W., GAZZINELLI, R. T., NETEA, M. G., KAZURA, J. W., DENT, A. E., FITZGERALD, K. A. & GOLENBOCK, D. T. 2018. Cutting Edge: Plasmodium falciparum Induces Trained Innate Immunity. *J Immunol,* 200**,** 1243-1248.

SLY, L. M., RAUH, M. J., KALESNIKOFF, J., SONG, C. H. & KRYSTAL, G. 2004. LPS-induced upregulation of SHIP is essential for endotoxin tolerance. *Immunity,* 21**,** 227-239.

SRIVASTAVA, N., IYER, S., SUDAN, R., YOUNGS, C., ENGELMAN, R. W., HOWARD, K. T., RUSSO, C. M., CHISHOLM, J. D. & KERR, W. G. 2016. A small-molecule inhibitor of SHIP1 reverses age- and diet-associated obesity and metabolic syndrome. *JCI Insight,* 1.

STENTON, G. R., MACKENZIE, L. F., TAM, P., CROSS, J. L., HARWIG, C., RAYMOND, J., TOEWS, J., CHERNOFF, D., MACRURY, T. & SZABO, C. 2013a. Characterization of AQX-1125, a small-molecule SHIP1 activator: Part 2. Efficacy studies in allergic and pulmonary inflammation models in vivo. *Br J Pharmacol,* 168**,** 1519-1529.

STENTON, G. R., MACKENZIE, L. F., TAM, P., CROSS, J. L., HARWIG, C., RAYMOND, J., TOEWS, J., WU, J., OGDEN, N., MACRURY, T. & SZABO, C. 2013b. Characterization of AQX-1125, a small-molecule SHIP1 activator: Part 1. Effects on inflammatory cell activation and chemotaxis in vitro and pharmacokinetic characterization in vivo. *Br J Pharmacol,* 168**,** 1506-1518.

STEVENS, W. B., NETEA, M. G., KATER, A. P. & VAN DER VELDEN, W. J. 2016. 'Trained immunity': consequences for lymphoid malignancies. *Haematologica,* 101**,** 1460-1468.

SUN, J. C., BEILKE, J. N. & LANIER, L. L. 2009. Adaptive immune features of natural killer cells. *Nature,* 457**,** 557-561.

TAMURA, N., HAZEKI, K., OKAZAKI, N., KAMETANI, Y., MURAKAMI, H., TAKABA, Y., ISHIKAWA, Y., NIGORIKAWA, K. & HAZEKI, O. 2009. Specific role of phosphoinositide 3-kinase p110alpha in the regulation of phagocytosis and pinocytosis in macrophages. *Biochem J,* 423**,** 99-108.

TARASENKO, T., KOLE, H. K., CHI, A. W., MENTINK-KANE, M. M., WYNN, T. A. & BOLLAND, S. 2007. T cell-specific deletion of the inositol phosphatase SHIP reveals its role in regulating Th1/Th2 and cytotoxic responses. *Proc Natl Acad Sci U S A,* 104**,** 11382-11387.

TAYLOR, P. R., TSONI, S. V., W5ILLMENT, J. A., DENNEHY, K. M., ROSAS, M., FINDON, H., HAYNES, K., STEELE, C., BOTTO, M., GORDON, S. & BROWN, G. D. 2007. Dectin-1 is required for beta-glucan recognition and control of fungal infection. *Nat Immunol,* 8**,** 31-38.

TRIBOULEY, J., TRIBOULEY-DURET, J. & APPRIOU, M. 1978. [Effect of Bacillus Callmette Guerin (BCG) on the receptivity of nude mice to Schistosoma mansoni]. *C R Seances Soc Biol Fil,* 172**,** 902-904.

TROTTA, R., PARIHAR, R., YU, J., BECKNELL, B., ALLARD, J., 2ND, WEN, J., DING, W., MAO, H., TRIDANDAPANI, S., CARSON, W. E. & CALIGIURI, M. A. 2005. Differential expression of SHIP1 in CD56bright and CD56dim NK cells provides

a molecular basis for distinct functional responses to monokine costimulation. *Blood,* 105**,** 3011-3018.

TROUTMAN, T. D., BAZAN, J. F. & PASARE, C. 2012. Toll-like receptors, signaling adapters and regulation of the pro-inflammatory response by PI3K. *Cell Cycle,* 11**,** 3559-3567.

USHACH, I. & ZLOTNIK, A. 2016. Biological role of granulocyte macrophage colony-stimulating factor (GM-CSF) and macrophage colony-stimulating factor (M-CSF) on cells of the myeloid lineage. *J Leukoc Biol,* 100**,** 481-489.

VAN 'T WOUT, J. W., POELL, R. & VAN FURTH, R. 1992. The role of BCG/PPD-activated macrophages in resistance against systemic candidiasis in mice. *Scand J Immunol,* 36**,** 713-719.

VAN DER HEIJDEN, C., NOZ, M. P., JOOSTEN, L. A. B., NETEA, M. G., RIKSEN, N. P. & KEATING, S. T. 2018. Epigenetics and Trained Immunity. *Antioxid Redox Signal,* 29**,** 1023-1040.

VAN DER MEER, J. W., JOOSTEN, L. A., RIKSEN, N. & NETEA, M. G. 2015. Trained immunity: A smart way to enhance innate immune defence. *Mol Immunol,* 68**,** 40-44.

VAN SPLUNTER, M., VAN OSCH, T. L. J., BRUGMAN, S., SAVELKOUL, H. F. J., JOOSTEN, L. A. B., NETEA, M. G. & VAN NEERVEN, R. J. J. 2018. Induction of Trained Innate Immunity in Human Monocytes by Bovine Milk and Milk-Derived Immunoglobulin G. *Nutrients,* 10.

VIERNES, D. R., CHOI, L. B., KERR, W. G. & CHISHOLM, J. D. 2014. Discovery and development of small molecule SHIP phosphatase modulators. *Med Res Rev,* 34**,** 795-824.

VO, T. T. & FRUMAN, D. A. 2015. INPP4B Is a Tumor Suppressor in the Context of PTEN Deficiency. *Cancer Discov,* 5**,** 697-700.

WALACHOWSKI, S., TABOURET, G., FABRE, M. & FOUCRAS, G. 2017. Molecular Analysis of a Short-term Model of beta-Glucans-Trained Immunity Highlights the Accessory Contribution of GM-CSF in Priming Mouse Macrophages Response. *Front Immunol,* 8**,** 1089.

WANG, J., WU, M., WEN, J., YANG, K., LI, M., ZHAN, X., FENG, L., LI, M. & HUANG, X. 2014. MicroRNA-155 induction by Mycobacterium bovis BCG enhances ROS production through targeting SHIP1. *Mol Immunol,* 62**,** 29-36.

WANG, J. W., HOWSON, J. M., GHANSAH, T., DESPONTS, C., NINOS, J. M., MAY, S. L., NGUYEN, K. H., TOYAMA-SORIMACHI, N. & KERR, W. G. 2002. Influence of SHIP on the NK repertoire and allogeneic bone marrow transplantation. *Science,* 295**,** 2094-2097.

WENDELN, A. C., DEGENHARDT, K., KAURANI, L., GERTIG, M., ULAS, T., JAIN, G., WAGNER, J., HASLER, L. M., WILD, K., SKODRAS, A., BLANK, T., STASZEWSKI, O., DATTA, M., CENTENO, T. P., CAPECE, V., ISLAM, M. R., KERIMOGLU, C., STAUFENBIEL, M., SCHULTZE, J. L., BEYER, M., PRINZ, M., JUCKER, M., FISCHER, A. & NEHER, J. J. 2018. Innate immune memory in the brain shapes neurological disease hallmarks. *Nature,* 556**,** 332-338.

WHITNEY, P. G., BAR, E., OSORIO, F., ROGERS, N. C., SCHRAML, B. U., DEDDOUCHE, S., LEIBUNDGUT-LANDMANN, S. & REIS E SOUSA, C. 2014.

Syk signaling in dendritic cells orchestrates innate resistance to systemic fungal infection. *PLoS Pathog,* 10**,** e1004276.

YAO, H., ZHANG, H., LAN, K., WANG, H., SU, Y., LI, D., SONG, Z., CUI, F., YIN, Y. & ZHANG, X. 2017. Purified Streptococcus pneumoniae Endopeptidase O (PepO) Enhances Particle Uptake by Macrophages in a Toll-Like Receptor 2- and miR-155-Dependent Manner. *Infect Immun,* 85.

ZHOU, P., KITAURA, H., TEITELBAUM, S. L., KRYSTAL, G., ROSS, F. P. & TAKESHITA, S. 2006. SHIP1 negatively regulates proliferation of osteoclast precursors via Akt-dependent alterations in D-type cyclins and p27. *J Immunol,* 177**,** 8777-8784.

ZHU, L., YANG, T., LI, L., SUN, L., HOU, Y., HU, X., ZHANG, L., TIAN, H., ZHAO, Q., PENG, J., ZHANG, H., WANG, R., YANG, Z., ZHANG, L. & ZHAO, Y. 2014. TSC1 controls macrophage polarization to prevent inflammatory disease. *Nat Commun,* 5**,** 4696.

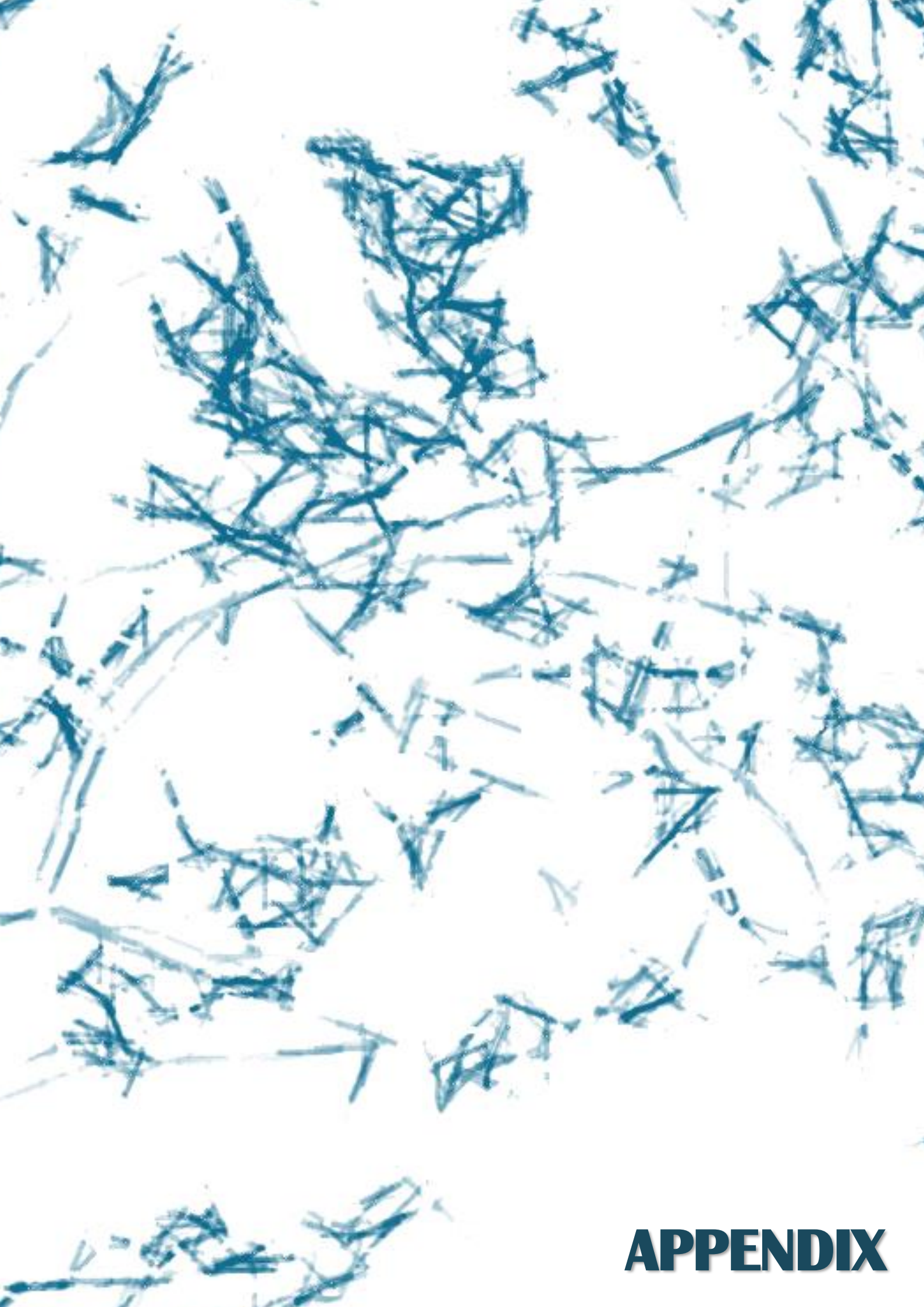

APPENDIX

Publication derived from this work

Saz-Leal P.*, Del Fresno C.*, Brandi P., Dungan O.M., Chisholm J.D., Kerr W.G., Sancho D. 2018. Targeting SHIP-1 in Myeloid Cells Enhances Trained Immunity and Boosts Response to Infection. *Cell Reports*. Accepted. https://doi.org/10.1016/j.celrep.2018.09.092.

Other publications during PhD training

Del Fresno C.*, **Saz-Leal P.***, Enamorado M., Wculek S.K., Martínez-Cano S., Blanco-Menéndez N., Schulz O., Gallizioli M., Miró-Mur F., Cano E., Planas A., Sancho D. (2018). DNGR-1 in dendritic cells limits tissue damage by dampening neutrophil recruitment. *Science*, 362 (6214):351-356. *** (Co-first authors)**.

Domínguez-Soto Á., Simón-Fuentes M., de Las Casas-Engel M., Cuevas V.D., López-Bravo M., Domínguez-Andrés J., **Saz-Leal P.**, Sancho D., Ardavín C., Ochoa-Grullón J., Sánchez-Ramón S., Vega M.A., Corbí A.L. (2018). IVIg Promote Cross-Tolerance against Inflammatory Stimuli In Vitro and In Vivo. *J Immunol*, 201 (1): 41-52.

Del Fresno C., Iborra S, **Saz-Leal P.**, Martínez-López M., Sancho D. (2018). Flexible Signaling of Myeloid C-Type Lectin Receptors in Immunity and Inflammation. *Front Immunol*, 9:804

Report

Cell Reports

Targeting SHIP-1 in Myeloid Cells Enhances Trained Immunity and Boosts Response to Infection

Graphical Abstract

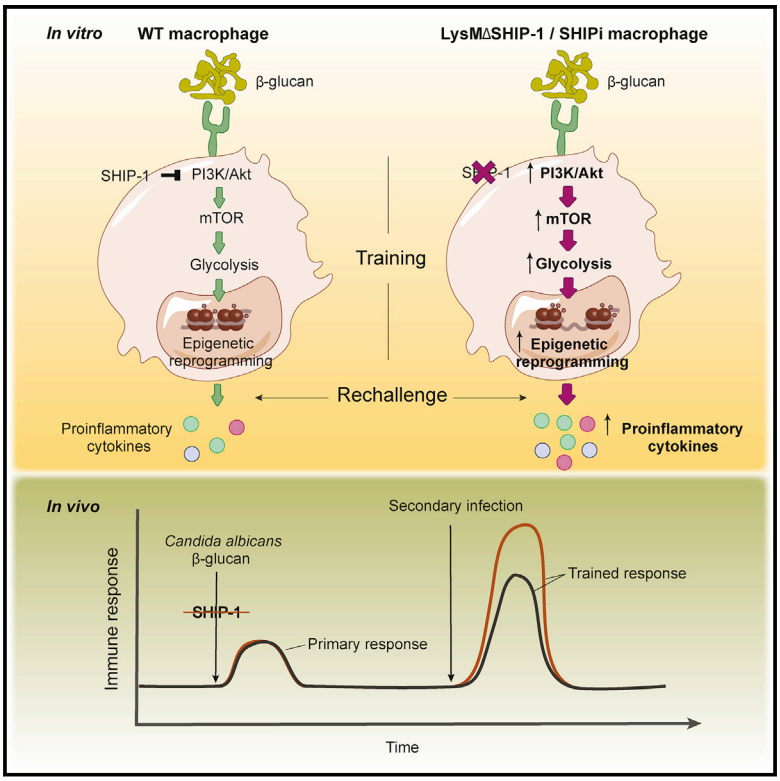

Highlights

- β-Glucan-induced trained immunity is enhanced by SHIP-1 deletion in macrophages
- SHIP-1 regulates molecular, metabolic, and epigenetic hallmarks of trained immunity
- Myeloid SHIP-1 deficiency improves protection conferred by trained immunity
- SHIP-1 pharmacological inhibition enhances trained immunity in mice and human cells

Authors

Paula Saz-Leal, Carlos del Fresno, Paola Brandi, ..., John D. Chisholm, William G. Kerr, David Sancho

Correspondence

dsancho@cnic.es

In Brief

Trained immunity leads to long-term protection, but strategies to boost it require further investigation. Saz-Leal et al. show that myeloid SHIP-1 deletion enhances trained immunity, improving the response to pathogen-specific or heterologous challenges. Pharmacological inhibition of SHIP-1 also potentiates this phenomenon, thereby revealing a potential tool to harness trained immunity.

Saz-Leal et al., 2018, Cell Reports *25*, 1–9
October 30, 2018
https://doi.org/10.1016/j.celrep.2018.09.092

CellPress

Please cite this article in press as: Saz-Leal et al., Targeting SHIP-1 in Myeloid Cells Enhances Trained Immunity and Boosts Response to Infection, Cell Reports (2018), https://doi.org/10.1016/j.celrep.2018.09.092

Cell Reports
Report

Targeting SHIP-1 in Myeloid Cells Enhances Trained Immunity and Boosts Response to Infection

Paula Saz-Leal,[1,6] Carlos del Fresno,[1,6] Paola Brandi,[1] Sarai Martínez-Cano,[1] Otto M. Dungan,[2] John D. Chisholm,[2] William G. Kerr,[2,3,4,5] and David Sancho[1,7,*]
[1]Immunobiology Lab, Centro Nacional de Investigaciones Cardiovasculares (CNIC), Melchor Fernández Almagro 3, Madrid, 28029, Spain
[2]Department of Chemistry, Syracuse University, Syracuse, NY 13210, USA
[3]Department of Microbiology and Immunology, State University of New York (SUNY) Upstate Medical University, Syracuse, NY 13210, USA
[4]Pediatrics Department, SUNY Upstate Medical University, Syracuse, NY, USA
[5]Centre d'Immunologie de Marseille-Luminy, Marseille, France
[6]These authors contributed equally
[7]Lead Contact
*Correspondence: dsancho@cnic.es
https://doi.org/10.1016/j.celrep.2018.09.092

SUMMARY

β-Glucan-induced trained immunity in myeloid cells leads to long-term protection against secondary infections. Although previous studies have characterized this phenomenon, strategies to boost trained immunity remain undefined. We found that β-glucan-trained macrophages from mice with a myeloid-specific deletion of the phosphatase SHIP-1 (LysMΔSHIP-1) showed enhanced proinflammatory cytokine production in response to lipopolysaccharide. Following β-glucan training, SHIP-1-deficient macrophages exhibited increased phosphorylation of Akt and mTOR targets, correlating with augmented glycolytic metabolism. Enhanced training in the absence of SHIP-1 relied on histone methylation and acetylation. Trained LysMΔSHIP-1 mice produced increased amounts of proinflammatory cytokines upon rechallenge *in vivo* and were better protected against *Candida albicans* infection compared with control littermates. Pharmacological inhibition of SHIP-1 enhanced trained immunity against *Candida* infection in mouse macrophages and human peripheral blood mononuclear cells. Our data establish proof of concept for improvement of trained immunity and a strategy to achieve it by targeting SHIP-1.

Q1 INTRODUCTION

Innate immune cells challenged with certain stimuli undergo long-lasting changes that result in improved response to a second challenge by the same or different microbial insult, a process referred to as trained immunity (Quintin et al., 2012). Stimuli driving trained immunity lead to a shift to aerobic glycolysis (Arts et al., 2016b), accompanied by sustained changes in the epigenome, mainly via histone methylation and acetylation (Netea et al., 2016). Among trained immunity inducers, exposure to a low dose of *Candida albicans* or the fungal cell wall component β-glucan protects mice from secondary lethal systemic candidiasis (Bistoni et al., 1986) or heterologous *Staphylococcus aureus* septicemia (Di Luzio and Williams, 1978). This acquired resistance does not rely on T/B lymphocytes or natural killer (NK) cells but occurs in a myeloid-dependent manner (Cheng et al., 2014; Quintin et al., 2012).

The C-type lectin receptor Dectin-1 is critical for *Candida albicans* or β-glucan sensing, leading to immune training of monocytes (Quintin et al., 2012). These primed macrophages show heightened production of proinflammatory cytokines to a wide variety of insults (Ifrim et al., 2013; Quintin et al., 2012). Dectin-1-mediated training relies on activation of the PI3K (phosphoinositide 3-kinase)/mTOR (mammalian target of rapamycin) pathway (Cheng et al., 2014). PI3K-induced Akt signaling is tightly regulated by phosphoinositide phosphatases, which counterbalance PI3K activity (Eramo and Mitchell, 2016). Among those phosphatases, the hematopoietic-restricted SHIP-1 (SH2-containing inositol 5′-phosphatase 1) (Kerr, 2011) is of particular interest, as we showed that it binds to the intracellular tail of Dectin-1 receptor in granulocyte-macrophage colony-stimulating factor (GM-CSF) bone marrow-derived cells (Blanco-Menéndez et al., 2015).

Because *Candida albicans*-induced trained immunity relies on Dectin-1 and PI3K signaling, and SHIP-1 couples to Dectin-1 and counteracts PI3K function, we postulated that SHIP-1 targeting could modulate trained immunity triggered by Dectin-1. Our results indicate that SHIP-1 has a regulatory role in β-glucan-induced training, affecting all hallmarks involved in that process. Moreover, *in vivo* SHIP-1 deficiency in the myeloid compartment improves protection conferred by trained immunity. Notably, enhanced proinflammatory cytokine production and better protection was also achieved by pharmacological SHIP-1 inhibition in both mice and human peripheral blood mononuclear cells (PBMCs), providing a potential therapeutic approach to boost trained immunity.

RESULTS

SHIP-1 Deletion Boosts β-Glucan-Induced Trained Immunity in Macrophages

Dectin-1 sensing of β-glucan induces trained immunity in myeloid cells, including PBMCs (Ifrim et al., 2013) or bone

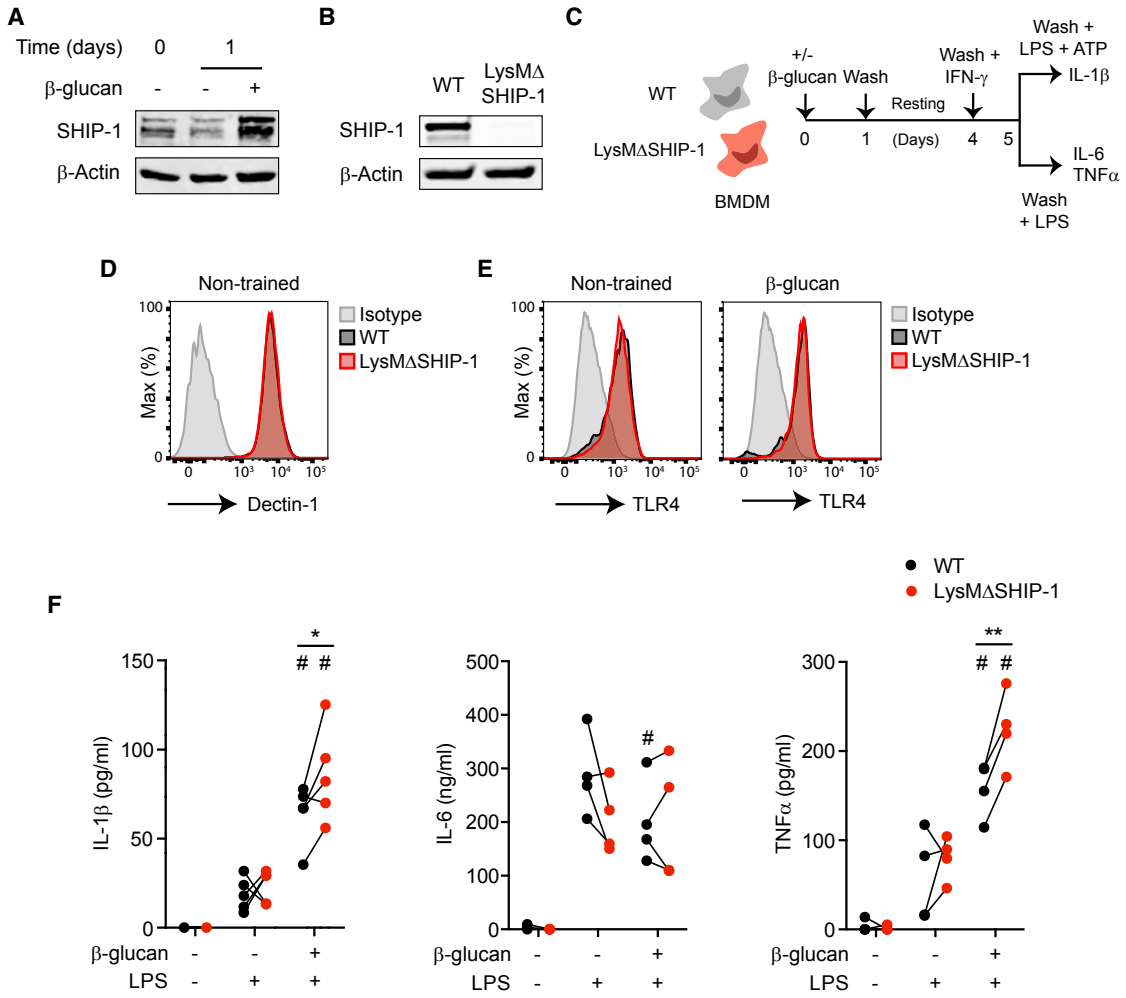

Figure 1. SHIP-1 Deletion Boosts β-Glucan-Induced Trained Immunity in Macrophages

(A) SHIP-1 expression by WB, normalized to β-actin, in bone marrow-derived macrophages (BMDMs) exposed (+) or not (−) to β-glucan (whole glucan particles) for the indicated time. Representative experiment of three performed.

(B) SHIP-1 protein expression in BMDMs. Representative experiment of six performed.

(C) Trained immunity *in vitro* model in mouse BMDMs. See also Figure S1A.

(D and E) Dectin-1 expression in BMDMs before β-glucan stimulation (D) or TLR4 expression both under non-trained (left) or β-glucan-primed (right) conditions, just before LPS stimulation (E), according to Figure 1C. FACS histograms representative of four independent experiments. See also Figures S1B and S1C.

(F) BMDMs were stimulated (+) or not (−) with β-glucan or LPS, and IL-1β (left), IL-6 (middle), and TNFα production (right) was analyzed in supernatants according to Figure 1C.

See also Figure S2. Independent experiments (n = 4 or 5) are shown. *$p < 0.05$ and **$p < 0.01$, paired Student's t test comparing wild-type (WT) and LysMΔSHIP-1. #$p < 0.05$, paired Student's t test comparing stimulated or not with β-glucan within the same genotype.

marrow-derived macrophages (BMDMs) (Walachowski et al., 2017). We initially stimulated BMDMs with purified particulate β-glucan from *S. cerevisiae*, a well-known ligand for Dectin-1 (Rosas et al., 2008). SHIP-1 basal expression in BMDMs was further induced after 1 day of β-glucan stimulation (Figure 1A). To study the potential involvement of SHIP-1 in Dectin-1-triggered trained immunity, we generated BMDMs from wild-type (WT) mice or mice bearing a myeloid-specific deletion of SHIP-1 in the myeloid compartment (LysMΔSHIP-1) (Collazo et al., 2012) (Figure 1B). Next, we adapted the proposed *in vitro* long-term scheme of trained immunity (Quintin et al., 2012) to IFN-γ-primed BMDMs, evaluating whether training with β-glucan boosts cytokine production in response to lipopolysaccharide (LPS) (Figure 1C). Of note, as previously described (Mosser and Zhang, 2008), IFN-γ priming was required to detect LPS-induced cytokines in BMDMs (Figure S1A), regardless of the induction of training. Surface expression of the receptors involved in β-glucan (Dectin-1; Figures 1D and S1B) and LPS (TLR4; Figures 1E and S1C) recognition were comparable between WT and LysMΔSHIP-1 BMDMs. We found that β-glucan-induced training resulted in increased cell viability in WT BMDMs (Figure S2), concurring with previous results (Bekkering et al., 2016; Garcia-Valtanen et al., 2017). Non-trained SHIP-1-deficient BMDMs showed higher viability than

their WT counterparts, but the relative cell number after β-glucan training was similar between genotypes (Figure S2). To ensure the analysis of cell-intrinsic responses as described (Bekkering et al., 2016), cytokine production was normalized to the relative cell number present in each treatment.

Pre-incubation of WT BMDMs with β-glucan prompted a greater production of IL-1β and TNFα in response to LPS (Figures 1F and S1A), reproducing trained immunity (Quintin et al., 2012). Notably, β-glucan-trained LysMΔSHIP-1 BMDMs showed an increased production of these trained immunity-associated cytokines compared with trained WT BMDMs (Figure 1F). Conversely, IL-6 was not induced following training or in the absence of SHIP-1 in this setting (Figure 1F). Of note, SHIP-1 deletion did not affect any of these inflammatory responses under non-trained conditions. These data indicate that SHIP-1 modulates the extent of LPS-induced proinflammatory cytokine production specifically during β-glucan training.

SHIP-1 Regulates Molecular and Metabolic Hallmarks of Trained Immunity

We tested whether the boost in β-glucan training in the absence of SHIP-1 was accompanied by regulation of key hallmarks involved in the process. Regarding the molecular pathway, Akt was phosphorylated in response to β-glucan in a time-dependent manner in WT BMDMs (Figure 2A, left, and Figure S3A), concurring with previous results (Cheng et al., 2014). Notably, LysMΔSHIP-1 BMDMs showed significantly increased and sustained Akt phosphorylation upon β-glucan stimulation (Figure 2A, left, and Figure S3A). The analysis of mTOR targets, S6 and 4EBP1, also revealed a maintained and significantly increased phosphorylation during the treatment with β-glucan in SHIP-1-deficient BMDMs (Figure 2A, right, and Figure S3B). Of note, a basal activation of the Akt pathway occurs in LysMΔSHIP-1 BMDMs. This is consistent with previous results in which the absence of SHIP-1 was associated with Akt overactivation and survival advantage (Antignano et al., 2010), which would concur with our results in non-trained BMDMs (Figure S2).

Next, we measured the extracellular acidification rate (ECAR) in β-glucan-trained BMDMs in a glycolysis stress test prior to LPS stimulation (Figure 2B). Training with β-glucan for 5 days increased ECAR in WT BMDMs, a metabolic shift that was significantly boosted in trained SHIP-1-deficient BMDMs (Figure 2B), as reflected by enhanced basal (Figure 2C) and maximal (Figure 2D) glycolysis, together with a higher glycolytic reserve (Figure 2E). Increase in glycolytic reserve is the first metabolic signature associated with SHIP-1-deficient BMDMs upon β-glucan training (Figure S4). Consistent with data on signaling pathway activation (Figures 2A and S3), basal enhanced glycolysis was found in LysMΔSHIP-1 BMDMs (Figures 2C–2E and S4), although it did not result in higher cytokine production unless β-glucan-induced training was established (Figure 1F). These results suggest that SHIP-1 controls the extent of the glycolytic switch. Therefore, SHIP-1 deficiency may promote a pro-glycolytic state that could boost inflammatory response upon β-glucan-trained conditions.

To assess whether SHIP-1 could affect epigenetic reprogramming induced by β-glucan, we tested the presence of the activating histone 3 Lys4 trimethylation (H3K4me3) (Cheng et al., 2014; Quintin et al., 2012). Chromatin immunoprecipitation (ChIP) analysis showed that H3K4me3 was specifically enriched by β-glucan training at TNFα promoter in WT BMDMs and further augmented in trained SHIP-1-deficient macrophages (Figure 2F), concurring with final enhanced TNFα production (Figure 1F). Moreover, inhibition of histone methyltransferases using 5′-deoxy-5′-(methylthio)adenosine (MTA) (Quintin et al., 2012) abolished TNFα overproduction in the absence of SHIP-1 upon training, whereas the histone demethylase inhibitor pargyline (Quintin et al., 2012) did not have any effect (Figure 2G). Considering that β-glucan-induced training relies also on histone acetylation, training in the presence of the histone deacetylase activator resveratrol (Cheng et al., 2014) or the histone acetyltransferase inhibitor EGCG (Ifrim et al., 2014) inhibited the enhanced TNFα produced by trained SHIP-1-deficient macrophages (Figure 2H). These results highlight SHIP-1 as a regulator of trained immunity by dampening the Akt/mTOR molecular pathway and the glycolytic switch and relying on the epigenetic reprogramming induced by β-glucan.

Myeloid-Specific Deletion of SHIP-1 Improves Trained Immunity *In Vivo*

The generation of trained immunity *in vivo* leads to cross-protection against diverse secondary infections (Netea et al., 2016). Signaling through PI3K is the canonical molecular pathway implicated in the development of these trained responses (Arts et al., 2016a; Cheng et al., 2014). To test the role of myeloid SHIP-1 in cytokine production under β-glucan training *in vivo*, WT and LysMΔSHIP-1 mice were challenged with LPS after training with β-glucan (Cheng et al., 2014), and serum cytokines were measured (Figure 3A). LPS-induced levels of IL-6 and TNFα were increased in sera from WT mice upon β-glucan pre-treatment (Figure 3B), indicative of the generation of a trained response (Quintin et al., 2012). Notably, serum levels of IL-1β, IL-6, and TNFα were further increased in LysMΔSHIP-1 trained mice compared with trained WT mice (Figure 3B), supporting the regulatory role of SHIP-1 upon β-glucan training also *in vivo*.

Protective response against lethal systemic *Candida albicans* infection by trained immunity relies on monocytes and macrophages (Quintin et al., 2012). After training with β-glucan, WT and LysMΔSHIP-1 mice were intravenously infected with a lethal dose of the clinical isolate *C. albicans* SC5314 (Figure 3C). Both WT and LysMΔSHIP-1 non-trained mice rapidly succumbed upon these infectious conditions (Figure 3D, dashed lines), indicating that SHIP-1 expression in the myeloid compartment is redundant for the primary response to lethal candidiasis. The protective effect of β-glucan administration against a lethal *C. albicans* infection was significantly improved in LysMΔSHIP-1 mice compared with WT littermates (Figure 3D, solid lines).

As trained immunity can be defined as a protection mechanism from secondary lethal *C. albicans* infection induced by a nonlethal encounter with the same pathogen (Quintin et al., 2012), we trained mice with a low dose of *C. albicans* followed by a lethal dose of the fungus (Figure 3E). Again, the training stimulus enlarged the survival time of WT mice and LysMΔSHIP-1 trained mice were more resistant than WT to lethal systemic candidiasis (Figure 3F, solid lines). Notably, we observed enhanced production of IL-1β and TNFα in *Candida*

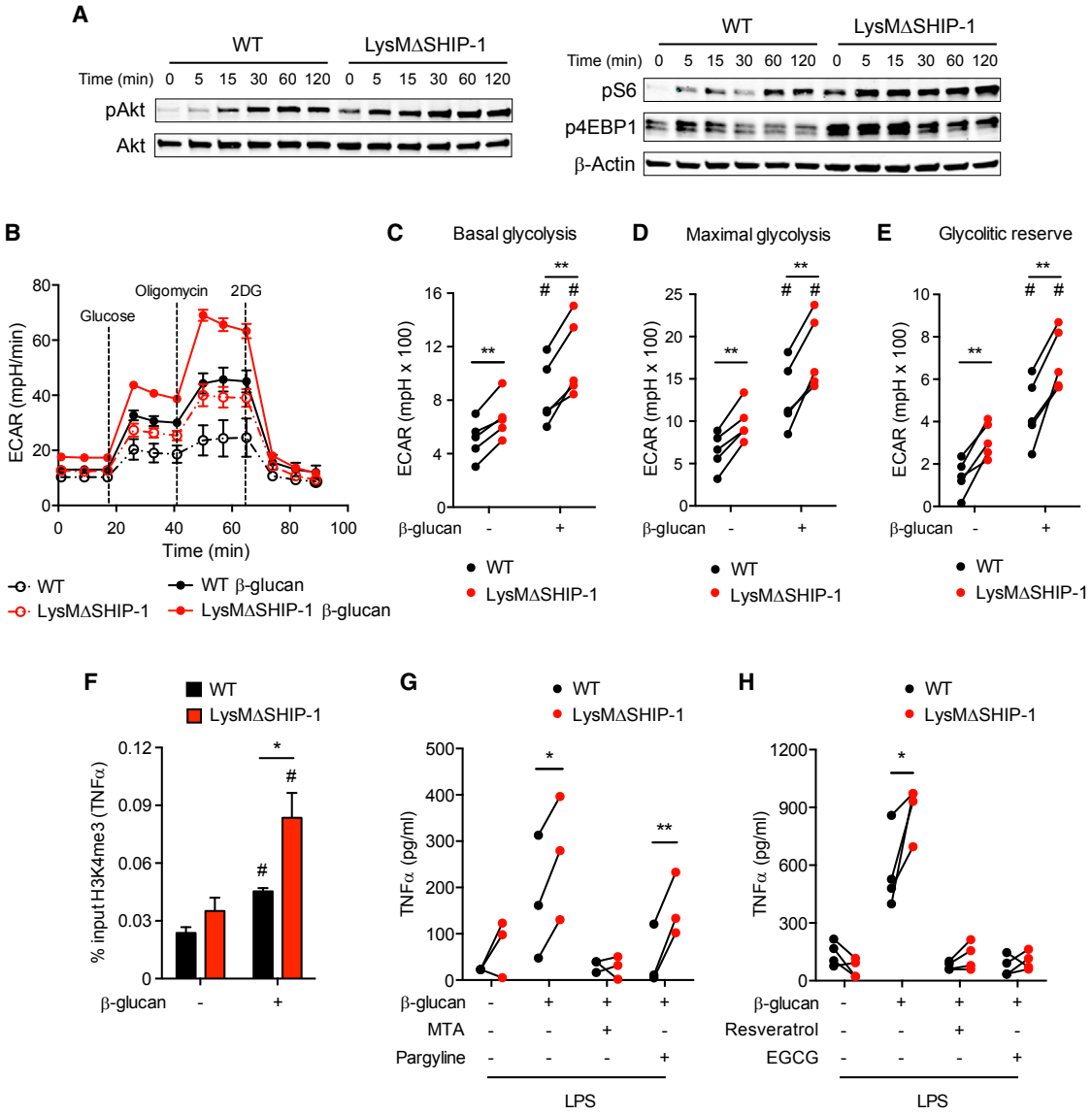

Figure 2. SHIP-1 Regulates Molecular and Metabolic Hallmarks of Trained Immunity

(A) BMDMs were exposed to β-glucan for the indicated time, and phospho-Akt, Akt, phospho-S6, phospho-4EBP1, and β-actin were analyzed by WB. Representative experiment of five performed. See also Figure S3.

(B–E) BMDMs were left untreated (dashed lines) or treated for 1 day with β-glucan (solid lines), washed, rested for 3 days, and re-plated in equal numbers for determination of extracellular acidification rate (ECAR) in a glycolysis stress test upon sequential addition of glucose, oligomycin, and 2-deoxyglucose (2DG) as indicated (B). Analysis of basal glycolysis (C), maximal glycolysis (D), and glycolytic reserve (E). See also Figure S4. Mean ± SEM (B) or individual data (C–E) of five independent cultures are shown.

(F) BMDMs were trained (+) or not (–) with β-glucan for 1 day, washed, and rested for 4 days and chromatin immunoprecipitation (ChIP) against H3K4me3 was performed in which enrichment on the TNFα promoter was analyzed using qPCR. Mean ± SEM of five independent experiments is shown.

(G and H) BMDMs were incubated (+) or not (–) with the methyltransferase inhibitor 5′-deoxy-5′-(methylthio)adenosine (MTA), the histone demethylase inhibitor pargyline (G), the histone deacetylase activator resveratrol, or the histone acetyltransferase inhibitor EGCG (H) for 30 min before β-glucan training and after wash-out. TNFα production was analyzed in supernatants after LPS stimulation according to Figure 1C. Individual data corresponding to three (G) or four (H) independent experiments are shown.

In (C)–(H), *p < 0.05 and **p < 0.01, paired Student's t test comparing WT and LysMΔSHIP-1. In (C)–(F), #p < 0.05, paired Student's t test comparing stimulated or not with β-glucan within the same genotype.

lethally infected kidneys from LysMΔSHIP-1 trained mice (Figure 3G), together with a decreased renal fungal burden (Figure 3H). These data indicate that SHIP-1 deficiency in myeloid cells enhances β-glucan- and *Candida*-induced trained immunity *in vivo*, improving the response to pathogen-specific or heterologous challenges.

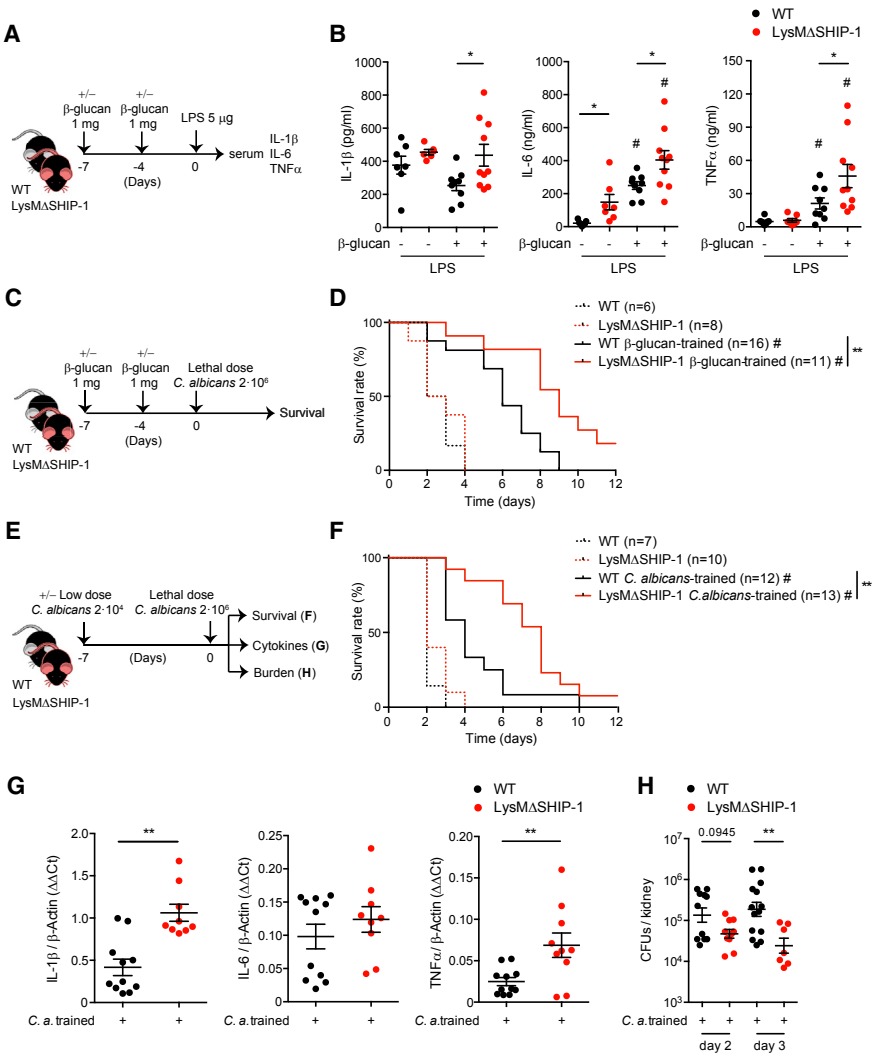

Figure 3. Myeloid-Specific Deletion of SHIP-1 Improves Trained Immunity *In Vivo*

(A) *In vivo* model of training by two intraperitoneal (i.p.) β-glucan injections and secondary i.p. LPS challenge for measuring serum cytokines.

(B) Mice were treated according to Figure 3A. Serum was collected after 60 min (TNFα) or 90 min (IL-1β and IL-6) of LPS challenge, and cytokines were analyzed.

(C) *In vivo* model of training as in (A) but with secondary *Candida albicans* lethal infection.

(D) Survival curve according to Figure 3C.

(E) *In vivo* model of training by a systemic infection with a low dose of *C. albicans* followed by a secondary lethal challenge with the same pathogen.

(F) Survival curve according to Figure 3E.

(G and H) Renal cytokines on day 2 post-infection (p.i.) (G) and kidney fungal burden (H) at indicated time points p.i. were evaluated in trained mice, following model in Figure 3E.

In (B), (G), and (H), single dots correspond to individual mice. Mean ± SEM of two (B and H) or three (G) pooled experiments is shown, including at least 5 mice per condition. *p < 0.05 and **p < 0.01, unpaired Student's t test comparing WT and LysMΔSHIP-1. #p < 0.05, unpaired Student's t test comparing the same genotype stimulated or not with β-glucan. In (D) and (F), a pool of two experiments is shown, including between 6 and 16 mice per group as indicated. **p < 0.01, log rank test between WT and LysMΔSHIP-1 mice. #p < 0.05, log rank test comparing trained or not with β-glucan (D) or *C. albicans* (F) within the same genotype.

Pharmacological Inhibition of SHIP-1 Enhances Trained Immunity

The relevance of the PI3K pathway in distinct pathologies has promoted the development of chemical SHIP-1 phosphatase inhibitors such as 3α-aminocholestane (3AC; SHIPi) (Brooks et al., 2010). We thus tested 3AC as a potential tool to boost trained immunity. BMDMs were trained with β-glucan in presence of different doses of 3AC (half maximal inhibitory concentration [IC_{50}] = 13.5 μM; Brooks et al., 2015), and LPS-induced TNFα was measured (Figure 4A). Upon β-glucan training, SHIP-1 inhibition boosted TNFα production in a dose-dependent manner (Figure 4B).

To analyze the effect of 3AC SHIPi under *in vivo* infectious conditions, mice were administered SHIPi twice on consecutive days following the published regimen (Gumbleton et al., 2017), and coincident with the second day of 3AC administration, mice were trained with a low dose of *C. albicans*. Seven days later, mice were lethally infected with the same fungus (Figure 4C). Inhibition of SHIP-1 did not affect the survival of non-trained mice (Figure 4D, dashed lines) but improved the survival of *Candida*-trained mice (Figure 4D, solid lines).

To further explore the potential relevance of the use of 3AC SHIPi, we trained human PBMCs in the presence of SHIPi, rested and stimulated with LPS, and cytokine production was measured (Figure 4E). This scheme mirrors the stimulation pattern proposed for human PBMCs elsewhere (Quintin et al., 2012). Importantly, SHIP-1 inhibition boosted all IL-1β, IL-6, and TNFα production in these β-glucan-trained human PBMCs (Figure 4F). Thus, our data indicate that SHIP-1 can be targeted with pharmacological inhibitors in both mice and human cells to boost trained immunity.

DISCUSSION

Herein, we define SHIP-1 in myeloid cells as a target to improve trained immunity. Additionally, we provide a pharmacological approach, the SHIP-1 inhibitor 3AC, improving training-induced resistance to *Candida* infection and trained immunity in human PBMCs. Because modulation of myeloid progenitors in the bone marrow is an integral component of trained immunity (Mitroulis et al., 2018), and 3AC administration expands the hematopoietic stem cell compartment (Brooks et al., 2015), SHIP-1

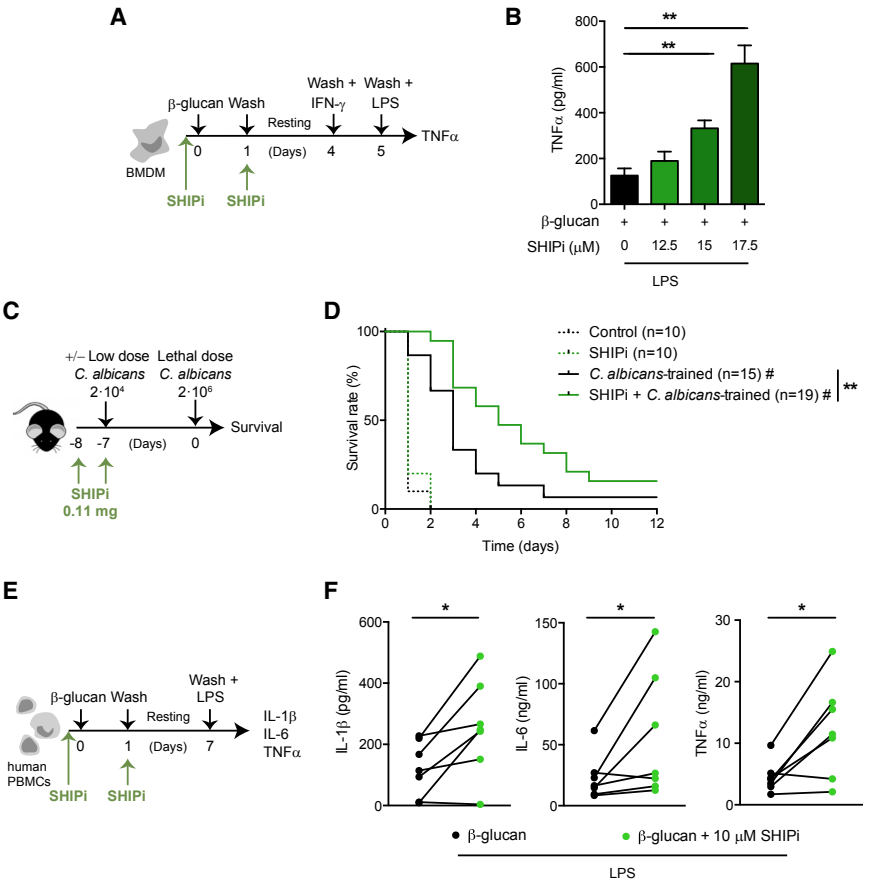

Figure 4. Pharmacological Inhibition of SHIP-1 Enhances Trained Immunity

(A) *In vitro* experimental model applied to mouse BMDMs, indicating when the SHIP-1 inhibitor (SHIPi) 3α-aminocholestane (3AC) was added.

(B) Mouse BMDMs were incubated with the SHIPi at the indicated concentrations. TNFα production was analyzed in supernatants of β-glucan-trained cells after LPS stimulation according to Figure 4A. Mean + SEM of four independent experiments is shown. **$p < 0.01$, paired Student's t test between SHIPi-treated and non-treated cells.

(C) *In vivo* model of training by a systemic infection with a low dose of *Candida albicans* in the presence of SHIPi followed by a second lethal challenge with the same pathogen. When indicated, the inhibitor was administered intraperitoneally.

(D) Survival curve of 0.3% hydroxypropylcellulose (control) or SHIPi-treated mice according to Figure 4C. A pool of two experiments is shown, including between 10 and 19 mice per group as indicated. **$p < 0.01$, log rank test between trained control and SHIPi-treated. #$p < 0.05$, log rank test comparing trained or not with *C. albicans* within the same treatment.

(E) *In vitro* experimental model applied to human peripheral blood mononuclear cells (PBMCs) indicating when SHIPi was added.

(F) IL-1β, IL-6, and TNFα production was analyzed in supernatants of β-glucan-trained human PBMCs after LPS stimulation according to Figure 4E. Samples from seven independent donors are shown. *$p < 0.05$, paired Student's t test.

inhibition could also influence this compartment. Although *Candida*-induced training and the primary response to the fungus are T/B cell independent (Bär et al., 2014; Quintin et al., 2012), systemic inhibition of SHIP-1 can also influence NK and T cells (Gumbleton et al., 2017), and we cannot rule out indirect effects on non-myeloid cells.

We show that SHIP-1 inhibition potentiates the canonical PI3K/Akt activation pathway, which also mediates trained immunity in response to other stimuli such as the bacillus Calmette-Guérin (BCG) vaccine (Arts et al., 2016a). SHIP-1 inhibition could represent a broad strategy to boost trained immunity. Indeed, SHIP-1 displays an inhibitory function in NOD2 signaling (Condé et al., 2012), the BCG-mediated trained immunity pathway (Kleinnijenhuis et al., 2012). Considering that BCG vaccination confers cross-protection to human viral infections (Arts et al., 2018b), SHIP-1 inhibitor could improve the protective effect of BCG.

Enhanced trained immunity could raise as an important host defense mechanism against infections or sepsis (Netea et al., 2016). However, because diverse endogenous danger signals from injured tissues can trigger innate immune memory hallmarks (Crișan et al., 2016b), caution is needed regarding the potential deleterious function of boosting trained immunity in diseases characterized by excessive inflammation. This notion could apply to atherosclerosis (Leentjens et al., 2018), cardiovascular events (Hoogeveen et al., 2017), gout (Crișan et al., 2016a), and a variety of autoimmune diseases and autoinflammatory disorders such as rheumatoid arthritis, systemic lupus erythematosus, and hyper-IgD syndrome (Arts et al., 2018a), in which monocytes and macrophages share a detrimental trained immunity-like phenotype. Similarly, boosting microglia-dependent training (Wendeln et al., 2018) through SHIP-1 inhibition could be detrimental for neurological disorders and stroke. Under these settings, SHIP-1 activators such as AQX-1125 (Stenton et al., 2013) could be potentially used to ameliorate an excessive and detrimental activation of trained immunity.

In conclusion, although studies on trained immunity have focused on the characterization of this phenomenon, strategies to enhance trained immunity deserve further investigation. Our data indicate that the trained immunity process can be boosted by targeting SHIP-1 in myeloid cells. Moreover, SHIP-1 inhibitors could be proposed as potential pharmacological tools to improve trained immunity in clinical settings in which enhancement of inflammatory responses is beneficial.

EXPERIMENTAL PROCEDURES

Mice and Human Samples

Mice were bred at Centro Nacional de Investigaciones Cardiovasculares (CNIC) under specific pathogen-free conditions. WT C57BL/6J mice were

used for SHIP-1 inhibition experiments. LysM$^{+/+}$SHIP-1$^{flox/flox}$ (WT) and LysM$^{Cre/+}$SHIP-1$^{flox/flox}$ (LysMΔSHIP-1) (Collazo et al., 2012) were kept as littermates. Experiments were conducted with 8- to 12-week-old age-matched mice (regardless of gender). Experiments were approved by the animal ethics committee at CNIC and conformed to Spanish law under Real Decreto 1201/2005. Animal procedures were also performed in accordance to European Union (EU) Directive 2010/63EU and Recommendation 2007/526/EC.

Buffy coats from healthy volunteers were obtained from the Andalusian Biobank after ethical approval was obtained from the local Instituto de Salud Carlos III (ISCIII) Research Ethics Committee (PI 36_2017).

Trained Immunity *In Vitro* Models

BMDMs

BMDMs (10^5) were plated in 96-well plates (200 μL final volume; Corning) and stimulated with R10 or 100 μg/mL β-glucan (whole glucan particles [WGPs]; Biothera) for 24 hr. Then, cells were washed and rested 3 days in culture medium. On day 4, unless indicated, BMDMs were washed again and primed with 25 ng/mL IFN-γ (BD Biosciences) for 24 hr. On day 5, a final wash was performed, and cells were stimulated with R10 or 1 μg/mL standard *Escherichia coli* LPS (EK; Invivogen). To measure IL-1β production, following 4 hr of LPS challenge, cells were further stimulated for 2 hr with 5 mM ATP (Sigma-Aldrich), needed for inflammasome activation and pro-IL-1β processing (Schroder and Tschopp, 2010), and supernatants were harvested for ELISA assay. For TNFα and IL-6, after 24 hr of LPS stimulation, supernatants were collected for ELISA.

When required, BMDMs were pre-incubated for 30 min prior to β-glucan stimulation with 500 μM MTA, 6 μM pargyline, 50 μM resveratrol, and 50 μM (-)-epigallocatechin-3-gallate (EGCG) (all from Sigma-Aldrich). SHIP-1 inhibitor (SHIPi; 3AC; Calbiochem) was also used at the indicated doses on β-glucan-trained BMDMs (toxic for non-trained cells). Inhibitors were also added in the first wash-out, before the resting period.

To assess receptor expression and cell viability, 6×10^5 BMDMs were plated in non-treated 24-well plates (1,200 μL final volume; Corning) and followed the training scheme described above. Dectin-1 expression was evaluated on day 0 prior to β-glucan addition. Cell viability and TLR4 expression were assessed on day 5 before LPS stimulation. At indicated times, cells were collected in PBS/EDTA and stained on ice-cold fluorescence-activated cell sorting (FACS) buffer (PBS/EDTA plus 3% fetal bovine serum [FBS]) for flow cytometry analysis.

For western blotting (WB) assays and ChIP analysis, 3×10^6 BMDMs were plated in six-well plates (3 mL final volume; Corning) and stimulated with R10 or 200 μg/mL β-glucan (to maintain mass/cell ratio) for given times. ChIP was performed on day 5, without IFN-γ priming, as detailed below.

To address metabolic status, 3×10^6 BMDMs were plated in non-treated 6-well plates (3 mL final volume; Corning) and followed the training scheme described above but with 200 μg/mL β-glucan (to maintain mass/cell ratio). On day 4, without IFN-γ priming, cells were detached in PBS/EDTA, plated at 10^5 cells/well, and rested overnight in R10 prior to the Seahorse XF glycolysis stress test (Agilent Technologies). When glycolytic metabolism was evaluated after overnight stimulation with β-glucan, BMDMs (10^5) were directly plated in 96-well Seahorse cell culture plates (200 μL final volume; Agilent Technologies) and stimulated with R10 or 100 μg/mL β-glucan the following day.

PBMCs

Total PBMCs (5×10^5) were plated in 96-well plates (200 μL final volume) and stimulated with 100 μg/mL β-glucan for 24 hr. Then cells were washed and rested for 6 days in culture medium. On day 7, PBMCs were stimulated with 1 μg/mL LPS (EK). After 24 hr, supernatants were collected for IL-1β, IL-6, and TNFα measurement by ELISA. When required, β-glucan-trained PBMCs were pre-incubated for 30 min with 10 μM 3AC (toxic for non-trained cells). Inhibitor was also added together with the first wash-out, before the resting period.

To assess cell viability, 3×10^6 total PBMCs were plated in 24-well plates (1,200 μL final volume; Corning) and followed the training scheme described here. On day 7, prior to LPS stimulation, cells were collected in PBS/EDTA and stained on ice-cold FACS buffer for flow cytometry analysis.

For normalization of cytokine production, the fold cell number in each condition was calculated as follows: live cell number/live cell number in average non-trained WT, according to Figure S2. In case of SHIP-1 inhibition experiments, non-treated cells were used as reference. Thus, cytokine production was normalized per cell number as (absolute cytokine value/fold cell number) in each condition.

In Vivo Models

Mice were trained with either two intraperitoneal (i.p.) injections of 1 mg β-glucan particles on days −7 and −4 or 2×10^4 *Candida albicans* intravenously (i.v.) on day −7. Sterile PBS was used as control. One week later, mice were challenged with 5 μg *E. coli* LPS (serotype O55:B5; Sigma-Aldrich) i.p., and blood was collected 60 min later to assess serum TNFα (Mouse TNFα DuoSet; R&D Systems) or 90 min later to evaluate serum IL-1β and IL-6. Alternatively, mice were lethally infected with 2×10^6 *C. albicans* i.v. and monitored daily for weight, general health, and survival, following institutional guidance. For qPCR analysis of renal cytokines, RNA was purified from whole kidneys on day 2 post-secondary infection (p.i.). Kidney fungal burden at indicated time points p.i. was determined by plating organ homogenates obtained mechanically over 70 μm cell strainers (BD Biosciences) after slicing the tissue, in serial dilutions on YPD agar plates; colony-forming units (CFUs) were counted after growth at 30°C for 48 hr, and data are shown as CFUs in total kidney. When required, mice were i.p. treated with 0.11 mg 3AC on days −8 and −7. 3AC was diluted in PBS 0.3% hydroxypropylcellulose (Sigma-Aldrich), used as control.

Quantification and Statistical Analysis

The statistical analysis was performed using Prism (GraphPad Software). Unless specified, statistical significance for comparison between two sample groups with a normal distribution (Shapiro-Wilk test for normality) was determined using two-tailed paired or unpaired Student's t test. When groups were too small to estimate normality, a Gaussian distribution was assumed. Comparison of survival curves was carried out using the log rank (Mantel-Cox) test. Outliers were identified by means of Tukey's range test. Differences were considered significant at $p < 0.05$ as indicated. Except when specified, only significant differences are shown. As indicated in figure legends, either a representative experiment or a pool is shown, and the number of repetitions of each experiment and number of experimental units (either cultures or mice) is indicated. *In vitro* experiments are shown as a pool of experiments, in which linked WT-LysMΔSHIP-1 dots represent independent cultures that were processed within the same experiment. In this way, an internal comparison between genotypes can be visually done. Different conditions within the same genotype in a particular experiment, although not connected by a matter of clarity, were also pair-analyzed, and statistically significant differences are indicated by pound signs (#).

SUPPLEMENTAL INFORMATION

Supplemental Information includes Supplemental Experimental Procedures and four figures and can be found with this article online at https://doi.org/10.1016/j.celrep.2018.09.092.

ACKNOWLEDGMENTS

We thank the members of the Immunobiology Lab for useful discussions. We thank the CNIC facilities and personnel, particularly Santiago Rodríguez and Ruben Mota, for their support. P.S.-L. is funded by grant BES-2015-072699 ("Ayudas para Contratos Predoctorales para la Formación de Doctores 2015") from the Spanish Ministry of Economy, Industry and Competitiveness (MINECO). C.d.F. is supported by the Asociación Española Contra el Cáncer (AECC) Foundation as a recipient of an "Ayuda Fundación Científica AECC a Personal Investigador en Cancer" grant. Work in the Sancho laboratory is funded by CNIC and grant SAF2016-79040-R from MINECO, Agencia Estatal de Investigación, and FEDER (European Fund for Regional Development); grant B2017/BMD-3733 Immunothercan-CM from Comunidad de Madrid; grant RD16/0015/0018-REEM from FIS-Instituto de Salud Carlos III, MINECO, and FEDER; Foundation Acteria; a Constantes y Vitales prize (Atresmedia); Foundation La Marató de TV3 (grant 201723); the European Commission (grant 635122-PROCROP H2020); and the European Research Council

Please cite this article in press as: Saz-Leal et al., Targeting SHIP-1 in Myeloid Cells Enhances Trained Immunity and Boosts Response to Infection, Cell Reports (2018), https://doi.org/10.1016/j.celrep.2018.09.092

(ERC-2016-Consolidator Grant 725091). CNIC is supported by MINECO and the Pro-CNIC Foundation and is a Severo Ochoa Center of Excellence (MINECO award SEV-2015-0505). W.G.K. is an Empire Scholar of the State of New York, the Murphy Family Professor of Children's Oncology Research, and is supported by funds from the Paige Arnold Butterfly Run.

AUTHOR CONTRIBUTIONS

P.S.-L., C.d.F., P.B., and S.M.-C. performed the experiments. W.G.K. shared reagents. O.M.D. and J.D.C. prepared 3AC for the pharmacological targeting to SHIP-1. P.S.-L., C.d.F., and D.S. conceived and designed experiments, analyzed data, and wrote the manuscript. All authors discussed the results and the manuscript.

DECLARATION OF INTERESTS

C.d.F., P.S.-L., J.D.C., W.G.K., and D.S. have patents pending and issued on the use of SHIPi in modulating immune function. W.G.K. is chief scientific officer at Alterna Therapeutics, which is devoted to developing SHIPi for therapeutic purposes. J.D.C. serves on the Scientific Advisory Board of Alterna Therapeutics. Both J.D.C. and W.G.K. hold equity in Alterna Therapeutics. All other authors declare no competing interests.

Received: April 10, 2018
Revised: August 14, 2018
Accepted: September 27, 2018
Published: October 30, 2018

REFERENCES

Antignano, F., Ibaraki, M., Ruschmann, J., Jagdeo, J., and Krystal, G. (2010). SHIP negatively regulates Flt3L-derived dendritic cell generation and positively regulates MyD88-independent TLR-induced maturation. J. Leukoc. Biol. *88*, 925–935.

Arts, R.J.W., Carvalho, A., La Rocca, C., Palma, C., Rodrigues, F., Silvestre, R., Kleinnijenhuis, J., Lachmandas, E., Gonçalves, L.G., Belinha, A., et al. (2016a). Immunometabolic pathways in BCG-induced trained immunity. Cell Rep. *17*, 2562–2571.

Arts, R.J., Joosten, L.A., and Netea, M.G. (2016b). Immunometabolic circuits in trained immunity. Semin. Immunol. *28*, 425–430.

Arts, R.J.W., Joosten, L.A.B., and Netea, M.G. (2018a). The potential role of trained immunity in autoimmune and autoinflammatory disorders. Front. Immunol. *9*, 298.

Arts, R.J.W., Moorlag, S., Novakovic, B., Li, Y., Wang, S.Y., Oosting, M., Kumar, V., Xavier, R.J., Wijmenga, C., Joosten, L.A.B., et al. (2018b). BCG vaccination protects against experimental viral infection in humans through the induction of cytokines associated with trained immunity. Cell Host Microbe *23*, 89–100.e5.

Bär, E., Whitney, P.G., Moor, K., Reis e Sousa, C., and LeibundGut-Landmann, S. (2014). IL-17 regulates systemic fungal immunity by controlling the functional competence of NK cells. Immunity *40*, 117–127.

Bekkering, S., Blok, B.A., Joosten, L.A., Riksen, N.P., van Crevel, R., and Netea, M.G. (2016). In vitro experimental model of trained innate immunity in human primary monocytes. Clin. Vaccine Immunol. *23*, 926–933.

Bistoni, F., Vecchiarelli, A., Cenci, E., Puccetti, P., Marconi, P., and Cassone, A. (1986). Evidence for macrophage-mediated protection against lethal Candida albicans infection. Infect. Immun. *51*, 668–674.

Blanco-Menéndez, N., Del Fresno, C., Fernandes, S., Calvo, E., Conde-Garrosa, R., Kerr, W.G., and Sancho, D. (2015). SHIP-1 couples to the Dectin-1 hemITAM and selectively modulates reactive oxygen species production in dendritic cells in response to Candida albicans. J. Immunol. *195*, 4466–4478.

Brooks, R., Fuhler, G.M., Iyer, S., Smith, M.J., Park, M.Y., Paraiso, K.H., Engelman, R.W., and Kerr, W.G. (2010). SHIP1 inhibition increases immunoregulatory capacity and triggers apoptosis of hematopoietic cancer cells. J. Immunol. *184*, 3582–3589.

Brooks, R., Iyer, S., Akada, H., Neelam, S., Russo, C.M., Chisholm, J.D., and Kerr, W.G. (2015). Coordinate expansion of murine hematopoietic and mesenchymal stem cell compartments by SHIPi. Stem Cells *33*, 848–858.

Cheng, S.C., Quintin, J., Cramer, R.A., Shepardson, K.M., Saeed, S., Kumar, V., Giamarellos-Bourboulis, E.J., Martens, J.H., Rao, N.A., Aghajanirefah, A., et al. (2014). mTOR- and HIF-1α-mediated aerobic glycolysis as metabolic basis for trained immunity. Science *345*, 1250684.

Collazo, M.M., Paraiso, K.H.T., Park, M.-Y., Hazen, A.L., and Kerr, W.G. (2012). Lineage extrinsic and intrinsic control of immunoregulatory cell numbers by SHIP. Eur. J. Immunol. *42*, 1785–1795.

Condé, C., Rambout, X., Lebrun, M., Lecat, A., Di Valentin, E., Dequiedt, F., Piette, J., Gloire, G., and Legrand, S. (2012). The inositol phosphatase SHIP-1 inhibits NOD2-induced NF-κB activation by disturbing the interaction of XIAP with RIP2. PLoS ONE *7*, e41005.

Crişan, T.O., Cleophas, M.C.P., Oosting, M., Lemmers, H., Toenhake-Dijkstra, H., Netea, M.G., Jansen, T.L., and Joosten, L.A.B. (2016a). Soluble uric acid primes TLR-induced proinflammatory cytokine production by human primary cells via inhibition of IL-1Ra. Ann. Rheum. Dis. *75*, 755–762.

Crişan, T.O., Netea, M.G., and Joosten, L.A. (2016b). Innate immune memory: Implications for host responses to damage-associated molecular patterns. Eur. J. Immunol. *46*, 817–828.

Di Luzio, N.R., and Williams, D.L. (1978). Protective effect of glucan against systemic Staphylococcus aureus septicemia in normal and leukemic mice. Infect. Immun. *20*, 804–810.

Eramo, M.J., and Mitchell, C.A. (2016). Regulation of PtdIns(3,4,5)P3/Akt signalling by inositol polyphosphate 5-phosphatases. Biochem. Soc. Trans. *44*, 240–252.

Garcia-Valtanen, P., Guzman-Genuino, R.M., Williams, D.L., Hayball, J.D., and Diener, K.R. (2017). Evaluation of trained immunity by β-1, 3 (d)-glucan on murine monocytes in vitro and duration of response in vivo. Immunol. Cell Biol. *95*, 601–610.

Gumbleton, M., Sudan, R., Fernandes, S., Engelman, R.W., Russo, C.M., Chisholm, J.D., and Kerr, W.G. (2017). Dual enhancement of T and NK cell function by pulsatile inhibition of SHIP1 improves antitumor immunity and survival. Sci. Signal. *10*, eaam5353.

Hoogeveen, R.M., Nahrendorf, M., Riksen, N.P., Netea, M.G., de Winther, M.P.J., Lutgens, E., Nordestgaard, B., Neidhart, M., Stroes, E.S.G., Catapano, A.L., and Bekkering, S. (2017). Monocyte and haematopoietic progenitor reprogramming as common mechanism underlying chronic inflammatory and cardiovascular diseases. Eur. Heart J. Published online October 24, 2017. https://doi.org/10.1093/eurheartj/ehx581.

Ifrim, D.C., Joosten, L.A., Kullberg, B.J., Jacobs, L., Jansen, T., Williams, D.L., Gow, N.A., van der Meer, J.W., Netea, M.G., and Quintin, J. (2013). Candida albicans primes TLR cytokine responses through a Dectin-1/Raf-1-mediated pathway. J. Immunol. *190*, 4129–4135.

Ifrim, D.C., Quintin, J., Joosten, L.A., Jacobs, C., Jansen, T., Jacobs, L., Gow, N.A., Williams, D.L., van der Meer, J.W., and Netea, M.G. (2014). Trained immunity or tolerance: opposing functional programs induced in human monocytes after engagement of various pattern recognition receptors. Clin. Vaccine Immunol. *21*, 534–545.

Kerr, W.G. (2011). Inhibitor and activator: dual functions for SHIP in immunity and cancer. Ann. N Y Acad. Sci. *1217*, 1–17.

Kleinnijenhuis, J., Quintin, J., Preijers, F., Joosten, L.A., Ifrim, D.C., Saeed, S., Jacobs, C., van Loenhout, J., de Jong, D., Stunnenberg, H.G., et al. (2012). Bacille Calmette-Guerin induces NOD2-dependent nonspecific protection from reinfection via epigenetic reprogramming of monocytes. Proc. Natl. Acad. Sci. U S A *109*, 17537–17542.

Leentjens, J., Bekkering, S., Joosten, L.A.B., Netea, M.G., Burgner, D.P., and Riksen, N.P. (2018). Trained innate immunity as a novel mechanism linking infection and the development of atherosclerosis. Circ. Res. *122*, 664–669.

Mitroulis, I., Ruppova, K., Wang, B., Chen, L.S., Grzybek, M., Grinenko, T., Eugster, A., Troullinaki, M., Palladini, A., Kourtzelis, I., et al. (2018). Modulation

of myelopoiesis progenitors is an integral component of trained immunity. Cell *172*, 147–161 e12.

Mosser, D.M., and Zhang, X. (2008). Activation of murine macrophages. Curr. Protoc. Immunol. *Chapter 14*, Unit 14.12.

Netea, M.G., Joosten, L.A., Latz, E., Mills, K.H., Natoli, G., Stunnenberg, H.G., O'Neill, L.A., and Xavier, R.J. (2016). Trained immunity: a program of innate immune memory in health and disease. Science *352*, aaf1098.

Quintin, J., Saeed, S., Martens, J.H.A., Giamarellos-Bourboulis, E.J., Ifrim, D.C., Logie, C., Jacobs, L., Jansen, T., Kullberg, B.J., Wijmenga, C., et al. (2012). Candida albicans infection affords protection against reinfection via functional reprogramming of monocytes. Cell Host Microbe *12*, 223–232.

Rosas, M., Liddiard, K., Kimberg, M., Faro-Trindade, I., McDonald, J.U., Williams, D.L., Brown, G.D., and Taylor, P.R. (2008). The induction of inflammation by dectin-1 in vivo is dependent on myeloid cell programming and the progression of phagocytosis. J. Immunol. *181*, 3549–3557.

Schroder, K., and Tschopp, J. (2010). The inflammasomes. Cell *140*, 821–832.

Stenton, G.R., Mackenzie, L.F., Tam, P., Cross, J.L., Harwig, C., Raymond, J., Toews, J., Chernoff, D., MacRury, T., and Szabo, C. (2013). Characterization of AQX-1125, a small-molecule SHIP1 activator: part 2. Efficacy studies in allergic and pulmonary inflammation models in vivo. Br. J. Pharmacol. *168*, 1519–1529.

Walachowski, S., Tabouret, G., Fabre, M., and Foucras, G. (2017). Molecular analysis of a short-term model of β-glucans-trained immunity highlights the accessory contribution of GM-CSF in priming mouse macrophages response. Front. Immunol. *8*, 1089.

Wendeln, A.-C., Degenhardt, K., Kaurani, L., Gertig, M., Ulas, T., Jain, G., Wagner, J., Häsler, L.M., Wild, K., Skodras, A., et al. (2018). Innate immune memory in the brain shapes neurological disease hallmarks. Nature *556*, 332–338.

Cell Reports, Volume *25*

Supplemental Information

Targeting SHIP-1 in Myeloid Cells Enhances Trained Immunity and Boosts Response to Infection

Paula Saz-Leal, Carlos del Fresno, Paola Brandi, Sarai Martínez-Cano, Otto M. Dungan, John D. Chisholm, William G. Kerr, and David Sancho

SUPPLEMENTAL INFORMATION

Figures S1-S4

Supplemental Experimental Procedures

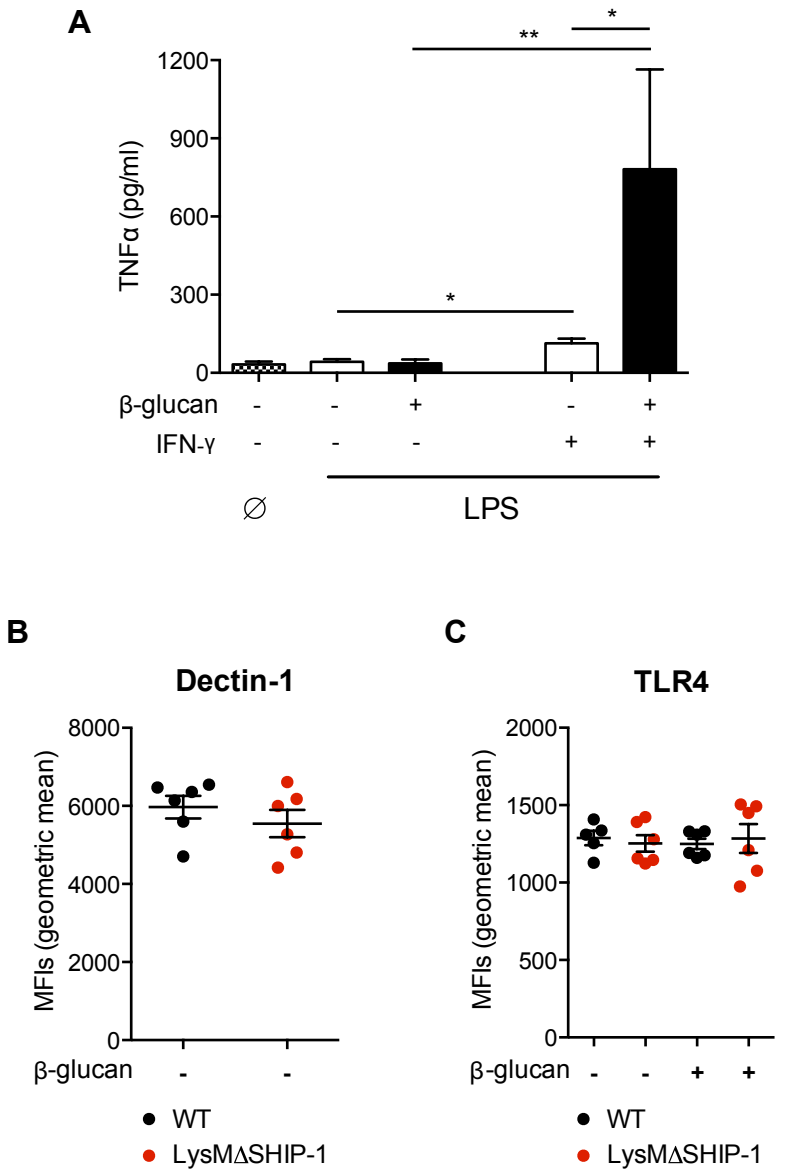

Figure S1 Experimental set-up of trained immunity *in vitro* model applied to BMDMs, related to Figure 1.

(A) WT and LysMΔSHIP-1 BMDMs were stimulated (+) or not (-) with β-glucan and primed (+) or not (-) with IFN-γ prior to LPS stimulation, according to the model in Figure 1C. (Ø) represent BMDMs without any stimuli. TNFα in supernatants was analyzed. Mean ± SEM from five independent experiments is shown. (B) Dectin-1 surface expression was analyzed by FACS in WT and LysMΔSHIP-1 BMDMs before β-glucan stimulation. (C) TLR4 surface expression was analyzed by FACS in WT and LysMΔSHIP-1 BMDMs both under non-trained (-) or β-glucan primed (+) conditions, before LPS stimulation. (B, C) Individual data and mean ± SEM from a pool of two experiments is shown including three BMDMs cultures per experiment. Each dot represents an independent cell culture.

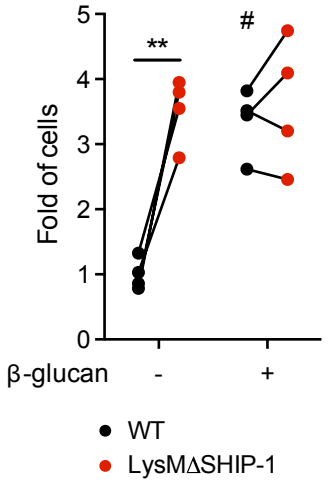

Figure S2. Relative amount of BMDMs recovered before LPS stimulation, related to Figure 1. WT and LysMΔSHIP-1 BMDMs were exposed (+) or not (-) to β-glucan according to model in Figure 1C. At day 5 and before LPS stimulation, the number of viable BMDMs was determined. Fold cell number was calculated by dividing live cell number in each experimental condition by the average number of WT non-trained cells in all the experiments. Individual data from four independent experiments are shown. $^{**}p < 0.01$, paired Student's *t*-test comparing WT and LysMΔSHIP-1. $\#p < 0.05$, paired Student's *t*-test comparing stimulated or not with β-glucan within the same genotype.

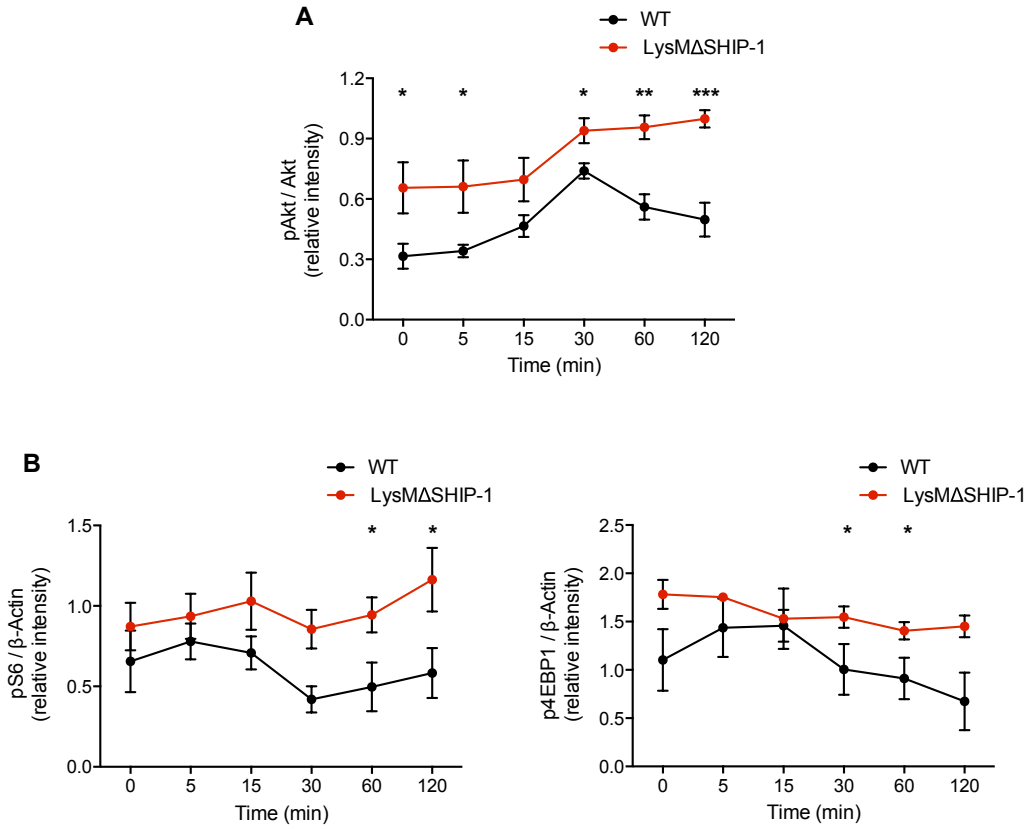

Figure S3. Quantification of WB kinetics, related to Figure 2. WT and LysMΔSHIP-1 BMDMs were exposed to β-glucan for the indicated time and phospho-Akt, Akt (A), phospho-S6, phospho-4EBP1 and β-Actin (B) analyzed by WB and quantified by ImageJ software. Relative band intensity is shown. Mean ± SEM from a pool of five experiments performed. *$p < 0.05$, **$p < 0.01$, ***p>0.001, paired Student's *t*-test comparing WT and LysMΔSHIP-1 at any time point.

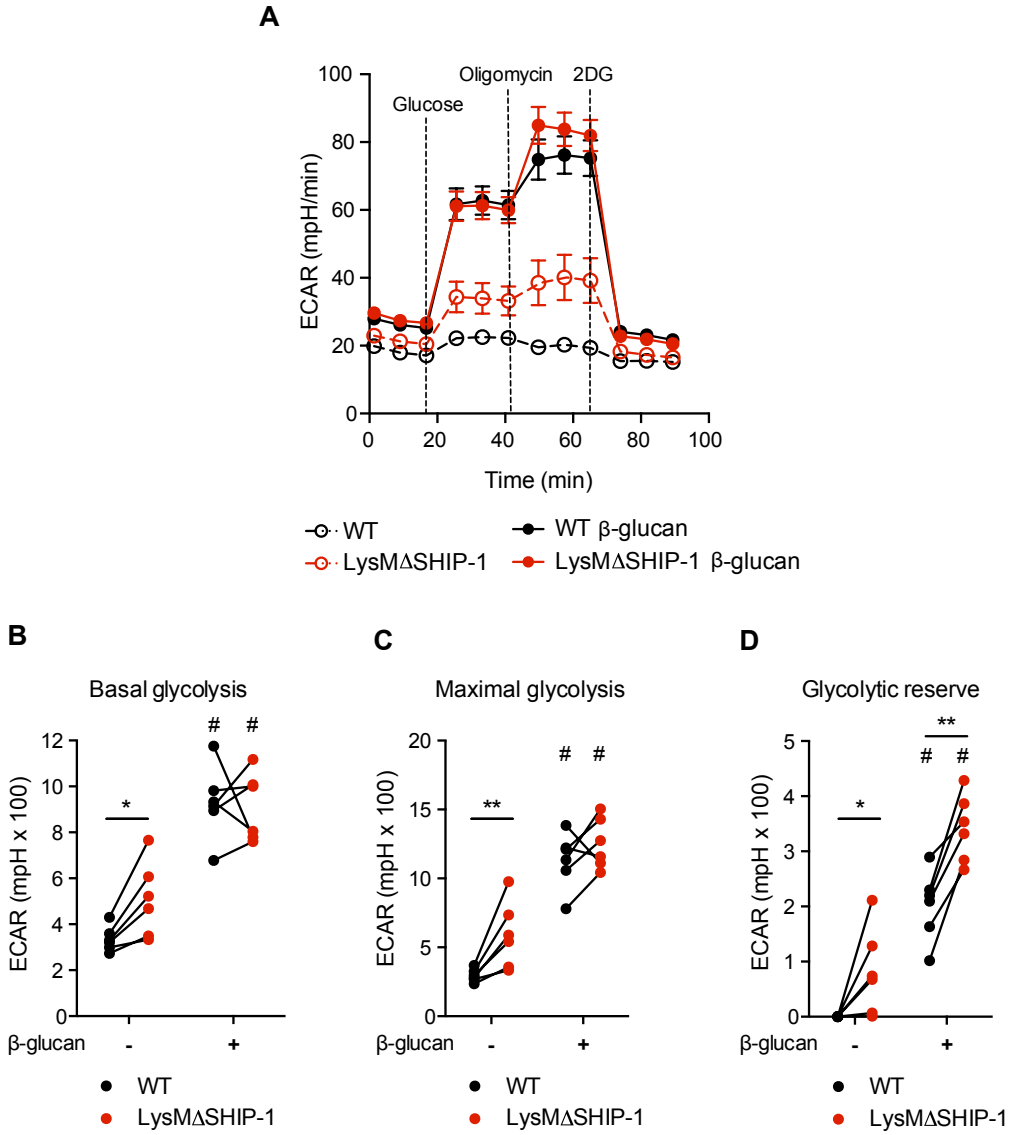

Figure S4. SHIP-1 controls the extent of the early glycolytic metabolism, related to Figure 2. (A-D) WT and LysMΔSHIP-1 BMDMs were left untreated (dashed lines, A) or treated overnight with β-glucan (solid lines, A) and extracellular acidification rate (ECAR) was determined. ECAR in a glycolysis stress test was analyzed upon sequential addition of glucose, oligomycin and 2-deoxyglucose (2DG) as indicated (A). Analysis of basal glycolysis (B), maximal glycolysis (C) and glycolytic reserve (D). (A-D) Mean ± SEM (A) or individual data (B-D) of six independent cultures are shown**.** (B-D) *$p < 0.05$, **$p <$ 0.01, paired Student's *t*-test comparing WT and LysMΔSHIP-1. #$p< 0.05$, paired Student's *t*-test comparing stimulated or not with β-glucan within the same genotype.

Supplemental Experimental Procedures

Candida albicans
Candida albicans (strain SC5314, kindly provided by Prof. C. Gil, Complutense University, Madrid, Spain) was grown on YPD-agar plates (Sigma) at 30ºC for 48h.

In vitro cell differentiation and culture

Mouse bone marrow-derived macrophage differentiation. To obtain mouse bone marrow-derived macrophages (BMDMs) from WT and LysMΔSHIP-1 mice, femurs were collected and flushed, and red blood cells were lysed using RBC Lysis Buffer (Sigma) for 3 minutes at room temperature (RT). Cell suspensions were plated in non-treated cell culture plates (Corning) in RPMI 1640 (Sigma) supplemented with 10% heat-inactivated fetal bovine serum (FBS, Sigma), 1 mM pyruvate (Lonza), 100 µM non-essential aminoacids (Thermo Fisher Scientific), 2 mM L-glutamine, 100 U/ml penicillin, 100 µg/ml streptomycin (all three from Lonza) and 50 µM 2-mercaptoethanol (Merck), herein called R10, plus M-CSF (30% mycoplasma-free L929 cell supernatant) at 37ºC for 5 days. At day 5, BMDMs were detached in phosphate buffered saline (PBS, Gibco) supplemented with 5 mM EDTA (PBS/EDTA, Life Technologies), counted, plated in R10 at the required concentration and rested overnight before any stimulation.

Peripheral blood mononuclear cells (PBMCs). PBMCs were isolated by differential centrifugation using Biocoll Separating Solution (Cultek). Cells were washed twice in PBS, resuspended in DMEM (Sigma) supplemented with 10% heat-inactivated FBS, 100 µM non-essential aminoacids, 2 mM L-glutamine, 100 U/ml penicillin, 100 µg/ml streptomycin and 50 µM 2-mercaptoethanol, herein called D10; counted and plated for stimulation.

ELISA

Mouse cytokines were analyzed in supernatants of BMDMs using the following reagents: for IL-1β, Mouse IL-1β/IL-1F2 DuoSet, R&D Systems; for IL-6, Purified rat anti-mouse IL-6, Biotin rat anti-mouse IL-6-both from BD Biosciences- and Streptavidin Horseradish Peroxidase (HRP) Conjugate from Invitrogen; for TNFα, OptEIA ELISA kit, BD Biosciences.
Human cytokines were analyzed in supernatants of PBMCs by using the Human IL-1β/IL-1F2 Duoset, Human IL-6 Duoset and Human TNFα DuoSet kits, all from R&D Systems.

Western Blot

Cell lysates were prepared in RIPA buffer containing protease and phosphatase inhibitors (Roche). Samples were run on Mini-PROTEAN TGX PRECAST Gels and transferred onto a nitrocellulose membrane (both from Bio-Rad Laboratories) for blotting with the following antibodies: β-Actin (C4) and SHIP-1 (P1C1) from Santa Cruz; pAkt (Ser473, #4058S), Akt (#2920S), pS6 (Ser235/236, #4858T) and p4EBP1 (Thr37/46, #9459S), all from Cell Signaling. Alexa Fluor-680 (Life Technologies) or Qdot-800 (Rockland) conjugated secondary antibodies were used. Gels were visualized in an Odyssey instrument (LI-COR) and band intensity was quantified by using ImageJ software (Bitplane).

Antibodies and flow cytometry

Samples were stained with the appropriate antibody cocktails in ice-cold FACS Buffer at 4ºC for 15 minutes. Antibodies included mouse PE-anti-TLR4 (BioLegend) and APC-anti-Dectin-1 (Bio-Rad). Dead cells were excluded by Hoechst 33258 (Invitrogen) incorporation. Purified anti-FcγRIII/II (2.4G2, TONBO Bioscience) was used to block murine Fc-receptors at 4ºC for 10 minutes in all the stainings. Events were acquired using FACSCanto 3L (BD Biosciences). Data were analyzed with FlowJo software (Tree Star).

Glycolytic flux evaluation

The assay was performed in DMEM supplemented with 1mM glutamine, 100 µg/ml penicillin, 100 µg/ml streptomycin. The pH was adjusted to 7.4 with KOH (herein called Seahorse medium). Cells were washed with PBS and 175µl of Seahorse medium was added. Plates were incubated at 37°C without CO_2 for 1h prior to the assay. Extracellular acidification rate (ECAR) was determined by using the glycolysis stress test in an XF-96 Extracellular Flux Analyzer (Agilent Technologies). Three consecutive measurements were performed under basal conditions and after sequential addition of 80 mM glucose (Merck), 9 µM oligomycin A (Sigma) and 500 mM 2-deoxy-glucose (2DG, Sigma). Basal and maximal glycolysis were defined as ECAR after addition of glucose and oligomycin, respectively. Glycolytic reserve was defined as the difference maximal and basal glycolysis.

Chromatin immunoprecipitation (ChIP) analysis

ChIP was performed using the Magna ChIP A – Chromatin Immunoprecipitation kit together with the ChIPAb+ Trimethyl-Histone3 (Lys4) (H3K4me3) – ChIP validated antibody, both from Millipore-Merck, following the provider's instructions. In brief, cells were fixed with 1% formaldehyde for 10 minutes at RT, exposed to glycine to quench unreacted formaldehyde and washed twice with ice-cold PBS supplemented with the provided protease inhibitor cocktail. After scraping the cells in ice-cold PBS, they were pelleted, lysed and sonicated for 15 minutes (30 seconds on/30 seconds off) at high intensity by using a Bioruptor UCD-200TM-TX water bath sonicator (Diagenode). Sonicates were diluted and incubated with antibodies plus protein A magnetic beads for 1 hour with rotation at 4 ºC. Beads were magnetically collected and washed extensively. Protein-DNA complexes were disrupted from the beads upon proteinase-K treatment and recovered DNA was purified. Immunoprecipitated DNA and input DNA were amplified by means of quantitative PCR with specific primers for the promoter region of TNFα (Fw: 5'-CAACTTTCCAAACCCTCTGC-3'; Rv: 5'-CTGGCTAGTCCCTTGCTGTC-3') with input DNA to generate a standard curve. ChIPdata are represented as a percentage of input.

RNA extraction and quantitative-PCR

RNeasy Plus Mini Kit, from Qiagen, was used for RNA extraction. cDNA was prepared using the High Capacity cDNA reverse transcription kit (Applied Biosystems, Foster City, CA). Quantitative PCR was performed in a 7900-FAST-384 instrument (Applied Biosystems) by using the GoTaq qPCR master mix from Promega. Primers used in this work (synthetized by Sigma) were as follows: β-actin Fw: 5′-GGCTGTATTCCCCTCCATCG-3′; β-actin Rv: 5′-CCAGTTGGTAACAATGCCATGT-3′; IL-1β Fw: 5'-CTGAACTCAACTGTGAAATGCCA-3'; IL-1β Rv: 5'-AAAGGTTTGGAAGCAGCCCT-3'; IL-6 Fw: CCGTGTGGTTACATCTACCCT-3'; IL-6 Rv: 5'-CGTGGTTCTGTTGATGACAGT-3' TNFα Fw: 5'-CCCTCACACTCAGATCATCTTCT-3'; TNFα Rv: 5'-GCTACGACGTGGGCTACAG-3'; mRNA levels were normalized to β-Actin expression. Data are shown as relative expression to β-Actin (ΔΔCt).

IMMUNOLOGY

DNGR-1 in dendritic cells limits tissue damage by dampening neutrophil recruitment

Carlos del Fresno[1]*†, Paula Saz-Leal[1]*, Michel Enamorado[1]‡, Stefanie K. Wculek[1], Sarai Martínez-Cano[1], Noelia Blanco-Menéndez[1], Oliver Schulz[2], Mattia Gallizioli[3], Francesc Miró-Mur[3], Eva Cano[4], Anna Planas[3,5], David Sancho[1]†

Host injury triggers feedback mechanisms that limit tissue damage. Conventional type 1 dendritic cells (cDC1s) express dendritic cell natural killer lectin group receptor-1 (DNGR-1), encoded by the gene *Clec9a*, which senses tissue damage and favors cross-presentation of dead-cell material to CD8$^+$ T cells. Here we find that DNGR-1 additionally reduces host-damaging inflammatory responses induced by sterile and infectious tissue injury in mice. DNGR-1 deficiency leads to exacerbated caerulein-induced necrotizing pancreatitis and increased pathology during systemic *Candida albicans* infection without affecting fungal burden. This effect is B and T cell–independent and attributable to increased neutrophilia in DNGR-1–deficient settings. Mechanistically, DNGR-1 engagement activates SHP-1 and inhibits MIP-2 (encoded by *Cxcl2*) production by cDC1s during *Candida* infection. This consequently restrains neutrophil recruitment and promotes disease tolerance. Thus, DNGR-1–mediated sensing of injury by cDC1s serves as a rheostat for the control of tissue damage, innate immunity, and immunopathology.

After sterile or infectious insults, injured tissues expose or release alarm signals that are detected by specific innate immune receptors on myeloid cells (*1*). This triggers an inflammatory response, which promotes the recruitment of myeloid cells into the damaged organ. This innate immune response must be tightly regulated to avoid additional tissue damage (*2*).

Among myeloid cell sensors of tissue damage, dendritic cell natural killer lectin group receptor-1 (DNGR-1; *Clec9a* gene) is a C-type lectin receptor (CLR) that detects F-actin exposed by damaged cells (*3*, *4*). DNGR-1 is mainly expressed by mouse and human conventional type 1 dendritic cells (cDC1s), including CD103$^+$CD11b$^-$ DCs in peripheral tissues (*5*, *6*). DNGR-1 favors the cross-presentation of dead cell–associated antigens to CD8$^+$ T cells (*7*–*9*). However, whether DNGR-1 plays any role in innate immunity is unknown. To address this issue, we used a mouse model of caerulein-induced acute necrotizing pancreatitis (Fig. 1A), which results in massive acinar cell death, leading to the infiltration of myeloid cells. This, in turn, triggers further pathology and edema (*10*). Upon caerulein treatment, there was increased pancreatic infiltration by neutrophils, but not monocytes, in DNGR-1–deficient (*Clec9a*$^{gfp/gfp}$) mice compared with that observed in wild-type (WT) mice (Fig. 1B). Neutrophil numbers in the bone marrow (BM) and blood were similar in both genotypes (fig. S1), ruling out an effect of DNGR-1 deficiency on neutrophil ontogeny and suggesting a local recruitment effect.

As a nongenetic approach, we used a DNGR-1–blocking antibody (*7*, *11*). Receptor blockade phenocopied the exacerbated pancreatic infiltration of neutrophils (Fig. 1C) but not monocytes (fig. S2A). Enhanced neutrophilia upon DNGR-1 blockade was lost in *Batf3*$^{-/-}$ mice (Fig. 1D and fig. S2B), which lack functional cDC1s (*12*), indicating that cDC1s are the key mediators. Pancreatic CXCR2-mediated neutrophil infiltration is pathological in acute pancreatitis (*13*). Consistently, caerulein-treated *Clec9a*$^{gfp/gfp}$ mice displayed exacerbated pancreatitis with increased serum lipase concentrations (Fig. 1E) and extended pancreatic edema (Fig. 1F).

The rapid kinetics of neutrophil infiltration suggested the involvement of an innate immune response. To test this, *Rag1*$^{-/-}$ (lacking B and T cells) and *Rag1*$^{-/-}$*Clec9a*$^{gfp/gfp}$ mice were subjected to caerulein-induced acute pancreatitis. Notably, the absence of DNGR-1 resulted in enhanced neutrophil infiltration (Fig. 1G and fig. S2C) and increased circulating lipase concentrations (Fig. 1H) in B and T cell–deficient mice. Thus, after tissue damage, DNGR-1 expressed on cDC1s regulates the recruitment of neutrophils without the involvement of B and T cells.

A reduction of neutrophil-mediated immunopathology is associated with disease tolerance upon infection, which limits the impact of damage-generating infectious challenges on host fitness without affecting pathogen burden (*14*, *15*). To test whether DNGR-1 affects disease tolerance, we used systemic *Candida albicans* infection, which generates extensive renal tissue necrosis (*16*). DNGR-1–deficient mice showed increased morbidity and mortality upon systemic candidiasis (Fig. 2, A and B), despite having a similar fungal burden (Fig. 2C). Extended pathology in the absence of DNGR-1 correlated with increased neutrophil infiltration in the kidney (Fig. 2, D and E). Neutrophil numbers in BM or blood of WT and *Clec9a*$^{gfp/gfp}$ mice were similar (fig. S3). DNGR-1 blockade in infected mice phenocopied increased neutrophilia (Fig. 2F), which was prevented in BATF3-deficient mice (Fig. 2G), indicating that cDC1s mediate the effect. Of note, *Rag1*$^{-/-}$*Clec9a*$^{gfp/gfp}$ mice also showed increased renal neutrophil numbers (Fig. 2H) and reduced survival after infection (Fig. 2I). Monocyte recruitment into *Candida*-infected kidneys was not significantly increased in any of the DNGR-1–deficient conditions (right panel of Fig. 2D and fig. S4). Thus, DNGR-1 dampens the recruitment of neutrophils to damaged tissues in both sterile and infectious settings in a B and T cell–independent manner.

Neutrophil-mediated renal immunopathology causes acute kidney failure and mortality during systemic candidiasis (*17*, *18*). Consistently, *C. albicans*–infected *Clec9a*$^{gfp/gfp}$ mice showed exacerbated kidney damage, with increased terminal deoxynucleotidyl transferase–mediated deoxyuridine triphosphate nick end labeling (TUNEL)–positive cells (Fig. 2J), increased concentrations of serum creatinine (Fig. 2K), and enhanced expression of kidney injury molecule-1 (KIM-1) (Fig. 2L). Kidney neutrophilia was increased in *Clec9a*$^{gfp/gfp}$ mice three days after infection (Fig. 2M), along with enhanced KIM-1 expression (Fig. 2N). Thus, exacerbated renal damage caused by neutrophils could underlie increased pathology in *Candida*-infected *Clec9a*$^{gfp/gfp}$ mice.

We tested whether DNGR-1–regulated neutrophilia drives tissue damage in sterile pancreatitis (Fig. 3A). Partial depletion of neutrophils with an antibody against Ly6G (anti-Ly6G, or 1A8 antibody) (fig. S5) reverted the enhanced edematous lesions found in isotype-treated *Clec9a*$^{gfp/gfp}$ mice upon caerulein treatment (Fig. 3B). Assessing the impact of neutrophils in *C. albicans* infection is more complex, because the depletion of neutrophils is lethal (*19*). To circumvent this, we first used fungizone to eliminate the fungus starting at day 3 postinfection (Fig. 3C and fig. S6A), after initial tissue damage by the infection (Fig. 2N). Removal of *C. albicans* did not affect the exacerbated neutrophil infiltration (Fig. 3D) or renal damage (Fig. 3E) observed in *Clec9a*$^{gfp/gfp}$ mice. Thus, after the initial damage, the presence of fungus was not essential for the DNGR-1–dependent effect. Neutrophil depletion with 1A8 antibody in the presence of fungizone (Fig. 3, C and F, and fig. S6B) prevented the enhanced renal damage found in isotype-treated *Clec9a*$^{gfp/gfp}$ mice (Fig. 3, G and H), even though fungal burden was equivalent between genotypes (Fig. 3I).

[1]Immunobiology Laboratory, Centro Nacional de Investigaciones Cardiovasculares (CNIC), Madrid, Spain. [2]Immunobiology Laboratory, The Francis Crick Institute, London, UK. [3]Institut d'Investigacions Biomèdiques August Pi i Sunyer (IDIBAPS), Barcelona, Spain. [4]Chronic Disease Programme–CROSADIS, Instituto De Salud Carlos III, Madrid, Spain. [5]Department of Brain Ischemia and Neurodegeneration, Institut d'Investigacions Biomèdiques de Barcelona (IIBB-CSIC), Barcelona, Spain.
*These authors contributed equally to this work.
†Corresponding author. Email: dsancho@cnic.es (D.S.); cdelfresno@cnic.es (C.d.F.) ‡Present address: Mucosal Immunology Section, Laboratory of Parasitic Diseases, NIAID, NIH, Bethesda, MD, USA.

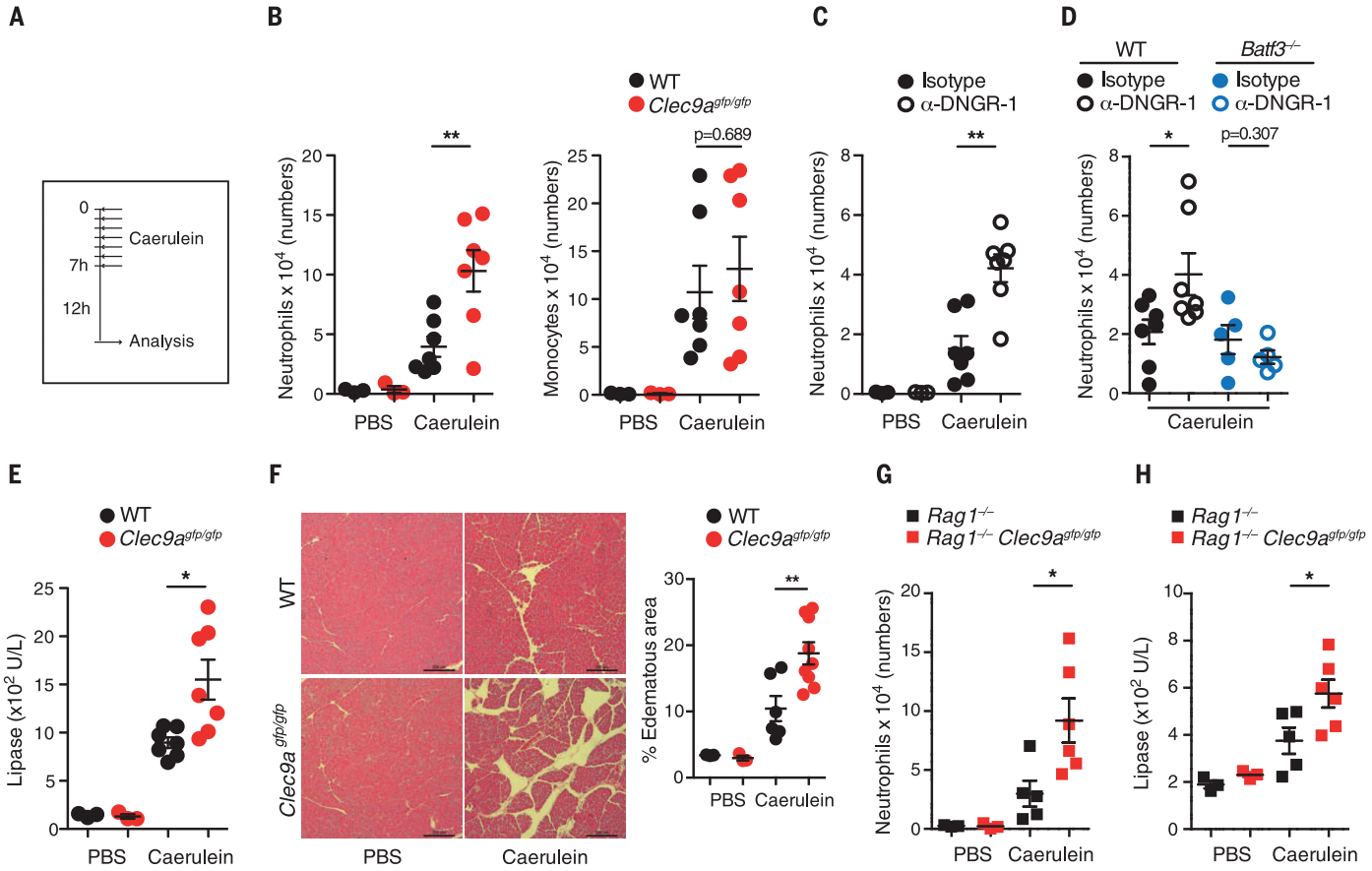

Fig. 1. DNGR-1 regulates neutrophil infiltration and tissue damage during acute pancreatitis. (**A**) Acute pancreatitis was induced by intraperitoneal injection of caerulein hourly for 6 hours in WT and DNGR-1–deficient (*Clec9a*$^{gfp/gfp}$) mice. Phosphate-buffered saline (PBS) injection was used as a control. Animals were analyzed 12 hours after the last injection. (**B**) Infiltrating neutrophils (left) and monocytes (right) in pancreas quantified by flow cytometry. (**C** and **D**) Anti–DNGR-1 (α-DNGR-1) or isotype control antibodies were intraperitoneally injected into WT (C) or WT and *Batf3*$^{-/-}$ (D) mice on the day before (day −1) and the day of (day 0) caerulein injection. Infiltrating neutrophils in pancreas were quantified by flow cytometry. (**E**) Concentrations of lipase were detected in serum from peripheral blood. U/L, units per liter. (**F**) Hematoxylin and eosin (H&E) staining in pancreatic sections (left). Representative images of $n = 5$ pancreata per experimental condition. Percentages of edematous area (right). (**G** and **H**) *Rag1*$^{-/-}$ and *Rag1*$^{-/-}$*Clec9a*$^{gfp/gfp}$ mice were subjected to pancreatitis as indicated in (A). Infiltrating neutrophils in pancreas quantified by flow cytometry (G) and serum lipase concentrations (H) are shown. In (B) to (H), each dot represents a single mouse. Data are means ± SEM of a representative experiment ($N \geq 2$ independent experiments). Significance was assessed by unpaired Student's *t* test between genotypes (B), (E), (F), (G), and (H) or treatments (C) and (D); $^{*}P < 0.05$, and $^{**}P < 0.01$.

Thus, neutrophil influx is the cellular mechanism driving the pathology in *Candida*-infected *Clec9a*$^{gfp/gfp}$ mice.

To decipher the mechanisms underlying the regulatory role of DNGR-1 on cDC1s in neutrophil infiltration, we used F-actin–myosin II complexes as DNGR-1 ligand (DNGR-1L) to robustly trigger the receptor (*20*). Plated DNGR-1L triggered signaling through the DNGR-1–SYK axis in B3Z-NFAT reporter cells (*7*) in a dose- (fig. S7A) and DNGR-1–dependent manner (fig. S7B). Then, we used a cDC1 cell line (MutuDC) (*21*) that expresses DNGR-1 as well as Dectin-1 (fig. S8A), a CLR critically involved in *C. albicans* recognition (*22*). Stimulation of MutuDCs with the Dectin-1 agonists whole β-glucan particles (WGP) or heat-killed *C. albicans* (*23*) induced the expression of proinflammatory factors such as *Tnf*, *Cxcl2*, and *Egr2*. This was reduced by concomitant exposure to DNGR-1L (Fig. 4A and fig. S8, B and C). Consistently, DNGR-1 triggering attenuated phospholipase Cγ2 (PLCγ2) phosphorylation and IκB degradation in response to WGP (Fig. 4B). DNGR-1 triggering had no impact on the response to toll-like receptor 9 (TLR9) ligand CpG (Fig. 4C and fig. S8, D and E), indicating specificity in the pathways modulated. Using a blocking antibody (fig. S8F), we confirmed that the effect elicited by DNGR-1L was DNGR-1 dependent (fig. S8G).

Regulatory phosphatases can couple to some immunoreceptor tyrosine-based activation motif (ITAM)–containing receptors (*24*, *25*). As DNGR-1 bears a hemi-ITAM (hemITAM) motif (*7*), we tested phosphatase activation upon DNGR-1L sensing. DNGR-1L induced SHP-1 phosphorylation (Fig. 4D) without affecting other CLR-related regulatory mechanisms (*26*, *27*) (fig. S8H). Treatment with the SHP inhibitor NSC-87877 (NSC) abolished the regulatory effect of DNGR-1L on responses elicited by WGP (Fig. 4E). Moreover, mice with SHP-1 depletion in the CD11c^{+} compartment (CD11cΔSHP-1) (*28*), including cDC1s, phenocopied the exacerbated neutrophil infiltration observed in DNGR-1–deficient mice (Fig. 4F and fig. S9). These observations are consistent with an involvement of SHP-1 in the molecular mechanism that adjusts inflammatory responses in cDC1s after DNGR-1 engagement.

MIP-2 (encoded by *Cxcl2*) is a CXCR2 ligand fundamental for neutrophil mobilization from the BM (*29*) and local recruitment to *C. albicans*–infected tissues (*30*). We hypothesized that the MIP-2–CXCR2 axis could be mediating the boosted neutrophilia in the absence of DNGR-1. Administration of pepducin, a peptide that inhibits CXCR2 signaling (*13*), reverted the enhanced renal neutrophil recruitment observed in *Clec9a*$^{gfp/gfp}$ upon *Candida* infection (Fig. 4G). To dissect the contribution of DNGR-1 to the MIP-2–mediated process in vivo, we infected mice with *C. albicans*. After 60 hours, we measured *Cxcl2* expression in the renal immune infiltrate (fig. S10). Of all 10 immune populations tested, only neutrophil

frequencies were increased in *Clec9a*$^{gfp/gfp}$ mice (fig. S11). *Cxcl2* was expressed by neutrophils, macrophages, cDC2s, and cDC1s, but expression was enhanced only in cDC1s in *Clec9a*$^{gfp/gfp}$ mice (Fig. 4H). This suggests that DNGR-1 limits *Cxcl2* expression in cDC1s during *C. albicans* infection.

To investigate the relevance of this increased MIP-2 production by cDC1s on neutrophil recruitment under DNGR-1–deficient conditions, we generated mixed BM chimeric mice with specific MIP-2 deficiency in cDC1s (*Batf3*$^{-/-}$:*Cxcl2*$^{-/-}$) (see methods and fig. S12). After infection with *C. albicans*, DNGR-1 blockade generated an exacerbated renal neutrophil recruitment

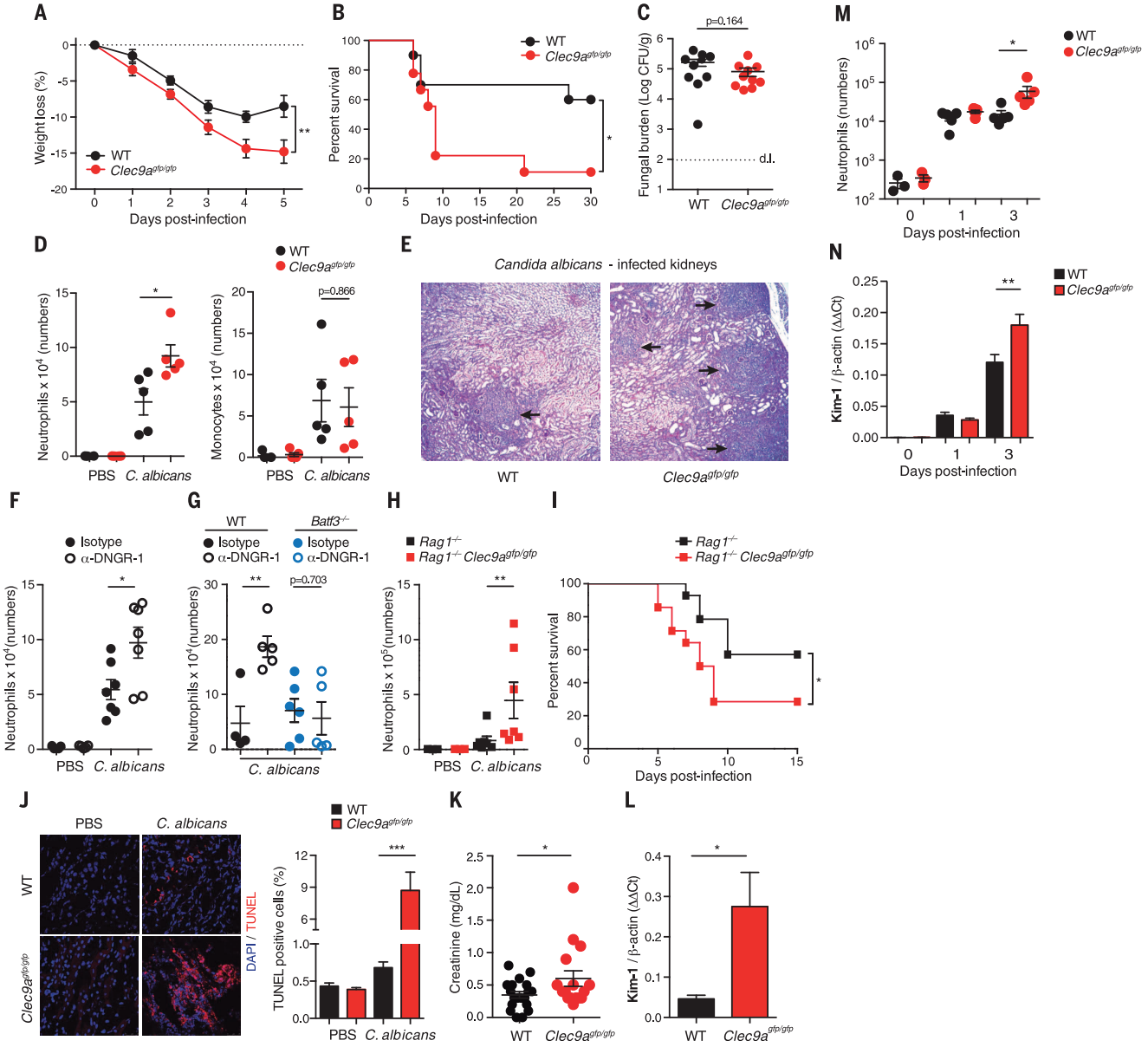

Fig. 2. DNGR-1 controls neutrophil recruitment and pathology associated with systemic candidiasis. *C. albicans* was intravenously injected into WT and *Clec9a*$^{gfp/gfp}$ mice. (**A** and **B**) Weight loss (A) and survival rate (B) were recorded. The dotted line in (A) shows the no-weight-loss reference. (**C** to **E**) After 6 days postinfection, renal fungal burden was detected (C), renal infiltrated neutrophils (left) and monocytes (right) were quantified by flow cytometry (D), and H&E staining was performed (E) (arrows indicate neutrophil accumulation). d.l., detection limit; CFU, colony forming unit. (**F** and **G**) Anti–DNGR-1 or isotype control antibodies were intraperitoneally injected in WT (F) or WT and *Batf3*$^{-/-}$ (G) mice on day −1 and daily after infection; infiltrating renal neutrophils were analyzed by flow cytometry. (**H** and **I**) *Rag1*$^{-/-}$ and *Rag1*$^{-/-}$*Clec9a*$^{gfp/gfp}$ mice were infected as indicated. Renal neutrophils (day 6 postinfection) were quantified by flow cytometry (H), and survival rate was determined (I). (**J**) 4′,6-diamidino-2-phenylindole (DAPI) and TUNEL staining in renal sections (left) and the percentage of TUNEL-positive cells (right). (**K** and **L**) Serum creatinine concentrations (K) and KIM-1 relative expression in total kidney (L) in WT and *Clec9a*$^{gfp/gfp}$ *Candida*-infected mice. β-actin expression was used for normalization. (**M** and **N**) Number of renal neutrophils (M) and KIM-1 expression in total kidney (N) at the indicated times postinfection. In (A), (C), (D), (F), (G), (H), and (M), data are means ± SEM of a representative experiment ($N \geq 2$ independent experiments), including at least five mice per condition. (B) and (I) show representative experiments ($N \geq 2$ independent experiments) with $n \geq 9$ mice per genotype. In (C), (D), (F), (G), (H), (K), and (M), each dot represents a single mouse. (E) and (J) show representative images of $n \geq 5$ kidneys per condition. In (K), (L), and (N), data are means ± SEM of ≥2 pooled experiments ($n \geq 5$ mice per experimental condition in each independent experiment). Significance was assessed by two-way analysis of variance (ANOVA) with Bonferroni post hoc test (A), log-rank (B) and (I), or unpaired Student's *t* test between genotypes (C), (D), (H), (J), (K), (L), (M), and (N) or treatments (F) and (G); $^{*}P < 0.05$, $^{**}P < 0.01$, and $^{***}P < 0.001$.

in *Batf3*$^{-/-}$:WT control chimeras (Fig. 4I). This boosted neutrophilia was lost in *Batf3*$^{-/-}$:*Cxcl2*$^{-/-}$ chimeras (Fig. 4I), thus relying on MIP-2 produced by cDC1s.

Furthermore, we crossed *Clec9a*$^{gfp/gfp}$ and *Cxcl2*$^{-/-}$ mice to further generate chimeric mice with cDC1s lacking both DNGR-1 and MIP-2 (*Batf3*$^{-/-}$:*Clec9a*$^{gfp/gfp}$ *Cxcl2*$^{-/-}$). Upon systemic candidiasis, *Batf3*$^{-/-}$:*Clec9a*$^{gfp/gfp}$ chimeras showed an exacerbated neutrophil infiltration into the kidney compared with *Batf3*$^{-/-}$:WT control chimeras (Fig. 4J). Notably, this boosted neutrophilia was lost in *Batf3*$^{-/-}$:*Clec9a*$^{gfp/gfp}$ *Cxcl2*$^{-/-}$ mice (Fig. 4J). Thus, in the absence of DNGR-1, MIP-2 produced by BATF3-dependent cDC1s is a key mediator for the enhanced neutrophil recruitment.

Infiltration of immune cells within injured tissues must balance pathogen control with increased damage caused by the inflammatory response. In particular, early infiltration by neutrophils to damaged tissues must be carefully regulated, because these cells can cause further tissue destruction (*13*, *17*, *18*). Disease tolerance to infections comprises mechanisms involved in the

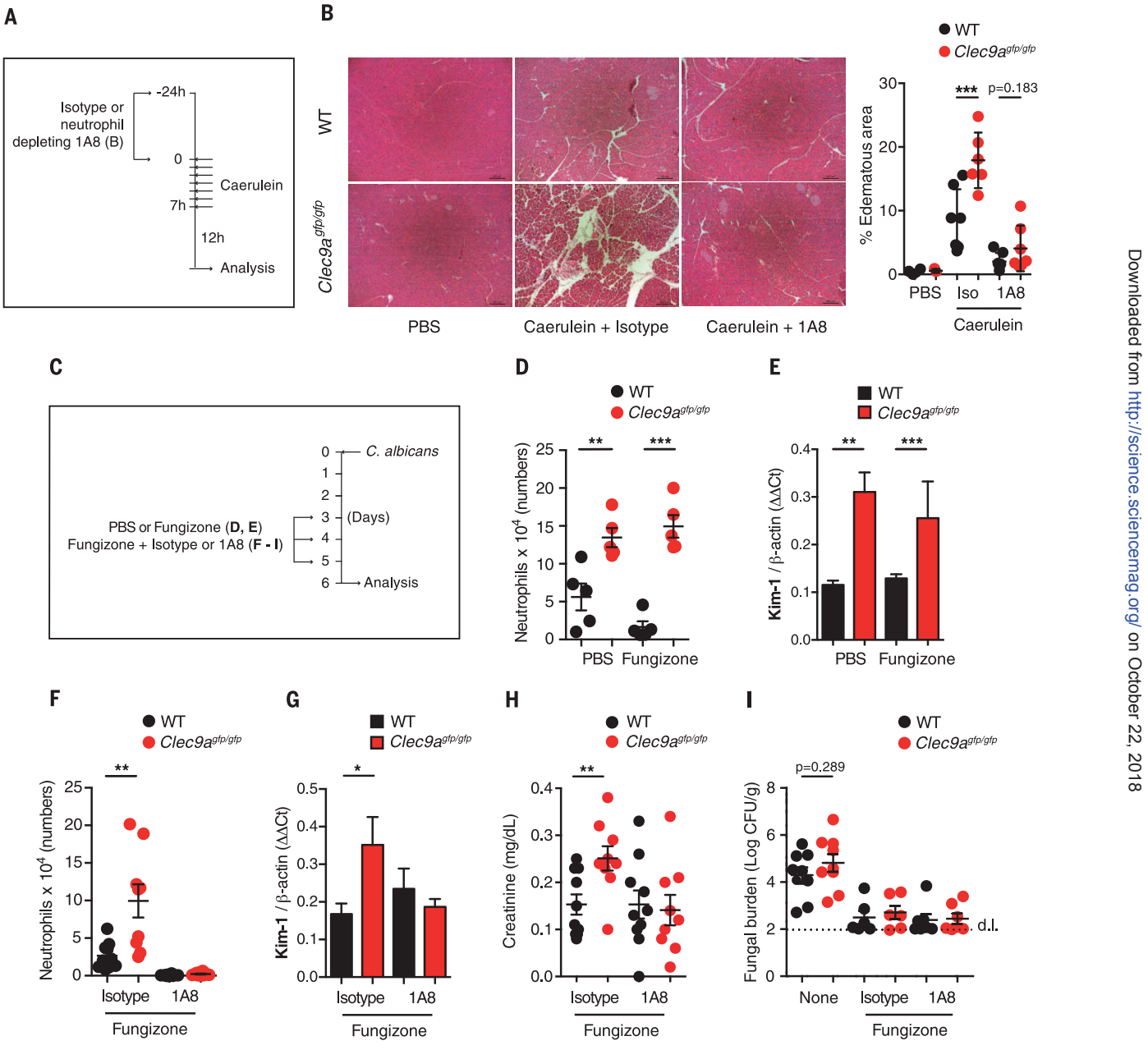

Fig. 3. DNGR-1 restrains tissue damage by dampening neutrophil-mediated immunopathology. (**A**) Representative scheme of pancreatitis induction. 1A8 neutrophil-depleting antibody or isotype (iso) control were administered intraperitoneally, as indicated. (**B**) H&E staining in pancreatic sections (left) and percentages of edematous area (right). Representative images of $n \geq 6$ pancreata per experimental condition. (**C**) Representative scheme of *C. albicans* infection; fungizone or PBS together or alone with 1A8 antibody or isotype control were intraperitoneally administered as indicated. (**D** to **I**) *C. albicans* was intravenously injected in WT and *Clec9a*$^{gfp/gfp}$ mice. After 6 days postinfection, renal-infiltrating neutrophils were quantified by flow cytometry (D) and (F), and KIM-1 expression in total kidney was measured (E) and (G). (H and I) Serum creatinine concentrations (H) and renal fungal burden (I). In (B) and (D) to (I), data are means ± SEM of a representative experiment ($N \geq 2$ independent experiments), including at least five mice per condition. Each dot represents a single mouse. Significance was assessed by unpaired Student's *t* test between genotypes; $^*P < 0.05$, $^{**}P < 0.01$, and $^{***}P < 0.001$.

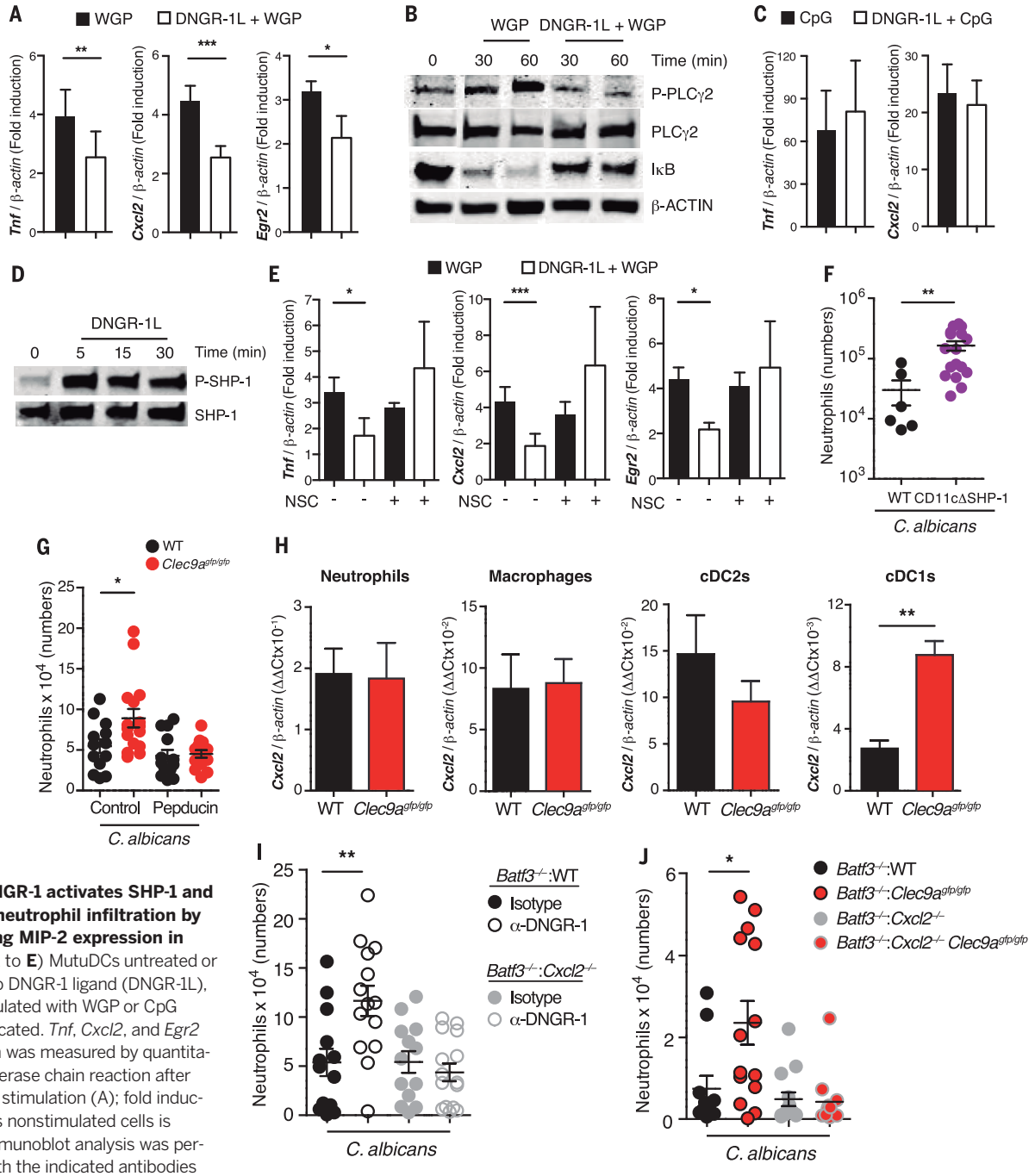

Fig. 4. DNGR-1 activates SHP-1 and controls neutrophil infiltration by dampening MIP-2 expression in cDC1s. (**A** to **E**) MutuDCs untreated or exposed to DNGR-1 ligand (DNGR-1L), were stimulated with WGP or CpG where indicated. *Tnf*, *Cxcl2*, and *Egr2* expression was measured by quantitative polymerase chain reaction after 4 hours of stimulation (A); fold induction versus nonstimulated cells is shown. Immunoblot analysis was performed with the indicated antibodies (B). P-PLCγ2, phosphorylated PLCγ2. In (C), *Tnf* and *Cxcl2* expression were measured as in (A). *Egr2* expression was not induced in response to CpG. MutuDCs were exposed to DNGR-1L and analyzed by immunoblot (D). P-SHP-1, phosphorylated SHP-1. In (E), *Tnf*, *Cxcl2*, and *Egr2* expression was measured in cells either preincubated with the SHP-inhibitor NSC (+) or not (−) and stimulated as in (A). (**F** to **J**) Mice were intravenously infected with *C. albicans*. Renal infiltrating neutrophils were quantified after 6 days in CD11cΔSHP-1 and WT littermates (F) and pepducin or control peptide-treated WT and *Clec9a*$^{gfp/gfp}$ mice (G). In (H), relative *Cxcl2* expression by immune cells in the kidney was measured 60 hours postinfection. In (I) and (J), renal infiltrating neutrophils were quantified at day 6 post infection. In (I), lethally irradiated B6/SJL CD45.1 recipient mice were reconstituted with a mixture of 50% BATF3-deficient BM cells (CD45.2, producing MIP-2 but lacking cDC1s) and 50% MIP-2–deficient BM cells (CD45.2, *Cxcl2*$^{-/-}$ mice). Thus, *Batf3*$^{-/-}$:*Cxcl2*$^{-/-}$ chimeric mice are defective for MIP-2 production only in cDC1s compared with control BM chimeras (*Batf3*$^{-/-}$:WT). Anti–DNGR-1 or isotype control antibodies were intraperitoneally injected on day −1 and daily after infection. In (J), neutrophil numbers are shown for the following mixed BM chimeric mice, generated as in (I): (i) *Batf3*$^{-/-}$:WT control chimeras; (ii) *Batf3*$^{-/-}$:*Clec9a*$^{gfp/gfp}$, which generate cDC1s lacking DNGR-1; (iii) *Batf3*$^{-/-}$:*Cxcl2*$^{-/-}$, which produce MIP-2–deficient cDC1s; and (iv) *Batf3*$^{-/-}$:*Clec9a*$^{gfp/gfp}$ *Cxcl2*$^{-/-}$, which generate cDC1s lacking both DNGR-1 and MIP-2. For (I) and (J), all cDC1s in the kidney were of donor origin (fig. S12, A and C), and the number of reconstituted cDC1s were equal in the different chimeric mice (fig. S12, B and D). In (A), (C), (E), and (H), data are means + SEM of pooled experiments, including $N \geq 3$ individual cultures or ≥4 mice per condition ($N \geq 4$ independent experiments). For (B) and (D), $N \geq 2$ representative immunoblots. In (F), (G), (I), and (J), data are means ± SEM of two pooled experiments. Each dot represents a single mouse. Significance was assessed by paired Student's *t* test between DNGR-1L–treated or untreated (A), (C), and (E) or between genotypes (H) or unpaired between genotypes (F), (G), (I), and (J); $*P < 0.05$, $**P < 0.01$, and $***P < 0.001$.

control of tissue damage. This concept of "tissue damage control" is not restricted to infections and can also be applied to the regulation of damage from sterile inflammation (*14*, *31*). Notably, mediators involved in tissue damage control under both sterile and infectious conditions can be shared (*31*). Our data suggest that DNGR-1 acts as a shared checkpoint for sterile and infectious tissue damage control. Detection of tissue damage by cDC1s through DNGR-1 would act as a checkpoint for neutrophil infiltration and further immunopathology. Deficient sensing of tissue damage in the absence of DNGR-1 leads to higher production of MIP-2 by cDC1s. This increased MIP-2 production can ignite neutrophil infiltration that drives immunopathology within the damaged organ (fig. S13). Thus, DNGR-1 acts as a necrosis-sensing receptor that, depending on the inflammatory context, may promote a regulatory tissue damage–control mechanism by cDC1s or may contribute to cross-priming during adaptive immunity–related responses (*7*–*9*). This capacity to develop two different host protective functions and the regulation and implications of this dual role remain to be investigated.

REFERENCES AND NOTES

1. P. Matzinger, *Science* **296**, 301–305 (2002).
2. K. L. Rock, H. Kono, *Annu. Rev. Pathol.* **3**, 99–126 (2008).
3. S. Ahrens *et al.*, *Immunity* **36**, 635–645 (2012).
4. J.-G. Zhang *et al.*, *Immunity* **36**, 646–657 (2012).
5. B. U. Schraml *et al.*, *Cell* **154**, 843–858 (2013).
6. L. F. Poulin *et al.*, *Blood* **119**, 6052–6062 (2012).
7. D. Sancho *et al.*, *Nature* **458**, 899–903 (2009).
8. S. Iborra *et al.*, *J. Clin. Invest.* **122**, 1628–1643 (2012).
9. S. Zelenay *et al.*, *J. Clin. Invest.* **122**, 1615–1627 (2012).
10. M. M. Lerch, F. S. Gorelick, *Gastroenterology* **144**, 1180–1193 (2013).
11. S. Iborra *et al.*, *Immunity* **45**, 847–860 (2016).
12. K. Hildner *et al.*, *Science* **322**, 1097–1100 (2008).
13. C. W. Steele *et al.*, *J. Pathol.* **237**, 85–97 (2015).
14. R. Medzhitov, D. S. Schneider, M. P. Soares, *Science* **335**, 936–941 (2012).
15. A. M. Jamieson *et al.*, *Science* **340**, 1230–1234 (2013).
16. J. F. Fisher, K. Kavanagh, J. D. Sobel, C. A. Kauffman, C. A. Newman, *Clin. Infect. Dis.* **52** (suppl. 6), S437–S451 (2011).
17. O. Majer *et al.*, *PLOS Pathog.* **8**, e1002811 (2012).
18. M. S. Lionakis *et al.*, *PLOS Pathog.* **8**, e1002865 (2012).
19. T. Dejima *et al.*, *Infect. Immun.* **79**, 4503–4510 (2011).
20. O. Schulz *et al.*, *Cell Reports* **24**, 419–428 (2018).
21. S. A. Fuertes Marraco *et al.*, *Front. Immunol.* **3**, 331 (2012).
22. R. A. Drummond, G. D. Brown, *Curr. Opin. Microbiol.* **14**, 392–399 (2011).
23. H. S. Goodridge *et al.*, *Nature* **472**, 471–475 (2011).
24. S. Ben Mkaddem *et al.*, *J. Clin. Invest.* **124**, 3945–3959 (2014).
25. S. Iborra *et al.*, *Immunity* **45**, 788–801 (2016).
26. N. Blanco-Menéndez *et al.*, *J. Immunol.* **195**, 4466–4478 (2015).
27. T. S. Freedman *et al.*, *eLife* **4**, e09183 (2015).
28. C. L. Abram, G. L. Roberge, L. I. Pao, B. G. Neel, C. A. Lowell, *Immunity* **38**, 489–501 (2013).
29. K. J. Eash, A. M. Greenbaum, P. K. Gopalan, D. C. Link, *J. Clin. Invest.* **120**, 2423–2431 (2010).
30. E. Balish *et al.*, *J. Leukoc. Biol.* **66**, 144–150 (1999).
31. S. R. Wu, P. Reddy, *Trends Immunol.* **38**, 231–235 (2017).

ACKNOWLEDGMENTS

We are grateful to C. Reis e Sousa and C. A. Lowell for sharing essential reagents. We thank C. Reis e Sousa and members of the D.S. laboratory for discussions and critical reading of the manuscript. We appreciate R. Mota for his advice on the pancreatitis model. We thank the staff at the CNIC facilities for technical support. **Funding:** C.d.F. is supported by the AECC Foundation as the recipient of an "Ayuda Fundación Científica AECC a personal investigador en cancer." P.S.-L. is funded by grant BES-2015-072699 from the Spanish Ministerio de Ciencia, Innovación y Universidades (MCIU). M.E. is the recipient of a CNIC International Ph.D. Programme fellowship "la Caixa"-Severo Ochoa OSLC-CNIC-2013-04. S.K.W. is supported by a European Molecular Biology Organization (EMBO) Long-Term Fellowship (grant ALTF 438-2016) and a CNIC-International Postdoctoral Programme Fellowship (grant 17230-2016). Work in the D.S. laboratory is funded by the CNIC and grant SAF2016-79040-R from MCIU, Agencia Estatal de Investigación, and Fondos Europeos de Desarrollo Regional (FEDER); B2017/BMD-3733 Immunothercan-CM from Comunidad de Madrid; RD16/0015/0018-REEM from FIS-Instituto de Salud Carlos III, MICINN, and FEDER; Acteria Foundation; Constantes y Vitales prize (Atresmedia); La Marató de TV3 Foundation (201723); the European Commission (635122-PROCROP H2020); and the European Research Council (ERC-2016-Consolidator Grant 725091). The CNIC is supported by the MCIU and the Pro-CNIC Foundation and is a Severo Ochoa Center of Excellence (SEV-2015-0505). **Author contributions:** Conceptualization: C.d.F., P.S.-L., and D.S.; methodology, investigation, analysis, and validation: C.d.F., P.S.-L., M.E., S.K.W., S.M.-C., N.B.-M., O.S., M.G., and F.M.-M.; resources: O.S., E.C., and A.P.; writing of original draft: C.d.F., P.S.-L., and D.S.; editing of draft: all authors; supervision, project administration, and funding acquisition: D.S. **Competing interests:** The authors declare no competing interests. **Data and materials availability:** All data needed to understand and assess the conclusions of this research are available in the main text and supplementary materials. *Batf3*$^{-/-}$ mice were obtained from K. M. Murphy under a material transfer agreement with Washington University and the Howard Hugues Medical Institute. The MuTu1940 DC cell line was obtained from H. Acha-Orbea under a material transfer agreement with the University of Laussanne.

SUPPLEMENTARY MATERIALS

www.sciencemag.org/content/362/6412/351/suppl/DC1
Materials and Methods
Figs. S1 to S13
References

29 May 2017; resubmitted 13 June 2018
Accepted 3 September 2018
10.1126/science.aan8423

IVIg Promote Cross-Tolerance against Inflammatory Stimuli In Vitro and In Vivo

Ángeles Domínguez-Soto,* Miriam Simón-Fuentes,* Mateo de las Casas-Engel,* Víctor D. Cuevas,* María López-Bravo,† Jorge Domínguez-Andrés,† Paula Saz-Leal,‡ David Sancho,‡ Carlos Ardavín,† Juliana Ochoa-Grullón,§ Silvia Sánchez-Ramón,§ Miguel A. Vega,* and Angel L. Corbí*

IVIg is an approved therapy for immunodeficiency and for several autoimmune and inflammatory diseases. However, the molecular basis for the IVIg anti-inflammatory activity remains to be fully explained and cannot be extrapolated from studies on animal models of disease. We now report that IVIg impairs the generation of human monocyte–derived anti-inflammatory macrophages by inducing JNK activation and activin A production and limits proinflammatory macrophage differentiation by inhibiting GM-CSF–driven STAT5 activation. In vivo, IVIg provokes a rapid increase in peripheral blood activin A, CCL2, and IL-6 levels, an effect that can be recapitulated in vitro on human monocytes. On differentiating monocytes, IVIg promotes the acquisition of altered transcriptional and cytokine profiles, reduces TLR expression and signaling, and upregulates negative regulators of TLR-initiated intracellular signaling. In line with these effects, in vivo IVIg infusion induces a state tolerant toward subsequent stimuli that results in reduced inflammatory cytokine production after LPS challenge in human peripheral blood and significant protection from LPS-induced death in mice. Therefore, IVIg conditions human macrophages toward the acquisition of a state of cross-tolerance against inflammatory stimuli, an effect that correlates with the net anti-inflammatory action of IVIg in vivo. ***The Journal of Immunology*****, 2018, 201: 41–52.**

Extensive macrophage accumulation is one of the hallmarks of inflammatory responses. During inflammation, monocytes egress from the bone marrow into the circulation (1, 2) and migrate into inflamed tissues (1, 3–5), where they give rise to distinct macrophage and dendritic cell subsets under the influence of tissue cellular and extracellular cues (6, 7). The high sensitivity of monocytes to the surrounding milieu is exemplified by their distinct responses to GM-CSF and M-CSF, which drive differentiation into functionally different macrophages (8). GM-CSF promotes proinflammatory macrophages (human monocyte–derived macrophages differentiated in the presence of GM-CSF [GM-MØ]) (9, 10) characterized by the expression of a "proinflammatory gene set" (11, 12). Conversely, M-CSF leads to tissue repair and anti-inflammatory/homeostatic macrophages (human monocyte–derived macrophages differentiated in the presence of M-CSF [M-MØ]) with robust IL-10–producing ability in response to pathogenic stimuli (9, 10, 13), which are transcriptionally defined by the expression of an "anti-inflammatory gene set" (11, 12, 14). Human GM-MØ and M-MØ are considered as proinflammatory and anti-inflammatory macrophages based on their respective profiles of stimuli-induced cytokines (9, 10, 15, 16) and because their specific gene signatures resemble those of macrophages from rheumatoid arthritis joints and tumor-associated macrophages, respectively (17). An adequate shift between the pro- and anti-inflammatory functions of macrophages is required for elimination of inflammatory insults and tissue repair (18, 19). Because deregulated macrophage polarization leads to the onset and maintenance of chronic inflammation (20–25), strategies for modulating macrophage polarization are of therapeutic use in chronic inflammatory diseases (26–30).

IVIg is a preparation of highly purified polyclonal and polyspecific IgG isolated from plasma of thousands of healthy donors. Besides substitutive treatment of patients with primary and secondary Ab deficiencies, IVIg is currently used in a large and growing number of autoimmune and systemic inflammatory disorders (31–34), as it exerts immunomodulatory effects on a variety of immune cells (31, 35, 36). Several non–mutually exclusive mechanisms have been proposed to explain the IVIg immunoregulatory action, including the sialic acid content of the Fc portion of the Abs and the interaction with ITAM-bearing Fc receptors (31, 32, 35–43). We have previously reported that IVIg

*Departamento de Biología Celular, Centro de Investigaciones Biológicas, Consejo Superior de Investigaciones Cientificas, 28040 Madrid, Spain; †Departamento de Inmunología y Oncología, Centro Nacional de Biotecnología, Consejo Superior de Investigaciones Cientificas, 28049 Madrid, Spain; ‡Fundación Centro Nacional de Investigaciones Cardiovasculares, Centro Nacional de Investigaciones Cardiovasculares, 28029 Madrid, Spain; and §Departamento de Inmunología Clínica, Hospital Universitario Clínico San Carlos, 28040 Madrid, Spain

ORCIDs: 0000-0002-2816-8070 (V.D.C.); 0000-0002-9091-1961 (J.D.-A.); 0000-0001-9585-6167 (S.S.-R.); 0000-0001-6151-4193 (M.A.V.).

Received for publication July 28, 2017. Accepted for publication April 18, 2018.

This work was supported by grants from the Ministerio de Economía y Competitividad (SAF2014-23801), the Instituto de Salud Carlos III (La Red de Investigación en Inflamación y Enfermedades Reumáticas, RIER RD12/009), and the Comunidad Autónoma de Madrid/FEDER (S2010/BMD-2350, RAPHYME Program) to A.L.C. and M.A.V. and by Instituto de Salud Carlos III Grant PI16/01428 to S.S.-R.

Address correspondence and reprint requests to Dr. Ángeles Domínguez-Soto and Dr. Angel L. Corbí, Centro de Investigaciones Biológicas, Consejo Superior de Investigaciones Cientificas, Ramiro de Maeztu, 9, 28040 Madrid, Spain. E-mail addresses: ads@cib.csic.es (Á.D.-S.) and acorbi@cib.csic.es (A.L.C.)

The online version of this article contains supplemental material.

Abbreviations used in this article: GM-BMDM, murine bone marrow–derived macrophage differentiated in the presence of GM-CSF; GM-MØ, human monocyte–derived macrophage differentiated in the presence of GM-CSF, proinflammatory macrophage; IVIg/GM-MØ, human monocyte–derived macrophage differentiated in the presence of GM-CSF and IVIg; IVIg/M-MØ, human monocyte–derived macrophage differentiated in the presence of M-CSF and IVIg; M-MØ, human monocyte–derived macrophage differentiated in the presence of M-CSF, anti-inflammatory/homeostatic macrophage; qRT-PCR, quantitative real-time PCR.

www.jimmunol.org/cgi/doi/10.4049/jimmunol.1701093

skews human and mouse macrophage polarization through FcγR-dependent mechanisms (44) and that the IVIg immunomodulatory activity is dependent on the polarization state of the responding macrophage, as IVIg limits the proinflammatory transcriptome and functions of GM-MØ but favors the acquisition of proinflammatory properties in M-MØ (44). In fact, IVIg potentiates inflammatory tissue-damaging responses in murine models of stroke and sepsis (44) and reduces tumor growth and metastasis in tumor models (44). However, extrapolation of the IVIg effects from animal models of disease to human pathology is not obvious because IVIg is prophylactically administered in most animal studies, whereas IVIg is used as a therapeutic strategy in humans (40).

We now report that IVIg modulates M-CSF– and GM-CSF–driven in vitro macrophage differentiation through distinct molecular mechanisms and conditions monocytes in vivo to acquire a state of tolerance against inflammatory stimuli. These findings provide novel insights into the anti-inflammatory activity of IVIg in vivo.

Materials and Methods

Macrophage differentiation, cell culture, and treatments

Human monocytes were purified from PBMCs by magnetic cell sorting using anti-CD14 microbeads (Miltenyi Biotec) (>95% $CD14^+$ cells) and cultured at 0.5×10^6 cells/ml for 7 d in RPMI 1640 supplemented with 10% FCS and either 1000 U/ml GM-CSF or 10 ng/ml M-CSF (ImmunoTools) to generate GM-MØ or M-MØ, respectively. Cytokines and IVIg (10 mg/ml; Privigen, CSL Behring) were added every 2 d, reaching 20–23 mg/ml of Igs at the end of the 7-d differentiation process. For activation, macrophages were treated with *Escherichia coli* 055:B5 LPS (10 ng/ml) for 24 h. Whenever indicated, a neutralizing Ab against human activin A (100 ng/ml; R&D Systems) was used. Murine bone marrow–derived macrophages differentiated in the presence of GM-CSF (GM-BMDMs) were generated using murine GM-CSF (1000 U/ml; PeproTech).

Quantitative real-time PCR

Total RNA was extracted using the RNeasy Mini Kit or the AllPrep DNA/RNA/Protein Mini Kit (Qiagen). cDNA was synthesized using the Reverse Transcription System kit (Applied Biosystems) (45). Oligonucleotides were designed with Universal ProbeLibrary software (Roche Life Sciences). Quantitative real-time PCR (qRT-PCR) was performed using custom-made microfluidic gene cards (Roche Life Sciences) or standard plates on a LightCycler 480 (Roche Life Sciences) (12). Where indicated, a panel of 28 genes differentially expressed between GM-MØ and M-MØ (and included within the previously defined proinflammatory gene set and anti-inflammatory gene set) was analyzed (11, 12). Assays were made in triplicate, and results were normalized according to the mean of the expression levels of *HPRT*, *SDHA*, and *TBP*. Results were expressed using the ΔΔCT method for quantitation.

Western blot

Cell lysates were subjected to SDS-PAGE and transferred onto an Immobilon-P polyvinylidene difluoride membrane (Millipore). After blocking the unoccupied sites with 5% BSA, protein detection was carried out with Abs against total and phosphorylated ERK1/2, total and phosphorylated JNK, IκBα, phosphorylated IRF3, phosphorylated STAT5, phosphorylated SHIP-1, A20 (Cell Signaling Technology), total and phosphorylated STAT1, phosphorylated STAT3 (BD Biosciences), or phosphorylated SHP-1 (Cell Signaling Technology) and using the SuperSignal West Pico Chemiluminescent system (Pierce). Protein loading was normalized using a mAb against GAPDH (sc-32233; Santa Cruz Biotechnology) or an Ab against human vinculin (Sigma-Aldrich).

Clinical samples and ex vivo LPS tolerance

Peripheral blood was obtained from 36 patients receiving IVIg therapy (400 mg/kg body weight), both before and after (5 h) IVIg infusion, and serum or plasma was recovered using standard procedures. Patients had been previously diagnosed with either common variable immunodeficiency and other inflammatory disorders ($n = 18$) or recurrent reproductive failure of inflammatory cause ($n = 18$). To assess cross-tolerance to LPS in ex vivo experiments, peripheral blood obtained from 10 patients receiving IVIg therapy, both before and after IVIg infusion, was maintained for 12 h at room temperature and treated with PBS or LPS (10 ng/ml) for 10 h, and plasma was recovered using standard procedures. Where indicated, monocytes were isolated from the peripheral blood of IVIg-treated patients using anti-CD14 microbeads (Miltenyi Biotec). All patients gave informed consent, and the Hospital Universitario Clínico San Carlos ethics committee approved the study.

In vivo endotoxin tolerance

For survival studies, mice ($n = 20$ mice per group) received PBS or IVIg i.p. (400 μl of a 100 mg/ml solution, 40 mg/mouse). After 26 h, mice were challenged i.p. with LPS (9 mg/kg in saline). Mouse survival was monitored every 12 h for 5 d. For survival studies, statistical analysis was performed using the Mantel–Cox log-rank test ($^{**}p < 0.01$).

Flow cytometry

Phenotypic analysis was carried out by flow cytometry as described previously (46) using either a mAb specific for human TLR4 (sc-13593; Santa Cruz Biotechnology) or an isotype-matched control Ab (Chemicon) and followed by staining with FITC-labeled Fab goat anti-mouse IgG. All incubations were done in the presence of 50 μg/ml human IgG to prevent binding through the Fc portion of the Abs.

ELISA

Culture supernatants from untreated or LPS-treated (24 h) human macrophages and plasma from patients were assayed for the presence of cytokines using a commercially available ELISA for human TNF-α, IL-12p40 (BD Pharmingen), CXCL10, IL-6, IL-10 (BioLegend), and activin A (R&D Systems). ELISA was performed following the protocols supplied by the manufacturers.

Statistical analysis

Unless otherwise indicated and for comparisons of means, statistical analysis was performed using the Student t test, and a p value <0.05 was considered significant ($^{*}p < 0.05$, $^{**}p < 0.01$, $^{***}p < 0.001$).

Results

IVIg blocks the acquisition of the anti-inflammatory transcriptional signature of M-MØ through JNK activation and activin A production

Peripheral blood monocytes are the immediate precursors of macrophages within inflamed tissues (47). Because IVIg modulates polarization of human macrophages (44), we sought to assess the IVIg effects on the ability of monocytes to differentiate into macrophages in vitro. To that end, monocytes were differentiated in the presence of therapeutic doses of IVIg. IVIg infusion as a replacement therapy (48) or as immunosuppressive therapy (31, 32, 36) raises peripheral blood IgG to 15–35 mg/ml (48–50) and increases IgG blood concentration by an average of 1.8-fold (mean of maximal IgG levels after IVIg infusion of 16.9 mg/ml). Therefore, monocytes were differentiated with either M-CSF or GM-CSF and with IVIg reaching a final concentration of 20–30 mg/ml at the end of the macrophage differentiation protocol. The presence of IVIg along M-CSF–driven differentiation generated macrophages (human monocyte–derived macrophages differentiated in the presence of M-CSF and IVIg [IVIg/M-MØ]) with significantly lower expression of the whole M-MØ–specific anti-inflammatory gene set and higher expression of several transcripts of the GM-MØ–specific proinflammatory gene set (Fig. 1A) (12, 51). The IVIg-induced transcriptomic changes were observed with IVIg concentrations as low as 1 mg/ml (Supplemental Fig. 1A) and were already detected 48 h after exposure to IVIg (Fig. 1B). The IVIg-induced changes were also evident at the protein level after 48 h of IVIg exposure, as indicated by the loss of expression of MAFB (Fig. 1C), which controls expression of most genes of the anti-inflammatory gene set (14), and the huge increase in the production of activin A (Fig. 1D), which drives the generation of

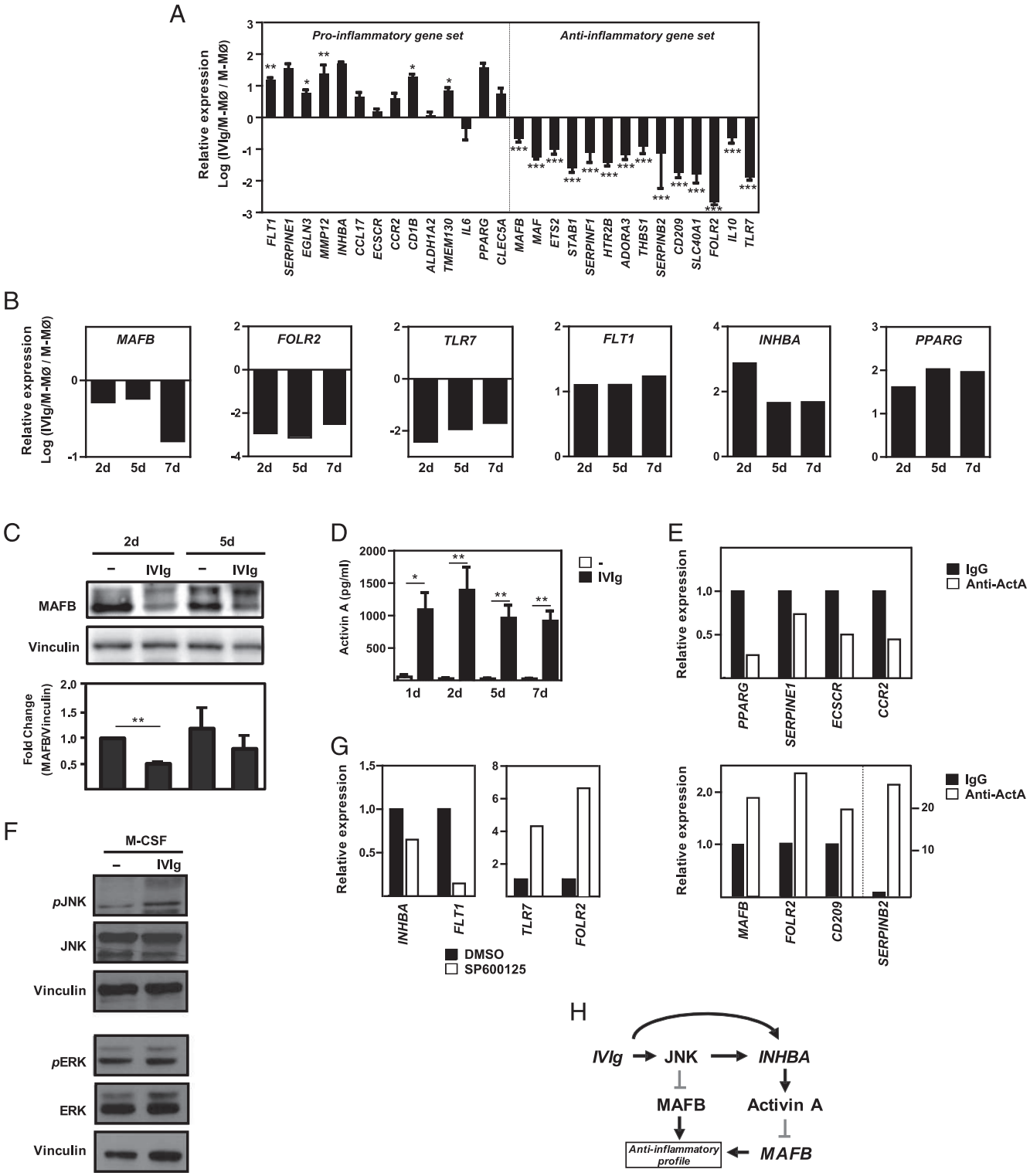

FIGURE 1. IVIg blocks the acquisition of the anti-inflammatory transcriptional signature of M-MØ through JNK activation and activin A production. (**A**) Relative expression of the indicated genes in IVIg/M-MØ, as determined by qRT-PCR. The experiment was done on monocytes from five independent donors, and shown is the mean ± SEM. (**B**) Expression of the indicated genes in monocytes differentiated under the influence of M-CSF with or without IVIg for 2, 5, or 7 d, as determined by qRT-PCR. Two independent experiments were performed and one of them is shown. In (A) and (B), results show the expression of each gene in IVIg/M-MØ relative to its expression in M-MØ. (**C**) Immunoblot analysis of MAFB protein levels in monocytes exposed to IVIg for 2 or 5 d. Protein levels of vinculin were determined in parallel to control for protein loading. Densitometric quantification of the relative MAFB protein levels in three independent experiments is shown in the lower panel. The expression of MAF in monocytes cultured for 2 d in the absence of IVIg was arbitrarily set to 1. (**D**) Activin A levels in culture supernatants of monocytes differentiated with M-CSF for the indicated periods of time and either in the absence or presence of IVIg. Each determination was performed in triplicate, and shown is the mean ± SEM of seven independent experiments. (**E**) Relative expression of the indicated genes in IVIg/M-MØ generated in the presence of 100 ng/ml of a blocking anti–activin A Ab (Anti-ActA) or an isotype-matched Ab (IgG), as determined by qRT-PCR. Shown are the relative mRNA levels of each gene (relative to *TBP* RNA levels) referred to its expression level when differentiation was done in the presence of an isotype-matched Ab (IgG). The experiment was done on monocytes from two independent donors, and one of the experiments is shown. (**F**) Immunoblot analysis of p-JNK, p-ERK, total JNK, and total ERK *(Figure legend continues)*

macrophages with proinflammatory activity (11, 12). The relevance of the IVIg-induced activin A production was demonstrated by the ability of a neutralizing anti–activin A Ab to partially reverse the IVIg-induced transcriptional changes (Fig. 1E). Moreover, IVIg/M-MØ–conditioned medium also exhibited an enhanced ability to limit tumor cell proliferation (data not shown), an activin A–dependent function that is exclusive to proinflammatory GM-MØ (12).

Regarding intracellular signaling, in M-CSF–exposed monocytes, IVIg did not affect the activation state of ERK or NF-κB (Fig. 1F, data not shown) but induced JNK phosphorylation (Fig. 1F), partly via Syk activation (Supplemental Fig. 2). The IVIg-induced JNK phosphorylation is particularly relevant because JNK activity drives the generation of macrophages with proinflammatory activity (52). In fact, the IVIg-induced transcriptional changes could also be impaired by inhibition of JNK activation, as evidenced by the weaker increase of *INHBA* (the activin A–encoding gene) and *FLT1* and the lower downregulation of *FOLR2* and *TLR7* (Fig. 1G). Because JNK activation contributes to *INHBA* expression (Fig. 1G) but also accelerates MAFB degradation (53), these results indicate that IVIg limits the transcriptional differentiation of monocytes into anti-inflammatory macrophages by triggering JNK activation and activin A production (Fig. 1H).

IVIg inhibits GM-CSF–induced STAT5 activation and impairs the acquisition of the GM-CSF–dependent transcriptional profile of proinflammatory GM-MØ

GM-CSF is a key driver of tissue inflammation whose levels are increased in blood from patients with inflammatory disorders, and it has become a therapeutic target in inflammatory diseases (54). We next evaluated the effect of IVIg on the GM-CSF–driven differentiation of human GM-MØ. The continuous presence of IVIg significantly impaired the upregulation of members of the proinflammatory gene set that characterizes proinflammatory GM-MØ (11, 12) (Fig. 2A) in a dose-dependent manner (Supplemental Fig. 1A). Like in the case of M-MØ, IVIg modulated gene expression after a single dose (48 h) (Fig. 2B). Interestingly, comparison of the transcriptional profile of macrophages generated in the absence or presence of IVIg revealed that the huge transcriptomic differences between GM-MØ and M-MØ (11, 12) are blunted when differentiation takes place in the continuous presence of IVIg and that IVIg/M-MØ exhibit a transcriptional profile that resembles the profiles of GM-MØ and human monocyte–derived macrophages differentiated in the presence of GM-CSF and IVIg (IVIg/GM-MØ) (Supplemental Fig. 1B). Thus, therapeutic concentrations of IVIg inhibit the transcriptional response of monocytes toward M-CSF or GM-CSF, impairing the generation of M-MØ or GM-MØ. In the case of GM-CSF–driven macrophage differentiation, IVIg exposure further increased the GM-CSF–induced phosphorylation of JNK in human monocytes (Fig. 2C, left panel). This IVIg-dependent enhancement of JNK activation did not translate into higher levels of activin A (Fig. 2A), probably because GM-CSF–induced JNK phosphorylation suffices to yield maximal INHBA gene expression. More importantly, IVIg drastically reduced the GM-CSF–induced STAT5 phosphorylation in human monocytes (Fig. 2C, right panel). Therefore, the ability of IVIg to impair the acquisition of the GM-CSF–dependent transcriptional profile correlates with its capacity to block STAT5 activation, which allows us to conclude that IVIg inhibits the transcriptional response of monocytes toward M-CSF or GM-CSF by distinct mechanisms.

IVIg disrupts the LPS responsiveness of proinflammatory GM-MØ and anti-inflammatory M-MØ

The defining functional feature of M-MØ and GM-MØ is their capacity to preferentially produce high levels of IL-10 and CCL2 (M-MØ) or proinflammatory cytokines (TNF-α, IL-12p40) (GM-MØ) in response to TLR ligands (13). Thus, we next compared the LPS responsiveness of macrophages generated in the absence (M-MØ, GM-MØ) or presence of IVIg (IVIg/M-MØ, IVIg/GM-MØ). Compared to M-MØ, IVIg/M-MØ exhibited a significantly lower production of LPS-induced CCL2, IL-10, and CXCL10 (reduction of LPS inducibility to 4.5% in M-MØ, $p = 3 \times 10^{-4}$) (Fig. 3A, left panels) as well as higher levels of LPS-induced TNF-α and IL-12p40 (Supplemental Fig. 1C). The distinct cytokine response of M-MØ and IVIg/M-MØ was also evident upon exposure to TLR2 ligands such as Pam3Cys or lipoteichoic acid (Fig. 3A, left panels). By contrast, IVIg/GM-MØ displayed a significantly lower LPS-induced expression of TNF-α, IL-12p40, CXCL10 (reduction of LPS inducibility to 0.06% in GM-MØ, $p = 2 \times 10^{-7}$) (Fig. 3A, right panels), IL-10, and IL-6 (Supplemental Fig. 1C), and a similar reduction was also observed in response to TLR2 ligands (Fig. 3A, right panels). Moreover, the effect of IVIg was not limited to stimuli-induced cytokines because assessment of the expression of genes whose LPS inducibility is cell type–specific (V.D. Cuevas and A.L. Corbí, unpublished observations) revealed that LPS enhanced the expression of *NLRP3* in IVIg/M-MØ (a property that is unique to GM-MØ), whereas *LMNB1* expression (whose LPS inducibility is M-MØ-specific) was not upregulated by LPS in IVIg/M-MØ (Fig. 3B). Furthermore, LPS treatment reduced *LMNB1* expression in IVIg/GM-MØ (but not in GM-MØ) and upregulated *NLRP3* expression in GM-MØ (but not in IVIg/GM-MØ) (Fig. 3B). Therefore, therapeutic concentrations of IVIg severely modify the LPS responsiveness of macrophages generated in the presence of either M-CSF or GM-CSF.

Monocyte exposure to IVIg impairs LPS-initiated signaling and enhances the expression of negative regulators of NF-κB signaling

To identify the molecular basis for the IVIg ability to disrupt the LPS-induced cytokine production in human macrophages, we analyzed whether IVIg alters LPS-initiated intracellular signals. IVIg/M-MØ exhibited lower levels of LPS-induced ERK activation and IκBα degradation than M-MØ (Fig. 4A, left panels), and a similar result was found upon LPS stimulation of IVIg/GM-MØ and GM-MØ (Fig. 4A, right panels). The LPS-induced activation of IRF3 and STAT3 was also significantly lower in IVIg/M-MØ and IVIg/GM-MØ than in M-MØ and GM-MØ (Fig. 4B). Moreover, and in line with the diminished production of LPS-induced CXCL10 (Fig. 3A), the LPS-induced activation of STAT1 was

in monocytes cultured with M-CSF overnight, starved for 2 h in M-CSF–free and serum-free medium, and then treated with IVIg before stimulation with M-CSF for 15 min. Protein levels of ERK, JNK, and vinculin were determined in parallel to control for protein loading. In each case, three independent experiments were performed, and one experiment is shown. (**G**) Relative expression of the indicated genes in IVIg/M-MØ generated in the absence (DMSO) or in the presence of the JNK inhibitor SP600125 (30 μM), as determined by qRT-PCR. Shown are the relative mRNA levels of each gene (relative to *TBP* RNA levels) referred to its expression level when differentiation was done in the presence of DMSO. Three independent experiments were done and one of them is shown. (**H**) Schematic representation of the effects of IVIg on the acquisition of the anti-inflammatory gene profile by human monocytes. $^{*}p < 0.05$, $^{**}p < 0.01$, $^{***}p < 0.001$.

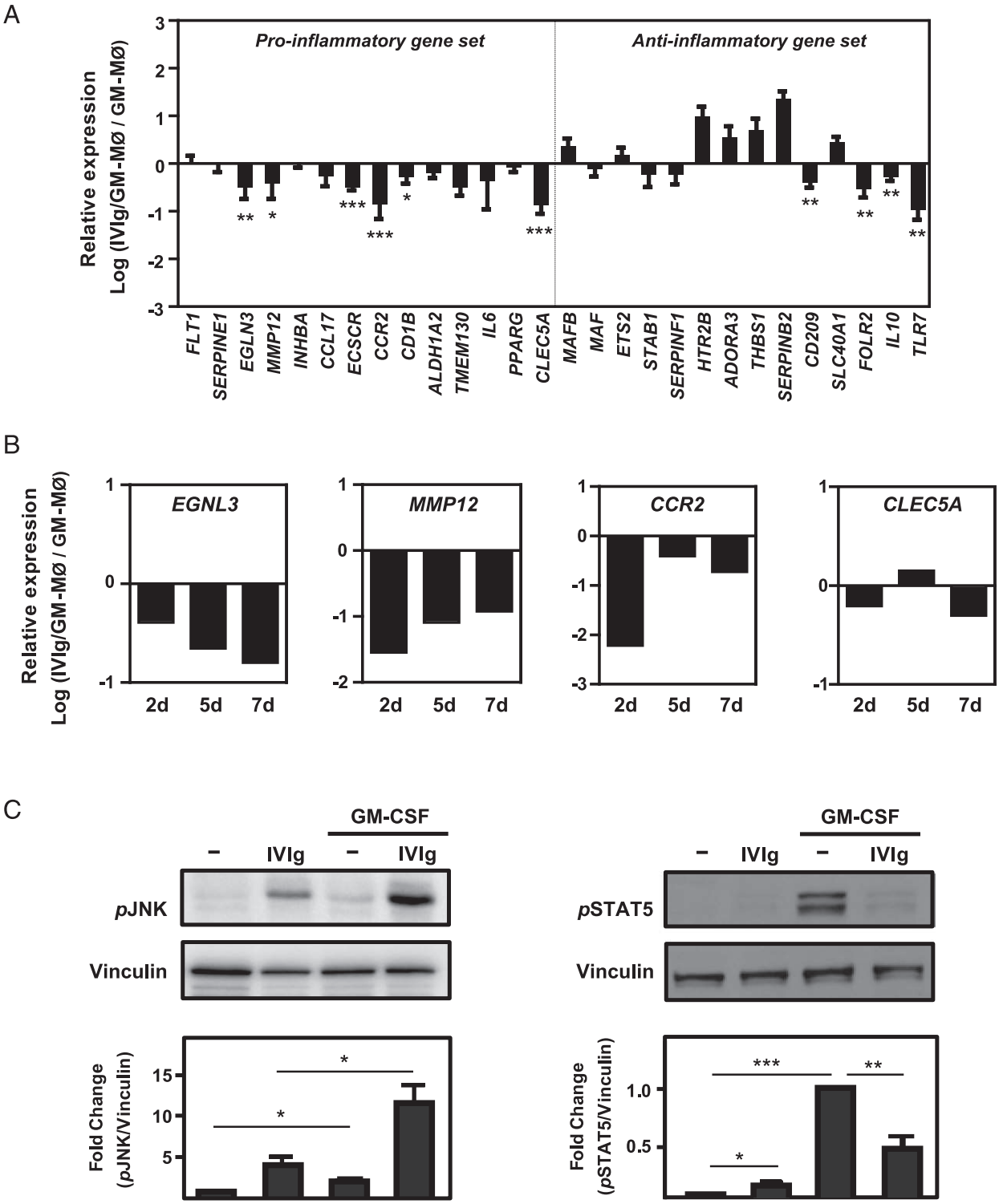

FIGURE 2. IVIg impairs the acquisition of the proinflammatory transcriptional signature of GM-MØ. (**A**) Relative expression of the indicated genes in IVIg/GM-MØ, as determined by qRT-PCR. The experiment was done on monocytes from five independent donors, and shown is the mean ± SEM. (**B**) Kinetics of the expression of the indicated genes along the differentiation of IVIg/GM-MØ, as determined by qRT-PCR. Two experiments were done on macrophages from independent donors, and one of them is shown. In (A) and (B), results show the expression of each gene in IVIg/GM-MØ relative to its expression in GM-MØ. (**C**) Immunoblot analysis of p-JNK (left panel) and p-STAT5 (right panel) in freshly isolated human monocytes untreated (-) or treated with IVIg before stimulation with GM-CSF for 15 min (for p-JNK) or 2 h (for p-STAT5). Protein levels of vinculin were determined in parallel to control for protein loading. Three independent experiments were performed whose densitometric analyses are shown. $*p < 0.05$, $**p < 0.01$, $***p < 0.001$.

also lower in IVIg/M-MØ and IVIg/GM-MØ (Fig. 4B). The weaker LPS-initiated signaling seen in macrophages generated in the presence of IVIg correlated with a diminished TLR4 cell surface expression (Fig. 4C) and reduced *TLR4* mRNA levels (Fig. 4D) in both IVIg/M-MØ and IVIg/GM-MØ. Therefore, the presence of therapeutic levels of IVIg during macrophage differentiation imposes a strong reduction in the signaling pathways that drive LPS-induced cytokine expression.

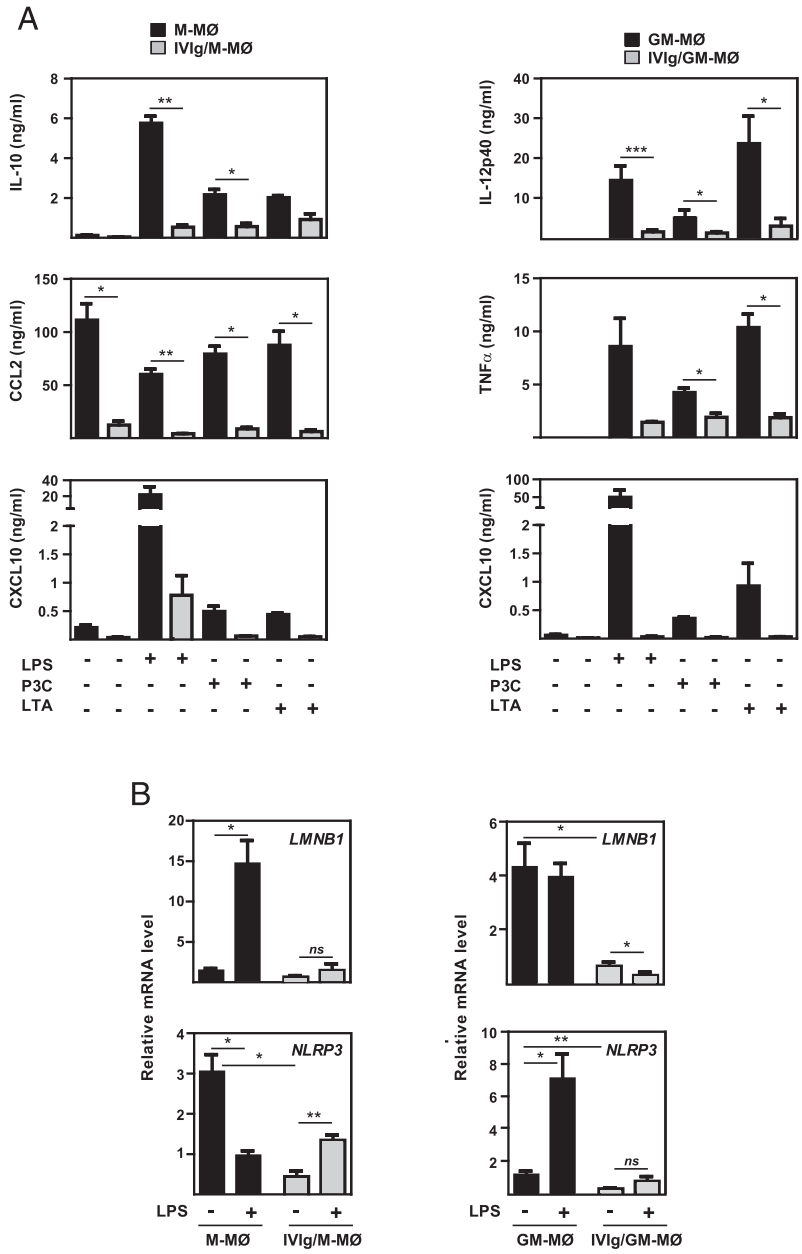

FIGURE 3. IVIg alters TLR responsiveness of M-MØ and GM-MØ. (**A**) Production of IL-10, CCL2, and CXCL10 in M-MØ and IVIg/M-MØ (left panels) or TNF-α, IL12p40, and CXCL10 in GM-MØ and IVIg/GM-MØ (right panels) that were either left untreated (-) or stimulated with 10 ng/ml LPS, 10 μg/ml Pam3CSK4, or 5 μg/ml LTA for 24 h, as determined by ELISA. Each determination was done in triplicate, and shown is the mean ± SEM of three independent experiments. (**B**) *NLRP3* and *LMNB1* mRNA expression levels in untreated (-) and LPS-treated (10 ng/ml, 4 h) M-MØ, IVIg/M-MØ, GM-MØ, and IVIg/GM-MØ, as determined by qRT-PCR. Results are expressed as relative mRNA levels (relative to *TBP* RNA levels). Mean ± SEM of three independent experiments is shown. $*p < 0.05$, $**p < 0.01$, $***p < 0.001$.

The fact that IVIg treatment leads to lower LPS-induced signaling and cytokine production is reminiscent of the endotoxin tolerance phenomenon (55). In fact, the acquisition of an LPS refractory state is compatible with the lower level of cell surface TLR4 and the weaker LPS-induced NF-κB activation seen in IVIg/M-MØ and IVIg/GM-MØ (Fig. 4A, 4C). To provide evidence for an IVIg-induced LPS refractory state in human macrophages, the expression and activation states of negative regulators of the LPS-initiated signaling pathway were assessed in IVIg/M-MØ and IVIg/GM-MØ. Compared with M-MØ, IVIg/M-MØ exhibited a higher expression of A20, an inhibitor of NF-κB activation (55) (Fig. 4E). Similarly, and compared with GM-MØ, IVIg/GM-MØ contained 1) higher levels of p-SHIP-1, which controls the PI3K cellular signaling pathway (56, 57); 2) considerably higher levels of A20, which inhibits NF-κB activation and contributes to limiting inflammation (58); and 3) higher levels of p-SHP-1, which negatively regulates TLR-mediated production of proinflammatory cytokines via inhibition of NF-κB and MAPK activation (59) (Fig. 4F). Therefore, macrophages generated in the presence of IVIg exhibit a number of features (diminished LPS-triggered intracellular signaling, reduced TLR4 expression, and higher p-SHIP-1, p-SHP-1, and A20 expression) that are compatible with IVIg promoting a state of cross-tolerance to LPS on differentiating monocytes.

IVIg treatment leads to a state of cross-tolerance to LPS in mice

Although IVIg exerts anti-inflammatory actions in mouse models of inflammatory disease (60, 61), its mechanisms of action differ between human and mouse, and results obtained with IVIg in mouse animal models of disease cannot be easily extrapolated (40). Despite this, we initially turned to the mouse system to determine the cell surface receptors implicated in the IVIg action and to assess the potential ability of IVIg to promote cross-tolerance to LPS. IVIg was found to modulate the phenotypic and functional profile of proinflammatory GM-BMDM (51, 62), as IVIg/GM-BMDM showed altered expression of polarization-specific genes (*Inhba, Clu, Emr1*) (51) (Fig. 5A) and produced

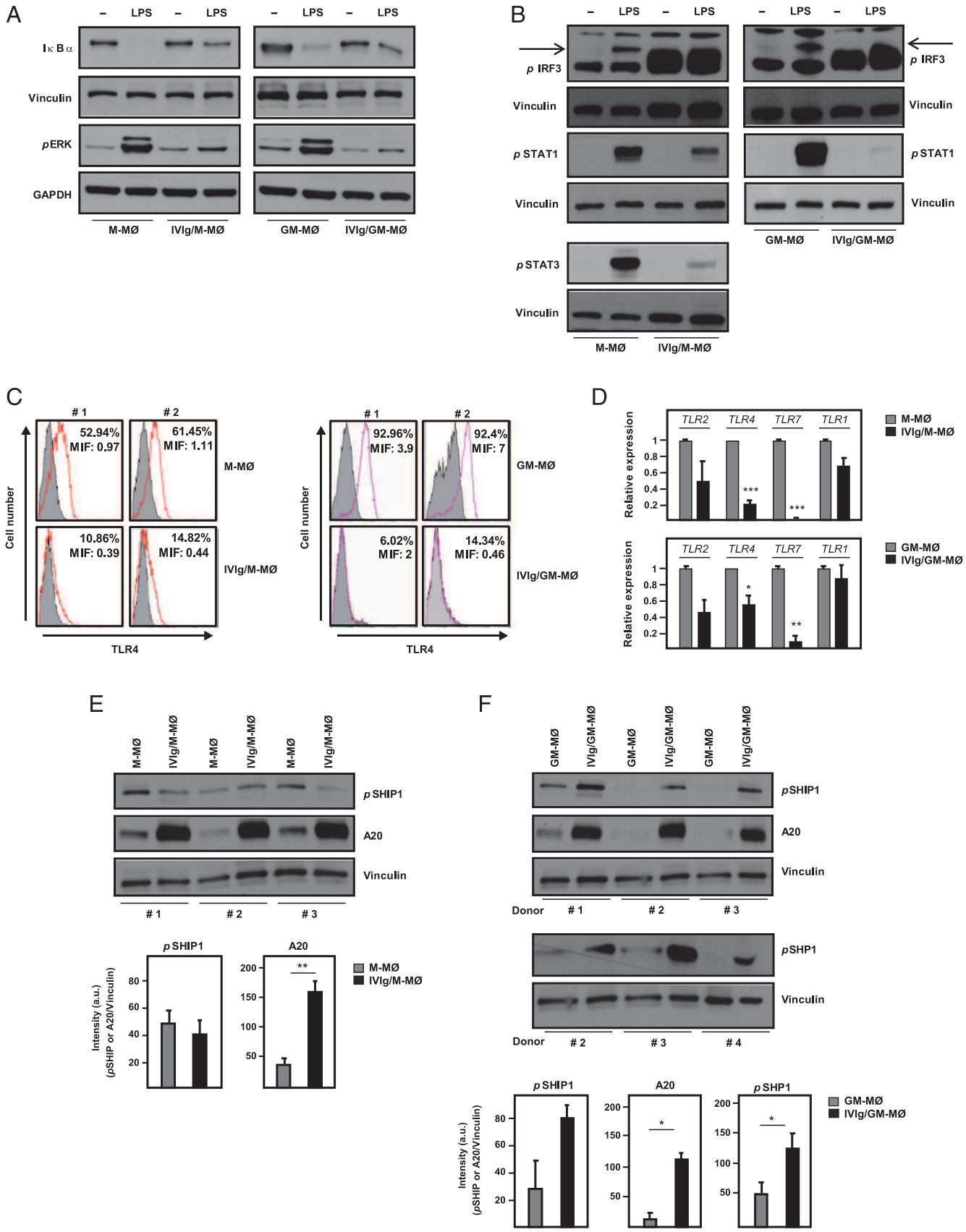

FIGURE 4. Human macrophage differentiation in the presence of IVIg impairs TLR4 signaling and enhances the expression of negative regulators of NF-κB signaling. (**A**) Immunoblot analysis of IκBα and p-ERK in M-MØ, IVIg/M-MØ (left panels), GM-MØ, and IVIg/GM-MØ (right panels) that were either untreated (-) or treated with 10 ng/ml LPS for 15 min. (**B**) Immunoblot analysis of p-IRF3, p-STAT3, and p-STAT1 in M-MØ, IVIg/M-MØ (left panels), GM-MØ, and IVIg/GM-MØ (right panels) that were either untreated (-) or treated with 10 ng/ml LPS for 2 h. Protein levels of GAPDH, STAT1, and vinculin were determined in parallel to control for protein loading. In each case, three independent experiments were performed, and one experiment is shown. (**C**) Cell surface expression of TLR4 (empty histograms) in M-MØ and IVIg/M-MØ (left panels) or GM-MØ and *(Figure legend continues)*

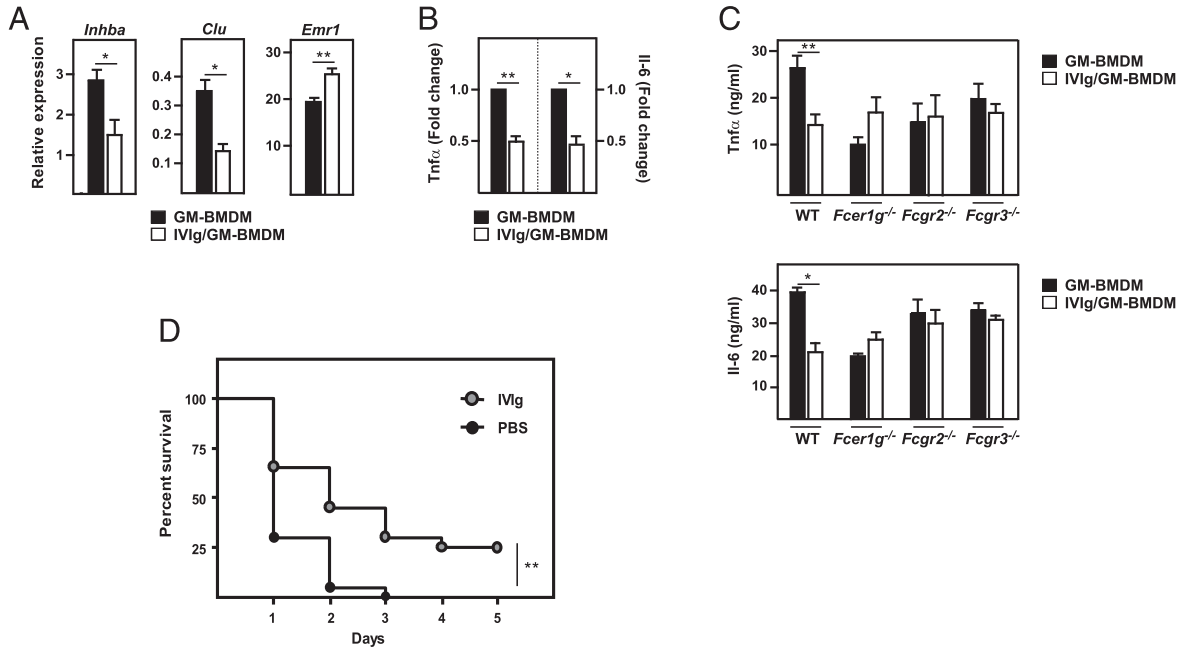

FIGURE 5. Effects of IVIg on mouse GM-BMDM differentiation and LPS responses in vivo. (**A**) Expression of polarization-associated genes in GM-BMDM and IVIg/GM-BMDM generated from C57BL/6 bone marrow, as determined by qRT-PCR. Relative expression indicates the expression of each marker relative to the expression of the *Tbp* gene. Shown is the mean ± SEM of three independent experiments. (**B**) LPS-induced release of Tnf-α and Il-6 from GM-BMDM and IVIg/GM-BMDM. Each determination was done in triplicate, and shown is the mean ± SEM of three independent experiments. (**C**) LPS-induced release of Tnf-α and Il-6 from GM-BMDM and IVIg/GM-BMDM generated from the bone marrow of wild type (WT), *Fcer1g*$^{-/-}$, *Fcgr2*$^{-/-}$, and *Fcgr3*$^{-/-}$ mice. Each determination was done in triplicate, and shown is the mean ± SEM of four independent experiments. (**D**) Survival of C57BL/6 mice pretreated with PBS or IVIg (40 μg/mouse) and then challenged 26 h later with a lethal dose of LPS (9 mg/kg). *$p < 0.05$, **$p < 0.01$.

lower levels of LPS-induced Tnf-α and Il-6 (Fig. 5B). The latter effects were dependent on Fcγ receptors, as deletion of *Fcgr3*, *Fcgr2*, or *Fcer1g* prevented the IVIg-mediated decrease in the LPS-induced secretion of Tnf-α and Il-6 (Fig. 5C), thus demonstrating that functional activating Fcγ receptors are required for the IVIg inhibition on the acquisition of proinflammatory functions in mouse macrophages. Because IVIg exerts a similar functional effect on human and mouse macrophages in vitro, the ability of IVIg to promote cross-tolerance to LPS was assessed using the endotoxin shock mouse model. To that end, mice were i.p. treated with IVIg (400 μl, 100 mg/ml) 26 h before receiving an i.p. injection of a lethal dose of LPS. IVIg-treated mice exhibited significantly higher survival than mice that had been pretreated with PBS (Fig. 5D). Therefore, in agreement with its ability to limit macrophage responses to LPS in vitro, IVIg is capable of inducing a state of endotoxin tolerance in mice.

IVIg infusion enhances inflammatory cytokine levels in peripheral blood

To evaluate whether IVIg can also promote tolerance to LPS in vivo in patients receiving IVIg therapy, we initially determined the ability of IVIg to alter the production of inflammatory cytokines in vivo. Cytokine determination on the peripheral blood of IVIg-treated patients with either immunodeficiency/inflammatory pathologic conditions (in which IVIg infusion increases IgG concentration from 11 to 19 mg/ml) (Fig. 6A, left panel) or recurrent reproductive failure of inflammatory causes (in which IVIg increases IgG concentration from 9.4 to 14.6 mg/ml) revealed a significant increase of IL-6, CCL2, and activin A 5 h after IVIg infusion (Fig. 6A, right panel). In vitro assessment of monocyte responses to IVIg (10 mg/ml) showed that IVIg is also capable of increasing the production of activin A, CCL2, and IL-6 from CD14^{+} monocytes from healthy donors (Fig. 6B). Therefore, infusion of IVIg results in enhanced levels of activin A, CCL2, and IL-6 in peripheral blood. Because the production of these cytokines by monocytes also increased after IVIg treatment in vitro, these results are compatible with IVIg promoting tolerance toward other stimuli in vivo.

IVIg infusion promotes monocytes to acquire tolerance toward inflammatory stimuli

The ability of IVIg to induce tolerance in vivo was then evaluated through the analysis of blood samples obtained from IVIg-treated patients. In the first set of experiments, CD14^{+} and CD14^{-} cells

IVIg/GM-MØ (right panels) from two independent donors, as determined by flow cytometry. Background fluorescence was determined using an isotype-matched Ab (gray histograms). The percentages of marker-positive cells and mean intensity of fluorescence (MIF) are indicated in each case. (**D**) Relative expression of the indicated TLR genes in M-MØ and IVIg/M-MØ (upper panel) and GM-MØ and GM-MØ plus IVIg (lower panel), as determined by qRT-PCR. Results are expressed as relative expression (relative to *TBP* mRNA levels) and refer to the expression level of each gene in GM-MØ. Shown is the mean ± SEM of three independent experiments. (**E**) Immunoblot analysis of p-SHIP-1 and A20 on M-MØ and IVIg/M-MØ derived from three independent monocyte preparations. Protein levels of vinculin were determined in parallel to control for protein loading. Densitometric quantification of the immunoblots relative to vinculin levels is shown in the lower panel. (**F**) Immunoblot analysis of p-SHIP-1, A20, and p-SHP-1 on GM-MØ and IVIg/GM-MØ derived from three independent monocyte preparations. Protein levels of vinculin were determined in parallel to control for protein loading. Densitometric quantification of the immunoblots relative to vinculin levels is shown in the lower panel. *$p < 0.05$, **$p < 0.01$, ***$p < 0.001$.

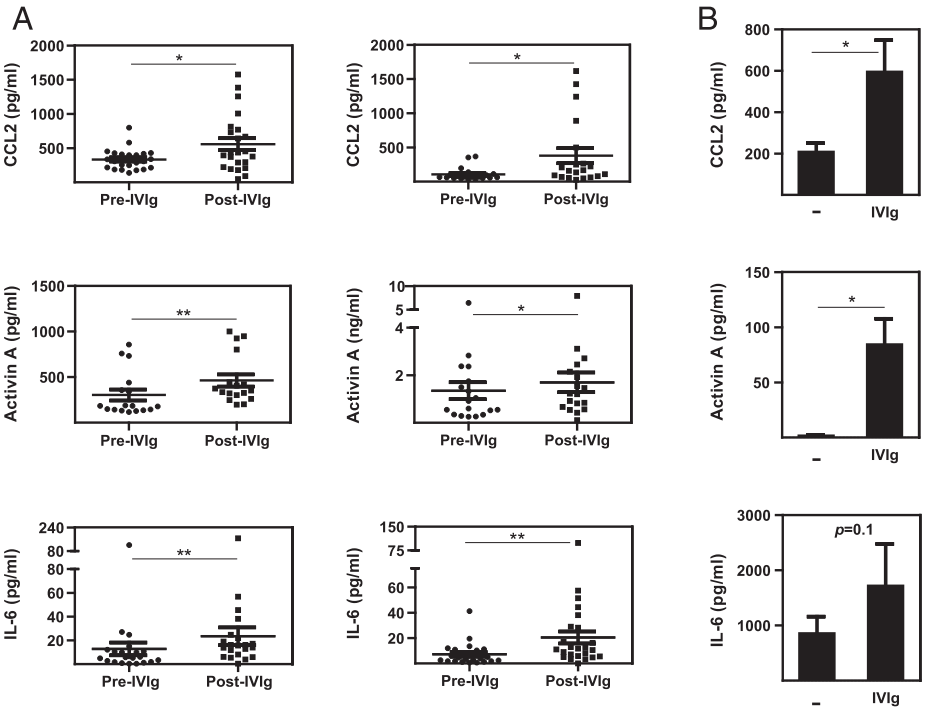

FIGURE 6. IVIg infusion leads to increased levels of inflammatory cytokines in peripheral blood in vivo and in monocytes in vitro. (**A**) Activin A, CCL2, and IL-6 levels in plasma or serum of patients with common variable immunodeficiency and other inflammatory disorders (n = 18, left panels) or recurrent reproductive failure of inflammatory cause (n = 18, right panels), both before (pre-IVIg) and 5 h after IVIg infusion (post-IVIg). Each determination was performed in triplicate, and shown is the mean ± SEM. (**B**) Activin A, CCL2, and IL-6 levels produced by $CD14^+$ monocytes from healthy subjects and either untreated (-) or exposed to IVIg (10 mg/ml) for 5 h. Eight independent experiments were performed, and shown is the mean ± SEM. $*p < 0.05$, $**p < 0.01$.

were isolated from the peripheral blood of patients both before and after IVIg infusion, and the production of LPS-induced TNF-α and IL-6 was determined in vitro. As shown in Fig. 7A and 7B, both cytokines were exclusively produced by $CD14^+$ monocytes, and more importantly, the LPS-upregulated levels of both cytokines were significantly lower in $CD14^+$ monocytes isolated from post-IVIg blood samples. Therefore, IVIg infusion renders monocytes less responsive toward a later stimulation by LPS. Next, and to confirm the induction of IVIg-mediated tolerance to LPS in whole blood, samples of peripheral blood were collected from patients both before and after IVIg infusion, maintained at room temperature for 12 h, and later challenged with either PBS or

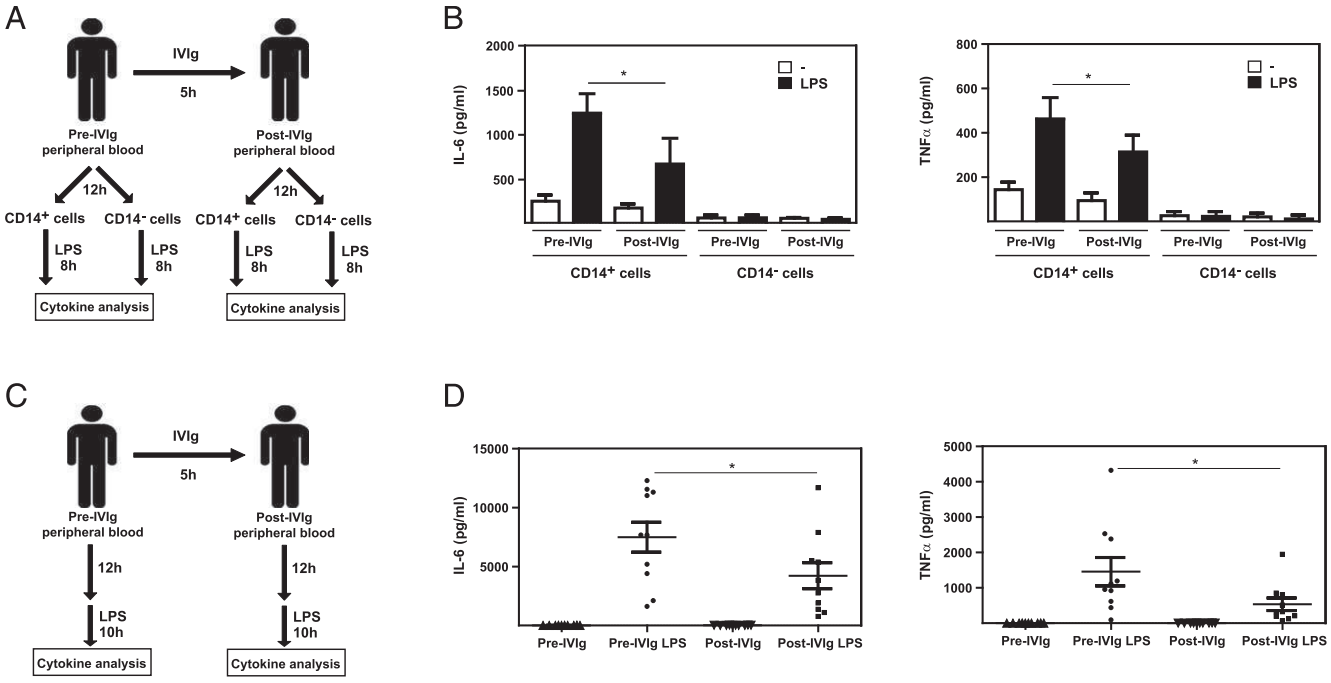

FIGURE 7. In vivo IVIg infusion promotes tolerance toward LPS. (**A**) Schematic representation of the experimental procedure used to assess LPS responsiveness of $CD14^+$ and $CD14^-$ cells isolated from the peripheral blood of IVIg-treated patients. (**B**) Whole blood was collected from IVIg-treated patients both before (pre-IVIg) and after receiving IVIg infusion (post-IVIg). After 12 h, $CD14^+$ and $CD14^-$ cells were isolated and treated with PBS (-) or LPS, and the levels of TNF-α and IL-6 were determined 8 h after stimulation. Each determination was performed in triplicate, and shown is the mean ± SEM of seven independent experiments. (**C**) Schematic representation of the experimental procedure used to assess IVIg-induced tolerance to LPS in the peripheral blood of IVIg-treated patients. (**D**) Whole blood was collected from IVIg-treated patients both before (pre-IVIg) and after receiving IVIg infusion (post-IVIg). After 12 h, blood was treated with PBS or LPS, and the levels of TNF-α and IL-6 were determined 10 h after stimulation. Each determination was performed in triplicate, and shown is the mean ± SEM of 10 independent experiments. $*p < 0.05$.

LPS (Fig. 7C). TNF-α and IL-6 were exclusively detected in LPS-treated blood samples, but significantly lower levels of both cytokines were found in the blood samples collected after IVIg infusion (Fig. 7D). Therefore, infusion of IVIg results in weaker proinflammatory cytokine response toward LPS in vivo, and this effect can be fully recapitulated with peripheral blood monocytes ex vivo (Fig. 7B). These results confirm that IVIg is capable of inducing a state of cross-tolerance to LPS in vivo and lead to the proposal that promotion of cross-tolerance toward other pathologic inflammatory stimuli underlies the net anti-inflammatory effect exerted by IVIg in vivo.

Discussion

The immunomodulatory action of IgG has widened the range of pathologic conditions for which IVIg therapy is either approved or has shown benefit (63, 64). Because of its beneficial actions on inflammatory pathologic conditions and its ability to limit tumor progression (44, 65, 66), we hypothesized that IVIg exerts its therapeutic action through modulation of the macrophage polarization state, whose deregulated control contributes to chronic inflammatory pathologic conditions, and found that IVIg shifts macrophage polarization at the functional and transcriptional levels (44). We now report that IVIg impairs the monocyte priming ability of M-CSF or GM-CSF through JNK activation and enhancement of activin A production (in the case of M-CSF) and also inhibits the GM-CSF–induced STAT5 activation. Besides, IVIg impairs the acquisition of the specific gene profiles and the TLR responses of proinflammatory and anti-inflammatory monocyte-derived macrophages. Importantly, the ability of IVIg to alter the LPS-induced macrophage cytokine profile correlates with the appearance of molecular parameters that limit TLR-initiated intracellular signaling and that characterize the state of endotoxin tolerance. In fact, we present evidence that IVIg promotes tolerance to LPS (cross-tolerance) in an endotoxin shock mouse model in vivo and that IVIg infusion results in weaker proinflammatory cytokine responses toward LPS in the peripheral blood of IVIg-treated patients.

Molecular analysis of the effects of IVIg has also led us to demonstrate that IVIg limits numerous intracellular signaling pathways in both human monocytes (GM-CSF–initiated STAT5 activation) and GM-MØ (LPS-triggered ERK, NF-κB, STAT1, and IRF3 activation). Blockade of intracellular signaling pathways is a common strategy for induction of tolerance. In the case of IVIg-treated human macrophages, the acquisition of the cross-tolerance state correlates with the appearance of molecular parameters that characterize desensitization in response to an inflammatory stimulus. Specifically, IVIg exposure results in lower TLR4 expression and higher levels of p-SHIP-1, p-SHP-1, and A20, all of which impair or inhibit LPS-triggered intracellular signaling. Therefore, IVIg shares with other tolerance-inducing agents the ability of increasing the expression of negative regulators of NF-κB signaling. Thus, A20 has been found to be partly responsible for the IVIg suppression of RANKL-induced osteoclastogenesis and TNF-α–induced bone resorption after engagement of Fcγ receptors (67). Therefore, similar to the case of LPS on human macrophages, IVIg might also induce a cross-tolerance state for RANKL and TNF-α, which share the NF-κB–activating activity with LPS.

The ability of IVIg to promote a tolerance state in macrophages can also explain its cell context–dependent effects. We previously showed that IVIg inhibits the proinflammatory functions of GM-MØ but enhances proinflammatory properties in M-MØ (44) and concluded that IVIg effects are cell type–dependent. However, NF-κB activation contributes to proinflammatory cytokine production in GM-MØ and IL-10 production in M-MØ. Considering that IVIg impairs NF-κB activation through the increase of negative regulators of NF-κB in both GM-MØ and M-MØ, this common molecular mechanism might underlie the opposite outcome of IVIg exposure in both types of macrophages: lower inflammatory cytokine production in GM-MØ and lower IL-10 production in M-MØ. Therefore, the opposite consequences of IVIg exposure to GM-MØ and M-MØ appear to be primarily a consequence of the distinct effector functions of both macrophage subtypes.

The capacity of IVIg to enhance the release of monocyte-derived cytokines, both in vitro and in vivo, clearly illustrates its monocyte-activating ability. The finding that activin A is one of the IVIg-induced cytokines has relevant implications and might also contribute to reconcile the pro- and anti-inflammatory actions of IVIg previously reported. Activin A is a member of the TGF-β family of factors (68) whose expression is high in inflammatory pathologic conditions (e.g., inflammatory bowel disease, rheumatoid arthritis, bacterial septicemia) and is induced with faster kinetics than other proinflammatory cytokines after LPS IV injection (69). Interestingly, activin A modulates inflammatory responses because it displays both proinflammatory and regulatory activities that resemble those exhibited by IVIg. Therefore, it is tempting to speculate that activin A critically contributes to the in vivo actions of IVIg. An additional implication of the IVIg-promoted increase of activin A relates to the function of activin A in promoting oocyte maturation, endometrial repair, decidualization, and maintaining pregnancy and to the fact that deregulation of the activin activities results in disorders of female reproduction and pregnancy (70). Previous reports indicate that low-dose IVIg overcome recurrent spontaneous abortions in women suffering from IgG subclass deficiency (71) and enhance clinical pregnancy and live birth rates in patients with recurrent reproductive failure of inflammatory cause (72). Therefore, the increase in activin A blood levels secondary to IVIg infusion might also contribute to the beneficial effects of IVIg on women with recurrent reproductive failure, a hypothesis that deserves further studies.

Numerous molecular and cellular mechanisms have been previously proposed to contribute to the IVIg immunoregulatory activity (31, 35, 37). The results reported in this article indicate that monocytes (and monocyte-derived macrophages) are involved in the effects of IVIg in vivo because IVIg infusion enhances the levels of monocyte-derived cytokines (e.g., activin A, CCL2, IL-6) in peripheral blood and alters the monocyte cytokine profile and macrophage differentiation capability in vitro. Therefore, IVIg targets monocytes (and monocyte-derived macrophages) and leads to the acquisition of a cross-tolerance state that underlies the apparent contradiction between its proinflammatory effects on monocytes and M-MØ in vitro and its immunosuppressive action in vivo (32, 41). According to this explanation, IVIg would shift monocytes/macrophages toward the acquisition of a proinflammatory profile, making IVIg-conditioned cells less sensitive to a subsequent exposure to TLR ligands. Consequently, IVIg-primed monocytes would be weakly responsive to further stimulation by any danger signals (e.g., TLR ligands) found after their entry into inflamed tissues. Therefore, monocyte exposure to IVIg would result in a lower level of macrophage activation within inflamed tissues and, consequently, would limit tissue damage (and pathologic conditions) triggered by an ongoing injury or an inflammation-provoking insult (danger signals or inflammatory stimuli). This hypothesis is supported by the ability of IVIg infusion to trigger an almost immediate increase in the level of inflammatory cytokines in peripheral blood, a result also reported by others (73, 74), and is compatible with the well-known therapeutic

benefits of IVIg in diseases like Kawasaki disease (75) and demyelinating polyneuropathy/Guillain–Barré syndrome (76), in which macrophages contribute to pathologic conditions.

Acknowledgments

We thank Dr. W.G. Kerr (State University of New York Upstate Medical University, Syracuse, NY) for providing SHIP-1 knockout mice.

Disclosures

The authors have no financial conflicts of interest.

References

1. Geissmann, F., M. G. Manz, S. Jung, M. H. Sieweke, M. Merad, and K. Ley. 2010. Development of monocytes, macrophages, and dendritic cells. *Science* 327: 656–661.
2. Fogg, D. K., C. Sibon, C. Miled, S. Jung, P. Aucouturier, D. R. Littman, A. Cumano, and F. Geissmann. 2006. A clonogenic bone marrow progenitor specific for macrophages and dendritic cells. *Science* 311: 83–87.
3. Chow, A., B. D. Brown, and M. Merad. 2011. Studying the mononuclear phagocyte system in the molecular age. *Nat. Rev. Immunol.* 11: 788–798.
4. Epelman, S., K. J. Lavine, and G. J. Randolph. 2014. Origin and functions of tissue macrophages. *Immunity* 41: 21–35.
5. Gomez Perdiguero, E., and F. Geissmann. 2013. Myb-independent macrophages: a family of cells that develops with their tissue of residence and is involved in its homeostasis. *Cold Spring Harb. Symp. Quant. Biol.* 78: 91–100.
6. Gordon, S., and P. R. Taylor. 2005. Monocyte and macrophage heterogeneity. *Nat. Rev. Immunol.* 5: 953–964.
7. Mosser, D. M., and J. P. Edwards. 2008. Exploring the full spectrum of macrophage activation. [Published erratum appears in 2010 *Nat. Rev. Immunol.* 10: 460.] *Nat. Rev. Immunol.* 8: 958–969.
8. Akagawa, K. S. 2002. Functional heterogeneity of colony-stimulating factor-induced human monocyte-derived macrophages. *Int. J. Hematol.* 76: 27–34.
9. Hamilton, J. A. 2008. Colony-stimulating factors in inflammation and autoimmunity. *Nat. Rev. Immunol.* 8: 533–544.
10. Fleetwood, A. J., T. Lawrence, J. A. Hamilton, and A. D. Cook. 2007. Granulocyte-macrophage colony-stimulating factor (CSF) and macrophage CSF-dependent macrophage phenotypes display differences in cytokine profiles and transcription factor activities: implications for CSF blockade in inflammation. *J. Immunol.* 178: 5245–5252.
11. González-Domínguez, É., Á. Domínguez-Soto, C. Nieto, J. L. Flores-Sevilla, M. Pacheco-Blanco, V. Campos-Peña, M. A. Meraz-Ríos, M. A. Vega, A. L. Corbí, and C. Sánchez-Torres. 2016. Atypical activin A and IL-10 production impairs human CD16+ monocyte differentiation into anti-inflammatory macrophages. *J. Immunol.* 196: 1327–1337.
12. Sierra-Filardi, E., A. Puig-Kröger, F. J. Blanco, C. Nieto, R. Bragado, M. I. Palomero, C. Bernabéu, M. A. Vega, and A. L. Corbí. 2011. Activin A skews macrophage polarization by promoting a proinflammatory phenotype and inhibiting the acquisition of anti-inflammatory macrophage markers. *Blood* 117: 5092–5101.
13. Verreck, F. A., T. de Boer, D. M. Langenberg, M. A. Hoeve, M. Kramer, E. Vaisberg, R. Kastelein, A. Kolk, R. de Waal-Malefyt, and T. H. Ottenhoff. 2004. Human IL-23-producing type 1 macrophages promote but IL-10-producing type 2 macrophages subvert immunity to (myco)bacteria. *Proc. Natl. Acad. Sci. USA* 101: 4560–4565.
14. Cuevas, V. D., L. Anta, R. Samaniego, E. Orta-Zavalza, J. Vladimir de la Rosa, G. Baujat, Á. Domínguez-Soto, P. Sánchez-Mateos, M. M. Escribese, A. Castrillo, et al. 2017. MAFB determines human macrophage anti-inflammatory polarization: relevance for the pathogenic mechanisms operating in multicentric carpotarsal osteolysis. *J. Immunol.* 198: 2070–2081.
15. Allavena, P., A. Sica, C. Garlanda, and A. Mantovani. 2008. The Yin-Yang of tumor-associated macrophages in neoplastic progression and immune surveillance. *Immunol. Rev.* 222: 155–161.
16. Murray, P. J., J. E. Allen, S. K. Biswas, E. A. Fisher, D. W. Gilroy, S. Goerdt, S. Gordon, J. A. Hamilton, L. B. Ivashkiv, T. Lawrence, et al. 2014. Macrophage activation and polarization: nomenclature and experimental guidelines. *Immunity* 41: 14–20.
17. Soler Palacios, B., L. Estrada-Capetillo, E. Izquierdo, G. Criado, C. Nieto, C. Municio, I. González-Alvaro, P. Sánchez-Mateos, J. L. Pablos, A. L. Corbí, and A. Puig-Kröger. 2015. Macrophages from the synovium of active rheumatoid arthritis exhibit an activin A-dependent pro-inflammatory profile. *J. Pathol.* 235: 515–526.
18. Ginhoux, F., and S. Jung. 2014. Monocytes and macrophages: developmental pathways and tissue homeostasis. *Nat. Rev. Immunol.* 14: 392–404.
19. Jantsch, J., K. J. Binger, D. N. Müller, and J. Titze. 2014. Macrophages in homeostatic immune function. *Front. Physiol.* 5: 146.
20. Wynn, T. A., A. Chawla, and J. W. Pollard. 2013. Macrophage biology in development, homeostasis and disease. *Nature* 496: 445–455.
21. Bosco, M. C., M. Puppo, F. Blengio, T. Fraone, P. Cappello, M. Giovarelli, and L. Varesio. 2008. Monocytes and dendritic cells in a hypoxic environment: spotlights on chemotaxis and migration. *Immunobiology* 213: 733–749.
22. Lynn, W. A., and J. Cohen. 1995. Management of septic shock. *J. Infect.* 30: 207–212.
23. Lumeng, C. N., J. L. Bodzin, and A. R. Saltiel. 2007. Obesity induces a phenotypic switch in adipose tissue macrophage polarization. *J. Clin. Invest.* 117: 175–184.
24. Gordon, S., and F. O. Martinez. 2010. Alternative activation of macrophages: mechanism and functions. *Immunity* 32: 593–604.
25. Ruffell, B., N. I. Affara, and L. M. Coussens. 2012. Differential macrophage programming in the tumor microenvironment. *Trends Immunol.* 33: 119–126.
26. Leuschner, F., P. Dutta, R. Gorbatov, T. I. Novobrantseva, J. S. Donahoe, G. Courties, K. M. Lee, J. I. Kim, J. F. Markmann, B. Marinelli, et al. 2011. Therapeutic siRNA silencing in inflammatory monocytes in mice. *Nat. Biotechnol.* 29: 1005–1010.
27. Shechter, R., O. Miller, G. Yovel, N. Rosenzweig, A. London, J. Ruckh, K. W. Kim, E. Klein, V. Kalchenko, P. Bendel, et al. 2013. Recruitment of beneficial M2 macrophages to injured spinal cord is orchestrated by remote brain choroid plexus. *Immunity* 38: 555–569.
28. Shechter, R., and M. Schwartz. 2013. Harnessing monocyte-derived macrophages to control central nervous system pathologies: no longer 'if' but 'how'. *J. Pathol.* 229: 332–346.
29. Dou, H., C. J. Destache, J. R. Morehead, R. L. Mosley, M. D. Boska, J. Kingsley, S. Gorantla, L. Poluektova, J. A. Nelson, M. Chaubal, et al. 2006. Development of a macrophage-based nanoparticle platform for antiretroviral drug delivery. *Blood* 108: 2827–2835.
30. Almouazen, E., S. Bourgeois, A. Boussaïd, P. Valot, C. Malleval, H. Fessi, S. Nataf, and S. Briançon. 2012. Development of a nanoparticle-based system for the delivery of retinoic acid into macrophages. *Int. J. Pharm.* 430: 207–215.
31. Kazatchkine, M. D., and S. V. Kaveri. 2001. Immunomodulation of autoimmune and inflammatory diseases with intravenous immune globulin. *N. Engl. J. Med.* 345: 747–755.
32. Gelfand, E. W. 2012. Intravenous immune globulin in autoimmune and inflammatory diseases. *N. Engl. J. Med.* 367: 2015–2025.
33. Dwyer, J. M. 1996. Immunoglobulins in autoimmunity: history and mechanisms of action. *Clin. Exp. Rheumatol.* 14(Suppl. 15): S3–S7.
34. Clynes, R. 2007. IVIG therapy: interfering with interferon-gamma. *Immunity* 26: 4–6.
35. Durandy, A., S. V. Kaveri, T. W. Kuijpers, M. Basta, S. Miescher, J. V. Ravetch, and R. Rieben. 2009. Intravenous immunoglobulins–understanding properties and mechanisms. *Clin. Exp. Immunol.* 158(Suppl. 1): 2–13.
36. Schwab, I., and F. Nimmerjahn. 2013. Intravenous immunoglobulin therapy: how does IgG modulate the immune system? *Nat. Rev. Immunol.* 13: 176–189.
37. Tha-In, T., J. Bayry, H. J. Metselaar, S. V. Kaveri, and J. Kwekkeboom. 2008. Modulation of the cellular immune system by intravenous immunoglobulin. *Trends Immunol.* 29: 608–615.
38. Ballow, M. 2011. The IgG molecule as a biological immune response modifier: mechanisms of action of intravenous immune serum globulin in autoimmune and inflammatory disorders. *J. Allergy Clin. Immunol.* 127: 315–323; quiz 324–325. 10.1016/j.jaci.2010.10.030
39. Negi, V. S., S. Elluru, S. Sibéril, S. Graff-Dubois, L. Mouthon, M. D. Kazatchkine, S. Lacroix-Desmazes, J. Bayry, and S. V. Kaveri. 2007. Intravenous immunoglobulin: an update on the clinical use and mechanisms of action. *J. Clin. Immunol.* 27: 233–245.
40. Tjon, A. S., R. van Gent, T. B. Geijtenbeek, and J. Kwekkeboom. 2015. Differences in anti-inflammatory actions of intravenous immunoglobulin between mice and men: more than meets the eye. *Front. Immunol.* 6: 197.
41. Corbí, A. L., S. Sánchez-Ramón, and A. Domínguez-Soto. 2016. The potential of intravenous immunoglobulins for cancer therapy: a road that is worth taking? *Immunotherapy* 8: 601–612.
42. Ben Mkaddem, S., M. Aloulou, M. Benhamou, and R. C. Monteiro. 2014. Role of FcγRIIIA (CD16) in IVIg-mediated anti-inflammatory function. *J. Clin. Immunol.* 34(Suppl. 1): S46–S50.
43. Aloulou, M., S. Ben Mkaddem, M. Biarnes-Pelicot, T. Boussetta, H. Souchet, E. Rossato, M. Benhamou, B. Crestani, Z. Zhu, U. Blank, et al. 2012. IgG1 and IVIg induce inhibitory ITAM signaling through FcγRIII controlling inflammatory responses. *Blood* 119: 3084–3096.
44. Domínguez-Soto, A., M. de las Casas-Engel, R. Bragado, J. Medina-Echeverz, L. Aragoneses-Fenoll, E. Martín-Gayo, N. van Rooijen, P. Berraondo, M. L. Toribio, M. A. Moro, et al. 2014. Intravenous immunoglobulin promotes antitumor responses by modulating macrophage polarization. *J. Immunol.* 193: 5181–5189.
45. Dominguez-Soto, A., L. Aragoneses-Fenoll, F. Gomez-Aguado, M. T. Corcuera, J. Claria, C. Garcia-Monzon, M. Bustos, and A. L. Corbi. 2009. The pathogen receptor liver and lymph node sinusoidal endotelial cell C-type lectin is expressed in human Kupffer cells and regulated by PU.1. *Hepatology* 49: 287–296.
46. Domínguez-Soto, A., A. Puig-Kröger, M. A. Vega, and A. L. Corbí. 2005. PU.1 regulates the tissue-specific expression of dendritic cell-specific intercellular adhesion molecule (ICAM)-3-grabbing nonintegrin. *J. Biol. Chem.* 280: 33123–33131.
47. Auffray, C., M. H. Sieweke, and F. Geissmann. 2009. Blood monocytes: development, heterogeneity, and relationship with dendritic cells. *Annu. Rev. Immunol.* 27: 669–692.
48. Kaveri, S. V., M. S. Maddur, P. Hegde, S. Lacroix-Desmazes, and J. Bayry. 2011. Intravenous immunoglobulins in immunodeficiencies: more than mere replacement therapy. *Clin. Exp. Immunol.* 164(Suppl. 2): 2–5.
49. Koleba, T., and M. H. Ensom. 2006. Pharmacokinetics of intravenous immunoglobulin: a systematic review. *Pharmacotherapy* 26: 813–827.
50. Sigman, K., F. Ghibu, W. Sommerville, B. J. Toledano, Y. Bastein, L. Cameron, Q. A. Hamid, and B. Mazer. 1998. Intravenous immunoglobulin inhibits IgE production in human B lymphocytes. *J. Allergy Clin. Immunol.* 102: 421–427.

51. Lacey, D. C., A. Achuthan, A. J. Fleetwood, H. Dinh, J. Roiniotis, G. M. Scholz, M. W. Chang, S. K. Beckman, A. D. Cook, and J. A. Hamilton. 2012. Defining GM-CSF- and macrophage-CSF-dependent macrophage responses by in vitro models. *J. Immunol.* 188: 5752–5765.
52. Han, M. S., D. Y. Jung, C. Morel, S. A. Lakhani, J. K. Kim, R. A. Flavell, and R. J. Davis. 2013. JNK expression by macrophages promotes obesity-induced insulin resistance and inflammation. *Science* 339: 218–222.
53. Tanahashi, H., K. Kito, T. Ito, and K. Yoshioka. 2010. MafB protein stability is regulated by the JNK and ubiquitin-proteasome pathways. *Arch. Biochem. Biophys.* 494: 94–100.
54. Wicks, I. P., and A. W. Roberts. 2016. Targeting GM-CSF in inflammatory diseases. *Nat. Rev. Rheumatol.* 12: 37–48.
55. Biswas, S. K., and E. Lopez-Collazo. 2009. Endotoxin tolerance: new mechanisms, molecules and clinical significance. *Trends Immunol.* 30: 475–487.
56. Beutler, B. 2004. SHIP, TGF-beta, and endotoxin tolerance. *Immunity* 21: 134–135.
57. Sly, L. M., M. J. Rauh, J. Kalesnikoff, C. H. Song, and G. Krystal. 2004. LPS-induced upregulation of SHIP is essential for endotoxin tolerance. *Immunity* 21: 227–239.
58. Boone, D. L., E. E. Turer, E. G. Lee, R. C. Ahmad, M. T. Wheeler, C. Tsui, P. Hurley, M. Chien, S. Chai, O. Hitotsumatsu, et al. 2004. The ubiquitin-modifying enzyme A20 is required for termination of Toll-like receptor responses. [Published erratum appears in 2005 *Nat. Immunol.* 6: 114.] *Nat. Immunol.* 5: 1052–1060.
59. An, H., J. Hou, J. Zhou, W. Zhao, H. Xu, Y. Zheng, Y. Yu, S. Liu, and X. Cao. 2008. Phosphatase SHP-1 promotes TLR- and RIG-I-activated production of type I interferon by inhibiting the kinase IRAK1. *Nat. Immunol.* 9: 542–550.
60. Anthony, R. M., T. Kobayashi, F. Wermeling, and J. V. Ravetch. 2011. Intravenous gammaglobulin suppresses inflammation through a novel T(H)2 pathway. *Nature* 475: 110–113.
61. Campbell, I. K., S. Miescher, D. R. Branch, P. J. Mott, A. H. Lazarus, D. Han, E. Maraskovsky, A. W. Zuercher, A. Neschadim, D. Leontyev, et al. 2014. Therapeutic effect of IVIG on inflammatory arthritis in mice is dependent on the Fc portion and independent of sialylation or basophils. *J. Immunol.* 192: 5031–5038.
62. Fleetwood, A. J., H. Dinh, A. D. Cook, P. J. Hertzog, and J. A. Hamilton. 2009. GM-CSF- and M-CSF-dependent macrophage phenotypes display differential dependence on type I interferon signaling. *J. Leukoc. Biol.* 86: 411–421.
63. Nimmerjahn, F., and J. V. Ravetch. 2008. Anti-inflammatory actions of intravenous immunoglobulin. *Annu. Rev. Immunol.* 26: 513–533.
64. Nimmerjahn, F., and J. V. Ravetch. 2007. Fc-receptors as regulators of immunity. *Adv. Immunol.* 96: 179–204.
65. Fishman, P., S. Bar-Yehuda, and Y. Shoenfeld. 2002. IVIg to prevent tumor metastases (Review). *Int. J. Oncol.* 21: 875–880.
66. Sapir, T., and Y. Shoenfeld. 2005. Uncovering the hidden potential of intravenous immunoglobulin as an anticancer therapy. *Clin. Rev. Allergy Immunol.* 29: 307–310.
67. Lee, M. J., E. Lim, S. Mun, S. Bae, K. Murata, L. B. Ivashkiv, and K. H. Park-Min. 2016. Intravenous immunoglobulin (IVIG) attenuates TNF-induced pathologic bone resorption and suppresses osteoclastogenesis by inducing A20 expression. *J. Cell. Physiol.* 231: 449–458.
68. Xia, Y., and A. L. Schneyer. 2009. The biology of activin: recent advances in structure, regulation and function. *J. Endocrinol.* 202: 1–12.
69. Sozzani, S., and T. Musso. 2011. The yin and yang of activin A. *Blood* 117: 5013–5015.
70. Florio, P., M. Gabbanini, L. E. Borges, L. Bonaccorsi, S. Pinzauti, F. M. Reis, P. Boy Torres, G. Rago, P. Litta, and F. Petraglia. 2010. Activins and related proteins in the establishment of pregnancy. *Reprod. Sci.* 17: 320–330.
71. Manfredi, G., L. Dell'Aera, and R. Liguori. 2015. Overcoming recurrent spontaneous abortions in women suffering from IgG subclass deficiency: high efficiency of low dose intravenous immunoglobulins treatment. *Eur. Ann. Allergy Clin. Immunol.* 47: 91–94.
72. Ramos-Medina, R., A. García-Segovia, J. Gil, J. Carbone, A. Aguarón de la Cruz, A. Seyfferth, B. Alonso, J. Alonso, J. A. León, D. Alecsandru, et al. 2014. Experience in IVIg therapy for selected women with recurrent reproductive failure and NK cell expansion. *Am. J. Reprod. Immunol.* 71: 458–466.
73. Loubaki, L., D. Chabot, and R. Bazin. 2015. Involvement of the TNF-α/TGF-β/IDO axis in IVIg-induced immune tolerance. *Cytokine* 71: 181–187.
74. Ibanez, C., P. Sune, A. Fierro, S. Rodriguez, M. Lopez, A. Alvarez, J. De Gracia, and J. B. Montoro. 2005. Modulating effects of intravenous immunoglobulins on serum cytokine levels in patients with primary hypogammaglobulinemia. *BioDrugs* 19: 59–65.
75. Leung, D. Y. 1989. The immunologic effects of IVIG in Kawasaki disease. *Int. Rev. Immunol.* 5: 197–202.
76. Dace, D. S., A. A. Khan, J. L. Stark, J. Kelly, A. H. Cross, and R. S. Apte. 2009. Interleukin-10 overexpression promotes Fas-ligand-dependent chronic macrophage-mediated demyelinating polyneuropathy. *PLoS One* 4: e7121.

frontiers in Immunology

REVIEW
published: 26 April 2018
doi: 10.3389/fimmu.2018.00804

Flexible Signaling of Myeloid C-Type Lectin Receptors in Immunity and Inflammation

Carlos del Fresno[1], Salvador Iborra[1,2], Paula Saz-Leal[1], María Martínez-López[1] and David Sancho[1]**

[1] *Immunobiology Laboratory, Centro Nacional de Investigaciones Cardiovasculares Carlos III (CNIC), Madrid, Spain,* [2] *Department of Immunology, School of Medicine, Universidad Complutense de Madrid, 12 de Octubre Health Research Institute (imas12), Madrid, Spain*

Myeloid C-type lectin receptors (CLRs) are important sensors of self and non-self that work in concert with other pattern recognition receptors (PRRs). CLRs have been previously classified based on their signaling motifs as activating or inhibitory receptors. However, specific features of the ligand binding process may result in distinct signaling through a single motif, resulting in the triggering of non-canonical pathways. In addition, CLR ligands are frequently exposed in complex structures that simultaneously bind different CLRs and other PRRs, which lead to integration of heterologous signaling among diverse receptors. Herein, we will review how sensing by myeloid CLRs and crosstalk with heterologous receptors is modulated by many factors affecting their signaling and resulting in differential outcomes for immunity and inflammation. Finding common features among those flexible responses initiated by diverse CLR-ligand partners will help to harness CLR function in immunity and inflammation.

Keywords: lectin receptors, signaling, monocytes, macrophages, dendritic cells, innate immunity, inflammation

OPEN ACCESS

Edited by:
Roland Lang, Universitätsklinikum Erlangen, Germany

Reviewed by:
Michael Rory Daws, University of Oslo, Norway
Marit Inngjerdingen, Oslo University Hospital, Norway
Yvette Van Kooyk, VU University Amsterdam, Netherlands

****Correspondence:***
Carlos del Fresno
carlos.delfresno@cnic.es;
David Sancho
dsancho@cnic.es

Specialty section:
This article was submitted to Molecular Innate Immunity, a section of the journal Frontiers in Immunology

Received: *19 December 2017*
Accepted: *03 April 2018*
Published: *26 April 2018*

Citation:
del Fresno C, Iborra S, Saz-Leal P, Martínez-López M and Sancho D (2018) Flexible Signaling of Myeloid C-Type Lectin Receptors in Immunity and Inflammation. Front. Immunol. 9:804. doi: 10.3389/fimmu.2018.00804

DIVERSITY OF SIGNALING MODULES IN MYELOID C-TYPE LECTIN RECEPTORS (CLRs)

The expression of diverse pattern recognition receptors (PRRs), including differential expression of CLRs, provides different subsets of immune cells with a repertoire to interpret and respond distinctly to the information coming from the environment. Myeloid cells are central for initiation and regulation of innate and adaptive immunity or tolerance and the CLR repertoire essentially contributes to myeloid cell function. We previously proposed a classification of myeloid CLRs based on their intracellular signaling motifs (1). While signaling motifs allow to predict effector responses following sensing by CLRs, this canonical response is subjected to modulation by the physical nature, affinity, and avidity of the ligand (2). Based on their intracellular signaling motifs, myeloid CLRs can be classified into the following broad categories (**Figure 1**): immunoreceptor tyrosine-based activating motif (ITAM)-coupled CLRs, hemi-ITAM-(hemITAM)-bearing CLRs, immunoreceptor tyrosine-based inhibitory motif (ITIM)-containing CLRs, and a group of CLRs lacking typical signaling motifs (1, 3, 4).

Immunoreceptor tyrosine-based activating motif-coupled CLRs have a classical ITAM motifs in their intracellular tail, consisting of YXXL tandem repeats, or can interact with ITAM-containing adaptor proteins, as Fc receptor γ (FcRγ) chain or DNAX-activation protein 12 (DAP12) (5). The majority of them, including Dectin-2 (*CLEC6A* in human, *Clec4n* in the mouse), Mincle (*CLEC4E*), MCL (*CLEC4D*), BDCA-2 (human *CLEC4C*), DCAR (mouse *Clec4b1*), DCAR1 (mouse *Clec4b2*), and mannose receptor (MR) (*MRC1*, CD206) utilize the FcRγ chain adaptor, while MDL-1

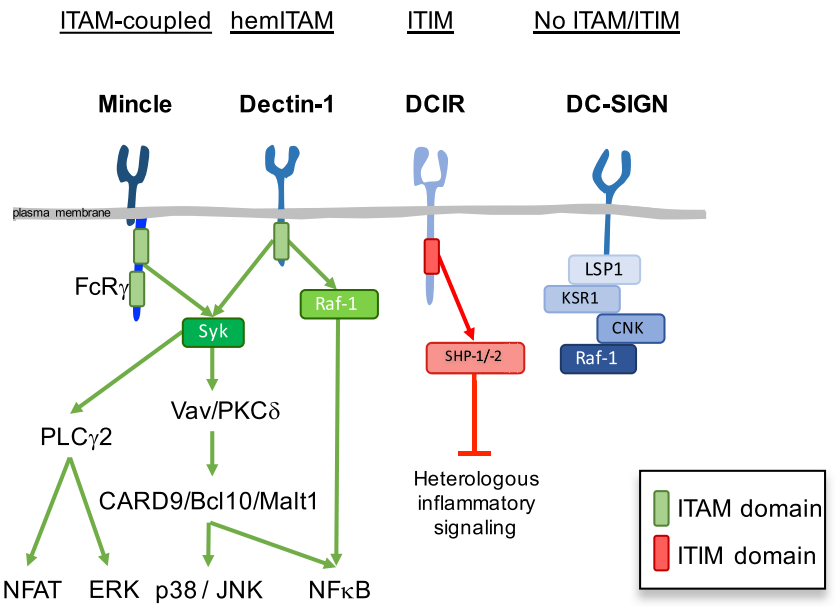

FIGURE 1 | Canonical signaling modules in myeloid C-type lectin receptors (CLRs). Based on canonical intracellular signaling motifs, myeloid CLRs can be classified into immunoreceptor tyrosine-based activating motif (ITAM)-coupled CLRs, hemi-ITAM-(hemITAM)-bearing CLRs, immunoreceptor tyrosine-based inhibitory motif (ITIM)-containing CLRs, and a group of CLRs lacking typical signaling motifs. Mincle, Dectin-1, DCIR, DC-SIGN, and their corresponding canonical signaling pathways and adaptors are depicted as prototypical examples of each category.

(*CLEC5A*) interacts with DAP12 (6–12). Hemi-ITAM-bearing CLRs contain a single tyrosine within an YXXL motif in their cytoplasmic domain (13, 14). Dectin-1 (*CLEC7A*), CLEC-2 (*CLEC1B*), DNGR-1 (*CLEC9A*), and SIGN-R3 (mouse *Cd209d*) belong to the hemITAM-based CLRs category (15–20).

These ITAM or hemITAM CLRs are considered activating receptors that couple to the spleen tyrosine kinase (Syk) (**Figure 1**) (15, 21, 22). Phosphorylation of the tyrosine(s) in the ITAM or hemITAM motifs generates docking sites for the SH2 domains of Syk, which undergoes a conformational change that permits autophosphorylation and activation (23). Mincle acts as a prototypical activating CLR after recognition of glycolipids in the cell wall of some fungal and bacterial pathogens (24–26). Through the full ITAM of the FcRγ chain adaptor, Mincle couples to Syk and activates Vav proteins and PKCδ, which lead to downstream activation of CARD9/Bcl10/Malt1 and MAPK pathways, thus resulting in the induction of several cytokines and chemokines, including TNF-α, macrophage inflammatory protein 2 (MIP-2; CXCL2), keratinocyte-derived chemokine (KC; CXCL1), and IL-6 (7, 27, 28). Production of inflammatory cytokines by myeloid cells, together with the generation of Th1 and Th17 responses, contribute to protective immunity upon recognition of some Mincle ligands (29–38).

Spleen tyrosine kinase activation downstream of the hemITAM-bearing CLR Dectin-1 leads to similar signaling pathways to those described for Mincle (**Figure 1**), with activation of the CARD9/Bcl10/Malt-1 module that promotes canonical NF-κB signaling (27, 28, 39). Dectin-1 can also activate MAPK (40, 41), NFAT through phospholipase C-γ2 (42, 43), and a Syk-independent non-canonical NF-κB activation relying on the activation of the Raf-1 kinase (44). These integrated pathways mediate production of reactive oxygen species (ROS) and cytokines, such as IL-1β, IL-6, IL-10, IL-12, TNF-α, and IL-23 to drive Th1 and Th17 differentiation, being essential for the development of antifungal immune responses (45–48). This axis is also activated in response to intestinal fungi, where Dectin-1 contributes to gut homeostasis (49).

Immunoreceptor tyrosine-based inhibitory motif-containing CLRs negatively regulate signaling initiated by kinase-associated heterologous receptors through the recruitment of tyrosine phosphatases, such as Src homology region 2 domain-containing phosphatase (SHP)-1 or -2 (**Figure 1**). Myeloid CLRs included in this group are human DCIR (*CLEC4A*), mDcir1 (*Clec4a2*), mDcir2 (*Clec4a4*), Clec12a (MICL, DCAL-2, KLRL1, CLL1), MAgH (*CLEC12B*), and Ly49Q (1, 50, 51). The ITIMs of both hDCIR and mDCIR1 have been shown to mediate inhibitory signaling through activation of the phosphatases, SHP-1 and SHP-2 (52–54). Activation of hDCIR on dendritic cells (DCs) leads to inhibition of TLR8-mediated IL-12 and TNF-α production and TLR9-induced IFN-α production (55, 56). Sensing endogenous ligands by DCIR modulates innate immunity to pathogens, such as *Plasmodium* or *Mycobacterium* (57, 58).

Myeloid CLRs that do not bear evident ITAM or ITIM domains include MMR (*MRC1*), DEC-205 (*LY75*), human DC-SIGN (*CD209*), mouse SIGN-R1 (*Cd209b*), Langerin (*CD207*), human MGL (*CLEC10A*), mouse Mgl1 (*Clec10a*), mouse Mgl2 (*Mgl2*), CLEC-1 (*CLEC1A*), human DCAL-1 (*CLECL1*), LOX-1 (*OLR1*), and LSECtin (*CLEC4G*). As an

example, DC-SIGN intracellular tail is associated with a signalosome composed of the scaffold proteins LSP1, KSR1, and CNK and the kinase Raf-1 in unstimulated DCs (59) (**Figure 1**). Similar to other CLRs in this group, DC-SIGN cannot promote DCs activation or cytokine secretion *per se*, but it rather modulates signaling by heterologous receptors (see below) or engages the endocytic machinery contributing to antigen processing and presentation to T cells (3).

Along this review, we will provide illustrative examples of how signaling pathways triggered by a CLR coupled to a particular canonical motif can vary depending on many factors. We will focus on Mincle, Dectin-1, DNGR-1, DCIR, and DC-SIGN as myeloid CLRs representative of each category of signaling motif. **Table 1** includes the signaling module coupled to each CLR surveyed in this review, common and gene names, category of flexible signaling source, signaling pathway involved, and the inflammatory outcome provided by such flexibility. In this **Table 1**, CLRs are grouped based on the signaling module they bear (left column) and graphically illustrates how the signaling pathways triggered by these receptors are more complex and versatile (right columns) than expected by their signaling modules.

SIGNALING FLEXIBILITY BEYOND THE CANONICAL MOTIFS

Motif Context and Receptor Location Modulate Signaling

Classifications of receptors based on intracellular structural motifs stand on the fact that those domains determine the molecular signaling pathways initiated after ligand recognition (1). However, in addition to the basic ITAM and ITIM motifs, subtle variations in the context of the canonical motifs profoundly affect the signal delivered. For example, DNGR-1 is a DC-specific hemITAM-bearing receptor that detects dead cells and promotes cross-presentation in sterile or infectious settings, without contributing to inflammation (**Figure 2A**), in contrast to the close-related Dectin-1 (19, 60–63). This deficiency to promote cytokine production through DNGR-1 hemITAM was linked to an isoleucine that precedes the tyrosine in DNGR-1 hemITAM and rescued by mutation to the glycine present in Dectin-1 hemITAM (60). Signaling flexibility can thus be intrinsically provided by the amino acid sequence of those motifs present in a CLR. In this regard, residues in the neck region of DNGR-1 allow the

TABLE 1 | Myeloid C-type lectin receptors (CLRs) surveyed in this review.

Signaling module	Common name	Gene name	Source of flexible signaling	Signaling pathway[a]	Flexibility outcome[b]
No immunoreceptor tyrosine-based activating motif (ITAM) or immunoreceptor tyrosine-based inhibitory motif (ITIM)	DC-SIGN	*CD209*	Homotetramerization	LSP1–KSR1–CNK–Raf-1	Intrinsic (80)
			Sensing self and non-self	LSP1–IKKε–Bcl3	Inhibitory (113–115)
				KSR1–CNK–Raf-1	Activating (59, 110)
			Heterologous modulation	(?)	Activating (148)
				Raf-1–MEK	Inhibitory (112)
			Heterotrimerization DC-SIGN/MR/MDL-1	DNAX-activation protein 12 (DAP12)	Activating (86)
ITAM	MDL-1	*CLEC5A*	Heterotrimerization DC-SIGN/MR/MDL-1	DAP12	Activating (86)
	Mannose receptor (MR)	*MRC1*	Heterotrimerization DC-SIGN/MR/MDL-1	DAP12	Activating (86)
			Inhibitory ITAM	Fc receptor γ (FcRγ)–Grb2–SHP-1	Inhibitory (12)
	Dectin-2	*CLEC6A*, *Clec4n*	Heterodimerization Dectin-2/MCL	FcRγ–spleen tyrosine kinase (Syk)–NF-κB p65	Activating (85)
	MCL	*CLEC4D*	Heterodimerization Mincle/MCL	FcRγ–Syk	Activating (81–84)
	Mincle	*CLEC4E*	Heterodimerization Mincle/MCL	FcRγ–Syk	Activating (81–84)
			Inhibitory ITAM	FcRγ–Syk–SHP-1	Inhibitory (91, 92)
			Sensing self	Retarded Syk	Inhibitory (104, 105)
				FcRγ–Syk	Activating (7, 100–103)
			Heterologous modulation	FcRγ–Syk	Activating (140, 141, 143)
				FcRγ–Syk–PKB–Mdm2	Inhibitory (146)
hemITAM	CLEC-2	*CLEC1B*	Homodimerization	Syk	Intrinsic (75, 76)
	DNGR-1	*CLEC9A*	Motif context	Syk	Intrinsic (19, 60–64)
	Dectin-1	*CLEC7A*	Subcellular location	Syk	Intrinsic (67–70)
			Ligand size-conditioned subcellular location	Syk–MAPK–reactive oxygen species	Intrinsic (71–74)
			Phosphatase association	SHP-1–PTEN–FcRγ SHIP-1	Inhibitory (93, 94)
				SHP-2–Syk	Activating (95)
			Heterologous modulation	Syk	Activating (124–126)
				PI3K–mTOR–HIF-1α	Activating (130–134)
				Syk–Pyk2–ERK–SOCS-1	Inhibitory (128)
ITIM	DCIR	*CLEC4A*, *Clec4a2*	Activating ITIM	IFNI–STAT1 SHP-2 hijacking (?)	Activating (58)
			Sensing self and non-self	(?)	Activating (57)
				SHP-2/SHIP-1	Inhibitory (108, 109)

[a]*Described in the indicated reference. In case it was not studied in depth, it might be incomplete.*

[b]*This column indicates the inflammatory balance provided by each source of signaling flexibility. "Intrinsic" refers to specific responses triggered by particular CLRs.*

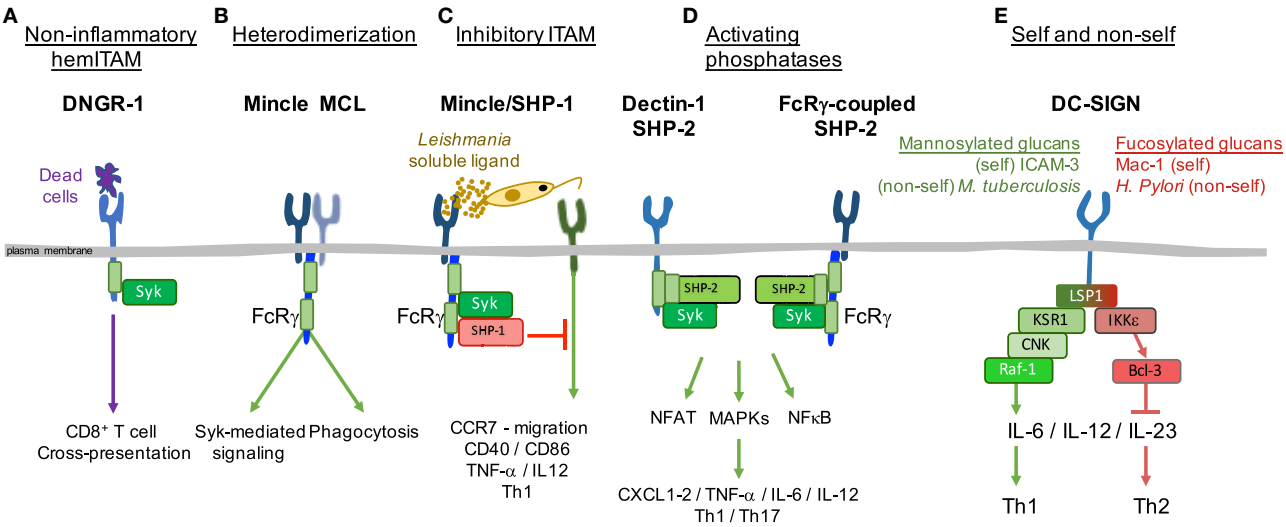

FIGURE 2 | Signaling flexibility downstream of C-type lectin receptors (CLRs). Signaling triggered downstream of CLRs goes beyond the canonical modules present in their intracellular domains and can be modulated by different processes. Some examples of such plasticity are represented. **(A)** DNGR-1 promotes cross-presentation of antigens to $CD8^+$ T cells, yet not directly contributing to inflammation. **(B)** Mincle and MCL dimerize, boosting phagocytosis, and spleen tyrosine kinase (Syk)-mediated inflammatory responses. **(C)** Sensing of a soluble ligand from *Leishmania* by Mincle triggers an inhibitory immunoreceptor tyrosine-based activating motif conformation downstream of Fc receptor γ (FcRγ), where SHP-1 dampens inflammatory responses triggered by heterologous receptors. **(D)** The phosphatase SHP-2 acts as a scaffold downstream of Dectin-1 and FcRγ-coupled CLRs, facilitating the recruitment of Syk and its inflammatory signaling. **(E)** Both self and non-self ligands share signaling pathways downstream of DC-SIGN depending on whether they are mannosylated or fucosylated glucans.

receptor to adopt different conformations that depend on pH and ionic strength, modulating its function as the receptor progresses through the endocytic pathway (64). Even the inflammatory response of mouse and human Dectin-1 to the same ligand varies because of minor interspecies variations in the signaling motif, with low valency ligands inducing proinflammatory genes through human but not mouse Dectin-1 (65).

Receptor location also affects CLR signaling and functions. A single CLR may be expressed in different cell types (66) as diverse isoforms that may differ in subcellular location. For example, two isoforms of Dectin-1 have been described to bind β-glucans (67); isoform A is characterized by the presence of a stalk region including an N-linked glycosylation site, which is missing in isoform B (68). This glycosylation determines the cell surface expression of isoform A, while non-glycosylated isoform B is retained intracellularly, thus conditioning the response to ligands (69) and the sensitivity to proteolytic cleavage (70).

The subcellular location of a CLR may not only depend on intrinsic features in its sequence, but also on the size of the particle where the ligand is recognized. For example, "frustrated" phagocytosis mediated by Dectin-1 in response to ligands exposed in large particles leads to enhanced cytokine response and ROS production compared with soluble ligands (71–73). Blockade of Dectin-1 internalization following ligand exposure leads to sustained MAPK activation (72), suggesting that endocytosis dampens Dectin-1 production of cytokines. Thus, formation of a phagocytic synapse by particulate β-glucan redistributes Dectin-1 and phosphatases along the cellular membrane, favoring proinflammatory signals including ROS production (73). In addition, the size of the ligand-containing particle and the consequent location of the receptor, can lead to qualitatively different responses. Dectin-1-mediated phagocytosis dampens the nuclear translocation of neutrophil elastase, controlling the extent of neutrophil extracellular traps (NET) formation in response to small pathogens (bacteria or yeast). Consequently, Dectin-1 blockade or deficiency leads to enhanced NETosis, as observed in response to non-phagocytic large pathogens (hyphae) (74).

Thus, the expected canonical response based on signaling modules can be altered both by slight modifications in motif context and the subcellular location of CLRs, taking into account that the latter may be affected by the size of the ligand recognized.

Multimerization of CLRs for Signaling

The signal transduction through several myeloid CLRs may also depend on their capacity to form dimers or multimers with other CLRs. CLRs bearing hemITAMs may require two phosphorylated tyrosines in a homodimer to bind Syk. It has been shown that CLEC-2 preexists as a dimer that aggregates following ligand binding (75, 76). The hemITAM motif of CLEC-2 is crucial for blood-lymph separation during development (77, 78). Of note, thrombus stability is dependent on CLEC-2 but not on the hemITAM, revealing a hemITAM-independent signaling for CLEC-2 (79).

DC-SIGN provides another example of homomultimerization, despite lacking ITAM or ITIM domains. This CLR appears assembled as a tetramer, allowing multiple interactions with diverse pathogens that differ in size, but also increasing ligand avidity (80). In addition, some CLRs form heterodimers, such as MCL and Mincle (11, 81). These two CLRs are interrelated as they both sense the mycobacterial glycolipid trehalose-6,6-dimycolate

(TDM), triggering an FcRγ-dependent pathway (11). Indeed, MCL and Mincle are co-regulated and depend on each other for their mutual surface expression (82, 83). However, the association of MCL with FcRγ in this complex is species-specific, being direct in mouse cells (11) but requiring Mincle in rat (81). Thus, the interaction between these CLRs would facilitate MCL signaling capacity *via* association with Mincle and translocation to the plasma membrane. On the other hand, Mincle would benefit the endocytic capacity of MCL (**Figure 2B**) and both receptors could increase affinity or specificity for their ligands (84). MCL also forms a heterodimeric pattern-recognition receptor with Dectin-2 (85), which has a high affinity for α-mannans on the surface of *Candida albicans* (*C. albicans)* hyphae.

Cooperative interaction is also found in the case of dengue virus binding with high affinity to MR and DC-SIGN, receptors that subsequently handle the virus to the lower affinity receptor CLEC5A, which mediates signal transduction (86).

All these examples illustrate how multimerization of CLRs, forming either homo- or hetero-complexes, facilitates a cooperative response to the ligand.

Is the Function of CLRs Inhibitory or Activating?

Another layer of complexity in CLR signaling stems from the ability of a single CLR to bind different ligands through its plastic C-type lectin domain. For instance, depending on their relative affinity or avidity, ligands may fine-tune signaling pathways downstream of ITAM motifs. Whereas the binding of high-avidity ligands to these receptors induces activating signals, the binding of low-avidity ligands leads to hypophosphorylation of the ITAM domain and preferential association of SH2-containing phosphatases like SHP-1, a configuration known as "inhibitory ITAM" (87). Although FcαRI receptor, which associates for signaling with the FcRγ chain, is the paradigmatic example of this inhibitory pathway (88–90), we have shown that CLRs associated with FcRγ chain may behave in the same fashion.

As an example, Mincle senses a soluble ligand derived from *Leishmania* that induces phosphorylation of SHP-1 coupled to FcRγ chain, inhibiting DC activation through heterologous receptors (**Figure 2C**) (91). In addition, SHP-1 contributes to deceleration of phagosome maturation upon TDM binding, suggesting an inhibitory signal downstream of Mincle during phagocytic processes (92). MR binds the FcRγ chain and, upon sensing *Mycobacterium tuberculosis*, recruits SHP-1 to the phagosome, thus limiting PI(3)P generation and delaying fusion with the lysosome, which promotes *M. tuberculosis* growth (12). Following treatment of DCs with curdlan or depleted zymosan (lacking TLR-stimulating properties), Dectin-1 signaling is modulated by the association of SHP-1 and PTEN to the FcRγ chain, hindering cytokine expression, DC maturation, and T-cell proliferation (93). ROS production downstream of Dectin-1 sensing of *C. albicans* is also tightly regulated by the SH2-domain containing inositol 5′ phosphatase (SHIP)-1 in response to Dectin-1 ligands (94). Thus, association of phosphatases to "activating" CLRs depending on the ligand nature, binding affinity, or avidity may contribute to maintenance of immune homeostasis.

Conversely, tyrosine phosphatases can contribute to activation. Contrary to SHP-1, the related tyrosine phosphatase SHP-2 acts as a scaffold, facilitating the recruitment of Syk to Dectin-1 or the adaptor FcRγ chain (95) (**Figure 2D**). In this way, DC-derived SHP-2 was crucial *in vivo* for the induction of TNF-α, IL-6, IL-12, and Th1 and Th17 anti-fungal responses upon *C. albicans* infection (95).

Immunoreceptor tyrosine-based inhibitory motif-coupled receptors can also deliver an activating signal. In a model of tuberculosis infection in non-human primates, DCIR deficiency impairs STAT1-mediated type I IFN signaling in DCs, leading to increased production of IL-12 and differentiation of T lymphocytes toward Th1. Thus, DCIR-deficient mice with increased Th1 immunity control *M. tuberculosis* better than WT animals, but also shown increased inflammation in the lungs mediated by TNF-α and inducible nitric oxide synthase (iNOS) (58). This study suggests that DCIR acts as an activating receptor for the STAT1-type I IFN signaling, and speculates that DCIR may function as a molecular sink binding unphosphorylated inactive SHP-2, therefore, limiting SHP-2′s capacity to deactivate STAT1.

The examples explained above illustrate a lack of correspondence between the canonical motif coupled to a CLR and the resulting signaling pathway. Association to kinases would lead to activating routes, while association to phosphatases would result in regulatory pathways, with some exceptions like the SHP-2-mediated CLR-induced activation (95). Association of kinases or phosphatases could be related to the strength of the initiating signal, with suboptimal phosphorylation leading to phosphatase binding to the hypo-phosporylated ITAM (inhibitory ITAM) (87). Due to the signaling flexibility offered by CLRs, a detailed empiric analysis for each CLR-ligand interaction in terms of type of ligand, concentration, and kinetics of exposition would be required to predict the signaling outcome.

Dealing With Self and Non-Self

C-type lectin receptors act as plastic receptors, some of them detecting self-ligands, other detecting non-self ligands, and many of them acting as dual receptors sensing self and non-self. It is possible that CLRs will behave as activating receptors when they sense non-self ligands, while CLRs bearing an ITIM motif will preferably bind self to dampen inflammation. However, in opposition to non-dangerous self, also known as "self-associated molecular patterns" (96, 97), Polly Matzinger proposed the existence of dangerous-self (damage-associated molecular patterns or DAMPs) exposed and/or released upon necrotic cell death (98, 99). In addition, tissue damage signals concomitant to infection can contribute to effector responses. Thus, DNGR-1 senses tissue damage concomitant with viral infections and facilitates antigen processing of viral antigens for cross-presentation to $CD8^+$ T cells, decoding the antigenicity rather than the adjuvanticity of the cargo (60–63). Some examples of CLRs dealing with self and non-self ligands are explained below.

Mincle is a plastic CLR promoting proinflammatory signals after sensing glycolipids in the cell wall of bacteria and fungi (24–26), but also sensing damaged self in the form of soluble SAP-130 following necrosis (7). Mincle sensing of β-glucosylceramide

(100) or cholesterol sulfate (101) promotes immunopathology (102, 103). Conversely, there are reports suggesting that Mincle sensing of SAP-130 can also drive immunosuppression (104). Moreover, human albumin abolishes innate immunity by directly binding Mincle receptor in the microglia after subarachnoid hemorrhage (105). Thus, Mincle is an example of CLR that deals with self and non-self ligands that may result in activating or inhibitory signals. However, the correlation of sensing self with an inhibitory response and sensing non-self with an activating response is not established. In this regard, non-self signals from pathogens may mimic self-inhibitory signals to escape immune surveillance, which could be the case for Mincle sensing of *Leishmania* (91).

DCIR is a myeloid CLR endowed with an ITIM motif that behaves as a self PRR. DCIR maintains the homeostasis of the immune system (106), since aged mice deficient for this CLR spontaneously develop several autoimmune disorders (107). Intravenous immunoglobulins bearing sialic acid induce a DCIR-mediated negative signal in DCs *via* SHP-2 and SHIP-1 that promotes Treg differentiation and dampens allergy (108). DCIR self-sensing can also occur in the context of infection, thus modulating the inflammatory response. DCIR-deficient mice exhibited severe inflammatory disease following Chikungunya virus infection (109). However, reduced adaptive T-cell responses in DCIR-deficient mice following cerebral malaria caused by *Plasmodium berghei* renders them more resistant (57). Since no evidence for direct interactions between DCIR and Chikungunya virus and *P. berghei* exists, we could hypothesize that DCIR may be recognizing DAMPs released during infection.

DC-SIGN illustrates how a single CLR deals differently with a variety of self and non-self ligands. DC-SIGN binds high mannose and fucose (LeX, LeY, LeA, LeB) that can be exposed in a variety of self receptors, such as ICAM-2, ICAM-3, CEACAM-1, Mac1 and CEA, or non-self proteins (structures in pathogens, including viruses, bacteria, fungi, and eukaryote parasites) (3, 110–115). Upon binding of mannosylated glucans, either self as those present on ICAM-3 (110) or non-self from *M. tuberculosis* (59), DC-SIGN couples to a LSP1–KSR1–CNK signalosome, leading to activation of Raf-1 and acetylation of the NF-κB p65 subunit, which results in enhancement of proinflammatory responses, including IL-12p70 and IL-6, although also promotes IL-10 transcription (59) (**Figure 2E**). In contrast, DC-SIGN recognition of fucosylated glucans as presented in self proteins, such as Mac1 (113) or non-self pathogens (*Helicobacter pylori*) (114), leads to dissociation of the LSP1-based signalosome and leaves just LSP1 associated with DC-SIGN. Phosphorylated LSP1 subsequently recruits IKKε and CYLD. IKKε activation inhibits CYLD deubiquitinase activity, facilitating nuclear translocation of ubiquitinated Bcl3 that represses TLR-induced proinflammatory cytokine expression, enhancing expression of IL-10 and Th2-attracting chemokines, and thus promoting Th2 polarization (114) (**Figure 2E**). In addition, IKKε collaborates with type I IFNR signaling to induce and activate the transcription factor ISGF3 that induces IL-27p28, a key cytokine for induction of T follicular helper cells (115). These results point to DC-SIGN as a dual receptor that, depending on the nature of the ligand, contributes to maintain homeostasis or initiates the immune response against some pathogens.

All these examples illustrate how a single CLR can trigger different signaling pathways depending on the recognition of self or non-self ligands. Current understanding of these processes is based on the study of individual CLRs. Deciphering common signaling patterns for self versus non-self sensing would allow harnessing immunity and inflammation by CLRs.

MODULATION OF HETEROLOGOUS SIGNALING BY MYELOID CLRs

In addition to the diverse response of a single CLR depending on the stimulus, it is fascinating how these signaling pathways interact with signals from heterologous receptors and lead to complex responses to stimuli that are simultaneously detected by several myeloid PRRs expressed in myeloid cells [see also Ref. (116, 117) for reviews focused on this topic]. In this section, we illustrate some examples of how myeloid CLRs cross-talk with surrounding heterologous receptors.

Dectin-1 Affects Simultaneous and Deferred Signaling Through Heterologous Receptors

Dectin-1 triggers a response after sensing infectious agents, such as diverse fungi and mycobacteria (118), *Salmonella typhimurium* (119) or *Leishmania infantum* (120). Dectin-1 may also promote proinflammatory signals following the detection of endogenous factors, such as vimentin from atherosclerotic plaques (121), galectin-9 from pancreatic carcinoma (122), or N-glucans on tumor cells (123). In addition to a prototypical activating CLR, Dectin-1 modulates signals simultaneously triggered through other PRRs. Dectin-1 cooperates with signals from TLR2/MyD88 to increase proinflammatory cytokine production (124–126). This synergy is exerted at the level of effector responses resulting in increased production of TNF-α, IL-12, and ROS (124) (**Figure 3A**, left). Dectin-1 also positively cooperates in the full activation of the NLRP3 inflammasome, participating in the priming and generation of pro-IL-1β and the induction of ROS required for NLRP3 activation (127). Conversely, Dectin-1 stimulation with depleted zymosan in bone marrow macrophages leads to Syk and Pyk2-ERK-dependent activation of SOCS-1 that downregulates IL-10 and IL-12p40 production induced by TLR9 stimulation (128) (**Figure 3A**, right). This effect would contribute to the Dectin-1 signature in priming Th17 responses (40, 128). In addition, Dectin-1 protects against chronic liver disease by suppressing TLR4 signaling. This effect is mediated by reducing TLR4 and CD14 expression, which are regulated by Dectin-1-dependent macrophage colony stimulating factor expression (129).

Apart from direct modulation of signaling pathways triggered simultaneously, Dectin-1 can leave a footprint that affects deferred signaling by heterologous receptors, a process named as trained immunity (130). Trained immunity after sensing of *C. albicans* or purified β-glucan *via* Dectin-1 results in enhanced protection to a lethal challenge with *Candida* and cross-protection

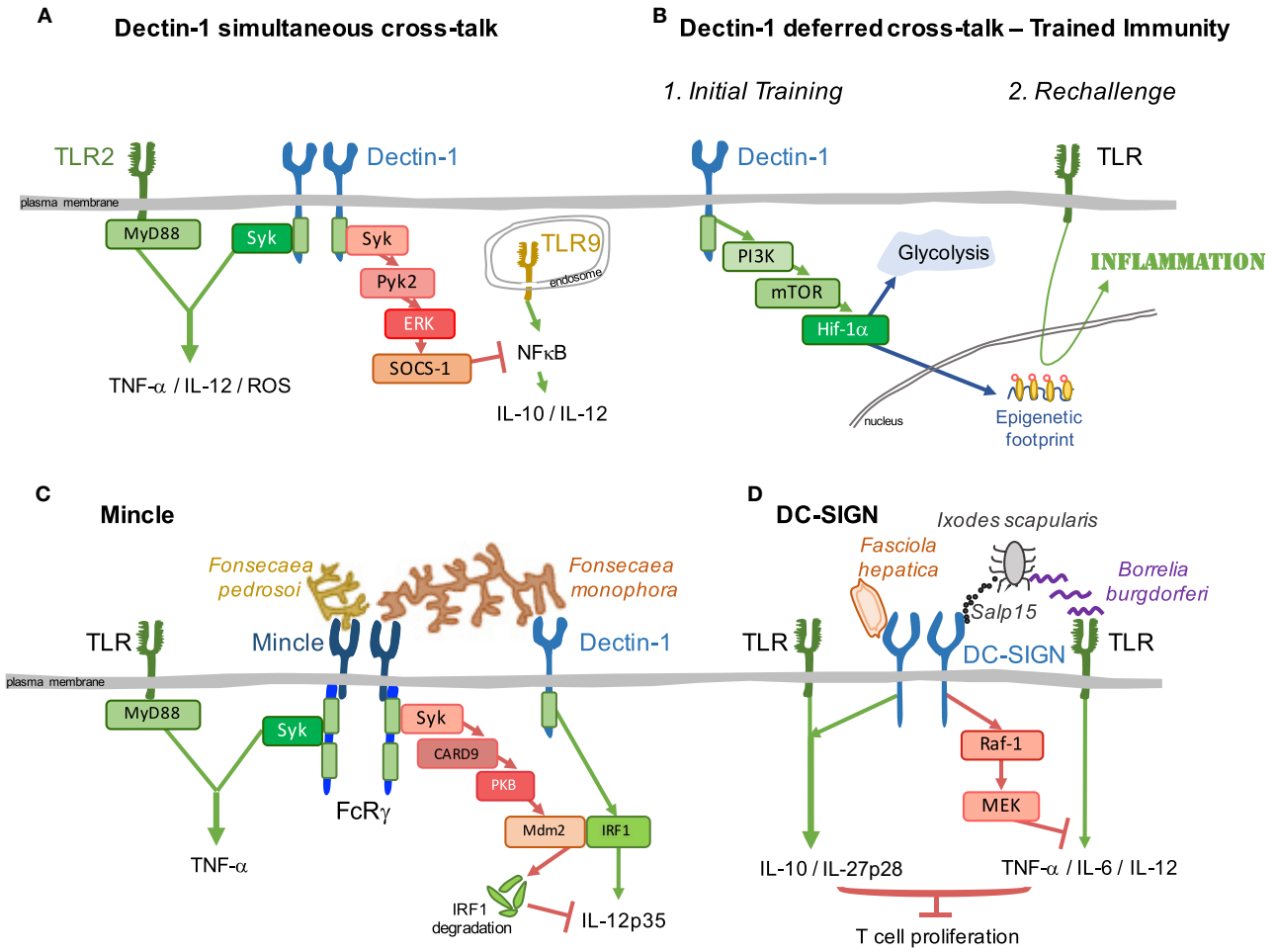

FIGURE 3 | Signaling crosstalk between myeloid C-type lectins and heterologous receptors. Signaling pathways initiated downstream of C-type lectin receptors (CLRs) interact with surrounding cascades triggered by heterologous receptors. Examples of such crosstalk are illustrated. **(A)** Dectin-1 coordinates with simultaneous signals from diverse TLRs to modulate the inflammatory response; this interaction can be either positive, as for TLR2/MyD88 (left), or negative, as for TLR9 through a Pyk2/ERK/SOCS-1-dependent pathway (right). **(B)** In addition, the axis Dectin-1/PI3K/mTOR/Hif-1α generates a switch toward glycolytic metabolism together with an epigenetic footprint, allowing for a "deferred" improved response to TLRs, boosting the inflammatory response. This process is known as trained immunity. **(C)** A full inflammatory response against *Fonsecaea pedrosoi* is achieved by synergistic stimulation between Mincle and ligands for TLRs coupled to the MyD88 adaptor (left). However, simultaneous recognition of *Fonsecaea monophora* by Mincle and Dectin-1 triggers a Mincle-PKB-Mdm2-dependent degradation of Dectin-1-activated IRF1, dampening the expression of protective IL-12p35 (right). **(D)** DC-SIGN recognition of *Fasciola hepatica* enhances TLR-induced IL-10 and IL-27p28 (left). Moreover, DC-SIGN sensing of the salivary protein Salp15 from the tick vector *Ixodes scapularis* dampens inflammatory responses triggered by *Borrelia burgdorferi* through TLRs (right). Both examples illustrate strategies to escape immune surveillance based on inhibition of T cell proliferation.

to *Staphylococcus aureus* infection (130, 131). This increased protection upon a later infection is linked to increased proinflammatory responses to delayed rechallenge with different TLR ligands, such as LPS or Pam_3Cys_4 (130) (**Figure 3B**), or bacteria, i.e., *Bacteroides fragilis, Escherichia coli, Staphylococcus aureus, Borrelia burgdorferi,* or *M. tuberculosis* (130, 132, 133). In monocytes, Dectin-1 signaling triggers the PI3K-Akt pathway, leading to activation of mTOR and HIF-1α (131). This leads to a shift from oxidative phosphorylation to aerobic glycolysis. Accumulation of fumarate, associated with glutamine replenishment of the TCA cycle, inhibits KDM5 histone demethylases, a key step for induction of monocyte epigenetic reprogramming that underlies the long-lasting effects of trained immunity (130, 134) (**Figure 3B**).

Apart from β-glucan or *Candida*, several other self and non-self ligands, such as chitin (135), BCG vaccine (136), and uric acid (137) induce trained immunity (137, 138). It would thus not be surprising that more CLRs could contribute to trained immunity. In this regard, although *C. albicans* mannans, potentially sensed by MR, Dectin-2, or Mincle (46), have shown not to prime human monocytes directly (130), they are essential for *C. albicans*-induced training (133). Furthermore, both Dectin-1 and MR are needed to trigger glycolysis upon *C. albicans* stimulation (139); this glycolytic switch constitutes a critical metabolic

step in trained immunity induction (131, 139). Trained immunity triggered by Dectin-1 and potentially other CLRs is thus a consequence of metabolic switch and epigenetic programming that affects deferred heterologous signaling.

Mincle-Triggered Regulatory Responses

As described before, Mincle triggers an FcRγ-mediated activating signal in response to different stimuli. In addition, Mincle engagement can deliver regulatory responses affecting signaling pathways triggered by heterologous PRRs, such as TLRs or other CLRs, for example, Dectin-1. This section will explore modulation of heterologous receptors by Mincle.

Mincle is induced following TLR activation (7). Following sensing of *Fonsecaea pedrosoi*, Mincle triggers an incomplete inflammatory response that requires synergistic TLR stimulation to induce a potent proinflammatory response (**Figure 3C**, left), needed to clear the infection in a mouse model of chromoblastomycosis (140). This cooperative activation through Mincle and TLRs is particularly effective in human newborn DCs. Co-stimulation using the Mincle agonist trehalose-6,6-dibehenate and the TLR7/8 agonist R848 led to enhanced caspase-1 and NF-κB activation, Th1 polarizing cytokine production and autologous Th1 polarization (141).

However, Mincle exhibits a dual role in promotion and subsequent resolution of inflammation. Mycobacteria express ligands for TLRs which induce expression of Mincle that can then detect TDM and contribute to inflammation. Mincle *via* the Syk/p38 axis can also lead to eIF5A hypusination that increases translation efficiency of iNOS, which is transcriptionally induced by TLR2 ligation (142). In this way, Mincle favors NO production that inhibits late-stage activation of NLRP3 inflammasome in TDM-induced inflammation, contributing to termination (142). Similarly, TLR2 sensing of *Corynebacterium* induces robust Mincle expression, which cooperatively detects corynebacterial glycolipids favoring production of granulocyte colony stimulating factor and NO (143).

Dectin-1 and Mincle are involved in the recognition of *Fonsecaea monophora*, a pleomorphic fungus also responsible for chromoblastomycosis (144, 145). Signaling triggered by Dectin-1 initiates protective immunity against the fungus by activating IRF1 and IL-12p35 transcription. However, these responses are dampened by the Mincle/Syk axis, in a process involving PI3K/PKB-mediated activation of the E3 ubiquitin ligase Mdm2, leading to degradation of IRF1 and repression of IL-12p35 production (**Figure 3C**, right). In this way, Mincle sensing of *F. monophora* dampens induction of protective Th1 immunity triggered by Dectin-1 (146). Mincle is also targeted by *Leishmania* parasites to evade the priming of Th1 immunity initiated by DCs. As explained above, Mincle recruits SHP-1 to an inhibitory ITAM configuration in the coupled FcRγ chain, and this results in inhibition of DC activation by heterologous receptors sensing *Leishmania* or LPS (91) (**Figure 2C**). Mincle ligation can also reduce TLR4-mediated inflammation, whereas Mincle deletion or knockdown results in exaggerated inflammation in response to LPS. This effect is mediated through the control of TLR4 correceptor CD14 expression (147).

Tailoring Immunity Through DC-SIGN

DC-SIGN engagement does not generally induce the expression of cytokines by itself, but rather modulates responses initiated by TLRs. Thus, glycans from the helminth *Fasciola hepatica* are recognized by DC-SIGN leading to enhanced TLR-induced IL-10 and IL-27p28, triggering a tolerogenic program that differentiates naive $CD4^+$ T cells into regulatory T cells (148) (**Figure 3D**, left). However, the interaction of DC-SIGN with the salivary protein Salp15 from the tick *Ixodes scapularis* dampens inflammatory responses triggered by *Borrelia burgdorferi*. Raf-1 activation downstream of DC-SIGN sensing Salp15 results in MEK-dependent decrease of IL-6 and TNF mRNA stability and impaired nucleosome remodeling at the IL-12p35 promoter, modulating TLR-induced DC activation and T cell proliferation (112) (**Figure 3D**, right).

All these examples clearly illustrate how signaling pathways triggered by CLRs can have an impact on responses mediated by surrounding heterologous receptors, adding an extra layer of complexity to our understanding of CLR-mediated responses.

CONCLUDING REMARKS

Classical sorting of myeloid CLRs based on the structure of the C-type lectin domain does not have functional significance. A more recent classification based on the presence of ITAM, hemITAM, or ITIM intracellular signaling motifs associated with the receptors has been useful as a starting point to predict the functional outcome of signaling CLRs (1). However, many factors may alter the expected canonical response. Minor variations in the context of the canonical motifs result in different signaling and effector outcomes (60, 65). Subcellular location depending on the isoform (69) or conformation of the receptor based on specific residues (64) also affects the function of the receptor. CLR signaling also depends on the size of the particle, where the ligand is recognized, affecting quantitatively the strength of the reaction (71–73) and also leading to qualitatively different responses (74, 149). Cooperative binding and signal transduction may be a consequence of multimerization. There are examples of homodimerization (75, 76) and formation of hetero-complexes (11, 81, 84–86). Hetero-complexes result in a mutual benefit for involved receptors, combining avidity for the ligand, capacity for endocytosis and/or signal transduction capabilities.

The plasticity of the C-type lectin domain allows binding to different ligands that, depending on their relative affinity or avidity, may trigger activating or inhibitory signaling pathways downstream of the same motifs. For example, low-avidity ligands drive a Syk-dependent association with SHP-1 to the ITAM domain (87, 88, 90), with a growing list of examples illustrating CLRs coupled to the FcRγ chain (12, 91–93). Conversely, tyrosine phosphatases may contribute to activation (95) and ITIM-containing CLRs may trigger activating signals (58). These results evidence the fine regulation of signaling though a single receptor based on differential interaction with diverse ligands, leading to the hypothesis that sensing self-ligands through CLRs could drive tolerance while non-self ligands could provoke immunity. However, dangerous-self could rather contribute to immunity and some non-self ligands could inhibit immune response for

evasion, making the final outcome of a single response rather unpredictable. In addition, the concerted sensing of complex ligands by a variety of PRRs leads to complex integrated responses. CLRs may affect signals of heterologous receptors that are simultaneously triggered, either enhancing or modulating the response (59, 91, 115, 124–126, 128, 142, 146). Of note, Dectin-1 induces a metabolic switch and epigenetic programming that affects deferred heterologous signaling (130, 131). In conclusion, understanding how different signaling pathways triggered by CLRs and heterologous receptors act in concert during sensing self and non-self remain a fascinating endeavor.

Research in the field of CLRs has gained much attention considering the diversity of members, ligands, expression pattern on clinically relevant cellular populations and their relevant function on the initiation, and regulation of immunity and inflammation. Some of these features have been illustrated here and offer multiple possibilities to harness CLR-triggered responses. However, CLR manipulation may lead to unexpected outcomes and needs to be tested empirically. In addition, deciphering molecular signatures common to signaling pathways triggered by CLRs in response to different ligands will help to understand their precise role in immunity and inflammation.

AUTHOR CONTRIBUTIONS

CF, SI, PS-L, MM-L, and DS conceived and wrote the manuscript. CF did the figures that were edited by all the authors.

ACKNOWLEDGMENTS

We thank the members of the immunobiology lab for useful discussions.

FUNDING

CF is supported by AECC Foundation as recipient of an "Ayuda Fundación Científica AECC a personal investigador en cancer." SI is funded by grant SAF2015-74561-JIN from the Spanish Ministry of Economy, Industry and Competitiveness (MINECO) and European Fund for Regional Development (FEDER). PS-L is funded by grant BES-2015-072699 ("Ayudas para contratos predoctorales para la formación de doctores 2015") from MINECO. MM-L received a FPU fellowship (AP2010-5935) from the Spanish Ministry of Education. Work in the DS laboratory is funded by the CNIC and grant SAF2016-79040-R from MINECO and FEDER; B2017/BMD-3733 Immunothercan-CM from Comunidad de Madrid; RD16/0015/0018-REEM from FIS-Instituto de Salud Carlos III, MINECO, and FEDER; Foundation Acteria; Constantes y Vitales prize (Atresmedia); Foundation La Marató de TV3 (201723); the European Commission (635122-PROCROP H2020); and the European Research Council (ERC-Consolidator Grant 725091). The CNIC is supported by the MINECO and the Pro-CNIC Foundation, and is a Severo Ochoa Center of Excellence (MINECO award SEV-2015-0505). The authors have no conflicting financial interests.

REFERENCES

1. Sancho D, Reis e Sousa C. Signaling by myeloid C-type lectin receptors in immunity and homeostasis. *Annu Rev Immunol* (2012) 30:491–529. doi:10.1146/annurev-immunol-031210-101352
2. Iborra S, Sancho D. Signalling versatility following self and non-self sensing by myeloid C-type lectin receptors. *Immunobiology* (2015) 220(2):175–84. doi:10.1016/j.imbio.2014.09.013
3. Geijtenbeek TB, Gringhuis SI. Signalling through C-type lectin receptors: shaping immune responses. *Nat Rev Immunol* (2009) 9(7):465–79. doi:10.1038/nri2569
4. Monteiro JT, Lepenies B. Myeloid C-type lectin receptors in viral recognition and antiviral immunity. *Viruses* (2017) 9(3):1–22. doi:10.3390/v9030059
5. Underhill DM, Goodridge HS. The many faces of ITAMs. *Trends Immunol* (2007) 28(2):66–73. doi:10.1016/j.it.2006.12.004
6. Sato K, Yang X-l, Yudate T, Chung J-S, Wu J, Luby-Phelps K, et al. Dectin-2 is a pattern recognition receptor for fungi that couples with the Fc receptor gamma chain to induce innate immune responses. *J Biol Chem* (2006) 281(50):38854–66. doi:10.1074/jbc.M606542200
7. Yamasaki S, Ishikawa E, Sakuma M, Hara H, Ogata K, Saito T. Mincle is an ITAM-coupled activating receptor that senses damaged cells. *Nat Immunol* (2008) 9(10):1179–88. doi:10.1038/ni.1651
8. Dzionek A, Sohma Y, Nagafune J, Cella M, Colonna M, Facchetti F, et al. BDCA-2, a novel plasmacytoid dendritic cell-specific type II C-type lectin, mediates antigen capture and is a potent inhibitor of interferon alpha/beta induction. *J Exp Med* (2001) 194(12):1823–34. doi:10.1084/jem.194.12.1823
9. Kaden SA, Kurig S, Vasters K, Hofmann K, Zaenker KS, Schmitz J, et al. Enhanced dendritic cell-induced immune responses mediated by the novel C-type lectin receptor mDCAR1. *J Immunol* (2009) 183(8):5069–78. doi:10.4049/jimmunol.0900908
10. Bakker AB, Baker E, Sutherland GR, Phillips JH, Lanier LL. Myeloid DAP12-associating lectin (MDL)-1 is a cell surface receptor involved in the activation of myeloid cells. *Proc Natl Acad Sci U S A* (1999) 96(17):9792–6. doi:10.1073/pnas.96.17.9792
11. Miyake Y, Toyonaga K, Mori D, Kakuta S, Hoshino Y, Oyamada A, et al. C-type lectin MCL is an FcRgamma-coupled receptor that mediates the adjuvanticity of mycobacterial cord factor. *Immunity* (2013) 38(5):1050–62. doi:10.1016/j.immuni.2013.03.010
12. Rajaram MVS, Arnett E, Azad AK, Guirado E, Ni B, Gerberick AD, et al. *M. tuberculosis*-initiated human mannose receptor signaling regulates macrophage recognition and vesicle trafficking by FcRgamma-chain, grb2, and SHP-1. *Cell Rep* (2017) 21(1):126–40. doi:10.1016/j.celrep.2017.09.034
13. Robinson MJ, Sancho D, Slack EC, LeibundGut-Landmann S, Reis e Sousa C. Myeloid C-type lectins in innate immunity. *Nat Immunol* (2006) 7(12):1258–65. doi:10.1038/ni1417
14. Osorio F, Reis e Sousa C. Myeloid C-type lectin receptors in pathogen recognition and host defense. *Immunity* (2011) 34(5):651–64. doi:10.1016/j.immuni.2011.05.001
15. Rogers NC, Slack EC, Edwards AD, Nolte MA, Schulz O, Schweighoffer E, et al. Syk-dependent cytokine induction by Dectin-1 reveals a novel pattern recognition pathway for C type lectins. *Immunity* (2005) 22(4):507–17. doi:10.1016/j.immuni.2005.03.004
16. Fuller GLJ, Williams JAE, Tomlinson MG, Eble JA, Hanna SL, Pöhlmann S, et al. The C-type lectin receptors CLEC-2 and Dectin-1, but not DC-SIGN, signal via a novel YXXL-dependent signaling cascade. *J Biol Chem* (2007) 282(17):12397–409. doi:10.1074/jbc.M609558200
17. Huysamen C, Willment JA, Dennehy KM, Brown GD. CLEC9A is a novel activation C-type lectin-like receptor expressed on BDCA3+ dendritic cells and a subset of monocytes. *J Biol Chem* (2008) 283(24):16693–701. doi:10.1074/jbc.M709923200
18. Sancho D, Mourao-Sa D, Joffre OP, Schulz O, Rogers NC, Pennington DJ, et al. Tumor therapy in mice via antigen targeting to a novel, DC-restricted C-type lectin. *J Clin Invest* (2008) 118(6):2098–110. doi:10.1172/JCI34584
19. Sancho D, Joffre OP, Keller AM, Rogers NC, Martínez D, Hernanz-Falcón P, et al. Identification of a dendritic cell receptor that couples sensing of necrosis to immunity. *Nature* (2009) 458(7240):899–903. doi:10.1038/nature07750

20. Tanne A, Ma B, Boudou F, Tailleux L, Botella H, Badell E, et al. A murine DC-SIGN homologue contributes to early host defense against *Mycobacterium tuberculosis*. *J Exp Med* (2009) 206(10):2205–20. doi:10.1084/jem.20090188
21. Underhill DM, Rossnagle E, Lowell CA, Simmons RM. Dectin-1 activates Syk tyrosine kinase in a dynamic subset of macrophages for reactive oxygen production. *Blood* (2005) 106(7):2543–50. doi:10.1182/blood-2005-03-1239
22. Kerrigan AM, Brown GD. Syk-coupled C-type lectins in immunity. *Trends Immunol* (2011) 32(4):151–6. doi:10.1016/j.it.2011.01.002
23. Mócsai A, Ruland J, Tybulewicz VLJ. The SYK tyrosine kinase: a crucial player in diverse biological functions. *Nat Rev Immunol* (2010) 10(6):387–402. doi:10.1038/nri2765
24. Ishikawa E, Ishikawa T, Morita YS, Toyonaga K, Yamada H, Takeuchi O, et al. Direct recognition of the mycobacterial glycolipid, trehalose dimycolate, by C-type lectin Mincle. *J Exp Med* (2009) 206(13):2879–88. doi:10.1084/jem.20091750
25. Schoenen H, Bodendorfer B, Hitchens K, Manzanero S, Werninghaus K, Nimmerjahn F, et al. Cutting edge: Mincle is essential for recognition and adjuvanticity of the mycobacterial cord factor and its synthetic analog trehalose-dibehenate. *J Immunol* (2010) 184(6):2756–60. doi:10.4049/jimmunol.0904013
26. Ishikawa T, Itoh F, Yoshida S, Saijo S, Matsuzawa T, Gonoi T, et al. Identification of distinct ligands for the C-type lectin receptors Mincle and Dectin-2 in the pathogenic fungus *Malassezia*. *Cell Host Microbe* (2013) 13(4):477–88. doi:10.1016/j.chom.2013.03.008
27. Strasser D, Neumann K, Bergmann H, Marakalala MJ, Guler R, Rojowska A, et al. Syk kinase-coupled C-type lectin receptors engage protein kinase C-sigma to elicit Card9 adaptor-mediated innate immunity. *Immunity* (2012) 36(1):32–42. doi:10.1016/j.immuni.2011.11.015
28. Roth S, Bergmann H, Jaeger M, Yeroslaviz A, Neumann K, Koenig PA, et al. Vav proteins are key regulators of Card9 signaling for innate antifungal immunity. *Cell Rep* (2016) 17(10):2572–83. doi:10.1016/j.celrep.2016.11.018
29. Vijayan D, Radford KJ, Beckhouse AG, Ashman RB, Wells CA. Mincle polarizes human monocyte and neutrophil responses to *Candida albicans*. *Immunol Cell Biol* (2012) 90(9):889–95. doi:10.1038/icb.2012.24
30. Wells CA, Salvage-Jones JA, Li X, Hitchens K, Butcher S, Murray RZ, et al. The macrophage-inducible C-type lectin, Mincle, is an essential component of the innate immune response to *Candida albicans*. *J Immunol* (2008) 180(11):7404–13. doi:10.4049/jimmunol.180.11.7404
31. Yamasaki S, Matsumoto M, Takeuchi O, Matsuzawa T, Ishikawa E, Sakuma M, et al. C-type lectin Mincle is an activating receptor for pathogenic fungus, *Malassezia*. *Proc Natl Acad Sci U S A* (2009) 106(6):1897–902. doi:10.1073/pnas.0805177106
32. Lee W-B, Kang J-S, Yan J-J, Lee MS, Jeon B-Y, Cho S-N, et al. Neutrophils promote mycobacterial trehalose dimycolate-induced lung inflammation via the Mincle pathway. *PLoS Pathog* (2012) 8(4):e1002614. doi:10.1371/journal.ppat.1002614
33. Schweneker K, Gorka O, Schweneker M, Poeck H, Tschopp J, Peschel C, et al. The mycobacterial cord factor adjuvant analogue trehalose-6,6'-dibehenate (TDB) activates the Nlrp3 inflammasome. *Immunobiology* (2013) 218(4):664–73. doi:10.1016/j.imbio.2012.07.029
34. Shenderov K, Barber DL, Mayer-Barber KD, Gurcha SS, Jankovic D, Feng CG, et al. Cord factor and peptidoglycan recapitulate the Th17-promoting adjuvant activity of mycobacteria through Mincle/CARD9 signaling and the inflammasome. *J Immunol* (2013) 190:5722–30. doi:10.4049/jimmunol.1203343
35. Ostrop J, Jozefowski K, Zimmermann S, Hofmann K, Strasser E, Lepenies B, et al. Contribution of Mincle-SYK signaling to activation of primary human APCs by mycobacterial cord factor and the novel adjuvant TDB. *J Immunol* (2015) 195(5):2417–28. doi:10.4049/jimmunol.1500102
36. Behler F, Maus R, Bohling J, Knippenberg S, Kirchhof G, Nagata M, et al. Macrophage-inducible C-type lectin Mincle-expressing dendritic cells contribute to control of splenic *Mycobacterium bovis* BCG infection in mice. *Infect Immun* (2015) 83(1):184–96. doi:10.1128/IAI.02500-14
37. Rabes A, Zimmermann S, Reppe K, Lang R, Seeberger PH, Suttorp N, et al. The C-Type lectin receptor Mincle binds to *Streptococcus pneumoniae* but plays a limited role in the anti-pneumococcal innate immune response. *PLoS One* (2015) 10(2):e0117022. doi:10.1371/journal.pone.0117022
38. Kottom TJ, Hebrink DM, Jenson PE, Nandakumar V, Wuthrich M, Wang H, et al. The interaction of pneumocystis with the C-type lectin receptor Mincle exerts a significant role in host defense against infection. *J Immunol* (2017) 198(9):3515–25. doi:10.4049/jimmunol.1600744
39. Gross O, Gewies A, Finger K, Schäfer M, Sparwasser T, Peschel C, et al. Card9 controls a non-TLR signalling pathway for innate anti-fungal immunity. *Nature* (2006) 442(7103):651–6. doi:10.1038/nature04926
40. LeibundGut-Landmann S, Gross O, Robinson MJ, Osorio F, Slack EC, Tsoni SV, et al. Syk- and CARD9-dependent coupling of innate immunity to the induction of T helper cells that produce interleukin 17. *Nat Immunol* (2007) 8(6):630–8. doi:10.1038/ni1460
41. Slack EC, Robinson MJ, Hernanz-Falcón P, Brown GD, Williams DL, Schweighoffer E, et al. Syk-dependent ERK activation regulates IL-2 and IL-10 production by DC stimulated with zymosan. *Eur J Immunol* (2007) 37(6):1600–12. doi:10.1002/eji.200636830
42. Goodridge HS, Simmons RM, Underhill DM. Dectin-1 stimulation by *Candida albicans* yeast or zymosan triggers NFAT activation in macrophages and dendritic cells. *J Immunol* (2007) 178(5):3107–15. doi:10.4049/jimmunol.178.5.3107
43. Xu S, Huo J, Lee K, Kurosaki T, Lam K. Phospholipase Cgamma 2 is critical for Dectin-1-mediated Ca2+ flux and cytokine production in dendritic cells. *J Biol Chem* (2009) 284:7038–46. doi:10.1074/jbc.M806650200
44. Gringhuis SI, den Dunnen J, Litjens M, van der Vlist M, Wevers B, Bruijns SC, et al. Dectin-1 directs T helper cell differentiation by controlling noncanonical NF-kappaB activation through Raf-1 and Syk. *Nat Immunol* (2009) 10(2):203–13. doi:10.1038/ni.1692
45. Rothfuchs AG, Bafica A, Feng CG, Egen JG, Williams DL, Brown GD, et al. Dectin-1 interaction with *Mycobacterium tuberculosis* leads to enhanced IL-12p40 production by splenic dendritic cells. *J Immunol* (2007) 179(6):3463–71. doi:10.4049/jimmunol.179.6.3463
46. Drummond RA, Brown GD. Signalling C-type lectins in antimicrobial immunity. *PLoS Pathog* (2013) 9(7):e1003417. doi:10.1371/journal.ppat.1003417
47. Saijo S, Fujikado N, Furuta T, Chung S-H, Kotaki H, Seki K, et al. Dectin-1 is required for host defense against *Pneumocystis carinii* but not against *Candida albicans*. *Nat Immunol* (2007) 8(1):39–46. doi:10.1038/ni1425
48. Taylor PR, Tsoni SV, Willment JA, Dennehy KM, Rosas M, Findon H, et al. Dectin-1 is required for beta-glucan recognition and control of fungal infection. *Nat Immunol* (2007) 8(1):31–8. doi:10.1038/ni1408
49. Iliev ID, Funari VA, Taylor KD, Nguyen Q, Reyes CN, Strom SP, et al. Interactions between commensal fungi and the C-type lectin receptor Dectin-1 influence colitis. *Science* (2012) 336(6086):1314–7. doi:10.1126/science.1221789
50. Kanazawa N. Dendritic cell immunoreceptors: C-type lectin receptors for pattern-recognition and signaling on antigen-presenting cells. *J Dermatol Sci* (2007) 45(2):77–86. doi:10.1016/j.jdermsci.2006.09.001
51. Marshall ASJ, Willment JA, Lin H-H, Williams DL, Gordon S, Brown GD. Identification and characterization of a novel human myeloid inhibitory C-type lectin-like receptor (MICL) that is predominantly expressed on granulocytes and monocytes. *J Biol Chem* (2004) 279(15):14792–802. doi:10.1074/jbc.M313127200
52. Kanazawa N, Okazaki T, Nishimura H, Tashiro K, Inaba K, Miyachi Y. DCIR acts as an inhibitory receptor depending on its immunoreceptor tyrosine-based inhibitory motif. *J Invest Dermatol* (2002) 118(2):261–6. doi:10.1046/j.0022-202x.2001.01633.x
53. Richard M, Thibault N, Veilleux P, Gareau-Pagé G, Beaulieu AD. Granulocyte macrophage-colony stimulating factor reduces the affinity of SHP-2 for the ITIM of CLECSF6 in neutrophils: a new mechanism of action for SHP-2. *Mol Immunol* (2006) 43(10):1716–21. doi:10.1016/j.molimm.2005.10.006
54. Lambert AA, Barabe F, Gilbert C, Tremblay MJ. DCIR-mediated enhancement of HIV-1 infection requires the ITIM-associated signal transduction pathway. *Blood* (2011) 117(24):6589–99. doi:10.1182/blood-2011-01-331363
55. Meyer-Wentrup F, Cambi A, Joosten B, Looman MW, de Vries IJM, Figdor CG, et al. DCIR is endocytosed into human dendritic cells and inhibits TLR8-mediated cytokine production. *J Leukoc Biol* (2009) 85(3):518–25. doi:10.1189/jlb.0608352
56. Meyer-Wentrup F, Benitez-Ribas D, Tacken PJ, Punt CJA, Figdor CG, de Vries IJM, et al. Targeting DCIR on human plasmacytoid dendritic cells results in antigen presentation and inhibits IFN-alpha production. *Blood* (2008) 111(8):4245–53. doi:10.1182/blood-2007-03-081398

57. Maglinao M, Klopfleisch R, Seeberger PH, Lepenies B. The C-type lectin receptor DCIR is crucial for the development of experimental cerebral malaria. *J Immunol* (2013) 191(5):2551–9. doi:10.4049/jimmunol.1203451
58. Troegeler A, Mercier I, Cougoule C, Pietretti D, Colom A, Duval C, et al. C-type lectin receptor DCIR modulates immunity to tuberculosis by sustaining type I interferon signaling in dendritic cells. *Proc Natl Acad Sci U S A* (2017) 114(4):E540–9. doi:10.1073/pnas.1613254114
59. Gringhuis SI, den Dunnen J, Litjens M, van der Vlist M, Geijtenbeek TB. Carbohydrate-specific signaling through the DC-SIGN signalosome tailors immunity to *Mycobacterium tuberculosis*, HIV-1 and *Helicobacter pylori*. *Nat Immunol* (2009) 10(10):1081–8. doi:10.1038/ni.1778
60. Zelenay S, Keller AM, Whitney PG, Schraml BU, Deddouche S, Rogers NC, et al. The dendritic cell receptor DNGR-1 controls endocytic handling of necrotic cell antigens to favor cross-priming of CTLs in virus-infected mice. *J Clin Invest* (2012) 122(5):1615–27. doi:10.1172/JCI60644DS1
61. Iborra S, Izquierdo HM, Martinez-Lopez M, Blanco-Menendez N, Reis e Sousa C, Sancho D. The DC receptor DNGR-1 mediates cross-priming of CTLs during vaccinia virus infection in mice. *J Clin Invest* (2012) 122(5):1628–43. doi:10.1172/JCI60660
62. Sancho D, Reis e Sousa C. Sensing of cell death by myeloid C-type lectin receptors. *Curr Opin Immunol* (2013) 25:46–52. doi:10.1016/j.coi.2012.12.007
63. Iborra S, Martinez-Lopez M, Khouili SC, Enamorado M, Cueto FJ, Conde-Garrosa R, et al. Optimal generation of tissue-resident but not circulating memory T cells during viral infection requires crosspriming by DNGR-1+ dendritic cells. *Immunity* (2016) 45(4):847–60. doi:10.1016/j.immuni.2016.08.019
64. Hanc P, Schulz O, Fischbach H, Martin SR, Kjaer S, Reis ESC. A pH- and ionic strength-dependent conformational change in the neck region regulates DNGR-1 function in dendritic cells. *EMBO J* (2016) 35(22):2484–97. doi:10.15252/embj.201694695
65. Takano T, Motozono C, Imai T, Sonoda KH, Nakanishi Y, Yamasaki S. Dectin-1 intracellular domain determines species-specific ligand spectrum by modulating receptor sensitivity. *J Biol Chem* (2017) 292(41):16933–41. doi:10.1074/jbc.M117.800847
66. Goodridge HS, Shimada T, Wolf AJ, Hsu Y-MS, Becker CA, Lin X, et al. Differential use of CARD9 by Dectin-1 in macrophages and dendritic cells. *J Immunol* (2009) 182(2):1146–54. doi:10.4049/jimmunol.182.2.1146
67. Willment JA, Gordon S, Brown GD. Characterization of the human beta-glucan receptor and its alternatively spliced isoforms. *J Biol Chem* (2001) 276(47):43818–23. doi:10.1074/jbc.M107715200
68. Yokota K, Takashima A, Bergstresser PR, Ariizumi K. Identification of a human homologue of the dendritic cell-associated C-type lectin-1, Dectin-1. *Gene* (2001) 272(1–2):51–60. doi:10.1016/S0378-1119(01)00528-5
69. Fischer M, Muller JP, Spies-Weisshart B, Grafe C, Kurzai O, Hunniger K, et al. Isoform localization of Dectin-1 regulates the signaling quality of anti-fungal immunity. *Eur J Immunol* (2017) 47(5):848–59. doi:10.1002/eji.201646849
70. Griffiths JS, Thompson A, Stott M, Benny A, Lewis NA, Taylor PR, et al. Differential susceptibility of Dectin-1 isoforms to functional inactivation by neutrophil and fungal proteases. *FASEB J* (2018). doi:10.1096/fj.201701145R
71. Rosas M, Liddiard K, Kimberg M, Faro-Trindade I, McDonald JU, Williams DL, et al. The induction of inflammation by Dectin-1 in vivo is dependent on myeloid cell programming and the progression of phagocytosis. *J Immunol* (2008) 181(5):3549–57. doi:10.4049/jimmunol.181.5.3549
72. Hernanz-Falcón P, Joffre O, Williams DL, Reis e Sousa C. Internalization of Dectin-1 terminates induction of inflammatory responses. *Eur J Immunol* (2009) 39(2):507–13. doi:10.1002/eji.200838687
73. Goodridge HS, Reyes CN, Becker CA, Katsumoto TR, Ma J, Wolf AJ, et al. Activation of the innate immune receptor Dectin-1 upon formation of a 'phagocytic synapse'. *Nature* (2011) 472(7344):471–5. doi:10.1038/nature10071
74. Branzk N, Lubojemska A, Hardison SE, Wang Q, Gutierrez MG, Brown GD, et al. Neutrophils sense microbe size and selectively release neutrophil extracellular traps in response to large pathogens. *Nat Immunol* (2014) 15(11):1017–25. doi:10.1038/ni.2987
75. Hughes CE, Pollitt AY, Mori J, Eble JA, Tomlinson MG, Hartwig JH, et al. CLEC-2 activates Syk through dimerization. *Blood* (2010) 115(14):2947–55. doi:10.1182/blood-2009-08-237834
76. Watson AA, Christou CM, James JR, Fenton-May AE, Moncayo GE, Mistry AR, et al. The platelet receptor CLEC-2 is active as a dimer. *Biochemistry* (2009) 48(46):10988–96. doi:10.1021/bi901427d
77. Suzuki-Inoue K, Inoue O, Ding G, Nishimura S, Hokamura K, Eto K, et al. Essential in vivo roles of the C-type lectin receptor CLEC-2: embryonic/neonatal lethality of CLEC-2-deficient mice by blood/lymphatic misconnections and impaired thrombus formation of CLEC-2-deficient platelets. *J Biol Chem* (2010) 285(32):24494–507. doi:10.1074/jbc.M110.130575
78. Bertozzi CC, Schmaier AA, Mericko P, Hess PR, Zou Z, Chen M, et al. Platelets regulate lymphatic vascular development through CLEC-2-SLP-76 signaling. *Blood* (2010) 116(4):661–70. doi:10.1182/blood-2010-02-270876
79. Haining EJ, Cherpokova D, Wolf K, Becker IC, Beck S, Eble JA, et al. CLEC-2 contributes to hemostasis independently of classical hemITAM signaling in mice. *Blood* (2017) 130(20):2224–8. doi:10.1182/blood-2017-03-771907
80. Garcia-Vallejo JJ, van Kooyk Y. The physiological role of DC-SIGN: a tale of mice and men. *Trends Immunol* (2013) 34(10):482–6. doi:10.1016/j.it.2013.03.001
81. Lobato-Pascual A, Saether PC, Fossum S, Dissen E, Daws MR. Mincle, the receptor for mycobacterial cord factor, forms a functional receptor complex with MCL and FcepsilonRI-gamma. *Eur J Immunol* (2013) 43(12):3167–74. doi:10.1002/eji.201343752
82. Miyake Y, Masatsugu OH, Yamasaki S. C-type lectin receptor MCL facilitates Mincle expression and signaling through complex formation. *J Immunol* (2015) 194(11):5366–74. doi:10.4049/jimmunol.1402429
83. Kerscher B, Dambuza IM, Christofi M, Reid DM, Yamasaki S, Willment JA, et al. Signalling through MyD88 drives surface expression of the mycobacterial receptors MCL (Clecsf8, Clec4d) and Mincle (Clec4e) following microbial stimulation. *Microbes Infect* (2016) 18(7–8):505–9. doi:10.1016/j.micinf.2016.03.007
84. Yamasaki S. Signaling while eating: MCL is coupled with Mincle. *Eur J Immunol* (2013) 43(12):3156–8. doi:10.1002/eji.201344131
85. Zhu L-L, Zhao X-Q, Jiang C, You Y, Chen X-P, Jiang Y-Y, et al. C-type lectin receptors Dectin-3 and Dectin-2 form a heterodimeric pattern-recognition receptor for host defense against fungal infection. *Immunity* (2013) 39(2):324–34. doi:10.1016/j.immuni.2013.05.017
86. Lo YL, Liou GG, Lyu JH, Hsiao M, Hsu TL, Wong CH. Dengue virus infection is through a cooperative interaction between a mannose receptor and CLEC5A on macrophage as a multivalent hetero-complex. *PLoS One* (2016) 11(11):e0166474. doi:10.1371/journal.pone.0166474
87. Blank U, Launay P, Benhamou M, Monteiro RC. Inhibitory ITAMs as novel regulators of immunity. *Immunol Rev* (2009) 232(1):59–71. doi:10.1111/j.1600-065X.2009.00832.x
88. Pasquier B, Launay P, Kanamaru Y, Moura IC, Pfirsch S, Ruffié C, et al. Identification of FcalphaRI as an inhibitory receptor that controls inflammation: dual role of FcRgamma ITAM. *Immunity* (2005) 22(1):31–42. doi:10.1016/j.immuni.2004.11.017
89. Aloulou M, Ben Mkaddem S, Biarnes-Pelicot M, Boussetta T, Souchet H, Rossato E, et al. IgG1 and IVIg induce inhibitory ITAM signaling through FcγRIII controlling inflammatory responses. *Blood* (2012) 119(13):3084–96. doi:10.1182/blood-2011-08-376046
90. Ben Mkaddem S, Hayem G, Jonsson F, Rossato E, Boedec E, Boussetta T, et al. Shifting FcgammaRIIA-ITAM from activation to inhibitory configuration ameliorates arthritis. *J Clin Invest* (2014) 124(9):3945–59. doi:10.1172/JCI74572
91. Iborra S, Martinez-Lopez M, Cueto FJ, Conde-Garrosa R, Del Fresno C, Izquierdo HM, et al. *Leishmania* uses Mincle to target an inhibitory ITAM signaling pathway in dendritic cells that dampens adaptive immunity to infection. *Immunity* (2016) 45(4):788–801. doi:10.1016/j.immuni.2016.09.012
92. Patin EC, Geffken AC, Willcocks S, Leschczyk C, Haas A, Nimmerjahn F, et al. Trehalose dimycolate interferes with FcgammaR-mediated phagosome maturation through Mincle, SHP-1 and FcgammaRIIB signalling. *PLoS One* (2017) 12(4):e0174973. doi:10.1371/journal.pone.0174973
93. Pan YG, Yu YL, Lin CC, Lanier LL, Chu CL. FcepsilonRI gamma-chain negatively modulates Dectin-1 responses in dendritic cells. *Front Immunol* (2017) 8:1424. doi:10.3389/fimmu.2017.01424
94. Blanco-Menendez N, Del Fresno C, Fernandes S, Calvo E, Conde-Garrosa R, Kerr WG, et al. SHIP-1 couples to the Dectin-1 hemITAM and selectively

modulates reactive oxygen species production in dendritic cells in response to *Candida albicans*. *J Immunol* (2015) 195(9):4466–78. doi:10.4049/jimmunol.1402874
95. Deng Z, Ma S, Zhou H, Zang A, Fang Y, Li T, et al. Tyrosine phosphatase SHP-2 mediates C-type lectin receptor-induced activation of the kinase Syk and anti-fungal TH17 responses. *Nat Immunol* (2015) 16(6):642–52. doi:10.1038/ni.3155
96. Elward K, Gasque P. "Eat me" and "don't eat me" signals govern the innate immune response and tissue repair in the CNS: emphasis on the critical role of the complement system. *Mol Immunol* (2003) 40(2–4):85–94. doi:10.1016/S0161-5890(03)00109-3
97. Varki A. Since there are PAMPs and DAMPs, there must be SAMPs? Glycan "self-associated molecular patterns" dampen innate immunity, but pathogens can mimic them. *Glycobiology* (2011) 21(9):1121–4. doi:10.1093/glycob/cwr087
98. Matzinger P. Tolerance, danger, and the extended family. *Annu Rev Immunol* (1994) 12:991–1045. doi:10.1146/annurev.iy.12.040194.005015
99. Matzinger P. The danger model: a renewed sense of self. *Science* (2002) 296(5566):301–5. doi:10.1126/science.1071059
100. Nagata M, Izumi Y, Ishikawa E, Kiyotake R, Doi R, Iwai S, et al. Intracellular metabolite beta-glucosylceramide is an endogenous Mincle ligand possessing immunostimulatory activity. *Proc Natl Acad Sci U S A* (2017) 114(16):E3285–94. doi:10.1073/pnas.1618133114
101. Kostarnoy AV, Gancheva PG, Lepenies B, Tukhvatulin AI, Dzharullaeva AS, Polyakov NB, et al. Receptor Mincle promotes skin allergies and is capable of recognizing cholesterol sulfate. *Proc Natl Acad Sci U S A* (2017) 114(13):E2758–65. doi:10.1073/pnas.1611665114
102. Suzuki Y, Nakano Y, Mishiro K, Takagi T, Tsuruma K, Nakamura M, et al. Involvement of Mincle and Syk in the changes to innate immunity after ischemic stroke. *Sci Rep* (2013) 3:3177. doi:10.1038/srep03177
103. Arumugam TV, Manzanero S, Furtado M, Biggins PJ, Hsieh YH, Gelderblom M, et al. An atypical role for the myeloid receptor Mincle in central nervous system injury. *J Cereb Blood Flow Metab* (2017) 37(6):2098–111. doi:10.1177/0271678X16661201
104. Seifert L, Werba G, Tiwari S, Ly NNG, Alothman S, Alqunaibit D, et al. The necrosome promotes pancreatic oncogenesis via CXCL1 and Mincle-induced immune suppression. *Nature* (2016) 532(7598):245–9. doi:10.1038/nature17403
105. Xie Y, Guo H, Wang L, Xu L, Zhang X, Yu L, et al. Human albumin attenuates excessive innate immunity via inhibition of microglial Mincle/Syk signaling in subarachnoid hemorrhage. *Brain Behav Immun* (2017) 60:346–60. doi:10.1016/j.bbi.2016.11.004
106. Fujikado N, Saijo S, Yonezawa T, Shimamori K, Ishii A, Sugai S, et al. Dcir deficiency causes development of autoimmune diseases in mice due to excess expansion of dendritic cells. *Nat Med* (2008) 14:176–80. doi:10.1038/nm1697
107. Maruhashi T, Kaifu T, Yabe R, Seno A, Chung SH, Fujikado N, et al. DCIR maintains bone homeostasis by regulating IFN-gamma production in T cells. *J Immunol* (2015) 194(12):5681–91. doi:10.4049/jimmunol.1500273
108. Massoud AH, Yona M, Xue D, Chouiali F, Alturaihi H, Ablona A, et al. Dendritic cell immunoreceptor: a novel receptor for intravenous immunoglobulin mediates induction of regulatory T cells. *J Allergy Clin Immunol* (2014) 133(3):853–63.e5. doi:10.1016/j.jaci.2013.09.029
109. Long KM, Whitmore AC, Ferris MT, Sempowski GD, McGee C, Trollinger B, et al. Dendritic cell immunoreceptor regulates Chikungunya virus pathogenesis in mice. *J Virol* (2013) 87(10):5697–706. doi:10.1128/JVI.01611-12
110. Geijtenbeek TB, Torensma R, van Vliet SJ, van Duijnhoven GC, Adema GJ, van Kooyk Y, et al. Identification of DC-SIGN, a novel dendritic cell-specific ICAM-3 receptor that supports primary immune responses. *Cell* (2000) 100(5):575–85. doi:10.1016/S0092-8674(00)80693-5
111. Geijtenbeek TBH, van Vliet SJ, Koppel EA, Sanchez-Hernandez M, Vandenbroucke-Grauls CMJE, Appelmelk B, et al. Mycobacteria target DC-SIGN to suppress dendritic cell function. *J Exp Med* (2003) 197(1):7–17. doi:10.1084/jem.20021229
112. Hovius JWR, de Jong MAWP, den Dunnen J, Litjens M, Fikrig E, van der Poll T, et al. Salp15 binding to DC-SIGN inhibits cytokine expression by impairing both nucleosome remodeling and mRNA stabilization. *PLoS Pathog* (2008) 4(2):e31. doi:10.1371/journal.ppat.0040031
113. van Gisbergen KPJM, Sanchez-Hernandez M, Geijtenbeek TBH, van Kooyk Y. Neutrophils mediate immune modulation of dendritic cells through glycosylation-dependent interactions between Mac-1 and DC-SIGN. *J Exp Med* (2005) 201(8):1281–92. doi:10.1084/jem.20041276
114. Gringhuis SI, Kaptein TM, Wevers BA, Mesman AW, Geijtenbeek TB. Fucose-specific DC-SIGN signalling directs T helper cell type-2 responses via IKKepsilon- and CYLD-dependent Bcl3 activation. *Nat Commun* (2014) 5:3898. doi:10.1038/ncomms4898
115. Gringhuis SI, Kaptein TM, Wevers BA, van der Vlist M, Klaver EJ, van Die I, et al. Fucose-based PAMPs prime dendritic cells for follicular T helper cell polarization via DC-SIGN-dependent IL-27 production. *Nat Commun* (2014) 5:5074. doi:10.1038/ncomms6074
116. Thaiss CA, Levy M, Itav S, Elinav E. Integration of innate immune signaling. *Trends Immunol* (2016) 37(2):84–101. doi:10.1016/j.it.2015.12.003
117. Ostrop J, Lang R. Contact, collaboration, and conflict: signal integration of Syk-coupled C-type lectin receptors. *J Immunol* (2017) 198(4):1403–14. doi:10.4049/jimmunol.1601665
118. Brown GD. Dectin-1: a signalling non-TLR pattern-recognition receptor. *Nat Rev Immunol* (2006) 6(1):33–43. doi:10.1038/nri1745
119. Jackson N, Compton E, Trowsdale J, Kelly AP. Recognition of *Salmonella* by Dectin-1 induces presentation of peptide antigen to type B T cells. *Eur J Immunol* (2014) 44(4):962–9. doi:10.1002/eji.201344065
120. Lefevre L, Lugo-Villarino G, Meunier E, Valentin A, Olagnier D, Authier H, et al. The C-type lectin receptors Dectin-1, MR, and SIGNR3 contribute both positively and negatively to the macrophage response to *Leishmania infantum*. *Immunity* (2013) 38(5):1038–49. doi:10.1016/j.immuni.2013.04.010
121. Thiagarajan PS, Yakubenko VP, Elsori DH, Yadav SP, Willard B, Tan CD, et al. Vimentin is an endogenous ligand for the pattern recognition receptor Dectin-1. *Cardiovasc Res* (2013) 99(3):494–504. doi:10.1093/cvr/cvt117
122. Daley D, Mani VR, Mohan N, Akkad N, Ochi A, Heindel DW, et al. Dectin 1 activation on macrophages by galectin 9 promotes pancreatic carcinoma and peritumoral immune tolerance. *Nat Med* (2017) 23(5):556–67. doi:10.1038/nm.4314
123. Chiba S, Ikushima H, Ueki H, Yanai H, Kimura Y, Hangai S, et al. Recognition of tumor cells by Dectin-1 orchestrates innate immune cells for anti-tumor responses. *Elife* (2014) 3:e04177. doi:10.7554/eLife.04177
124. Gantner BN, Simmons RM, Canavera SJ, Akira S, Underhill DM. Collaborative induction of inflammatory responses by Dectin-1 and toll-like receptor 2. *J Exp Med* (2003) 197(9):1107–17. doi:10.1084/jem.20021787
125. Viriyakosol S, Fierer J, Brown GD, Kirkland TN. Innate immunity to the pathogenic fungus *Coccidioides posadasii* is dependent on toll-like receptor 2 and Dectin-1. *Infect Immun* (2005) 73(3):1553–60. doi:10.1128/iai.73.3.1553-1560.2005
126. Yadav M, Schorey JS. The beta-glucan receptor Dectin-1 functions together with TLR2 to mediate macrophage activation by mycobacteria. *Blood* (2006) 108(9):3168–75. doi:10.1182/blood-2006-05-024406
127. Gross O, Poeck H, Bscheider M, Dostert C, Hannesschläger N, Endres S, et al. Syk kinase signalling couples to the Nlrp3 inflammasome for anti-fungal host defence. *Nature* (2009) 459:433–6. doi:10.1038/nature07965
128. Eberle ME, Dalpke AH. Dectin-1 stimulation induces suppressor of cytokine signaling 1, thereby modulating TLR signaling and T cell responses. *J Immunol* (2012) 188(11):5644–54. doi:10.4049/jimmunol.1103068
129. Seifert L, Deutsch M, Alothman S, Alqunaibit D, Werba G, Pansari M, et al. Dectin-1 regulates hepatic fibrosis and hepatocarcinogenesis by suppressing TLR4 signaling pathways. *Cell Rep* (2015) 13(9):1909–21. doi:10.1016/j.celrep.2015.10.058
130. Quintin J, Saeed S, Martens JHA, Giamarellos-Bourboulis EJ, Ifrim DC, Logie C, et al. *Candida albicans* infection affords protection against reinfection via functional reprogramming of monocytes. *Cell Host Microbe* (2012) 12(2):223–32. doi:10.1016/j.chom.2012.06.006
131. Cheng SC, Quintin J, Cramer RA, Shepardson KM, Saeed S, Kumar V, et al. mTOR- and HIF-1alpha-mediated aerobic glycolysis as metabolic basis for trained immunity. *Science* (2014) 345(6204):1250684. doi:10.1126/science.1250684
132. Buffen K, Oosting M, Quintin J, Ng A, Kleinnijenhuis J, Kumar V, et al. Autophagy controls BCG-induced trained immunity and the response to intravesical BCG therapy for bladder cancer. *PLoS Pathog* (2014) 10(10):e1004485. doi:10.1371/journal.ppat.1004485

133. Ifrim DC, Joosten LA, Kullberg BJ, Jacobs L, Jansen T, Williams DL, et al. *Candida albicans* primes TLR cytokine responses through a Dectin-1/Raf-1-mediated pathway. *J Immunol* (2013) 190(8):4129–35. doi:10.4049/jimmunol.1202611
134. Arts RJ, Novakovic B, Ter Horst R, Carvalho A, Bekkering S, Lachmandas E, et al. Glutaminolysis and fumarate accumulation integrate immunometabolic and epigenetic programs in trained immunity. *Cell Metab* (2016) 24(6):807–19. doi:10.1016/j.cmet.2016.10.008
135. Rizzetto L, Ifrim DC, Moretti S, Tocci N, Cheng SC, Quintin J, et al. Fungal chitin induces trained immunity in human monocytes during cross-talk of the host with *Saccharomyces cerevisiae*. *J Biol Chem* (2016) 291(15):7961–72. doi:10.1074/jbc.M115.699645
136. Kleinnijenhuis J, Quintin J, Preijers F, Joosten LA, Ifrim DC, Saeed S, et al. Bacille Calmette-Guerin induces NOD2-dependent nonspecific protection from reinfection via epigenetic reprogramming of monocytes. *Proc Natl Acad Sci U S A* (2012) 109(43):17537–42. doi:10.1073/pnas.1202870109
137. Crisan TO, Netea MG, Joosten LA. Innate immune memory: implications for host responses to damage-associated molecular patterns. *Eur J Immunol* (2016) 46(4):817–28. doi:10.1002/eji.201545497
138. Netea MG, Joosten LA, Latz E, Mills KH, Natoli G, Stunnenberg HG, et al. Trained immunity: a program of innate immune memory in health and disease. *Science* (2016) 352(6284):aaf1098. doi:10.1126/science.aaf1098
139. Domínguez-Andrés J, Arts RJW, ter Horst R, Gresnigt MS, Smeekens SP, Ratter JM, et al. Rewiring monocyte glucose metabolism via C-type lectin signaling protects against disseminated candidiasis. *PLoS Pathog* (2017) 13:e1006632. doi:10.1371/journal.ppat.1006632
140. Sousa, MdG, Reid DM, Schweighoffer E, Tybulewicz V, Ruland J, et al. Restoration of pattern recognition receptor costimulation to treat chromoblastomycosis, a chronic fungal infection of the skin. *Cell Host Microbe* (2011) 9(5):436–43. doi:10.1016/j.chom.2011.04.005
141. van Haren SD, Dowling DJ, Foppen W, Christensen D, Andersen P, Reed SG, et al. Age-specific adjuvant synergy: dual TLR7/8 and Mincle activation of human newborn dendritic cells enables Th1 polarization. *J Immunol* (2016) 197(11):4413–24. doi:10.4049/jimmunol.1600282
142. Lee WB, Kang JS, Choi WY, Zhang Q, Kim CH, Choi UY, et al. Mincle-mediated translational regulation is required for strong nitric oxide production and inflammation resolution. *Nat Commun* (2016) 7:11322. doi:10.1038/ncomms11322
143. Schick J, Etschel P, Bailo R, Ott L, Bhatt A, Lepenies B, et al. Toll-like receptor 2 and Mincle cooperatively sense corynebacterial cell wall glycolipids. *Infect Immun* (2017) 85(7):1–14. doi:10.1128/IAI.00075-17
144. Wuthrich M, Wang H, Li M, Lerksuthirat T, Hardison SE, Brown GD, et al. *Fonsecaea pedrosoi*-induced Th17-cell differentiation in mice is fostered by Dectin-2 and suppressed by Mincle recognition. *Eur J Immunol* (2015) 45(9):2542–52. doi:10.1002/eji.201545591
145. Siqueira IM, de Castro RJA, Leonhardt LCM, Jeronimo MS, Soares AC, Raiol T, et al. Modulation of the immune response by *Fonsecaea pedrosoi* morphotypes in the course of experimental chromoblastomycosis and their role on inflammatory response chronicity. *PLoS Negl Trop Dis* (2017) 11(3):e0005461. doi:10.1371/journal.pntd.0005461
146. Wevers BA, Kaptein TM, Zijlstra-Willems EM, Theelen B, Boekhout T, Geijtenbeek TB, et al. Fungal engagement of the C-type lectin Mincle suppresses Dectin-1-induced antifungal immunity. *Cell Host Microbe* (2014) 15(4):494–505. doi:10.1016/j.chom.2014.03.008
147. Greco SH, Mahmood SK, Vahle AK, Ochi A, Batel J, Deutsch M, et al. Mincle suppresses toll-like receptor 4 activation. *J Leukoc Biol* (2016) 100(1):185–94. doi:10.1189/jlb.3A0515-185R
148. Rodriguez E, Kalay H, Noya V, Brossard N, Giacomini C, van Kooyk Y, et al. *Fasciola hepatica* glycoconjugates immuneregulate dendritic cells through the dendritic cell-specific intercellular adhesion molecule-3-grabbing non-integrin inducing T cell anergy. *Sci Rep* (2017) 7:46748. doi:10.1038/srep46748
149. Warnatsch A, Tsourouktsoglou TD, Branzk N, Wang Q, Reincke S, Herbst S, et al. Reactive oxygen species localization programs inflammation to clear microbes of different size. *Immunity* (2017) 46(3):421–32. doi:10.1016/j.immuni.2017.02.013

Conflict of Interest Statement: The authors declare that the research was conducted in the absence of any commercial or financial relationships that could be construed as a potential conflict of interest.